

Developing concurrent transcranial magnetic stimulation and electroencephalography to study prefrontal cortex neurophysiology in people with schizophrenia.

Nigel C. Rogasch

Monash Alfred Psychiatry Research Centre
Central Clinical School
Faculty of Medicine, Nursing and Health Sciences
Monash University

A thesis submitted for the degree of Doctor of Philosophy
(Neuroscience)

October 2013

Notice 1

Under the Copyright Act 1968, this thesis must be used only under the normal conditions of scholarly fair dealing. In particular no results or conclusions should be extracted from it, nor should it be copied or closely paraphrased in whole or in part without the written consent of the author. Proper written acknowledgement should be made for any assistance obtained from this thesis.

Notice 2

I certify that I have made all reasonable efforts to secure copyright permissions for third-party content included in this thesis and have not knowingly added copyright content to my work without the owner's permission

CONTENTS

ABSTRACT	i
LIST OF PUBLICATIONS	iii
DECLARATIONS.....	vi
ACKNOWLEDGEMENTS	xvii
CHAPTER ONE: Introduction and overview.....	1
Schizophrenia	1
The pathophysiology of working memory deficits in schizophrenia.....	3
Transcranial magnetic stimulation	8
Combined transcranial magnetic stimulation and electroencephalography to study prefrontal cortex networks.....	10
Aims.....	12
Overview	14
CHAPTER TWO: TMS and schizophrenia	17
Preamble to review paper.....	17
Paper 1: Cortical Inhibition, Excitation, and Connectivity in Schizophrenia: A Review of Insights from Transcranial Magnetic Stimulation.....	18
CHAPTER THREE: Concurrent TMS and EEG.....	40
Preamble to review paper.....	40
Paper 2: Assessing cortical network properties using TMS-EEG.....	41
CHAPTER FOUR: Artifacts in TMS-EEG recordings	59
Preamble to empirical paper.....	59
Paper 3: Short-Latency Artifacts Associated with Concurrent TMS-EEG.....	60
CHAPTER FIVE: Removing TMS-EEG artifacts using ICA	69
Preamble to empirical paper.....	69
Paper 4: Removing artifacts from TMS-EEG recordings using independent component analysis: importance for assessing prefrontal cortex network properties.....	70

CHAPTER SIX: Mechanisms underlying TMS-evoked potentials in motor cortex	121
Preamble to empirical paper	121
Paper 5: Mechanisms underlying long-interval cortical inhibition in the human motor cortex: a TMS-EEG study.....	123
CHAPTER SEVEN: Mechanisms underlying TMS-evoked potentials in DLPFC.....	133
Preamble to empirical paper	133
Paper 6: Mechanisms underlying markers of cortical inhibition in the dorsolateral prefrontal cortex: a TMS-EEG study.....	134
CHAPTER EIGHT: DLPFC function in people with schizophrenia	165
Preamble to empirical paper	165
Paper 7: Dorsolateral prefrontal cortex network properties are altered in schizophrenia: implications for working memory.....	166
CHAPTER NINE: Discussion and conclusions	193
Summary of main findings.....	193
<i>Study one (chapter four): Short-Latency Artifacts Associated with Concurrent TMS-EEG.</i>	193
<i>Study two (Chapter 5): Removing artifacts from TMS-EEG recordings using independent component analysis: importance for assessing prefrontal cortex network properties.</i>	194
<i>Study three (Chapter 6): Mechanisms underlying long-interval cortical inhibition in the human motor cortex: a TMS-EEG study.</i>	195
<i>Study four (Chapter 7): Mechanisms underlying markers of cortical inhibition in the dorsolateral prefrontal cortex: a TMS-EEG study.</i>	195
<i>Study five (Chapter 8): Dorsolateral prefrontal cortex network properties are altered in schizophrenia: implications for working memory.</i>	196
Implications	197
<i>TMS-EEG methods</i>	197
<i>Evaluating cortical mechanisms with TMS.....</i>	201
<i>Understanding SCZ pathophysiology.....</i>	205
Limitations	209
Future directions	211
Conclusions.....	213
REFERENCES	214
APPENDICES.....	230

Appendix A	230
Appendix B	231
Appendix C	233
Appendix D	235
Appendix E.....	236
Appendix F.....	238
Appendix G	240

ABSTRACT

Cognitive impairment such as deficits in working memory - the ability to retain and manipulate information over a brief period - are core features of schizophrenia. Such deficits may result from dysfunctional cortical inhibition in the dorsolateral prefrontal cortex (DLPFC). One method potentially suited to studying inhibitory circuits in the DLPFC is concurrent transcranial magnetic stimulation and electroencephalography (TMS-EEG). Merging these methods is technically challenging, resulting in artifacts which obscure recording of TMS-evoked neural activity. Furthermore, little is known about the mechanisms that underlie TMS-evoked cortical potentials (TEPs) from the DLPFC. The broad aim of this thesis was to develop and validate TMS-EEG methods to study DLPFC neurophysiology in people with and without schizophrenia.

Five studies are reported. The first describes EEG artifacts following TMS. Phantom heads (melons) and human participants were used to investigate the effects of different experimental arrangements (stimulators, pulse types, stimulation site, intensity, paired-pulse conditions) on TMS-evoked EEG artifacts. This study demonstrated the pervasive nature of TMS-evoked scalp muscle artifacts over the DLPFC.

In the second study, independent component analysis (ICA - a method of blind source separation) was assessed to identify and remove artifacts from EEG recordings following TMS over the DLPFC. Five subtypes of artifact were identified including muscle, blink and auditory artifacts. We provided evidence that each of these artifacts could be removed with reasonable confidence using ICA, revealing otherwise obscured TMS-evoked neural activity.

In study three and four we examined the underlying mechanisms of TEPs. We compared suppression of TEPs with motor evoked potentials (MEPs) following long-interval cortical inhibition (LICI - a paired-pulse TMS paradigm) over the motor cortex (study three) and variations in TEP LICI over the DLPFC between individuals (study four). We demonstrated that modulation of LICI strength differed between TEP peaks,

suggesting early peaks (P30, N40) reflected excitatory neurotransmission, whereas latter peaks (N100) reflected the inhibitory mechanism responsible for LICl.

In the final study, we compared TMS-evoked DLPFC network properties between people with and without schizophrenia. People with schizophrenia displayed a reduced N100 and reduced TMS-evoked high frequency oscillations in fronto-parietal and interhemispheric networks compared with controls. Importantly, TMS-evoked gamma oscillations (30-45 Hz; dependent on cortical inhibition) in the DLPFC were particularly reduced in a sub-group of schizophrenia participants with low working memory capacity. These findings support impaired inhibitory neurotransmission in the DLPFC of people with schizophrenia and suggest the ability of the DLPFC to generate high frequency oscillations may contribute to schizophrenia-related working memory deficits.

This thesis describes the application of TMS-EEG to study cortical neurophysiology in both healthy and disease states. The findings demonstrate that TMS-evoked neural activity can be recorded from the DLPFC following artifact removal and provide insight into inhibitory mechanisms within the DLPFC. Moreover, alterations in DLPFC function assessed using TMS-EEG may underlie reduced working memory capacity in people with schizophrenia. These findings have significant implications for the development of TMS-EEG as a neurophysiological technique, our knowledge of inhibitory mechanisms in the human cortex and our understanding of working memory deficits in schizophrenia.

LIST OF PUBLICATIONS

PEER-REVIEWED PAPERS PUBLISHED DURING CANDIDATURE

1. **Rogasch NC**, Daskalakis ZJ, Fitzgerald PB. (In press). Cortical Inhibition, Excitation, and Connectivity in Schizophrenia: A Review of Insights from Transcranial Magnetic Stimulation. *Schizophrenia Bulletin*.
2. **Rogasch NC**, Fitzgerald PB. (2013). Assessing cortical network properties using TMS-EEG. *Human Brain Mapping*. 109(1):1652-69.
3. **Rogasch NC**, Thomson RH, Daskalakis ZJ, Fitzgerald PB. (In press). Short-Latency Artifacts Associated with Concurrent TMS-EEG. *Brain Stimulation*.
4. **Rogasch NC**, Daskalakis ZJ, Fitzgerald PB. (2013). Mechanisms underlying long-interval cortical inhibition in the human motor cortex: a TMS-EEG study. *Journal of Neurophysiology*. 109(1):89-99.

PAPERS SUBMITTED DURING CANDIDATURE FOR PEER-REVIEW

5. **Rogasch NC**, Thomson RH, Farzan F, Fitzgibbon BM, Bailey NW, Hernandez-Pavon JC, Daskalakis ZJ, Fitzgerald PB. Removing artifacts from TMS-EEG recordings using independent component analysis: importance for assessing prefrontal cortex network properties.
6. **Rogasch NC**, Daskalakis ZJ, Fitzgerald PB. Mechanisms underlying markers of cortical inhibition in the dorsolateral prefrontal cortex: a TMS-EEG study.
7. **Rogasch NC**, Rajji TK, Tran LC, Bailey NW, Fitzgibbon BM, Daskalakis ZJ, Fitzgerald PB. Dorsolateral prefrontal cortex network properties are altered in schizophrenia: implications for working memory.

CONFERENCE PRESENTATIONS AND POSTERS DURING CANDIDATURE

1. **Rogasch NC**, Fitzgerald PB. Long interval cortical inhibition measured in humans using concurrent TMS-EEG. Poster presentation, Australian Cognitive Neurosciences Conference (November 26-29, 2010). Melbourne, Australia.
2. **Rogasch NC**, Fitzgerald PB. Optimal parameters for measuring long-interval cortical inhibition using TMS-EEG. Poster presentation, Society for Neuroscience (November 12-16, 2011). Washington DC, USA.
3. **Rogasch NC**, Rajji TK, Tran LC, Fitzgerald PB, Daskalakis ZJ. Plasticity in the prefrontal cortex: relationship with working memory and schizophrenia. Poster presentation, Biological Psychiatry Australia (October 29-30, 2012). Melbourne, Australia.
4. **Rogasch NC**, Rajji TK, Tran LC, Fitzgerald PB, Daskalakis ZJ. Plasticity induced in the prefrontal cortex is impaired in people with schizophrenia. Oral presentation, Australian Neuroscience Society Annual Meeting (January 29- February 1, 2013). Melbourne, Australia.
5. **Rogasch NC**, Rajji TK, Tran LC, Fitzgerald PB, Daskalakis ZJ. Brain stimulation-induced associative plasticity is reduced in the prefrontal cortex of people with schizophrenia. Invited oral presentation, Australasian Schizophrenia Conference (May 13-14, 2013). Melbourne, Australia.
6. **Rogasch NC**, Rajji TK, Tran LC, Fitzgerald PB, Daskalakis ZJ. Brain stimulation-induced associative plasticity is reduced in the prefrontal cortex of people with schizophrenia. Oral presentation, World Congress of Biological Psychiatry (June 22-27, 2013). Kyoto, Japan.

7. **Rogasch NC**, Thomson RH, Bailey NW, Daskalakis ZJ, Fitzgerald PB. Artifacts associated with combined TMS-EEG. Oral presentation, Australasian Brain Stimulation Meeting (July 25-26, 2013). Melbourne, Australia.

DECLARATIONS

Monash University

Declaration for thesis based or partially based on conjointly published or unpublished work

General Declaration

In accordance with Monash University Doctorate Regulation 17.2 Doctor of Philosophy and Research Master's regulations the following declarations are made:

I hereby declare that this thesis contains no material which has been accepted for the award of any other degree or diploma at any university or equivalent institution and that, to the best of my knowledge and belief, this thesis contains no material previously published or written by another person, except where due reference is made in the text of the thesis.

This thesis includes four original papers published in peer reviewed journals and three unpublished papers. The core theme of the thesis is development of combined transcranial magnetic stimulation and electroencephalography to study prefrontal cortex neurophysiology in people with schizophrenia. The ideas, development and writing up of all the papers in the thesis were the principal responsibility of myself, the candidate, working within the Central Clinical School under the supervision of Professor Paul Fitzgerald.

The inclusion of co-authors reflects the fact that the work came from active collaboration between researchers and acknowledges input into team-based research.

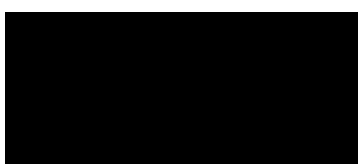
In the case of 2, 3, 4, 5, 6, 7 and 8 my contribution to the work involved the following:

Project design (in consultation with my supervisors and co-authors); review of appropriate literature; securing ethics approval; recruitment of participants; data collection; conducting data analysis; writing of papers. Supervisors and co-authors provided input into completed manuscript drafts.

Thesis chapter	Publication title	Publication status*	Nature and extent of candidate's contribution
2	Cortical Inhibition, Excitation, and Connectivity in Schizophrenia: A Review of Insights from Transcranial Magnetic Stimulation.	In press	As above
3	Assessing cortical network properties using TMS-EEG	Published	As above
4	Short-Latency Artifacts Associated with Concurrent TMS-EEG.	In press	As above
5	Removing artifacts from TMS-EEG recordings using independent component analysis: importance for assessing prefrontal cortex network properties.	Submitted	As above
6	Mechanisms underlying long-interval cortical inhibition in the human motor cortex: a TMS-EEG study.	Published	As above
7	Mechanisms underlying markers of cortical inhibition in the dorsolateral prefrontal cortex: a TMS-EEG study.	Submitted	As above
8	Dorsolateral prefrontal cortex network properties are altered in schizophrenia: implications for working memory.	Submitted	As above

I have renumbered sections of submitted or published papers in order to generate a consistent presentation within the thesis.

Signed:



Date: 8/10/13

Declaration for Thesis Chapter 2

Declaration by candidate

In the case of Chapter 2, the nature and extent of my contribution to the work was the following:

Nature of contribution	Extent of contribution (%)
Literature review, writing of manuscript	90

The following co-authors contributed to the work. If co-authors are students at Monash University, the extent of their contribution in percentage terms is stated:

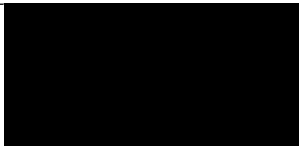
Name	Nature of contribution	Extent of contribution (%) for student co-authors only
Jeff Daskalakis	Review of manuscript.	Not applicable
Paul Fitzgerald	Review of manuscript, supervisory input.	Not applicable

The undersigned hereby certify that the above declaration correctly reflects the nature and extent of the candidate's and co-authors' contributions to this work.

Candidate's
Signature

	Date 8/10/13
---	--------------

Co-author 1
Signature

	Date 8/10/13
---	--------------

Main
Supervisor's
Signature

	Date 8/10/13
---	--------------

Declaration for Thesis Chapter 3

Declaration by candidate

In the case of Chapter 2, the nature and extent of my contribution to the work was the following:

Nature of contribution	Extent of contribution (%)
Literature review, writing of manuscript	95

The following co-authors contributed to the work. If co-authors are students at Monash University, the extent of their contribution in percentage terms is stated:

Name	Nature of contribution	Extent of contribution (%) for student co-authors only
Paul Fitzgerald	Review of manuscript, supervisory input.	Not applicable

The undersigned hereby certify that the above declaration correctly reflects the nature and extent of the candidate's and co-authors' contributions to this work.

**Candidate's
Signature**

	Date 8/10/13
---	---------------------

**Main
Supervisor's
Signature**

	Date 8/10/13
---	---------------------

Declaration for Thesis Chapter 4

Declaration by candidate

In the case of Chapter 4, the nature and extent of my contribution to the work was the following:

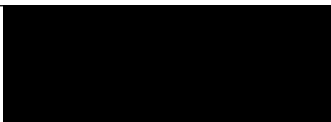
Nature of contribution	Extent of contribution (%)
Project design, participant recruitment, data collection, data analysis, writing of manuscript.	90

The following co-authors contributed to the work. If co-authors are students at Monash University, the extent of their contribution in percentage terms is stated:

Name	Nature of contribution	Extent of contribution (%) for student co-authors only
Richard Thomson	Technical advice, data collection, review of manuscript.	Not applicable
Jeff Daskalakis	Review of manuscript.	Not applicable
Paul Fitzgerald	Review of manuscript, supervisory input.	Not applicable

The undersigned hereby certify that the above declaration correctly reflects the nature and extent of the candidate's and co-authors' contributions to this work.

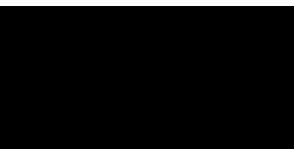
Candidate's
Signature

	Date 8/10/13
---	--------------

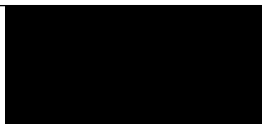
Co-author 1
Signature

	Date 8/10/13
---	--------------

Co-author 2
Signature

	Date 8/10/13
---	--------------

Main
Supervisor's
Signature

	Date 8/10/13
---	--------------

Declaration for Thesis Chapter 5

Declaration by candidate

In the case of Chapter 5, the nature and extent of my contribution to the work was the following:

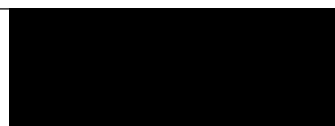
Nature of contribution	Extent of contribution (%)
Project design, ethics application and approval, participant recruitment, data collection, data analysis, writing of manuscript.	85

The following co-authors contributed to the work. If co-authors are students at Monash University, the extent of their contribution in percentage terms is stated:

Name	Nature of contribution	Extent of contribution (%) for student co-authors only
Richard Thomson	Technical advice, review of manuscript.	Not applicable
Faranak Farzan	Technical advice, review of manuscript.	Not applicable
Bernadette Fitzgibbon	Data collection, review of manuscript.	Not applicable
Neil Bailey	Data analysis, review of manuscript.	Not applicable
Julio Hernandez-Pavon	Technical advice, review of manuscript.	Not applicable
Jeff Daskalakis	Review of manuscript.	Not applicable
Paul Fitzgerald	Review of manuscript, supervisory input.	Not applicable

The undersigned hereby certify that the above declaration correctly reflects the nature and extent of the candidate's and co-authors' contributions to this work.

Candidate's
Signature



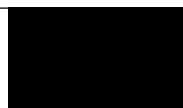
Date 8/10/13

Co-author 1
Signature



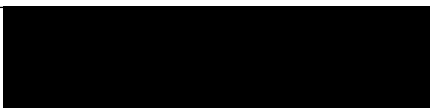
Date 8/10/13

Co-author 2
Signature



Date 8/10/13

Co-author 3
Signature



Date 8/10/13

**Co-author 4
Signature**

		Date 8/10/13
---	--	---------------------

**Co-author 5
Signature**

		Date 8/10/13
---	--	---------------------

**Co-author 6
Signature**

		Date 8/10/13
---	--	---------------------

**Main
Supervisor's
Signature**

		Date 8/10/13
---	--	---------------------

Declaration for Thesis Chapter 6

Declaration by candidate

In the case of Chapter 6, the nature and extent of my contribution to the work was the following:

Nature of contribution	Extent of contribution (%)
Project design, participant recruitment, data collection, data analysis, writing of manuscript.	90

The following co-authors contributed to the work. If co-authors are students at Monash University, the extent of their contribution in percentage terms is stated:

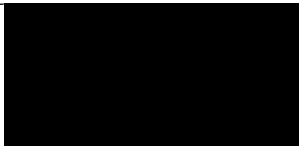
Name	Nature of contribution	Extent of contribution (%) for student co-authors only
Jeff Daskalakis	Review of manuscript.	Not applicable
Paul Fitzgerald	Review of manuscript, supervisory input.	Not applicable

The undersigned hereby certify that the above declaration correctly reflects the nature and extent of the candidate's and co-authors' contributions to this work.

Candidate's
Signature

	Date 8/10/13
---	--------------

Co-author 1
Signature

	Date 8/10/13
---	--------------

Main
Supervisor's
Signature

	Date 8/10/13
---	--------------

Declaration for Thesis Chapter 7

Declaration by candidate

In the case of Chapter 7, the nature and extent of my contribution to the work was the following:

Nature of contribution	Extent of contribution (%)
Project design, ethics submission, participant recruitment, data collection, data analysis, writing of manuscript.	90

The following co-authors contributed to the work. If co-authors are students at Monash University, the extent of their contribution in percentage terms is stated:

Name	Nature of contribution	Extent of contribution (%) for student co-authors only
Jeff Daskalakis	Review of manuscript.	Not applicable
Paul Fitzgerald	Review of manuscript, supervisory input.	Not applicable

The undersigned hereby certify that the above declaration correctly reflects the nature and extent of the candidate's and co-authors' contributions to this work.

Candidate's
Signature

	Date 8/10/13
---	--------------

Co-author 1
Signature

	Date 8/10/13
---	--------------

Main
Supervisor's
Signature

	Date 8/10/13
---	--------------

Declaration for Thesis Chapter 8

Declaration by candidate

In the case of Chapter 8, the nature and extent of my contribution to the work was the following:

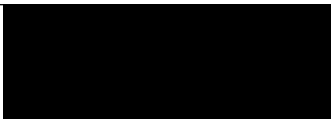
Nature of contribution	Extent of contribution (%)
Project design, ethics application and approval, participant recruitment, data collection, data analysis, writing of manuscript.	85

The following co-authors contributed to the work. If co-authors are students at Monash University, the extent of their contribution in percentage terms is stated:

Name	Nature of contribution	Extent of contribution (%) for student co-authors only
Tarek Rajji	Design of experiment, review of manuscript.	Not applicable
Lisa Tran	Data collection, review of manuscript.	Not applicable
Neil Bailey	Task design, review of manuscript.	Not applicable
Bernadette Fitzgibbon	Data collection, review of manuscript.	Not applicable
Jeff Daskalakis	Design of experiment, review of manuscript.	Not applicable
Paul Fitzgerald	Design of experiment, review of manuscript, supervisory input.	Not applicable

The undersigned hereby certify that the above declaration correctly reflects the nature and extent of the candidate's and co-authors' contributions to this work.

Candidate's
Signature

	Date 8/10/13
---	--------------

Co-author 1
Signature

	Date 8/10/13
---	--------------

Co-author 2
Signature

	Date 8/10/13
---	--------------

**Co-author 3
Signature**

		Date 8/10/13
---	--	---------------------

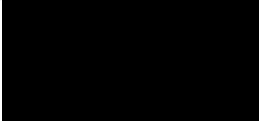
**Co-author 4
Signature**

		Date 8/10/13
---	--	---------------------

**Co-author 5
Signature**

		Date 8/10/13
---	--	---------------------

**Main
Supervisor's
Signature**

		Date 8/10/13
---	--	---------------------

ACKNOWLEDGEMENTS

There are many people who have either directly or indirectly contributed to this thesis, for which I am extremely grateful. First and foremost, my greatest thanks goes to my supervisor, Paul Fitzgerald. Paul, I couldn't have asked for any more in a supervisor. You have provided incredible guidance and insight throughout my PhD. Your passion for brain stimulation and your willingness to push the boundaries are a consistent source of inspiration. You have also provided me with so many opportunities, both big and small – thank you so much. If only you supported a decent football team...

To my un-official supervisor abroad, Jeff Daskalakis, a massive thank you for inviting me to join your lab in Canada. My time with you and your team completed my PhD experience. I learned so much in my short stay at your lab and have so many fond memories. Thank you for the kindness and generosity that you have shown me throughout my PhD. Go Leafs!

A number of other people also made significant contributions to this thesis. My thanks goes to Richard Thomson, who absorbed so much of my angst, stress and frustration with TMS-EEG and provided so much technical support with his endless knowledge. To Neil Bailey and Bernadette Fitzgibbon, thanks so much for your help and support guys. You both made my PhD incredibly fun and enjoyable! I couldn't have asked for better work mates. To Tarek Rajji and Lisa Tran, thanks so much for taking care of me in Canada, sharing ideas and the hours and hours of PAS (which didn't even make it in to the thesis). To Faranak Farzan and Julio Hernandez-Pavon, you both entered my PhD at a time when I was in need of some inspiration. Thank you both so much for sharing your knowledge and passion for TMS-EEG.

My warmest thanks goes to all of the members of MAPrc. I count myself incredibly fortunate to have worked with such a great group of people! In particular, a massive shout out to Pete 'the birdman' Enticott

and Kate ‘the hammer’ Hoy, who have provided so much support, guidance and friendship throughout my candidature. To all the guys at CAMH, thanks also for all of your help, support and Friday night beers. I really appreciate the way you all accepted me into your lab and made me feel so at home.

To my friends, both old and new, who have provided support, care and a welcome relief from my PhD. Thank you all for your understanding and the fun times we have shared together over the years.

A huge thank you must go to my family. It has been a long road of study and you guys have been there all the way. Thank you so much for your continued love and support, no matter what I do.

Finally, to my beautiful fiancé Sonja. I couldn’t have brought this PhD baby into the world without you. Your love, support, understanding and kindness (and delicious cooking) have kept me going. I cannot thank you enough!

CHAPTER ONE

Introduction and overview

Schizophrenia

Schizophrenia (SCZ) is a debilitating mental illness that affects between 0.5-1% of the population (Saha, Chant, Welham, & McGrath, 2005). SCZ has a heterogeneous presentation of symptoms including positive (disorganised thought, delusions and hallucinations), negative (anhedonia and amotivation) and cognitive (poor memory and executive functioning) symptoms (van Os & Kapur, 2009). These symptoms have devastating impact on social and occupational behaviour and, although psychotic symptoms can be managed by medication, functional outcomes of the illness remain poor (Green, 1996). For instance, people with SCZ are overrepresented in unemployment (Marwaha & Johnson, 2004), homelessness (Foster, Gable, & Buckley, 2012) and prevalence of preventable diseases such as diabetes and cardiovascular disease (McEvoy et al., 2005). Sadly, as many as 10% of sufferers will eventually take their own lives (Saha, Chant, & McGrath, 2007). As a result of these factors, many face a lifetime of disability (Wiersma et al., 2000) and the average lifespan of people with SCZ is almost 20 years shorter than the average population (Colton & Manderscheid, 2006). Therefore, SCZ not only has devastating effects on the lives of sufferers, but is also associated with considerable emotional burden on families and a large economic burden on society through access to the medical system and lost productivity (Fitzgerald et al., 2009; Murray et al., 2013).

For the majority of people, SCZ is a lifetime illness following the onset of symptoms (Harrison, 2001). Symptoms usually first present in early adolescence, particularly in males, and onset is rare in early life or after middle age (van Os & Kapur, 2009). The exact cause of SCZ remains unclear, however risk of developing SCZ increases proportionally with the degree of genetic relatedness to an affected individual (Baron, Gruen, Asnis, & Kane, 1983). Accordingly, genome-wide association studies have identified a number of specific common risk alleles, many of which are involved in neurodevelopment and synaptic function (Doherty, O'Donovan, & Owen, 2012). However, the degree of risk conferred by these singular nucleotide polymorphisms (SNPs) appears low. Rare structural variants such as copy number variants and

translocations appear to have larger causative effects than SNPs, but most are not specific to SCZ and often only occur in single families (Malhotra & Sebat, 2012). Along with the concordance rates in identical twin studies (~50%; Cannon, Kaprio, Lönqvist, Huttunen, & Koskenvuo, 1998), this data suggest that a purely genetic explanation of SCZ is insufficient. A large body of research has identified a raft of environmental factors that confer additional risk to the development of SCZ. Migrant status, older fathers, exposure to the antibody *Toxoplasmosis Gondii*, prenatal famine, lifetime cannabis use, obstetrical complications, urban rearing and winter or spring births all convey additional, albeit mild, increases in developing SCZ (MacDonald & Schulz, 2009). This complex interplay between genetic and environmental factors is still poorly understood and, as a result, there are currently no biological tests that are diagnostic for SCZ. Instead, the diagnosis of SCZ is based on a clinical syndrome, that is, the clustering of certain behaviours with certain positive and negative symptoms (American Psychiatric Association, 2000).

Although SCZ is characterised by positive and negative symptoms, cognitive symptoms occur with a relatively high frequency amongst sufferers (Gold, 2004; Heinrichs & Zakzanis, 1998), so much so that many now consider these symptoms as core features of the illness (Barch & Ceaser, 2012; Silver, Feldman, Bilker, & Gur, 2003). This notion is backed by a growing body of evidence. Firstly, several cross-sectional and longitudinal studies have documented cognitive impairments before the onset of psychotic symptoms (Sørensen et al., 2010; Woodberry, Giuliano, & Seidman, 2008), which may even exist through childhood (Reichenberg et al., 2010). Cognitive impairments also exist in first degree relatives, although to a lesser extent (Snitz, Macdonald, & Carter, 2006) and these cognitive impairments generally persist throughout illness duration (Hoff et al., 1999) and remain unaffected by current pharmacological treatments (Goldberg et al., 2007). Finally, cognitive impairment is the strongest predictor of functional outcome of the illness (Bowie, Reichenberg, Patterson, Heaton, & Harvey, 2006; Green, 1996). This body of evidence is leading a re-conceptualisation of SCZ as a neurodevelopmental disorder that primarily affects cognition (Insel, 2010). The lack of current treatments and the strong link between cognition and functionality has spurred a large research effort to understand the pathophysiological mechanisms responsible for these symptoms (Lewis,

Hashimoto, & Volk, 2005). Understanding these mechanisms is paramount for the effective development of novel treatments specifically targeting cognitive symptoms in SCZ (Bray, Leweke, Kapur, & Meyer-Lindenberg, 2010).

The pathophysiology of working memory deficits in schizophrenia

Deficits in working memory (WM; the ability to maintain and manipulate information over a brief period; Baddeley, 1992) have received particular attention in SCZ research (Silver et al., 2003). WM plays a central role in general cognitive function and impairments are prevalent in SCZ (Forbes, Carrick, McIntosh, & Lawrie, 2009). Neurophysiological studies in non-human primates have provided much insight in to the cellular networks underlying WM (Goldman-Rakic, 1995). These studies have demonstrated that persistent neuronal activity in specific memory fields across the dorsolateral prefrontal cortex (DLPFC; Funahashi, 2006; Siegel, Warden, & Miller, 2009) and posterior parietal cortex (Pesaran, Pezaris, Sahani, Mitra, & Andersen, 2002) are required for WM performance. In humans, the DLPFC consists of a region of cortex spanning the superior, middle and inferior frontal gyri (Brodmann areas 9 and 46) and is involved in higher order functions such as planning, organisation and cognitive control (Miller & Cohen, 2001). Accordingly, fronto-parietal networks show increased hemodynamic activity during WM tasks in healthy humans during functional magnetic resonance imaging (fMRI) and positron emission tomography (PET) studies (Braver et al., 1997; Jonides et al., 1993; McCarthy et al., 1994; Petrides, Alivisatos, Meyer, & Evans, 1993; Smith, Jonides, & Koeppe, 1996; Swartz et al., 1995). However, the exact pneumatic role of these areas remains somewhat unclear, with some studies suggesting both the DLPFC and posterior parietal cortex maintain information during WM (Curtis & D'Esposito, 2003), while others suggest that information is stored in the parietal cortex while the DLPFC plays a top-down supporting role, possibly increasing memory capacity (Edin et al., 2009). Regardless, abnormalities in hemodynamic activation of the DLPFC during WM are one of the most widely replicated findings in SCZ, suggesting the DLPFC abnormalities may underlie WM deficits (Barch & Ceaser, 2012; Minzenberg, Laird, Thelen, Carter, & Glahn, 2009). The nature of these abnormalities is not straight forward, with some studies reporting decreased (Curtis et al., 1998; Volz et al.,

1999), while others increased (Manoach et al., 2000) DLPFC activity in SCZ. These findings have been reconciled by demonstrating an inverted U shape activation pattern in the DLPFC, where activity increases with WM load until memory capacity is exceeded after which it decreases (Callicott et al., 1999). As people with SCZ have lower WM capacity, the DLPFC activity tends to be higher in SCZ at low loads, but lower in high loads once WM capacity has been exceeded relative to controls (Callicott et al., 2003). Similar, but weaker patterns have also been demonstrated in individuals at high risk of psychosis (Morey et al., 2005) and first degree relatives (Meda et al., 2008), suggesting these findings are not a result of medication or chronicity of illness. Although these findings appear robust, one limitation is the lack of information fMRI and PET studies provide on the mechanisms underlying dysfunctional DLPFC activation.

In order to explain DLPFC dysfunction, studies have focused on DLPFC anatomy. Evidence from structural magnetic resonance imaging (MRI) and diffusion tensor imaging (DTI) studies suggest that anatomical changes may accompany functional DLPFC changes in SCZ. Cortical thinning in the DLPFC of people with SCZ is a widely replicated finding (Minzenberg et al., 2009), as are subtle changes in the fractional anisotropy (a coarse measure of white matter tract integrity) between the DLPFC, thalamus and anterior cingulate gyrus (Ellison-Wright & Bullmore, 2010). Post mortem studies have provided further evidence of the cytoarchitectural changes that might underlie these alterations in gross anatomy observed in MRI studies. Early studies reported increased neuronal density (Selemon, Rajkowska, & Goldman-Rakic, 1995), decreases in cortical thickness (Selemon et al., 1995) and reduced dendritic spine density on pyramidal neurons in the DLPFC of people with SCZ (Glantz & Lewis, 2000), suggesting reduced excitatory inputs from subcortical structures such as the thalamus. Reelin, a protein involved in migration of cortical neurons during development, was also found to be decreased in SCZ (Impagnatiello et al., 1998).

Changes in inhibitory interneurons are perhaps the most widespread and replicated of post mortem findings (Lewis et al., 2005). Glutamic acid decarboxylase 67 (GAD67), an enzyme involved in synthesis of γ -

amino butyric acid (GABA; the primary inhibitory neurotransmitter in the mature cortex), and GABA membrane transporter 1 (GAT1; a protein responsible for GABA reuptake) are both reduced in the DLPFC of people with SCZ (Akbarian et al., 1995; Hashimoto et al., 2003; Volk, Austin, Pierri, Sampson, & Lewis, 2001; Volk, Austin, Pierri, Sampson, & Lewis, 2000). These changes are prominent on a particular sub-class of inhibitory interneurons expressing the protein parvalbumin (PV), occurring on ~50% of interneurons (Hashimoto et al., 2003). These changes are accompanied by increased expression of postsynaptic GABA_A receptors (one of two GABA receptor sub-types), possibly reflecting a compensatory mechanism (Benes, Vincent, Marie, & Khan, 1996). Interestingly, recent studies have suggested that reduction in markers of PV-containing interneuron function may result from hypofunction of glutamatergic n-methyl-d-aspartate (NMDA) receptors on these interneurons (Bitanirwe, Lim, Kelley, Kaneko, & Woo, 2009; Gonzalez-Burgos & Lewis, 2012). Taken together, these findings suggest synthesis and release of GABA is decreased in the DLPFC of people with SCZ. Although these findings appear strongest in the DLPFC, alterations in inhibitory interneurons have also been reported in numerous other cortical regions such as motor, sensory and limbic regions, suggesting possible global GABA deficits in SCZ (Hashimoto et al., 2008; Thompson, Weickert, Wyatt, & Webster, 2009).

Translating the findings from post mortem studies to living humans has proven challenging due to methodological limitations. *In vivo* attempts to measure cortical GABA levels using magnetic resonance spectroscopy in the DLPFC have produced mixed results (Goto, Yoshimura, Moriya, et al., 2009; Kegeles et al., 2012). This method does not have the resolution to detect subtle changes in GABA synthesis and release from particular interneuron subtypes, however one study has demonstrated a relationship between WM performance and GABA levels in participants with early-stage SCZ (Goto, Yoshimura, Kakeda, et al., 2009). At a functional level, alterations in the PV-inhibitory interneurons predict that cortical inhibition, the suppression of cortical activity by GABA neurotransmission, should be abnormal in people with SCZ. In support, P50 suppression, an electroencephalographic (EEG) measure of sensorimotor gating that is dependent on cortical inhibition (Hershman, Freedman, & Bickford, 1995), is reduced in the auditory cortex of participants with SCZ (Freedman et al., 1996, 2000), although this finding bears little relevance to DLPFC

dysfunction during WM. To fully appreciate the role of cortical inhibition in neural dynamics and coordinated cortical function in regions such as the DLPFC, one must first return to animal studies.

Brain slice (Whittington, Traub, & Jefferys, 1995) and optogenetic studies in animals (Cardin et al., 2009; Sohal, Zhang, Yizhar, & Deisseroth, 2009) have revealed the importance of PV-positive interneurons in generating and maintaining cortical oscillations, particularly in the gamma band (30-80 Hz). Oscillations reflect synchronous firing of neuronal ensembles (Buzsáki & Draguhn, 2004) and high frequency oscillations such as gamma are thought to represent a key mechanism for the encoding and maintenance of information within cortical networks (Lisman & Buzsáki, 2008; Lisman & Idiart, 1995; Singer & Gray, 1995). The fast spiking nature of PV-positive interneurons and the intrinsic properties of GABA_A receptors (fast acting, ligand-gated ion channels) are well suited for entraining networks at a gamma frequency (Buzsáki & Wang, 2012). Results from these animal studies combined with computer modelling have resulted in two models explaining the role of PV-interneurons and postsynaptic GABA_A receptors in generating gamma oscillations (Gonzalez-Burgos & Lewis, 2008). The interneuron network gamma (ING) model suggests that gamma oscillations can be entrained by reciprocal feedback between interneurons, which then act upon pyramidal cells (Whittington, Traub, Kopell, Ermentrout, & Buhl, 2000). The pyramidal interneuron network gamma (PING) model suggests that recurrent feedback between interneurons and pyramidal cells drives phasic activity at gamma frequencies (Whittington et al., 2000). Regardless, in both models successful generation and maintenance of gamma oscillations are dependent on PV-positive interneurons and GABA_A receptors. A second class of GABA receptor, the slower acting, G-protein coupled GABA_B receptor, may also play a role in the modulation of gamma oscillations (Kohl & Paulsen, 2010). GABA_B receptors are located both post-synaptically on pyramidal neurons and pre-synaptically on inhibitory interneurons (Chalifoux & Carter, 2011), allowing direct inhibitory control of gamma entrainment. Accordingly, GABA_B agonists reduce gamma oscillations in rat hippocampal slice experiments (Brown, Davies, & Randall, 2007). Taken together, cortical inhibitory function is essential for the generation and control of gamma oscillations, which may

represent a mechanism in which information can be maintained for short periods within the cortex during WM.

Based on the above evidence, dysfunctional cortical inhibition in the DLPFC of SCZ could manifest in abnormal cortical oscillations, particularly in gamma band frequencies. In humans, fluctuations in cortical electrical currents resulting from oscillatory activity are either measured through the scalp using EEG, or by measuring the magnetic fields generated by these currents using magnetoencephalography (MEG; Buzsáki, Anastassiou, & Koch, 2012). Using these methods, increases in gamma oscillations with increased WM load have been demonstrated in healthy individuals (Howard, 2003; Tallon-Baudry, Bertrand, Peronnet, & Pernier, 1998). Interestingly, recent concurrent EEG and fMRI data has demonstrated a positive correlation between gamma oscillations and hemodynamic activity during WM, suggesting the two techniques may reflect at least partially overlapping mechanisms (Michels et al., 2010). In participants with SCZ, abnormalities in gamma oscillatory activity during various cognitive and sensory tasks have been observed across several stages of the illness, including early and late stages (Sun et al., 2011; Uhlhaas & Singer, 2010). Both increases (Barr et al., 2010; Basar-Eroglu et al., 2007) and decreases (Cho, Konecky, & Carter, 2006; Haenschel et al., 2009; Minzenberg et al., 2010) in gamma band activity have been reported in the DLPFC during WM in SCZ, which may reflect a similar inverted U relationship of gamma and WM load as observed in fMRI studies. In support of a role of abnormal cortical inhibition in this process, SCZ participants treated with a selective GABA_A-agonist showed improved WM performance and increased gamma band activation (Lewis et al., 2008). However, a subsequent randomised control trial using the same drug failed to find any overall benefit for cognitive impairment (Buchanan et al., 2011).

To summarise, convergent findings from various neuroimaging modalities support impaired activation of the DLPFC during WM in SCZ. Anatomical studies have demonstrated deficits in PV-positive inhibitory interneurons in the DLPFC and other cortical regions of SCZ. Cortical inhibition resulting from these

interneurons is critical for generation and maintenance of gamma oscillations, which is a candidate mechanism for WM storage. Accordingly, DLPFC gamma activity is impaired during WM in participants with SCZ. Taken together, this evidence has led to the hypothesis that WM deficits in SCZ result from dysfunctional cortical inhibition in the DLPFC, which in turn leads to abnormal generation and control of gamma oscillations and results in an impaired ability of DLPFC-parietal networks to maintain information over brief periods (Gonzalez-Burgos & Lewis, 2008). Although appealing in their argument, the above studies do not address two fundamental questions critical to this hypothesis. First, it is unclear whether activation of the DLPFC is the limiting factor in WM impairment. As the DLPFC plays a top-down role in cognitive control, activation of this region is dependent on adequate sensory input (Tsujimoto & Sawaguchi, 2004). Binding of sensory information also involves gamma activity and sensory integration deficits are widespread across all sensory modalities in SCZ (Spencer et al., 2003, 2004; Spencer, Niznikiewicz, Shenton, & McCarley, 2008). It is possible that abnormal DLPFC activation during WM may be secondary, or even a compensatory response, to insufficient sensory information and encoding deficits and may not directly reflect impaired DLPFC function (Dias, Butler, Hoptman, & Javitt, 2011). Second, *in vivo* evidence for cortical inhibitory deficits in SCZ are either indirect (i.e. gamma oscillations) or not specific to DLPFC (i.e. P50 suppression). Therefore, it remains unclear if cortical inhibition is actually deficient in the DLPFC of people with SCZ (Kegeles et al., 2012). To address these issues, a method is required that 1) activates the DLPFC in a task-independent manner therefore bypassing sensory systems and 2) provides a direct measure of cortical inhibitory function in the DLPFC.

Transcranial magnetic stimulation

One method suited to addressing these issues is transcranial magnetic stimulation (TMS). TMS non-invasively depolarises cortical neurons in conscious humans using the principle of electromagnetic induction (Barker, Jalilou, & Freeston, 1985). In this method, a large, but brief (~50-100 μ s) electrical current is passed through plastic-shielded copper coils in either a circular or figure-of-eight arrangement. When held over the head, the electric current creates a time-varying magnetic field that passes through the

scalp and generates an inverse electrical field in conductive tissue such as cortical grey matter. At sufficient intensities, this induced electric field alters the membrane potential of neurons, resulting in depolarisation and neuronal firing (Hallett, 2007; Rothwell, Thompson, Day, Boyd, & Marsden, 1991; Rothwell, 1997). A single TMS pulse results in a cascade of excitatory and inhibitory neurotransmission, which alters membrane potentials in cortical networks for several 100 ms beyond stimulation (Kujirai et al., 1993; Paulus et al., 2008; Valls-Solé, Pascual-Leone, Wassermann, & Hallett, 1992). This method has been used to investigate cortical function across several fields, including cognitive neuroscience (Pascual-Leone, Walsh, & Rothwell, 2000), visual physiology (Merabet, Theoret, & Pascual-Leone, 2003) and motor physiology (Reis et al., 2008). The motor cortex is particularly suited to TMS research as transynaptic activation of corticospinal output neurons following TMS results in measurable electromyographic (EMG) responses in peripheral muscle (motor evoked potentials; MEPs) controlled by the stimulated region (Amassian, Cracco, & Maccabee, 1989; Amassian, Eberle, Maccabee, & Cracco, 1992). MEP amplitude is considered a basic index of excitability within the corticospinal system and can be used to infer cortical function. By exploiting differing properties of cortical interneurons and pyramidal cells (i.e. differences in threshold), various single and paired-pulse TMS paradigms have been designed to assess specific excitatory and inhibitory networks within the motor cortex, including measures of GABA_A-mediated (Kujirai et al., 1993; Ziemann, Lönnecker, Steinhoff, & Paulus, 1996) and GABA_B-mediated (Fuhr, Agostino, & Hallett, 1991; McDonnell, Orekhov, & Ziemann, 2006; Valls-Solé et al., 1992; Werhahn, Kunesch, Noachtar, Benecke, & Classen, 1999) cortical inhibition and glutamatergic excitation (Kujirai et al., 1993; Ziemann, Tergau, Wischer, Hildebrandt, & Paulus, 1998; Ziemann, Tergau, Wassermann, et al., 1998). Using this approach, direct evidence for cortical inhibitory deficits in SCZ has been obtained from the motor cortex, supporting the evidence from anatomical studies (Daskalakis et al., 2002; Fitzgerald, Brown, Daskalakis, DeCastella, & Kulkarni, 2002; Fitzgerald et al., 2003; Fitzgerald, Brown, Daskalakis, & Kulkarni, 2002). A detailed discussion on the use of TMS to investigate motor physiology in SCZ can be found in Chapter 2. Although inhibitory deficits in the motor cortex are an excellent proof of principle for wider deficits of inhibitory function in SCZ, a method for measuring neurophysiological mechanisms in non-motor regions is required in order to study these cortical properties in the DLPFC.

Combined transcranial magnetic stimulation and electroencephalography to study prefrontal cortex networks

The ability to directly measure TMS-evoked cortical activity is required to successfully allow the use of TMS to study cortical inhibition outside of the motor cortex. To achieve this goal, TMS has recently been combined with other neuroimaging modalities such as EEG (Ilmoniemi et al., 1997). This approach conveys several advantages compared with TMS-EMG. Firstly, EEG allows assessment of TMS-evoked activity from theoretically any cortical surface near the scalp (Ilmoniemi et al., 1997; Massimini et al., 2005), hence providing access to the DLPFC (Kähkönen, Komssi, Wilenius, & Ilmoniemi, 2005; Kähkönen, Wilenius, Nikulin, Ollikainen, & Ilmoniemi, 2003). Secondly, cortical excitability can be assessed using TMS without the potential confounds of the spinal cord and motor neurons associated with TMS-EMG (Komssi et al., 2002; Komssi, Kähkönen, & Ilmoniemi, 2004). Finally, TMS-EEG provides insight in to numerous aspects of TMS-evoked cortical function beyond corticospinal output. For instance, EEG provides data both on the stimulated region and on the activity of other regions causally connected to the stimulated region (Cona, Zavaglia, Massimini, Rosanova, & Ursino, 2011; Massimini et al., 2005; Voineskos et al., 2010), therefore providing a measure of effective or directional connectivity within the brain. In addition, a single TMS pulse evokes a brief period of coordinated network activity measured as cortical oscillations from the stimulated brain region (Brignani, Manganotti, Rossini, & Miniussi, 2008; Fuggetta, Fiaschi, & Manganotti, 2005; Paus, Sipila, & Strafella, 2001; Van Der Werf & Paus, 2006). The properties (i.e. resonant frequency) of these oscillations differ between brain regions, suggesting TMS-evoked oscillations reflect intrinsic properties of local cortical networks (Rosanova et al., 2009). Finally, studies from the motor cortex suggest different properties of TMS-evoked potentials across time, such as peak amplitude and slope, may provide information on the dominant mechanism of that period, such as TMS-evoked glutamatergic excitation or GABAergic inhibition (Bonato, Miniussi, & Rossini, 2006; Komssi et al., 2004; Nikulin, Kicic, Kahkonen, & Ilmoniemi, 2003). A detailed discussion on the current state of knowledge of using TMS-EEG to assess cortical network properties can be found in Chapter 3.

Considering these points, TMS-EEG is an excellent candidate method to study DLPFC activation in a task-independent manner, allowing controlled stimulation of the cortex between individuals without requiring sensory input. Furthermore, the properties of the TMS-evoked cortical response may allow a direct measure of inhibitory neurotransmission from the motor cortex, although the translation of these findings to regions such as the DLPFC requires confirmation and further exploration.

Despite the clear advantages conferred by TMS-EEG, the technique has been plagued by technical challenges (Ilmoniemi & Kicić, 2010). The large magnetic field generated by TMS saturates necessarily sensitive EEG amplifiers, preventing recording of signal for several hundreds of milliseconds (Cracco, Amassian, Maccabee, & Cracco, 1989; Izumi et al., 1997). To circumvent these issues, several hardware solutions have been developed such as sample-and-hold circuits which pin the amplifier and prevent saturation (Ilmoniemi et al., 1997; Virtanen, Ruohonen, Näätänen, & Ilmoniemi, 1999) and amplifiers with large recording ranges that capture the TMS-artifact with minimal saturation (Veniero, Bortoletto, & Miniussi, 2009). However, the artifact profile resulting from these systems can differ substantially. This point is particularly relevant following the realisation that certain existing, non-specialised EEG amplifiers are also capable of recording TMS-evoked activity, such as DC-coupled amplifiers (Daskalakis, Farzan, Barr, Maller, et al., 2008; Fitzgerald et al., 2008). Given that many laboratories already own EEG amplifiers, and the purchase of specialised TMS-EEG systems is often prohibitive due to cost, the use of non-specialised EEG systems in TMS-EEG research is steadily increasing (Fitzgerald, 2010; Levitt-Binnun et al., 2010). Despite this increase, few studies have systematically described the artifact profiles resulting from the use of TMS with these systems, limiting the confidence in the resulting data (Veniero et al., 2009; Virtanen et al., 1999). Furthermore, additional sources of artifact such as charges stored at the skin/electrode interface or in the electrode recording circuit (Julkunen et al., 2008), electromotive forces (Sekiguchi, Takeuchi, Kadota, Kohno, & Nakajima, 2011), vibration of the TMS coil and capacitor recharge artifacts from the TMS machine (Veniero et al., 2009) can also obscure recording of neural activity. Even small changes in experimental

arrangement have the potential to introduce or exacerbate any number of these artifacts, meaning artifacts that are not present in one experiment may appear in another. Finally, TMS can result in unwanted physiological artifacts, the presence of which changes between different cortical regions. For instance, the loud click of the TMS coil results in auditory-evoked potentials unrelated to TMS-evoked cortical activity (Nikouline, Ruohonen, & Ilmoniemi, 1999; Tiitinen et al., 1999), TMS over lateral scalp positions such as the DLPFC can result in inadvertent stimulation of scalp muscles (Korhonen et al., 2011; Mäki & Ilmoniemi, 2011; Mutanen, Mäki, & Ilmoniemi, 2012) and TMS over frontal regions can evoke a blink response (Bruckmann et al., 2012), all of which obscure neural EEG activity. Although some online and offline methods exist for preventing and removing some of these artifacts (Hernandez-Pavon et al., 2012; Korhonen et al., 2011; Litvak et al., 2007; Massimini et al., 2005; Morbidi et al., 2007; Tiitinen et al., 1999), a detailed understanding of the effectiveness of many of these methods is lacking. Therefore, the presence of these artifacts severely limits the use and confidence of EEG in recording TMS-evoked neural activity.

To summarise, combined TMS-EEG is an excellent candidate technique to study DLPFC function in people with SCZ. However, the presence of artifacts in TMS-EEG recordings have the potential to severely limit its usefulness. In particular, the current knowledge regarding recording artifacts in non-specialised EEG amplifiers and physiological artifacts following TMS of non-motor regions does not allow for confident measures of TMS-evoked cortical activity from the DLPFC. In addition, although evidence exists supporting the use of TMS-EEG to assess excitatory and inhibitory mechanisms in the motor cortex, little is known about how these findings translate in to non-motor regions such as the DLPFC.

Aims

The broad aim of this thesis was to develop and validate TMS-EEG methods to study DLPFC neurophysiology in people with and without schizophrenia. To achieve this goal, three specific aims were developed:

Aim 1: The first aim of this thesis was to identify recording and physiological artifacts in non-specialised TMS-EEG arrangements and develop validated methods to either prevent or remove these artifacts over non-motor regions, therefore improving confidence in measuring TMS-evoked neural activity from the DLPFC.

Aim 2: The second aim of this thesis was to further validate the use of TMS-EEG to study cortical excitation and inhibition in the motor cortex and to assess whether these findings translate to other cortical regions, such as the DLPFC.

Aim 3: Having established and validated methods, the final aim of this thesis was to compare DLPFC network properties between people with and without schizophrenia using TMS-EEG and to relate TMS-evoked DLPFC function to WM performance.

To achieve these aims, four experimental studies have been completed:

1. A detailed description of artifacts resulting from different TMS-EEG arrangements such as different stimulator combinations, different scalp positions (motor, DLPFC) and different TMS paradigms (i.e. single vs. paired). Recordings were made using a non-specialised EEG amplifier.
2. A comparison between TMS-evoked potentials (EEG) and motor-evoked potentials (EMG) to measure cortical inhibition using a well validated paired-pulse TMS paradigm over motor cortex (long-interval cortical inhibition) in healthy participants.

3. A study assessing whether TMS-EEG findings from the motor cortex translate in to the DLPFC using paired pulse TMS. Data from this study was also used to assess independent component analysis as a method to identify and remove artifacts following DLPFC stimulation.
4. A comparison of DLPFC network properties between people with and without schizophrenia using TMS-EEG. Participants also completed a WM task and people with participants with SCZ completed an evaluation of symptom severity.

Overview

This thesis consists of nine chapters including seven manuscripts (four published/in press, three in submission). In Chapter 1, we have presented an overview of the background and aims of the thesis.

Chapter 2 presents a published review on the use of TMS to study cortical function in schizophrenia. In this review we focus on the insights TMS has provided into the fidelity of inhibitory and excitatory neuronal populations in the motor cortex of people with schizophrenia. We also discuss the use of TMS to study the connectivity between remote brain regions and specific neuronal populations in the motor cortex and how these connections are effected in schizophrenia. Finally, we review the existing studies that have used TMS-EEG to study non-motor cortical function in SCZ.

In Chapter 3, we present a second published review on the use of TMS-EEG to study cortical network properties. This review covers four main topics. First, we describe the known artifacts that are associated with TMS-EEG. Second, we discuss the physiological information contained within TMS-evoked potentials. Third, we review the evidence for using TMS-EEG to study cortical inhibition and neural plasticity. Finally, we review the use of TMS-EEG in assessing both resting and active cortical networks.

Chapter 4 contains the first published empirical paper on short-latency artifacts associated with TMS-EEG. In this paper we use a phantom model (a melon) to describe recording artifacts resulting from different TMS stimulators and a non-specialised EEG amplifier and provide suggestions on how to control for these artifacts. Next, we describe an early physiological artifact in humans and how this artifact is affected by different parameters such as stimulation site, stimulation intensity and paired-pulse paradigms. We conclude that this artifact results from stimulation of scalp muscles and can mask neural activity following stimulation over both motor and prefrontal cortices if not adequately controlled for or removed.

Chapter 5 contains the third empirical paper, currently in submission, which describes the use of independent component analysis (ICA; a statistical method of blind source separation) in identifying and removing different types of artifacts following prefrontal cortex TMS-EEG. This chapter also provides a detailed description on the effect each artifact type has on TMS-evoked neural activity.

In Chapter 6 we present a fourth published empirical paper describing the mechanisms of long-interval cortical inhibition (a paired-pulse TMS paradigm) assessed using both TMS-evoked potentials (EEG) and MEPs measured from small hand muscles (EMG). By comparing methods, we found that early components of the TMS-evoked potential (i.e. P30) were modulated in a fashion consistent with excitatory neurotransmission, whereas later components (i.e. N100) were consistent with inhibitory neurotransmission. These findings suggest that specific physiological mechanisms can be measured from TMS-evoked potentials in the motor cortex.

In Chapter 7 we present an empirical paper, currently in submission, which assesses whether the paired-pulse findings from the motor cortex translate in to the DLPFC. We found that a similar relationship

between early (N40) and late (N100) components following paired pulse TMS in the DLPFC, suggesting that excitatory and inhibitory neurotransmission can also be assessed from this region using TMS-EEG.

Chapter 8 contains the final empirical paper, currently in submission, which compares the DLPFC network properties between people with and without schizophrenia. We found reduced N100 slope and amplitude (marker of inhibitory neurotransmission) and increased P180 (potential marker of excitatory neurotransmission) in people with SCZ. In addition, we found that SCZ participants with low WM capacity also showed reduced TMS-evoked gamma activity over the DLPFC compared with other SCZ participants and controls, supporting a link between reduced DLPFC activation and WM impairments.

The implications of the results from the experimental chapters are integrated in a general discussion in Chapter 9. In addition, methodological limitations and directions for future research are also discussed. The thesis closes with a brief summary of the main findings and final conclusions.

CHAPTER TWO

TMS and schizophrenia

Rogasch NC, Daskalakis ZJ, Fitzgerald PB. (In press). Cortical Inhibition, Excitation, and Connectivity in Schizophrenia: A Review of Insights from Transcranial Magnetic Stimulation. *Schizophrenia Bulletin*.

Preamble to review paper

The following published paper provides a review of using transcranial magnetic stimulation to assess cortical neurophysiology in people with SCZ. This review provides a consensus on the fidelity of mechanisms such as cortical inhibition, excitability and connectivity within the motor cortex of people with SCZ and how disruption of these mechanisms could infer wider cortical dysfunction. In addition, we also review the use of combined TMS-EEG to study motor and non-motor regions in SCZ.

Due to copyright, readers are directed to the following reference:

Rogasch NC, Daskalakis ZJ, Fitzgerald PB. (In press). Cortical Inhibition, Excitation, and Connectivity in Schizophrenia: A Review of Insights from Transcranial Magnetic Stimulation. *Schizophrenia Bulletin*. doi:10.1093/schbul/sbt078

CHAPTER THREE

Concurrent TMS and EEG

Rogasch NC, Fitzgerald PB. (2013). Assessing cortical network properties using TMS-EEG. *Human Brain Mapping*. 109(1):1652-69.

Preamble to review paper

In the previous chapter (Chapter 2) we introduced the use of TMS-EEG to study non-motor cortical function in people with SCZ. The combination of TMS-EEG is relatively new to neuroscience and has only gained wide spread use in the past several years. As a result, the methodological constraints and the nature of information provided by this technique are still in early stages. In the following published review paper, we provide an overview of the current state of knowledge regarding the use of TMS to study cortical network properties. The first section focuses on artifacts associated with TMS-EEG. The next three sections discuss the evidence for using TMS-EEG to assess cortical mechanisms such as excitability, inhibition, connectivity and oscillations, and examples of how TMS-EEG has furthered knowledge on cortical function.

Due to copyright, readers are directed to the following reference:

Rogasch NC, Fitzgerald PB. (2013). Assessing cortical network properties using TMS-EEG. *Human Brain Mapping*. 109(1):1652-69. DOI: 10.1002/hbm.22016

CHAPTER FOUR

Artifacts in TMS-EEG recordings

Rogasch NC, Thomson RH, Daskalakis ZJ, Fitzgerald PB. (In press). Short-Latency Artifacts Associated with Concurrent TMS-EEG. *Brain Stimulation*.

Preamble to empirical paper

As discussed in Chapter 3, artifacts resulting from the interaction between TMS and EEG recording equipment, or unwanted stimulation of non-neural elements such as muscles, are the main limiting factor for TMS-EEG research. Separating TMS-evoked cortical activity from artifactual activity is therefore paramount for the success of this technique. Furthermore, determining the earliest possible time that neural activity can be confidently recorded is of particular importance (Veniero et al., 2009). Studying the combination of non-specialised TMS and EEG equipment is becoming increasingly relevant, as many laboratories are combining existing equipment to perform TMS-EEG research (Daskalakis, Farzan, Barr, Maller, et al., 2008; Fitzgerald et al., 2008; Levitt-Binnun et al., 2010). However, few of these arrangements have been formally tested to identify potential artifacts. The following chapter presents the first detailed description of recording artifacts in a non-specialised, DC-coupled EEG amplifier following stimulation with two popular brands of TMS stimulator (magstim and magventure). In this published paper, TMS-evoked EEG artifacts were recorded from both phantom (melon) and human participants to separate recording and physiological artifacts. In addition, the effect of different conditions (stimulation site, intensity, paired-pulse paradigms) on artifact properties were tested in human participants. Using this data, we also provide insight in to the origin of a large, early, bipolar TMS-evoked potential observed in human experiments, the origin of which is a point of controversy within the field.

Due to copyright, readers are directed to the following reference:

Rogasch NC, Thomson RH, Daskalakis ZJ, Fitzgerald PB. (2013). Short-Latency Artifacts Associated with Concurrent TMS-EEG. *Brain Stimulation*. Nov; 6(6):868-76. DOI: 10.1016/j.brs.2013.04.004.

CHAPTER FIVE

Removing TMS-EEG artifacts using ICA

Rogasch NC, Thomson RH, Farzan F, Fitzgibbon BM, Bailey NW, Hernandez-Pavon JC, Daskalakis ZJ, Fitzgerald PB. Removing artifacts from TMS-EEG recordings using independent component analysis: importance for assessing prefrontal cortex network properties. (Submitted).

Preamble to empirical paper

In Chapter 4, we established that recording artifacts had largely recovered within 10 ms following TMS using our experimental arrangement. However physiological artifacts such as TMS-evoked scalp muscle activity and blinks contaminated EEG signal up to 100 ms, particularly over the DLPFC. Therefore, a method was required to separate TMS-evoked neural activity from artifact activity in order for TMS-EEG over the DLPFC to be useful. Independent component analysis (ICA) is a validated method of blind source separation suited for this application (Onton, Westerfield, Townsend, & Makeig, 2006) which has been implemented in several TMS-EEG studies (Hamidi, Slagter, Tononi, & Postle, 2010; Hernandez-Pavon et al., 2012; Korhonen et al., 2011). However, certain properties of TMS-evoked artifacts such as the size of muscle artifacts (Hernandez-Pavon et al., 2012) and the time-locked nature of blink artifacts (Li & Principe, 2006) weakens several assumptions of ICA, potentially invalidating recovered data. The following chapter provides a detailed account of identifying and removing artifacts from TMS-EEG recordings over the DLPFC. Importantly, evidence is provided on the effect of removing TMS-evoked artifacts using ICA on underlying neural activity. Finally, this study describes how each artifact type distorts measures of TMS-evoked cortical activity, further demonstrating the importance of controlling for artifacts.

Removing artifacts from TMS-EEG recordings using independent component analysis: importance for assessing prefrontal cortex network properties.

Nigel C. Rogasch¹, Richard H. Thomson¹, Faranak Farzan², Bernadette M. Fitzgibbon¹, Neil W. Bailey¹, Julio C. Hernandez-Pavon³, Zafiris J. Daskalakis² and Paul B. Fitzgerald¹

1. Monash Alfred Psychiatry Research Centre, Central Clinical School, The Alfred and Monash University, Melbourne, Australia
2. Temerty Centre for Therapeutic Brain Intervention, Centre for Addiction and Mental Health, University of Toronto, Toronto, Ontario, Canada
3. Department of Biomedical Engineering and Computational Science, Aalto University, Aalto, Finland

Running head: Prefrontal cortex TMS-EEG and ICA

Key words: Transcranial magnetic stimulation, electroencephalography, independent component analysis, physiological artifacts, dorsolateral prefrontal cortex.

Word count (abstract): 364

Word count (main text): 6,512

Figures: 8

Correspondence: Nigel C. Rogasch
Monash Alfred Psychiatry Research Centre
Level 4, 607 St. Kilda rd.
Melbourne,
Victoria, Australia, 3004

ABSTRACT

Introduction: The combination of transcranial magnetic stimulation and electroencephalography (TMS-EEG) is emerging as a powerful tool for causally investigating cortical mechanisms and networks. However, various artifacts contaminate TMS-EEG recordings, particularly over regions such as the dorsolateral prefrontal cortex (DLPFC). The aim of this study was to substantiate removal of artifacts from TMS-EEG recordings using independent component analysis (ICA) following stimulation of the DLPFC.

Methods: 30 healthy volunteers (32.2 ± 11 years, 8 female) received 75 single TMS pulses to the left DLPFC while EEG was recorded from 57 electrodes. A subset of 9 volunteers also received 50 sham pulses. The large TMS artifact and early muscle activity (-2 to ~20 ms) were removed using interpolation and the remaining EEG signal was processed in two separate ICA runs using the fastICA algorithm. Five sub-types of TMS-related artifacts were manually identified: fast decay artifacts, slow decay artifacts, blink artifacts, auditory artifacts and bad channels. The source of proposed blink and auditory artifacts were confirmed by concatenating known artifacts (i.e. voluntary blinks or auditory evoked potentials resulting from sham TMS) to the TMS trials before ICA and assessing grouping of resultant independent components (ICs). Finally, we assessed the effect of removing specific artifact types on TMS-evoked potentials (TEPs) and TMS-evoked oscillations following DLPFC stimulation.

Results: ICs from both fast and slow recovering artifacts correlated with TMS-evoked muscle activity size, whereas blinks and auditory ICs combined with known concatenated artifacts following ICA, confirming their source. Individual artifact sub-types characteristically distorted each measure of DLPFC function at a group level with the exception of bad channels. When free of artifact, TEPs from DLPFC spread from the site of stimulation to remote brain regions in the contralateral prefrontal cortex, ipsilateral parietal cortex and bilateral occipital cortex within the first 120 ms of the pulse. TMS-evoked oscillations in the upper beta/gamma bands were strongest at the site of stimulation and alpha/lower beta oscillations were evoked in contralateral frontal, temporal and motor cortex as well as central parieto/occipital cortex.

Conclusions: Various different artifacts contaminate TMS-EEG recordings over the DLPFC. However these can be reliably removed using ICA. When artifacts were successfully removed, TMS could be used to probe the intrinsic properties of DLPFC and wider connected networks.

HIGHLIGHTS

- The origin of different electroencephalographic artifacts following transcranial magnetic stimulation (TMS) over dorsolateral prefrontal cortex identified using independent component analysis (ICA) were confirmed and included decay artifacts, blinks and an auditory evoked response.
- Decay artifacts, blink artifacts and auditory artifacts can be removed using (ICA) with minimal impact on TMS-evoked neural activity.
- Failure to remove these artifacts severely distorts prefrontal network properties such as TMS-evoked potentials and TMS-evoked oscillations both at the site of stimulation and across the scalp.

ABBREVIATIONS

TMS, transcranial magnetic stimulation

EEG, electroencephalography

TEP, TMS-evoked potential

DLPFC, dorsolateral prefrontal cortex

PCA, principle component analysis

ICA, independent component analysis

IC, independent component

MEP, motor evoked potential

Ag/AgCl, silver-silver chloride

APB, abductor pollicis brevis

RMT, resting motor threshold

GMFA, global mean field amplitude

ROI, region of interest

1. INTRODUCTION

Transcranial magnetic stimulation (TMS) is a non-invasive form of brain stimulation used to assess and modulate cortical function in humans. TMS utilises a fast, time-varying magnetic field to induce an electrical field in the cortical tissue, resulting in non-invasive depolarisation of cortical neurons (Hallett, 2007). Increasingly, electroencephalography (EEG) has been used to directly record the cortical potentials evoked by TMS (TMS-evoked potentials; TEPs; Ilmoniemi et al., 1997). TEPs reveal various aspects of functional network properties such as reactivity, effective connectivity and resonant oscillatory tuning (Daskalakis et al., 2012; Rogasch and Fitzgerald, 2013; Siebner et al., 2009). By applying an external input to the cortex, TMS-EEG allows a direct functional assessment of specific cortical regions in a controlled manner without the need to engage the participants in a task (Massimini et al., 2005; Rosanova et al., 2012). This approach has proven useful for studying cortical function in both healthy (Komssi and Kähkönen, 2006) and clinical populations (Farzan et al., 2010; Rogasch et al., 2013a).

Despite the value gained by combining TMS with EEG, the technique is plagued by methodological issues (Ilmoniemi and Kicić, 2010). The magnetic pulse generated by TMS results in saturation of traditional EEG amplifiers which can take hundreds of milliseconds to recover, precluding the recording of neural signal. Several hardware solutions have been developed to circumvent this problem, such as sample-and-hold circuits (Ilmoniemi et al., 1997; Virtanen et al., 1999) and DC-coupled amplifiers with a large operating range, which prevent or minimize amplifier saturation and allow recording of TEPs within 5-10 ms following TMS (Bonato et al., 2006; Daskalakis et al., 2008; Rogasch et al., 2013c; Veniero et al., 2009). However, TMS also results in a number of physiological EEG artifacts which can mask TMS-evoked neural activity. For instance, TMS over lateral brain areas such as the dorsolateral prefrontal cortex (DLPFC) or temporal cortex can stimulate scalp muscles, resulting in large electromyographic artifacts (Korhonen et al., 2011; Mutanen et al., 2012; Rogasch et al., 2013c). TMS over frontal regions can also result in a blink startle response which significantly affects signal over anterior electrodes (Bruckmann et al., 2012; Rogasch et al., 2013c). Finally, discharge of the TMS coil is accompanied by a loud click which results in confounding auditory-evoked potentials (Nikouline et al., 1999; Tiitinen et al., 1999). Some of these artifacts can be avoided. For instance,

auditory artifacts can be minimized by masking the click (Massimini et al., 2005; Ter Braack et al., 2013) and muscle activation can be avoided by stimulating away from scalp muscles (Mutanen et al., 2012; Rogasch et al., 2013c) or manipulating coil angles (Mutanen et al., 2012). However, this is not always possible, especially if the region of interest is lateral or if the specific experimental design does not allow for auditory masking.

Various methods have been proposed to remove artifacts from TMS-EEG recordings offline, including template subtraction (Bender et al., 2005; Thut et al., 2005), principle component analysis (PCA; Litvak et al., 2011; Mäki and Ilmoniemi, 2011; ter Braack et al., 2013) and independent component analysis (ICA; Hamidi et al., 2010; Hernandez-Pavon et al., 2012; Iwahashi et al., 2008; Korhonen et al., 2011). ICA is a method of blind source separation that separates the EEG signal into temporally independent components (ICs; Makeig et al., 1997). This method follows three basic assumptions; 1) the EEG signal is a linear combination of activity from multiple cortical and non-cortical sources, 2) these sources are stationary in space and 3) the time course of activity from these sources is independent (Onton et al., 2006). ICA has been validated for separating cortical and non-cortical sources such as eye blinks (Plöchl et al., 2012) and muscle activity (McMenamin et al., 2010) as well as separating independent cortical sources from EEG recordings (Jung et al., 2001; Makeig et al., 1997; Onton et al., 2006). Accordingly, an increasing number of TMS-EEG studies have used ICA to correct muscle and blink artifacts (Hamidi et al., 2010; Hernandez-Pavon et al., 2012; Iwahashi et al., 2008; Korhonen et al., 2011; Rajji et al., 2013; Verhagen et al., 2013; Vernet et al., 2013). However, several properties specific to TMS-EEG artifacts pose considerable problems for ICA algorithms. First, TMS-evoked muscle activity from areas such as DLPFC is several orders of magnitude larger than neural activity and is therefore difficult to accurately remove. Although ICA can successfully recover the time course of neural sources under these circumstances, the topographies of these components are severely distorted, invalidating the data (Hernandez-Pavon et al., 2012). Second, artifacts such as TMS-evoked blinks can be time-locked to TEPs such as the N100. This time-locking weakens the assumption of temporal independence and can result in mixing of independent sources into a single common IC, overcorrecting the data if removed (Li and Principe, 2006).

Without addressing these issues and justifying artifact selection, confidence in ICA-corrected TMS-EEG data is considerably diminished. Therefore, the principal aim of the current study was to justify and validate the use of ICA for removing artifacts from TMS-EEG recordings following DLPFC stimulation. In this study, we use ICA to identify potential artifacts in EEG recordings caused by TMS over DLPFC using ICA. Second, we provide evidence that characterize the origin of each artifact component. Third, we attempt to evaluate whether removing different artifacts inadvertently alters TMS-evoked neural activity. Fourth, we describe the TMS-evoked properties of the DLPFC assessed from the artifact corrected TMS-EEG data (TEPs and TMS-evoked oscillations). Finally, we demonstrate the impact of each different artifact type on TMS-evoked neural activity, demonstrating their need for removal.

2. MATERIALS AND METHODS

30 healthy volunteers (32.2 ± 11 years, 8 female) received single pulse TMS to the left DLPFC while EEG was recorded. A subset of 9 participants also received sham TMS to the left DLPFC. All participants provided informed consent prior to participation. Experimental procedures were approved by the Alfred Hospital, Monash University and the Centre for Addiction and Mental Health Human Research Ethics Committees.

2.2 Transcranial magnetic stimulation

Monophasic TMS pulses were delivered using a figure of eight coil (wing diameter = 7 cm) connected to two magstim 200 units via a bistim module (Magstim Ltd., UK). The TMS coil was held tangentially over the scalp with the handle at a 45° angle to the midline resulting in a posterior-anterior current flow in the underlying cortex. Stimulation intensity was determined over left motor cortex and motor evoked potentials (MEPs) were recorded using Ag/AgCl electrodes positioned in a tendon-belly montage over the right abductor pollicis brevis (APB) muscle. EMG signal was amplified (1000x) band-pass filtered (10-1000 Hz; PowerLab, ADInstruments, New Zealand) digitised (2000 Hz; Micro1401, Cambridge Electronic Design Ltd., UK), epoched around the stimulus (-200 to 500 ms) and displayed on a computer screen online. The coil was moved until the position resulting in maximal MEPs was determined. Resting motor threshold (RMT) was then determined as the minimum intensity required to evoke at least 3 of 6 MEPs $> 50\mu\text{V}$ in amplitude (Conforto et al., 2004). TMS intensity was then modified until a stable MEP of ~ 1 mV in peak-to-peak amplitude was achieved and this intensity was used throughout the experiment (maximum stimulator output = 68.2 ± 11 %; percentage of RMT = 120.3 ± 6 %).

For DLPFC stimulation, the coil was positioned so the centre rested between the F3 and F5 electrodes. This positioning method provides the closest estimate to DLPFC position (border of BA9 and BA46) without using neuronavigational techniques (Fitzgerald et al., 2009; Rusjan et al., 2010). The edge of the coil was marked on the cap using a felt-tipped pen, a method which enables reliable re-positioning of the coil within 1 mm (Rogasch et al., 2013c). The coil was held in place by an experimenter throughout the session. Participants received 75 single pulses while sitting quietly with eyes open and looking directly ahead. For sham

stimulation, the coil was held with the front of the coil perpendicular to the scalp and the wing resting over the same prefrontal position of the head. 50 sham pulses were delivered. TMS frequency was 0.2 Hz (10% jitter) throughout the experiment.

2.3 Electroencephalography

EEG was recorded using a cap with 57 electrodes (sintered Ag/AgCl) in standard 10-20 positions (Quickcap, Compumedics Ltd., Australia). EEG signal was amplified (1000x), filtered (DC-3500 Hz) and digitised (20 kHz; Synamps2, Compumedics Ltd.), and recorded on a computer for offline analysis. This arrangement along with the DC-coupling and large recording range of the amplifier captures the TMS artifact with minimal amplifier saturation and allows recording of neural signal within ~5-10 ms following a pulse (Rogasch et al., 2013c; Veniero et al., 2009). Electrode impedances were regularly checked and kept as low as possible throughout the experiment (<5 k Ω).

2.4 Analysis

Analysis of EEG data was performed using EEGLAB (Delorme and Makeig, 2004), field trip (Oostenveld et al., 2011) and custom scripts all on the MATLAB platform (R2013a, The Mathworks, USA). EEG data were epoched around the TMS pulse (-1000 to 1000 ms), baseline corrected (-500 to -110 ms) and bad channels (e.g. those that were disconnected or with poor contact) were removed. To prevent large artifacts distorting neural components following ICA (Hernandez-Pavon et al., 2012), data containing the TMS pulse artifact and peaks of large, early bipolar artifact were removed and the remaining data traces were concatenated together. In order to allow consistent decomposition of any remaining decay artifacts by ICA, the window for data removal was adjusted for each participant from -2 ms to the time when signal had returned to ~150 μ V (16.6 ± 6 ms, never later than 25 ms; see fig. 1A). Following removal and concatenation, data were downsampled to 1 kHz and trials containing any large, paroxysmal artifacts were removed. In order to allow further pre-processing such as filtering, the data were submitted to a first run through the fastICA algorithm (Hyvärinen and Oja, 2000) and the component representing the large, fast decay artifact was selected based on amplitude and removed (see fig. 1B). Data from the removed window were then interpolated using a

cubic function and all data were filtered using a butterworth, zero-phase band-pass filter (1-80 Hz). Epochs were then manually inspected and trials containing excessive muscle activity (i.e. from jaw clenching) or other anomalous activity were removed. The data was then submitted to a second round of fastICA. Following ICA, artifact components were manually identified based on four sub-type categories: slow decay artifacts, blink artifacts, auditory artifacts and bad electrode artifacts (see supplementary materials for details). Five separate files were then created; a file with one of the four artifact categories removed and a file with all artifact components removed. Following artifact removal, missing channels were interpolated and data from each electrode were re-referenced to the average of all channels. Finally, butterfly plots were inspected for unusual activity (i.e. a single electrode with much larger signal than all others). If unusual activity was detected, suggesting that an artifact component had been missed, the component identification and processing steps were repeated until this activity was removed.

-----Insert figure 1-----

To investigate the origin of the identified components, components identified as artifacts were compared with introduced artifacts of known origin. As both the fast and slow decay artifacts were hypothesised as related to the large bipolar waveform occurring in the first 6-15 ms, the amount of EEG signal removed by these components was correlated with bipolar waveform size. The size of the bipolar artifact was assessed by calculating the area under the curve of the global mean field amplitude (GMFA; Lehmann and Skrandies, 1980) between 6-15 ms (prior to muscle artifact removal). GMFA identifies the maximum amplitude of the evoked field and is used to index the effect of TMS on global brain activity (Komssi et al., 2004). The amount of EEG signal removed by the fast and slow decay artifacts was calculated as the difference in area under the curve of the GMFA before and after the components were removed (fast = 25-50, slow = 25-100 ms). For the blink artifact, trials containing voluntary blinks recorded prior to the start of the TMS block (40 blinks at approximately once per second) were concatenated to the TMS trials before ICA. Although voluntary blinks are much larger and have a longer duration than spontaneous blinks or blinks evoked by TMS, the activity should combine in to a single IC if the source is the same regardless of size (Plöchl et al., 2012). Following this

logic, sham TMS trials (i.e. auditory-evoked potentials) were concatenated with real TMS trials prior to ICA to confirm the source of the auditory artifact.

To assess whether reducing the early artifact size to $\sim 150 \mu\text{V}$ prior to ICA was sufficient to minimise mixing of neural and artifact signal, this method was compared with a compression method that improves decomposition of neural components in the presence of high amplitude artifacts (Hernandez-Pavon et al., 2012; Korhonen et al., 2011). Singular value decomposition was used to truncate the data to the 30 largest principle components before the second round of ICA (Hernandez-Pavon et al., 2012). Compressing the data helps prevent mixing of neural and high amplitude artifacts, thereby conserving the topography of neural components. To assess whether removing the blink component was also removing time-locked TMS-evoked neural activity, removal of the TMS blink component was compared with removal of the combined voluntary and TMS blink component. This approach has proven useful in separating time-locked auditory and blink event-related potentials which are mixed into a single IC following an auditory startle task (Li and Principe, 2006). Finally, to assess whether removing the auditory component was inadvertently removing TMS-evoked neural activity, removal following TMS alone was compared with removal following combined sham and real TMS.

2.5 Reproducibility

As identification of artifactual ICs was performed manually and is therefore inherently subjective, IC identification was repeated by a second experimenter to confirm reproducibility (first=NCR, second=NWB). The dataset was randomly reduced to 15 participants using the randperm function in MATLAB. Prior to analysis, the second experimenter was shown two examples of artifact component selection. An instruction manual was provided for additional reference (supplementary material).

2.6 Measuring cortical network properties following TMS

To investigate cortical network properties following TMS over DLPFC, TEPs (time domain) and TMS-evoked oscillations (frequency domain) were assessed following removal of all artifacts. Two different analysis

approaches were utilised. To capture the effect of TMS on local networks a region of interest (ROI) analysis was performed on the F3 electrode. To capture connectivity of DLPFC with wider cortical networks, analysis of all electrodes was included. To assess the effect of retaining artifacts on cortical network properties, all but one type of artifact was removed for each artifact and the signal was compared with artifact corrected signal on the these measures.

Time domain analysis: For ROI analysis, three peaks at F3 were examined; N40, P60 and N100. The N40 latency was calculated at the negative peak closest to 40 ms between 25-55 ms and the amplitude was calculated as the average signal between ± 5 ms of the peak latency. The P60 latency was calculated at the positive peak closest to 60 ms between 45-75 ms and the amplitude was calculated as the average signal between ± 5 ms of the peak latency. The N100 latency was calculated at the negative peak closest to 100 ms between 85-145 ms and the amplitude was calculated as the average signal between ± 10 ms of the peak latency. For connectivity analysis, activity across all electrodes between 25-500 ms was assessed.

Frequency domain analysis. TMS-evoked oscillations were obtained using wavelet decomposition (3.5 oscillation cycles, steps of 1 Hz between 8-45 Hz) on averaged trials for each individual electrode. Oscillations were normalised by dividing the relative post TMS power by mean baseline power (-600 to -100) in each frequency bin. For ROI analysis at the F3 electrode, oscillations were averaged across discrete frequency bands (alpha 8-12 Hz, lower beta 13-20 Hz, upper beta 21-30 Hz, gamma 31-45 Hz). Delta (1-4 Hz) and theta (4-8 Hz) band activity were not assessed in the current study due to limitations of the epoch width. As lower and higher frequencies occur across different time periods, alpha and lower beta oscillations were analysed between 25-250 ms and upper beta and gamma between 25-150 ms. For connectivity analysis of TMS-evoked oscillations, time-frequency analysis from all electrodes was assessed between 25-300 ms and across all individual frequencies.

2.7 Statistics

Comparisons of artifact retention on ROI analysis (peak latencies, peak amplitudes, TMS-evoked frequency bands) were made between corrected and uncorrected signal using paired t-tests. Correlations of GMFA area under the curve were performed using Pearson's correlations (with and without outliers removed).

Comparisons of artifact removal on global EEG signal (space and time) and comparisons of artifact retention on connectivity measures of TMS-evoked potentials (space and time) and TMS-evoked oscillations (space, time and frequency) were performed using non-parametric, cluster-based permutation statistics (Maris and Oostenveld, 2007). This approach controls for multiple-comparisons across any combination of space, time and frequency. Clusters were defined as two or more neighbouring electrodes in which the t-statistic at a given time or frequency point exceeded a threshold of $p < 0.05$ (dependent t-test). Electrodes, time points and/or frequency bins with above-threshold values were used for subsequent cluster-based permutation analysis. Monte Carlo p-values were calculated on 2000 random permutations and a value of $p < 0.05$ was used as the cluster-statistic significance threshold for all analyses.

3. RESULTS

3.1 Identifying and removing artifact components using ICA

3.1.1 Decay artifacts

TMS over DLPFC resulted in a large bipolar waveform with peaks around 5 and 8 ms in all participants (fig. 1A). The size (maximum amplitude range = 74 to 5,679 μV , mean = $2,131 \pm 1,522 \mu\text{V}$; several orders of magnitude larger than neural activity), topography and properties of this waveform are consistent with scalp muscle activation, (Mutanen et al., 2012; Rogasch et al., 2013c), however other residual artifacts and cortical potentials could also contribute (Julkunen et al., 2009; Veniero et al., 2010). Bipolar artifact size trended towards a significant correlation with TMS intensity ($r=0.29$, $p=0.11$), suggesting higher TMS intensities resulted in larger artifact. Following removal of the main TMS artifact and the bipolar artifact using interpolation (see section 2.4 for details), the first ICA run consistently decomposed the fast decay into a single component (fig. 1B for example). Removing this component resulted in significant reduction in EEG signal lasting up to 52 ms in two electrode clusters spanning the majority of the scalp (both clusters $p<0.05$). The difference in GMFA between uncorrected and corrected traces significantly correlated with the GMFA of the bipolar peaks occurring between 6-15 ms ($r=0.88$, $p<0.001$), supporting that the fast decay component represented the tail end of this activity (fig. 1C). We could not detect any significant systematic differences in scalp topography following removal of the fast decay component using this method and using data compression prior to ICA ($p>0.05$). This suggests that mixing of neural and artifact components was minimal, supporting successful ICA decomposition. All additional analyses were performed following a second ICA run after removal of the fast decay artifact and additional processing steps (see section 2.4).

The second round of ICA revealed between 1-5 components consistent with slow decay components in most participants (27/30). These components were particularly prominent in participants with large bipolar artifacts, were considerably smaller in amplitude than the fast decay component and were slower to recover (fig. 1D for example). Removal of these components resulted in significant reduction in EEG signal in two electrode clusters spanning the majority of the scalp (34-160 ms, $p=0.005$; 35-188 ms, $p=0.002$; fig. 1E). We could also not detect any significant systematic differences in scalp topography following removal of the slow

decay component between this method and using data compression prior to ICA ($p>0.05$), further supporting successful ICA decomposition. The difference in GMFA between uncorrected and corrected traces also significantly correlated with the GMFA of the bipolar peaks ($r=0.65$, $p<0.001$), supporting a relationship between the slow decay components and this artifact (fig. 1F).

3.1.2 Blink artifacts.

Either one ($n=25$) or two ($n=4$) components consistent with TMS-evoked blinks were present in all but one participant. TMS-evoked blinks typically occurred with a peak at ~ 90 ms and topography concentrated over anterior electrodes (fig. 2A). To assess whether this component was blink related, trials containing voluntary blinks were concatenated to the TMS trials prior to ICA. Signal related to voluntary blinks combined with signal related to TMS-evoked blinks into the same independent components in all but one participant (28/29; fig. 1B for example), strongly supporting a non-cortical origin of this component.

Removal of the blink component resulted in reduced EEG signal over a cluster of bilateral anterior electrodes (68-164 ms, $p=0.007$) and two clusters of bilateral posterior electrodes (29-61 ms, $p=0.019$; 67-165 ms, $p<0.001$; fig. 1C). The amount of signal removed by the blink component suggested a correlation with TMS intensity ($r=0.29$, $p=0.12$) and that higher TMS intensities resulted in larger blinks. To assess whether removing the blink component also inadvertently removed neural signal, removal of the TMS blink component was compared with removal of the combined voluntary and TMS blink. The addition of voluntary blinks before ICA resulted in significantly less signal removal over a cluster of electrodes spanning from left temporal to central regions (61-144 ms, $p=0.003$; fig. 1D). To assess whether suppressing data prior to ICA also separated these sources, data compression prior to ICA was compared with both the straight TMS blink condition and the combined voluntary blink and TMS condition. Removal of the blink following ICA with data compression also resulted in significantly more removal of signal than the combined voluntary and TMS blink (60-121 ms, $p=0.019$).

----Insert figure 2-----

3.1.3 Auditory artifacts.

Sham TMS performed in nine participants resulted in a biphasic waveform with peaks between 80-100 ms and 150-200 ms over fronto-central regions, consistent with an auditory-evoked potential (fig. 3A for example). One (n=29) or two (n=1) components with similar properties were also observed following active TMS in all participants (fig. 3B). To confirm this component was an auditory-evoked potential, sham trials were concatenated to the active TMS trials prior to ICA in nine participants. Auditory-evoked potentials following sham stimulation combined with potentials following active TMS in all nine participants, further supporting a non TMS-evoked origin of this component (fig. 3C for example).

Removal of the auditory component resulted in significant reduction in EEG signal in four separate clusters across all thirty participants. EEG amplitude was significantly reduced in two clusters with fronto-central topographies across consecutive time periods (71-126 ms, $p=0.015$; 136-275 ms, $p<0.001$; fig. 3D). The remaining two clusters were concentrated over posterior electrodes and displayed opposing polarities and similar time periods to the first two clusters (72-126 ms, $p=0.006$; 135-273 ms, $p<0.001$). The amount of signal removed by the auditory component did not correlate with TMS intensity ($r=0.07$, $p=0.68$). In addition, we could not detect any significant difference between signal correction using combined sham/active TMS compared with TMS alone ($p=0.16$, $n=9$), suggesting auditory-evoked potentials could be removed without removing TMS-evoked neural activity. To assess the effect of removing the auditory component on the auditory evoked potential, corrected and uncorrected data from the sham trials were compared. Removing the auditory artifact significantly reduced the signal in sham trials ($p<0.05$; fig. 3E for example), suggesting that the majority of the auditory evoked potential was successfully removed.

-----Insert figure 3-----

3.1.4 Bad electrode artifacts.

In each participant, multiple components (range = 10-24) were present in which the topography centred on a single electrode. The majority of these components did not display activity time locked to the TMS pulse and were consistent with small drift artifacts resulting from idiosyncratic differences between electrodes,

persistent muscle activity or line noise (see supplementary material). However, 1-2 components typically from electrodes under the coil did display activity time-locked to the TMS pulse which could pass for TMS-evoked neural activity (fig. 4A for example). When considered relative to other channels, these components typically accounted for outlier activity in individual channels (figure 4B-C). Neural activity typically contributes a common signal to adjacent electrodes, so such outliers are unlikely to result from neural activity. For instance, such localised signal could result from interruptions to the electrode-skin interface caused by coil vibration/movement or small, residual charges stored in these specific electrode circuits.

We could not detect any significant systematic difference in EEG signal after removing bad electrode components across participants ($p > 0.05$). However, it should be noted that severely noisy channels were removed prior to ICA. Instead, removing these remaining components appeared to improve signal-to-noise ratio in a characteristic way for each individual participant, particularly in electrodes under the coil. There was a significant correlation between the amount of signal removed by bad electrodes and TMS intensity ($p = 0.035$, $r = 0.39$), suggesting higher TMS intensities resulted in larger artifacts from bad electrodes.

-----Insert figure 4-----

3.2 Reliability.

There was no significant difference in the number of components removed ($p = 0.12$) or in the corrected EEG signal between experimenters ($p = 0.40$), suggesting removal of artifacts using ICA was both reproducible and reliable using the above method.

3.3 The importance of removing artifacts for measuring prefrontal network properties

3.3.1 TMS-evoked potentials.

Removal of artifacts revealed a complex pattern of evoked activity both at the site of stimulation and across the scalp following TMS over DLPFC. Three consistent deflections were observed in the electrode under the coil (F3); a negative peak at 40.3 ± 7 ms (N40; distinguishable in 29 participants), a positive peak at 61.9 ± 11

ms (P60; distinguishable in 29 participants) and second negative peak at 113.2 ± 14 ms (N100; distinguishable in 29 participants). Across the grand average of all electrodes, five clear peaks at ~40, 60, 80, 120 and 190 ms were observed within the first 200 ms following TMS (fig. 5). A sixth early peak between 20-30 ms was also present, however as interpolation lasted up to 25 ms in some participants, this peak was not considered for analysis. Early peaks displayed voltage distributions focused over bilateral frontal cortex, contralateral temporal and motor cortex and ipsilateral parietal cortex, whereas latter peaks displayed fronto-central and occipital distributions. The spatiotemporal evolution of this signal suggests that TMS not only stimulates neurons within the DLPFC, but also activates larger networks in which the DLPFC presumably plays a causal role.

-----Insert figure 5-----

Figure 6 A-B describe the uncorrected (no artifacts removed) and corrected (all artifacts removed) signals. To assess the effect of individual artifacts on measuring TEPs, all but one of the artifact sub-types were removed and compared with the corrected signal. If not removed, the slow decay components significantly altered the amplitude of N40, P60 and N120 peaks at the F3 electrode (all $p < 0.05$). Across space and time, the slow decay artifact significantly distorted EEG signal amplitude and topography between 35 – 500 ms (2 positive, 3 negative clusters; all $p < 0.05$; fig 6C). This primarily affected a cluster of central electrodes as well as a second more posterior cluster.

The blink artifact significantly altered the amplitude and latency of N40 ($p < 0.005$) and N100 ($p < 0.001$) and the latency of P60 ($p < 0.001$) at F3. Across space and time, the blink artifact increased EEG amplitude across two consecutive time frames, firstly between 67-165 ms and then between 198-439 ms (2 positive, 2 negative clusters; all $p < 0.05$; fig. 6D). In both cases, a cluster of anterior and cluster of posterior electrodes were affected. Combining voluntary eye-blinks prior to ICA had no significant effect on N40, P60 or N120 amplitude (all $p > 0.6$) or latency (all $p > 0.7$). Across space and time, combining voluntary blinks increased EEG amplitude between 197-276 ms in a central and posterior cluster compared with not combining blinks (1 positive, 1 negative cluster; $p < 0.05$), however there was no significant effect prior to this time.

The auditory evoked potential had no significant effect on either amplitude or latency of any peak at F3, however differences in amplitude trended towards significance for both P60 ($p=0.07$) and N120 ($p=0.06$). Across space and time, the auditory artifact increased EEG amplitude across three time frames, 71-126 ms, 135-275 ms and 346-500 ms (3 positive clusters, 3 negative clusters; $p<0.05$; fig6E). Over each time frame, a cluster of fronto-central and a cluster of posterior electrodes were affected.

Bad electrodes significantly increased P60 amplitude ($p=0.025$), but had no significant effect on N40 or N120 (all $p>0.1$) or latency of any peak (all $p>0.3$) at F3. There was no significant effect of bad electrodes on EEG signal across space and time ($p>0.3$; fig. 6F).

-----Insert figure 6-----

3.3.2 TMS-evoked oscillations.

Removal of artifacts revealed a broad range of evoked cortical oscillations both at the site of stimulation and over remote cortical regions following DLPFC TMS. At the F3 electrode, the largest oscillation increase occurred in the upper-beta and gamma frequencies (20-40 Hz), peaking at ~40 ms and persisting for ~100 ms (fig. 7A). Lower-beta and alpha oscillations (8-20 Hz) were also increased for ~150 ms. Across space, time and frequency, 20-45 Hz oscillations were increased in most regions within the first 100 ms, with the largest increases over left frontal cortex. Increases in alpha oscillations (8-12 Hz) were largely concentrated over the left frontal cortex for the first 100 ms, however propagated to the contralateral frontal and motor regions and to parieto-occipital regions between 100-250 ms (fig. 7B-C). Propagation of oscillatory activity both in space and time suggests outputs from the DLPFC can entrain oscillations in distant brain regions.

-----Insert figure 7-----

To assess the effect of artifacts on measuring TMS-evoked oscillations, all but one of the artifact sub-types were removed for each artifact and compared with the corrected signal. If the slow decay component was not removed, it significantly increased lower-beta ($p=0.039$) and tended to increase alpha oscillations ($p=0.064$) at the F3 electrode, but did not significantly alter upper-beta or gamma oscillations (both $p>0.05$). Across space, time and frequency, the slow decay artifact increased oscillations across all frequencies (8-45 Hz) in the first 50 ms and increased alpha oscillations (8-12 Hz) up to 150, particularly for electrodes on the side of stimulation (one significant cluster, $p<0.001$; fig. 8A).

At F3, the blink artifact significantly increased alpha ($p=0.018$) and lower-beta ($p=0.025$) oscillations, but did not significantly alter upper-beta ($p=0.687$) or gamma ($p=0.640$) oscillations. Across space, time and frequency, the blink artifact significantly increased 18-45 Hz oscillations between 80-120 ms across frontal and posterior electrodes (one significant cluster, $p<0.001$; fig. 8B), particularly in the 8-12 Hz band over frontal electrodes. Combining voluntary eye-blinks prior to ICA did not significantly affect TMS-evoked oscillations for any frequency band at the F3 electrode (all $p>0.05$) or across space, time and frequency ($p=0.3$) compared with not combining blinks.

At F3, the auditory evoked potential increased oscillations in the alpha ($p=0.024$), upper beta ($p=0.034$) and gamma ($p=0.021$), but not lower beta ($p=0.360$) bands. Across space, time and frequency, the auditory evoked potential significantly increased 18-45 Hz oscillations over two time periods at ~70 ms and ~140 ms in fronto-central and posterior electrodes (one significant cluster, $p<0.001$; fig. 8C). The auditory evoked potential also increased 8-12 Hz oscillations in fronto-central electrodes up to 300 ms.

Bad electrodes had no significant effect on any frequency band at F3 (all $p>0.3$). Across space, time and frequency, bad electrodes significantly increased upper beta oscillations over a cluster of parietal electrodes up to 80 ms (one negative cluster, $p=0.044$).

-----Insert figure 8-----

4. DISCUSSION

The current study demonstrates a number of novel findings. First, we have provided evidence that decay, blink and auditory artifacts can be identified using ICA in TMS-EEG recordings. Second, we have demonstrated that these artifacts can be removed with minimal impact on TMS-evoked activity following stimulation of the DLPFC. Finally, we have also established that if not removed, each artifact characteristically distorts measures of DLPFC function obtained from TMS-EEG recordings.

4.1 Identification and removal of artifacts.

The most pervasive artifact following TMS over DLPFC, particularly for early signal, seemed to result from a large bipolar waveform most likely resulting from inadvertent stimulation of scalp muscles. The fast decay artifact was tightly correlated with the size of the bipolar waveform and is likely to directly reflect the recovery phase of this artifact (Mutanen et al., 2012; Rogasch et al., 2013c). However, we have also described a slow decay artifact that takes longer to recover and was also related to bipolar artifact size. The topography of this artifact was different to that of the fast decay component suggesting a different origin. The twitch associated with TMS-evoked muscle stimulation causes a visible movement on the scalp which could interrupt the electrode-skin interface, possibly contributing to this component (ter Braack et al., 2013). Alternatively, charges stored at the electrode-skin interface or in the electrode circuit could also contribute (Julkunen et al., 2008; Sekiguchi et al., 2011). Removal of both fast and slow decay components produced identical results when a compression method was used which is useful in preventing mixing of neural and artifact components (Hernandez-Pavon et al., 2012). However, it remains unclear if reducing the data to an amplitude of $\sim 150 \mu\text{V}$ following interpolation was sufficient to prevent distortion of neural components resulting from large artifacts. Future comparisons with validated suppression techniques such as PCA, white noise and wavelet analysis are required to address this issue (Hernandez-Pavon et al., 2012).

We have also described and confirmed the source of a time-locked blink artifact that was prominent in our recordings and has also been described by others (Bruckmann et al., 2012). TMS-evoked blinks have received little attention compared with other artifacts, yet are vital to control for in light of the temporal association

with peaks of interest such as the N100 (Bruckmann et al., 2012). Removing the blink artifact using different ICA methods altered the amount of signal removed. For instance, combining voluntary blinks with TMS-evoked data resulted in less signal being removed around 100 ms than with straight TMS data, or with TMS data compressed prior to ICA. A similar dissociation between methods occurs following removal of blink artifacts in an auditory startle task using ICA (Li and Principe, 2006). One interpretation of this finding is that adding voluntary blinks aids the algorithm in separating a time-locked neural component which is mixed with the blink component (Li and Principe, 2006). Alternatively, combining large voluntary blinks may force ICA to decompose the data differently, leading to under-correction. Regardless, examination of the final corrected signal (i.e. with all artifacts removed) revealed no difference between correction methods within 200 ms (i.e. TMS alone compared with combined voluntary blinks and TMS). This suggests that the additional signal recovered following the combined condition was removed with another artifact type. Given the possible association of this signal with auditory evoked activity (Li and Principe, 2006), this additional signal could have been removed with the auditory artifact. Although not conclusive, the above evidence suggests that blink artifacts can also be removed with reasonable confidence that the underlying TMS-evoked activity is minimally affected.

Auditory evoked potentials caused by the loud clicking of TMS are another common artifact occurring independent of stimulation site. We provide the first evidence to our knowledge that this auditory artifact can be identified and removed using ICA. As the auditory artifact also represents neuronal activity, it is impossible to be completely confident that removal does not affect the TMS-evoked potential. However, several lines of evidence suggest TMS-evoked neural activity is mostly conserved. First, removing auditory components from combined sham and real TMS resulted in the same amount of correction as removing auditory components from real TMS alone, suggesting that non-auditory neural activity was not inadvertently removed with this component. Second, removing the auditory component with combined sham and real TMS removed the auditory evoked potential in the sham trials, suggesting this method was adequate for artifact removal. Finally, the corrected pattern of TMS-evoked neural activity over DLPFC (N100 and P180) is consistent with other studies that have controlled for auditory artifacts by subtracting sham

data (Kähkönen et al., 2003) or by auditory masking (Ferrarelli et al., 2008). Removing the auditory artifact using ICA could prove useful for studies not able to use auditory masking, and may aid in controlling for both the air and bone conducted aspects of the auditory-evoked potential. However, from a practical perspective, the auditory artifact was the most difficult to identify due to similarities with other neural components. Confidence in selecting this IC can be greatly improved by combining sham trials. Therefore, future studies wishing to utilize this method would greatly benefit from either including a sham condition or interleaving auditory clicks with real TMS trials.

4.2 TMS-evoked potentials and oscillations over DLPFC

The decay, blink and auditory artifacts all significantly altered measures of local and global TMS-evoked activation if not corrected. This finding highlights the importance of removing these artifacts to accurately measure DLPFC function with TMS-EEG. Although bad channel artifacts did not significantly affect the group data, removing these artifacts did improve signal-to-noise ratio on an individual level, justifying their removal. When artifact-corrected, the EEG signal revealed six clear TEP peaks within the first 200 ms following TMS over DLPFC. The latencies of 5 of these peaks (27, 40, 60, 100 and 180 ms) accurately replicate peaks shown in earlier studies on DLPFC TEPs (Kähkönen et al., 2004, 2003; S Kähkönen et al., 2005; Seppo Kähkönen et al., 2005; Lioumis et al., 2009). Importantly, the voltage distribution of these peaks is also consistent across studies (see figure 5 from S Kähkönen et al., 2005). We observed an additional peak at 80 ms which may have been revealed after blink and auditory artifacts were removed. The origin and physiological mechanisms responsible for these peaks remains unclear. A growing body of evidence from the motor cortex suggests that early peaks at the site of stimulation may represent excitatory neurotransmission (Bonato et al., 2006; Komssi et al., 2004; Mäki and Ilmoniemi, 2010; Rogasch et al., 2013b), whereas latter peaks such as the N100 are consistent with inhibitory neurotransmission mediated by GABA_B receptors (Bender et al., 2005; Bonnard et al., 2009; Bruckmann et al., 2012; Farzan et al., 2013; Kicić et al., 2008; Nikulin et al., 2003; Rogasch et al., 2013b; Spieser et al., 2010). Whether the same is true for the DLPFC requires further investigation.

In the frequency domain, TMS over DLPFC evoked predominantly upper beta and gamma band oscillations during the first 100 ms at the site of stimulation. Previous TMS-EEG studies that have also reported high frequency TMS-evoked oscillations from frontal sites such as the superior frontal gyrus (Ferrarelli et al., 2012) and premotor cortex (Ferrarelli et al., 2008; Rosanova et al., 2009). TMS-evoked oscillations likely reflect the intrinsic organisation of local DLPFC networks as well as connectivity between other cortical and sub-cortical regions (Cona et al., 2011; Rosanova et al., 2009; Van Der Werf et al., 2006). We also report that stimulation of the DLPFC can entrain alpha, lower beta and gamma oscillations in distant cortical regions such as ipsilateral prefrontal and temporo-motor cortex and bilateral parieto-occipital cortex. This finding is consistent with the top-down role of the DLPFC in generating oscillations in connected brain regions, a mechanism thought critical for working memory and selective attention performance (Benchenane et al., 2011; Fell and Axmacher, 2011; Zanto et al., 2011).

4.3 Limitations

Additional artifacts to those assessed here could also affect TMS-EEG recordings from DLPFC. For instance, somatosensory-evoked potentials resulting from TMS-evoked muscle activity or from stimulation of the trigeminal nerve could also contribute to the EEG signal. Future studies directly addressing these sources of artifact are required. From a practical perspective, manually identifying artifacts from a large number of components (>50) was both laborious and time consuming. In addition, having such a large number of components often resulted in the splitting of artifacts into multiple components. This made artifact identification difficult and potentially increases the risk of rater error. Using compression methods to limit the number of components to those representing the majority of activity may prove useful to minimize this problem. Finally, a large amount of data was removed following ICA to reveal the relatively small TMS-evoked EEG signal (for example fig. 6A-B). Although we have provided evidence that neural signal can be recovered with reasonable confidence using this method, complete certainty that TMS-evoked neural activity was not altered by removing these artifacts is not possible.

5. CONCLUSIONS

TMS over DLPFC results in multiple artifacts in EEG recordings, such as TMS-evoked muscle activity, blinks and auditory evoked potentials. If not removed, these artifacts distort measures of TMS-evoked neural activity such as cortical reactivity, connectivity and oscillations. ICA can be used to both identify and remove these artifacts with minimal impact on TMS-evoked neural activity. The artifact free data provides valuable information on cortical network properties, which can be used to study DLPFC function in both healthy and clinical populations.

Acknowledgements: The authors wish to thank all volunteers for their participation. The following work will contribute to the doctoral thesis of NCR. NCR is supported by a postgraduate biomedical research scholarship (607223) from the National Health and Medical Research Council (NHMRC) of Australia. PBF is supported by a NHMRC Practitioner Fellowship.

Disclosures and conflict of interests: PBF has received equipment for research from MagVenture A/S, Medtronic Ltd and Brainsway Ltd and funding for research from Cervel Neurotech. In the last 5 years, ZJD received external funding through Brainsway Inc and a travel allowance through Pfizer and Merck. ZJD has also received speaker funding through Sepracor Inc, AstraZeneca and served on the advisory board for Hoffmann-La Roche Limited. NCR, RHT, FF, BMF, NWB and JCH report no conflicts of interest.

REFERENCES

- Benchenane, K., Tiesinga, P.H., Battaglia, F.P., 2011. Oscillations in the prefrontal cortex: a gateway to memory and attention. *Curr. Opin. Neurobiol.* 21, 475–85.
- Bender, S., Basseler, K., Sebastian, I., Resch, F., Kammer, T., Oelkers-Ax, R., Weisbrod, M., 2005. Electroencephalographic response to transcranial magnetic stimulation in children: Evidence for giant inhibitory potentials. *Ann. Neurol.* 58, 58–67.
- Bonato, C., Miniussi, C., Rossini, P.M., 2006. Transcranial magnetic stimulation and cortical evoked potentials: a TMS/EEG co-registration study. *Clin. Neurophysiol.* 117, 1699–707.
- Bonnard, M., Spieser, L., Meziane, H.B., de Graaf, J.B., Pailhous, J., 2009. Prior intention can locally tune inhibitory processes in the primary motor cortex: direct evidence from combined TMS-EEG. *Eur. J. Neurosci.* 30, 913–23.
- Bruckmann, S., Hauk, D., Roessner, V., Resch, F., Freitag, C.M., Kammer, T., Ziemann, U., Rothenberger, A., Weisbrod, M., Bender, S., 2012. Cortical inhibition in attention deficit hyperactivity disorder: new insights from the electroencephalographic response to transcranial magnetic stimulation. *Brain* 135, 2215–30.
- Cona, F., Zavaglia, M., Massimini, M., Rosanova, M., Ursino, M., 2011. A neural mass model of interconnected regions simulates rhythm propagation observed via TMS-EEG. *Neuroimage* 57, 1045–58.
- Conforto, A.B., Z'Graggen, W.J., Kohl, A.S., Rösler, K.M., Kaelin-Lang, A., 2004. Impact of coil position and electrophysiological monitoring on determination of motor thresholds to transcranial magnetic stimulation. *Clin. Neurophysiol.* 115, 812–9.
- Daskalakis, Z.J., Farzan, F., Barr, M.S., Maller, J.J., Chen, R., Fitzgerald, P.B., 2008. Long-interval cortical inhibition from the dorsolateral prefrontal cortex: a TMS-EEG study. *Neuropsychopharmacology* 33, 2860–9.
- Daskalakis, Z.J., Farzan, F., Radhu, N., Fitzgerald, P.B., 2012. Combined transcranial magnetic stimulation and electroencephalography: its past, present and future. *Brain Res.* 1463, 93–107.
- Delorme, A., Makeig, S., 2004. EEGLAB: an open source toolbox for analysis of single-trial EEG dynamics including independent component analysis. *J. Neurosci. Methods* 134, 9–21.
- Farzan, F., Barr, M.S., Hoppenbrouwers, S.S., Fitzgerald, P.B., Chen, R., Pascual-Leone, A., Daskalakis, Z.J., 2013. The EEG correlates of the TMS-induced EMG silent period in humans. *Neuroimage* 83C, 120–134.
- Farzan, F., Barr, M.S., Levinson, A.J., Chen, R., Wong, W., Fitzgerald, P.B., Daskalakis, Z.J., 2010. Evidence for gamma inhibition deficits in the dorsolateral prefrontal cortex of patients with schizophrenia. *Brain* 133, 1505–14.
- Fell, J., Axmacher, N., 2011. The role of phase synchronization in memory processes. *Nat. Rev. Neurosci.* 12, 105–18.
- Ferrarelli, F., Massimini, M., Peterson, M.J., Riedner, B. a, Lazar, M., Murphy, M.J., Huber, R., Rosanova, M., Alexander, A.L., Kalin, N., Tononi, G., 2008. Reduced evoked gamma oscillations in the frontal cortex in schizophrenia patients: a TMS/EEG study. *Am. J. Psychiatry* 165, 996–1005.

- Ferrarelli, F., Sarasso, S., Guller, Y., Riedner, B. a, Peterson, M.J., Bellesi, M., Massimini, M., Postle, B.R., Tononi, G., 2012. Reduced natural oscillatory frequency of frontal thalamocortical circuits in schizophrenia. *Arch. Gen. Psychiatry* 69, 766–74.
- Fitzgerald, P.B., Maller, J.J., Hoy, K.E., Thomson, R., Daskalakis, Z.J., 2009. Exploring the optimal site for the localization of dorsolateral prefrontal cortex in brain stimulation experiments. *Brain Stimul.* 2, 234–7.
- Hallett, M., 2007. Transcranial magnetic stimulation: a primer. *Neuron* 55, 187–99.
- Hamidi, M., Slagter, H. a, Tononi, G., Postle, B.R., 2010. Brain responses evoked by high-frequency repetitive transcranial magnetic stimulation: an event-related potential study. *Brain Stimul.* 3, 2–14.
- Hernandez-Pavon, J.C., Metsomaa, J., Mutanen, T., Stenroos, M., Mäki, H., Ilmoniemi, R.J., Sarvas, J., 2012. Uncovering neural independent components from highly artifactual TMS-evoked EEG data. *J. Neurosci. Methods* 209, 144–57.
- Hyvärinen, a, Oja, E., 2000. Independent component analysis: algorithms and applications. *Neural Netw.* 13, 411–30.
- Ilmoniemi, R.J., Kicić, D., 2010. Methodology for combined TMS and EEG. *Brain Topogr.* 22, 233–48.
- Ilmoniemi, R.J., Virtanen, J., Ruohonen, J., Karhu, J., Aronen, H.J., Näätänen, R., Katila, T., 1997. Neuronal responses to magnetic stimulation reveal cortical reactivity and connectivity. *Neuroreport* 8, 3537–40.
- Iwahashi, M., Arimatsu, T., Ueno, S., Iramina, K., 2008. Differences in evoked EEG by transcranial magnetic stimulation at various stimulus points on the head. *Conf. Proc. IEEE Eng. Med. Biol. Soc.* 2008, 2570–3.
- Julkunen, P., Pääkkönen, a, Hukkanen, T., Könönen, M., Tiihonen, P., Vanhatalo, S., Karhu, J., 2008. Efficient reduction of stimulus artefact in TMS-EEG by epithelial short-circuiting by mini-punctures. *Clin. Neurophysiol.* 119, 475–81.
- Julkunen, P., Säisänen, L., Sarasti, M., Könönen, M., 2009. Effect of electrode cap on measured cortical motor threshold. *J. Neurosci. Methods* 176, 225–9.
- Jung, T.-P., Makeig, S., McKeown, M.J., Bell, A.J., Lee, T.-W., Sejnowski, T.J., 2001. Imaging Brain Dynamics Using Independent Component Analysis. *Proc. IEEE. Inst. Electr. Electron. Eng.* 89, 1107–1122.
- Kähkönen, S., Komssi, S., Wilenius, J., Ilmoniemi, R.J., 2005. Prefrontal transcranial magnetic stimulation produces intensity-dependent EEG responses in humans. *Neuroimage* 24, 955–60.
- Kähkönen, Seppo, Komssi, S., Wilenius, J., Ilmoniemi, R.J., 2005. Prefrontal TMS produces smaller EEG responses than motor-cortex TMS: implications for rTMS treatment in depression. *Psychopharmacology (Berl)*. 181, 16–20.
- Kähkönen, S., Wilenius, J., Komssi, S., Ilmoniemi, R.J., 2004. Distinct differences in cortical reactivity of motor and prefrontal cortices to magnetic stimulation. *Clin. Neurophysiol.* 115, 583–8.
- Kähkönen, S., Wilenius, J., Nikulin, V. V, Ollikainen, M., Ilmoniemi, R.J., 2003. Alcohol reduces prefrontal cortical excitability in humans: a combined TMS and EEG study. *Neuropsychopharmacology* 28, 747–54.
- Kicić, D., Lioumis, P., Ilmoniemi, R.J., Nikulin, V. V, 2008. Bilateral changes in excitability of sensorimotor cortices during unilateral movement: combined electroencephalographic and transcranial magnetic stimulation study. *Neuroscience* 152, 1119–29.

- Komssi, S., Kähkönen, S., 2006. The novelty value of the combined use of electroencephalography and transcranial magnetic stimulation for neuroscience research. *Brain Res. Rev.* 52, 183–92.
- Komssi, S., Kähkönen, S., Ilmoniemi, R.J., 2004. The effect of stimulus intensity on brain responses evoked by transcranial magnetic stimulation. *Hum. Brain Mapp.* 21, 154–64.
- Korhonen, R.J., Hernandez-Pavon, J.C., Metsomaa, J., Mäki, H., Ilmoniemi, R.J., Sarvas, J., 2011. Removal of large muscle artifacts from transcranial magnetic stimulation-evoked EEG by independent component analysis. *Med. Biol. Eng. Comput.* 49, 397–407.
- Lehmann, D., Skrandies, W., 1980. Reference-free identification of components of checkerboard-evoked multichannel potential fields. *Electroencephalogr. Clin. Neurophysiol.* 48, 609–21.
- Li, R., Principe, J.C., 2006. Blinking artifact removal in cognitive EEG data using ICA. *Conf. Proc. IEEE Eng. Med. Biol. Soc.* 1, 5273–6.
- Lioumis, P., Kicić, D., Savolainen, P., Mäkelä, J.P., Kähkönen, S., 2009. Reproducibility of TMS-Evoked EEG responses. *Hum. Brain Mapp.* 30, 1387–96.
- Litvak, V., Mattout, J., Kiebel, S., Phillips, C., Henson, R., Kilner, J., Barnes, G., Oostenveld, R., Daunizeau, J., Flandin, G., Penny, W., Friston, K., 2011. EEG and MEG data analysis in SPM8. *Comput. Intell. Neurosci.* 2011, 852961.
- Makeig, S., Jung, T.P., Bell, a J., Ghahremani, D., Sejnowski, T.J., 1997. Blind separation of auditory event-related brain responses into independent components. *Proc. Natl. Acad. Sci. U. S. A.* 94, 10979–84.
- Mäki, H., Ilmoniemi, R.J., 2010. The relationship between peripheral and early cortical activation induced by transcranial magnetic stimulation. *Neurosci. Lett.* 478, 24–8.
- Mäki, H., Ilmoniemi, R.J., 2011. Projecting out muscle artifacts from TMS-evoked EEG. *Neuroimage* 54, 2706–10.
- Maris, E., Oostenveld, R., 2007. Nonparametric statistical testing of EEG- and MEG-data. *J. Neurosci. Methods* 164, 177–90.
- Massimini, M., Ferrarelli, F., Huber, R., Esser, S.K., Singh, H., Tononi, G., 2005. Breakdown of cortical effective connectivity during sleep. *Science* 309, 2228–32.
- McMenamin, B.W., Shackman, A.J., Maxwell, J.S., Bachhuber, D.R.W., Koppenhaver, A.M., Greischar, L.L., Davidson, R.J., 2010. Validation of ICA-based myogenic artifact correction for scalp and source-localized EEG. *Neuroimage* 49, 2416–32.
- Mutanen, T., Mäki, H., Ilmoniemi, R.J., 2012. The effect of stimulus parameters on TMS-EEG muscle artifacts. *Brain Stimul.* 1–6.
- Nikouline, V., Ruohonen, J., Ilmoniemi, R.J., 1999. The role of the coil click in TMS assessed with simultaneous EEG. *Clin. Neurophysiol.* 110, 1325–8.
- Nikulin, V. V., Kicic, D., Kahkonen, S., Ilmoniemi, R.J., 2003. Modulation of electroencephalographic responses to transcranial magnetic stimulation: evidence for changes in cortical excitability related to movement. *Eur. J. Neurosci.* 18, 1206–1212.

- Onton, J., Westerfield, M., Townsend, J., Makeig, S., 2006. Imaging human EEG dynamics using independent component analysis. *Neurosci. Biobehav. Rev.* 30, 808–22.
- Oostenveld, R., Fries, P., Maris, E., Schoffelen, J.-M., 2011. FieldTrip: Open source software for advanced analysis of MEG, EEG, and invasive electrophysiological data. *Comput. Intell. Neurosci.* 2011, 156869.
- Plöchl, M., Ossandón, J.P., König, P., 2012. Combining EEG and eye tracking: identification, characterization, and correction of eye movement artifacts in electroencephalographic data. *Front. Hum. Neurosci.* 6, 278.
- Rajji, T.K., Sun, Y., Zomorodi-Moghaddam, R., Farzan, F., Blumberger, D.M., Mulsant, B.H., Fitzgerald, P.B., Daskalakis, Z.J., 2013. PAS-Induced Potentiation of Cortical-Evoked Activity in the Dorsolateral Prefrontal Cortex. *Neuropsychopharmacology* 1–8.
- Rogasch, N.C., Daskalakis, Z.J., Fitzgerald, P.B., 2013a. Cortical Inhibition, Excitation, and Connectivity in Schizophrenia: A Review of Insights From Transcranial Magnetic Stimulation. *Schizophr. Bull.* 1–12.
- Rogasch, N.C., Daskalakis, Z.J., Fitzgerald, P.B., 2013b. Mechanisms underlying long-interval cortical inhibition in the human motor cortex: a TMS-EEG study. *J. Neurophysiol.* 109, 89–98.
- Rogasch, N.C., Fitzgerald, P.B., 2013. Assessing cortical network properties using TMS-EEG. *Hum. Brain Mapp.* 34, 1652–69.
- Rogasch, N.C., Thomson, R.H., Daskalakis, Z.J., Fitzgerald, P.B., 2013c. Short-Latency Artifacts Associated with Concurrent TMS-EEG. *Brain Stimul.* 1–9.
- Rosanova, M., Casali, A., Bellina, V., Resta, F., Mariotti, M., Massimini, M., 2009. Natural frequencies of human corticothalamic circuits. *J. Neurosci.* 29, 7679–85.
- Rosanova, M., Gosseries, O., Casarotto, S., Boly, M., Casali, A.G., Bruno, M.-A., Mariotti, M., Boveroux, P., Tononi, G., Laureys, S., Massimini, M., 2012. Recovery of cortical effective connectivity and recovery of consciousness in vegetative patients. *Brain* 135, 1308–20.
- Rusjan, P.M., Barr, M.S., Farzan, F., Arenovich, T., Maller, J.J., Fitzgerald, P.B., Daskalakis, Z.J., 2010. Optimal transcranial magnetic stimulation coil placement for targeting the dorsolateral prefrontal cortex using novel magnetic resonance image-guided neuronavigation. *Hum. Brain Mapp.* 31, 1643–52.
- Sekiguchi, H., Takeuchi, S., Kadota, H., Kohno, Y., Nakajima, Y., 2011. TMS-induced artifacts on EEG can be reduced by rearrangement of the electrode's lead wire before recording. *Clin. Neurophysiol.* 122, 984–90.
- Siebner, H.R., Bergmann, T.O., Bestmann, S., Massimini, M., Johansen-Berg, H., Mochizuki, H., Bohning, D.E., Boorman, E.D., Groppa, S., Miniussi, C., Pascual-Leone, A., Huber, R., Taylor, P.C.J., Ilmoniemi, R.J., De Gennaro, L., Strafella, A.P., Kähkönen, S., Klöppel, S., Frisoni, G.B., George, M.S., Hallett, M., Brandt, S., Rushworth, M.F., Ziemann, U., Rothwell, J.C., Ward, N., Cohen, L.G., Baudewig, J., Paus, T., Ugawa, Y., Rossini, P.M., 2009. Consensus paper: combining transcranial stimulation with neuroimaging. *Brain Stimul.* 2, 58–80.
- Spieser, L., Meziane, H.B., Bonnard, M., 2010. Cortical mechanisms underlying stretch reflex adaptation to intention: a combined EEG-TMS study. *Neuroimage* 52, 316–25.
- Ter Braack, E.M., de Jonge, B., van Putten, M.J. a M., 2013. Reduction of TMS induced artifacts in EEG using principal component analysis. *IEEE Trans. Neural Syst. Rehabil. Eng.* 21, 376–82.

- Ter Braack, E.M., de Vos, C.C., van Putten, M.J. a M., 2013. Masking the Auditory Evoked Potential in TMS-EEG: A Comparison of Various Methods. *Brain Topogr.*
- Thut, G., Ives, J.R., Kampmann, F., Pastor, M. a, Pascual-Leone, A., 2005. A new device and protocol for combining TMS and online recordings of EEG and evoked potentials. *J. Neurosci. Methods* 141, 207–17.
- Tiitinen, H., Virtanen, J., Ilmoniemi, R.J., Kamppuri, J., Ollikainen, M., Ruohonen, J., Näätänen, R., 1999. Separation of contamination caused by coil clicks from responses elicited by transcranial magnetic stimulation. *Clin. Neurophysiol.* 110, 982–5.
- Van Der Werf, Y.D., Sadikot, A.F., Strafella, A.P., Paus, T., 2006. The neural response to transcranial magnetic stimulation of the human motor cortex. II. Thalamocortical contributions. *Exp. Brain Res.* 175, 246–55.
- Veniero, D., Bortoletto, M., Miniussi, C., 2009. TMS-EEG co-registration: on TMS-induced artifact. *Clin. Neurophysiol.* 120, 1392–9.
- Veniero, D., Maioli, C., Miniussi, C., 2010. Potentiation of short-latency cortical responses by high-frequency repetitive transcranial magnetic stimulation. *J. Neurophysiol.* 104, 1578–88.
- Verhagen, L., Dijkerman, H.C., Medendorp, W.P., Toni, I., 2013. Hierarchical organization of parietofrontal circuits during goal-directed action. *J. Neurosci.* 33, 6492–503.
- Vernet, M., Bashir, S., Yoo, W.-K., Perez, J.M., Najib, U., Pascual-Leone, A., 2013. Insights on the neural basis of motor plasticity induced by theta burst stimulation from TMS-EEG. *Eur. J. Neurosci.* 37, 598–606.
- Virtanen, J., Ruohonen, J., Näätänen, R., Ilmoniemi, R.J., 1999. Instrumentation for the measurement of electric brain responses to transcranial magnetic stimulation. *Med. Biol. Eng. Comput.* 37, 322–6.
- Zanto, T.P., Rubens, M.T., Thangavel, A., Gazzaley, A., 2011. Causal role of the prefrontal cortex in top-down modulation of visual processing and working memory. *Nat. Neurosci.* 14, 656–61.

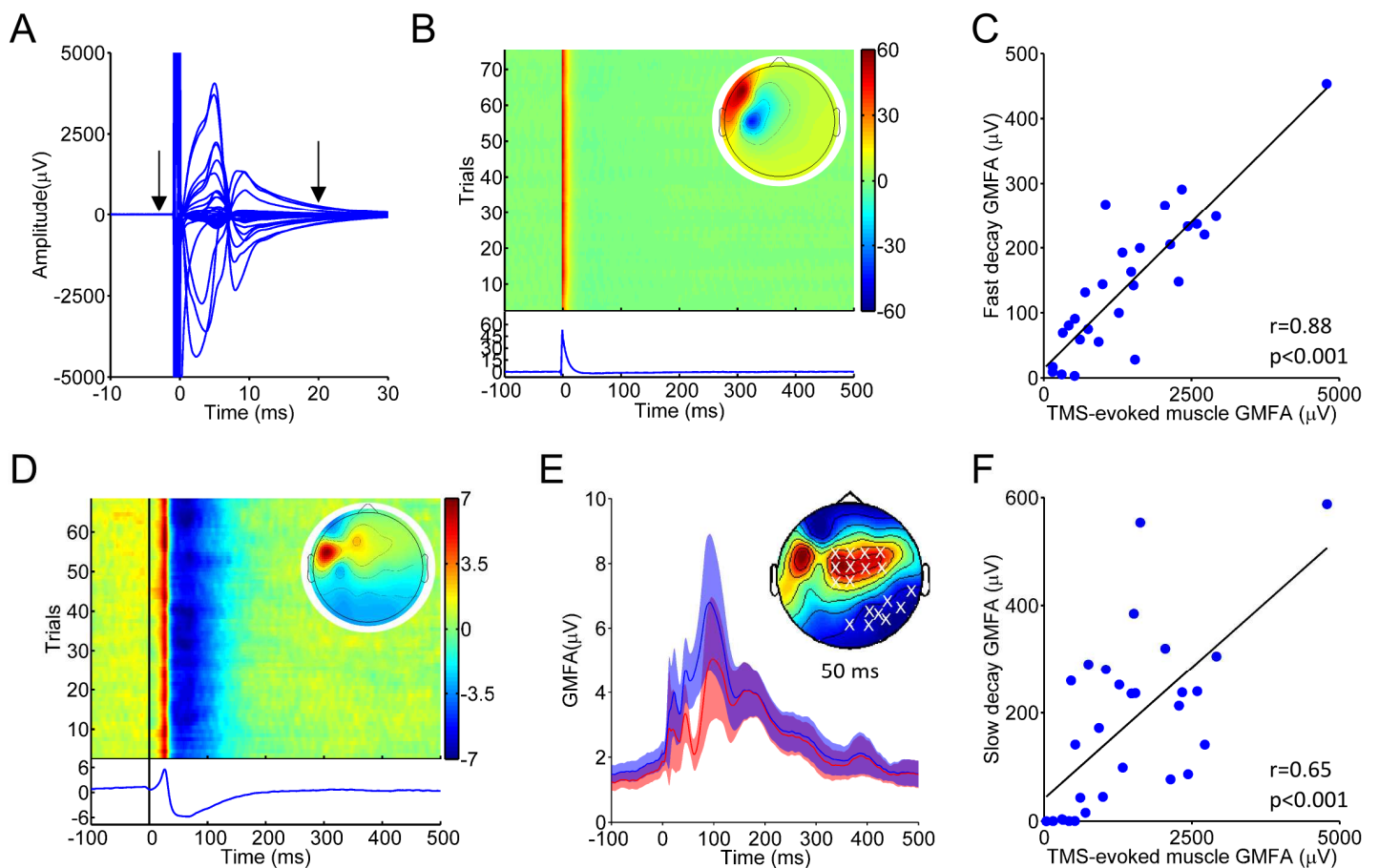


Figure 1: Decay artifact components. A) TMS pulse and TMS-evoked muscle activity (peaks at ~5 and 8 ms) in a representative individual. Arrows indicate the time frame of data to be removed prior to the first ICA run. B) Independent component representing the fast decay artifact following the first ICA run. C) Correlation between signal removed with the fast decay component and TMS-evoked muscle activity size across all participants (GMFA, global mean field amplitude). D) Independent component representing the slow decay artifact following the second ICA run. E) GMFA traces averaged across all participants (shaded line = 95% confidence interval). Red= signal with the slow decay component removed, blue = signal without the slow decay component removed. White crosses on topoplots indicate electrodes significantly altered following removal of the slow decay component at the 50 ms time point (cluster-based statistics, $p<0.05$). F) Correlation between the signal removed with the slow decay component and TMS-evoked muscle activity size across all participants.

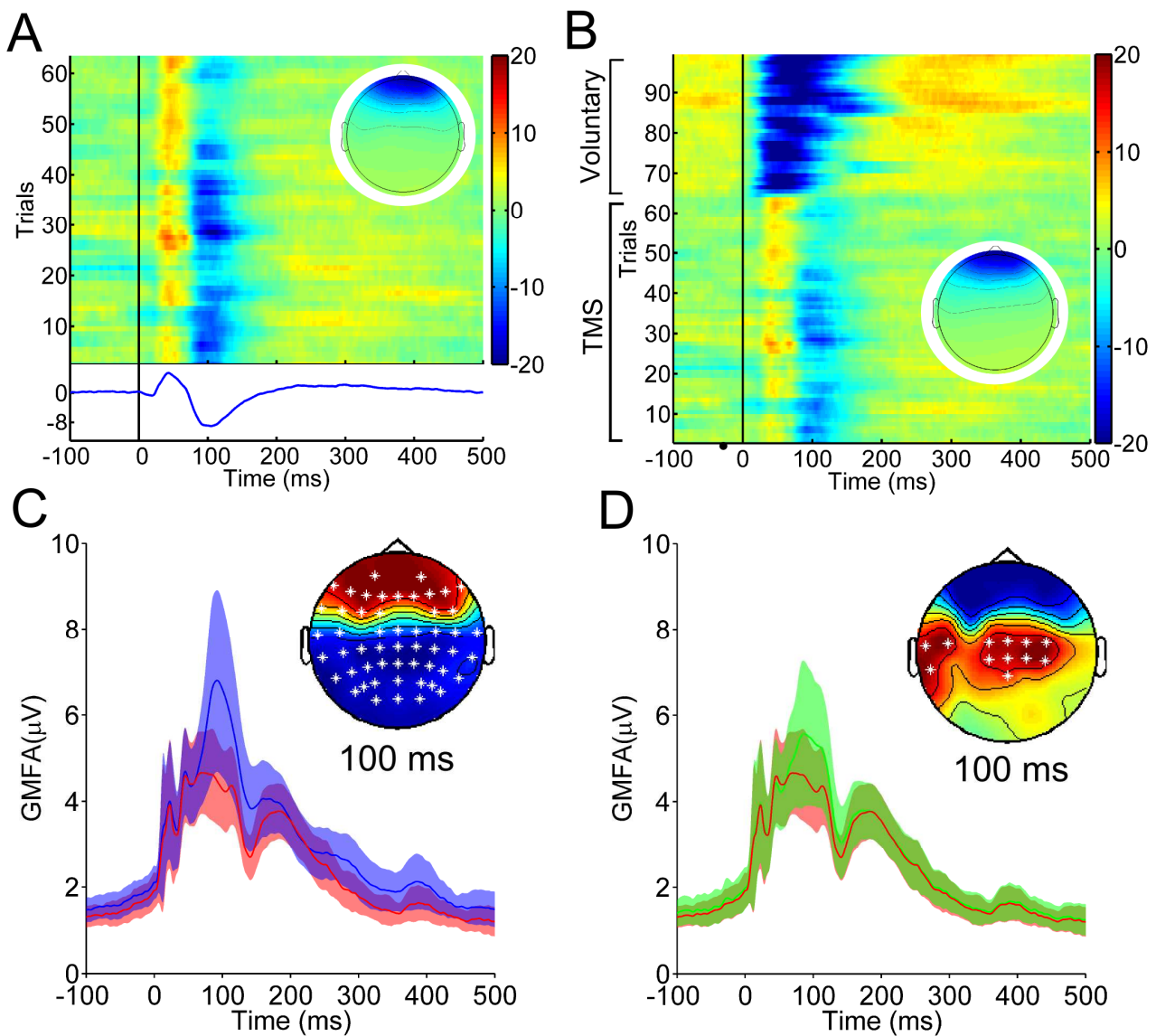


Figure 2: Blink artifact components. A) Independent component representing a blink artifact. B) Activity from the component in A combined with voluntary blinks, confirming that the source of the component was not neural. C-D) Global mean field amplitude (GMFA) traces averaged across all participants (shaded line = 95% confidence interval). Red = signal with the blink component removed, blue = signal without the blink component removed, green = signal with the combined voluntary and TMS blink component removed. White crosses on topoplots in C indicate electrodes significantly altered following removal of the blink component at the 100 ms time point (cluster-based statistics, $p < 0.05$). White crosses on topoplots in D indicate electrodes with significantly less signal following removal of the TMS blink component compared with removal of the combined voluntary and TMS blink component (cluster-based statistics, $p < 0.05$; 100 ms time point).

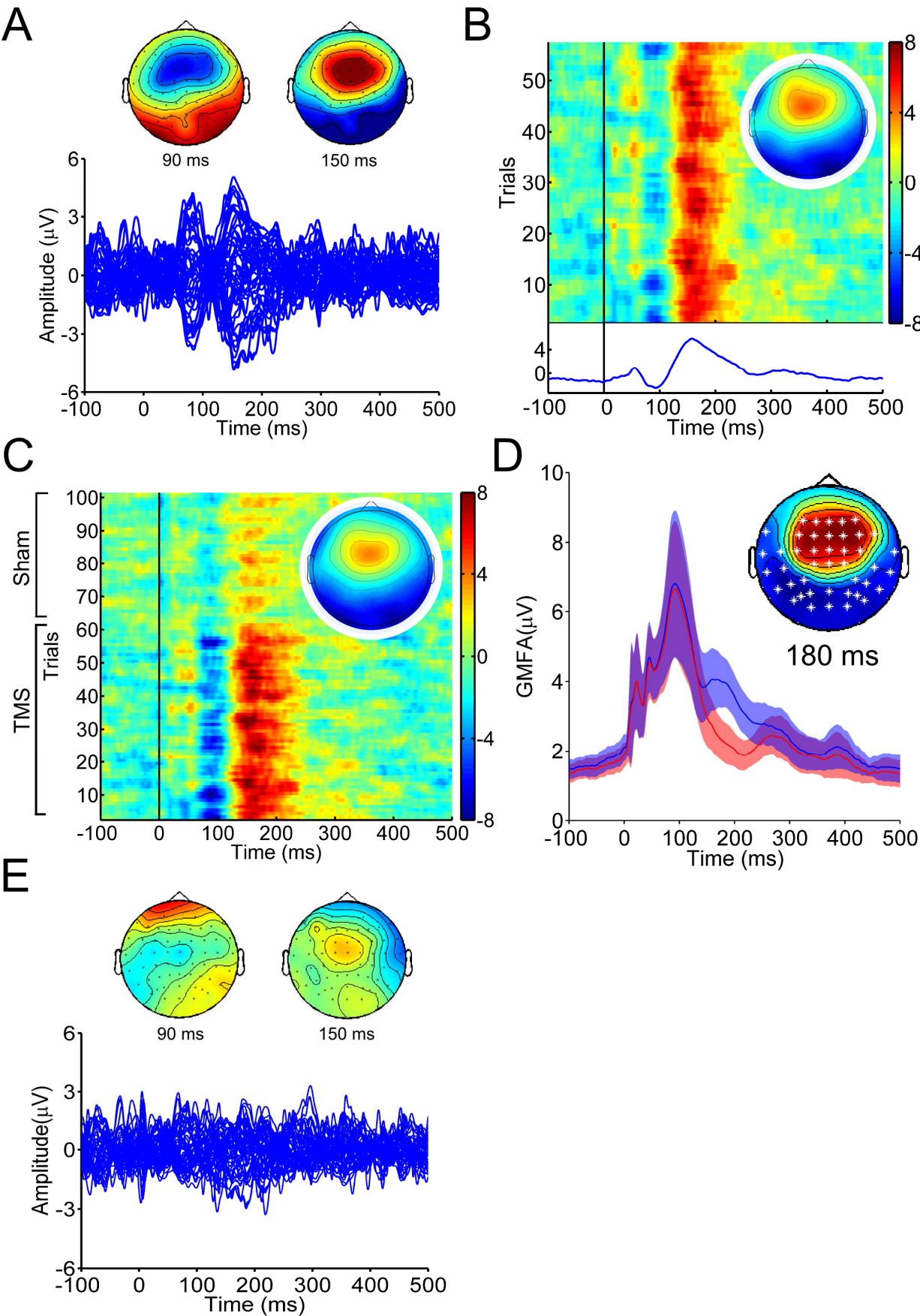


Figure 3: Auditory artifact components. A) Butterfly plot showing auditory-evoked potentials following sham TMS with peak topographies in a representative individual. B) Independent component representing auditory activity following real TMS. C) Activity from the component in B combined with sham TMS, confirming that the source of the component was unlikely related to TMS-evoked potentials. D) Global mean field amplitude (GMFA) traces averaged across all participants (shaded line = 95% confidence interval). Red = signal with the auditory component removed, blue = signal without the auditory component removed. White crosses on topoplot indicate electrodes significantly altered following removal of the auditory component at the 180 ms time point (cluster-based statistics, $p < 0.05$). E) Butterfly plot of sham trials from individual in A following removal of the auditory component.

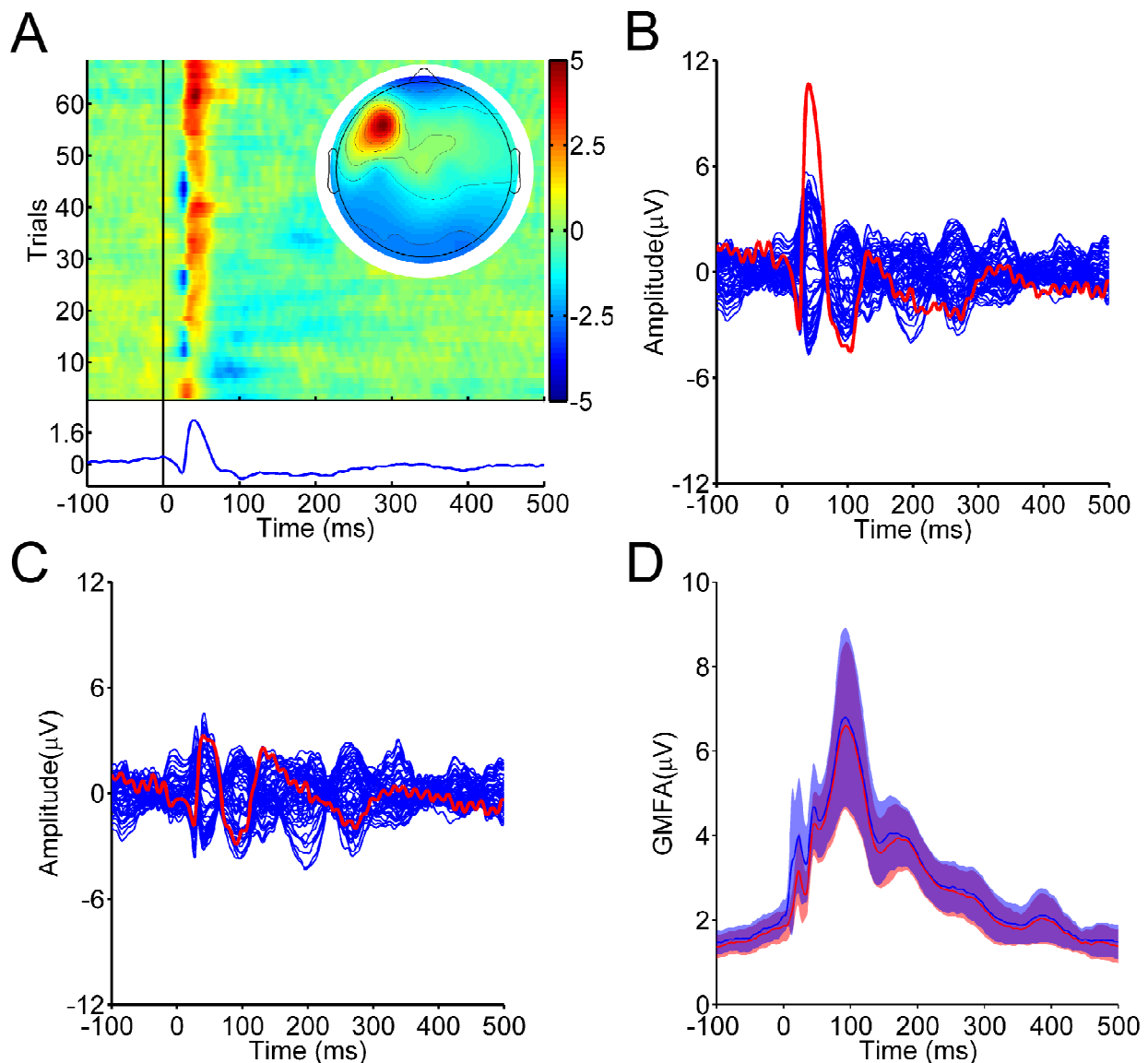


Figure 4: Bad electrode artifact components. A) Independent component representing a bad electrode, most likely resulting from coil-electrode contact. B) Butterfly plot showing TMS-evoked potentials without the component in A removed. Activity from this component largely contributes to the outlier electrode highlighted in red. C) Butterfly plot showing TMS-evoked potentials with component in A removed. D) Global mean field amplitude (GMFA) traces averaged across all participants (shaded line = 95% confidence interval). Red = signal with bad electrode components removed, blue = signal without bad electrode components removed. Removing bad electrode components did not significantly alter EEG signal in the group data (cluster-based statistics, $p > 0.05$).

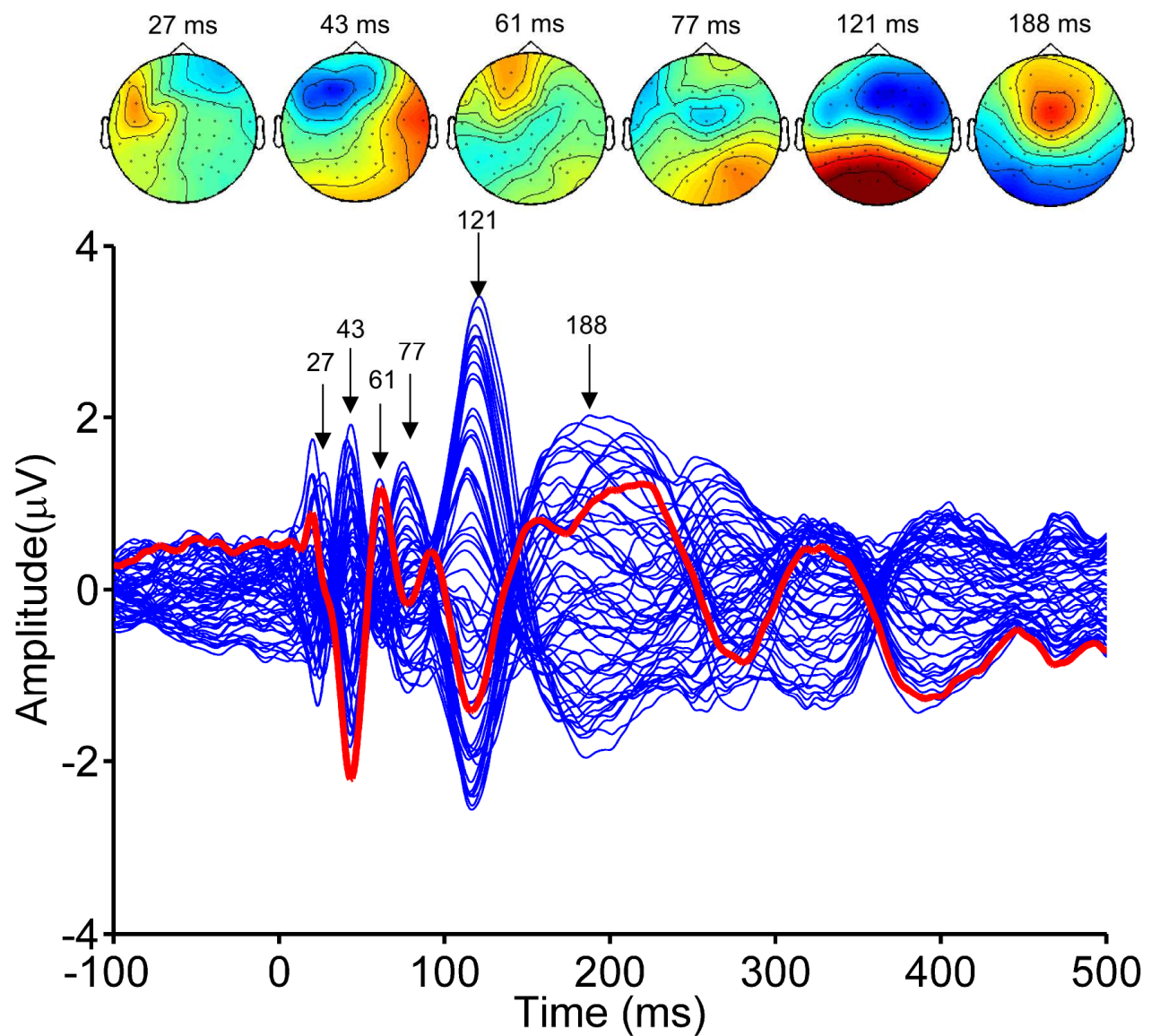


Figure 5: Spatiotemporal spread of the TMS-evoked potential following stimulation over left dorsolateral prefrontal cortex with artifacts removed (average across all participants). Voltage densities for each of the six peaks indicated by the arrows are plotted above. Red line = the electrode under the coil (F3).

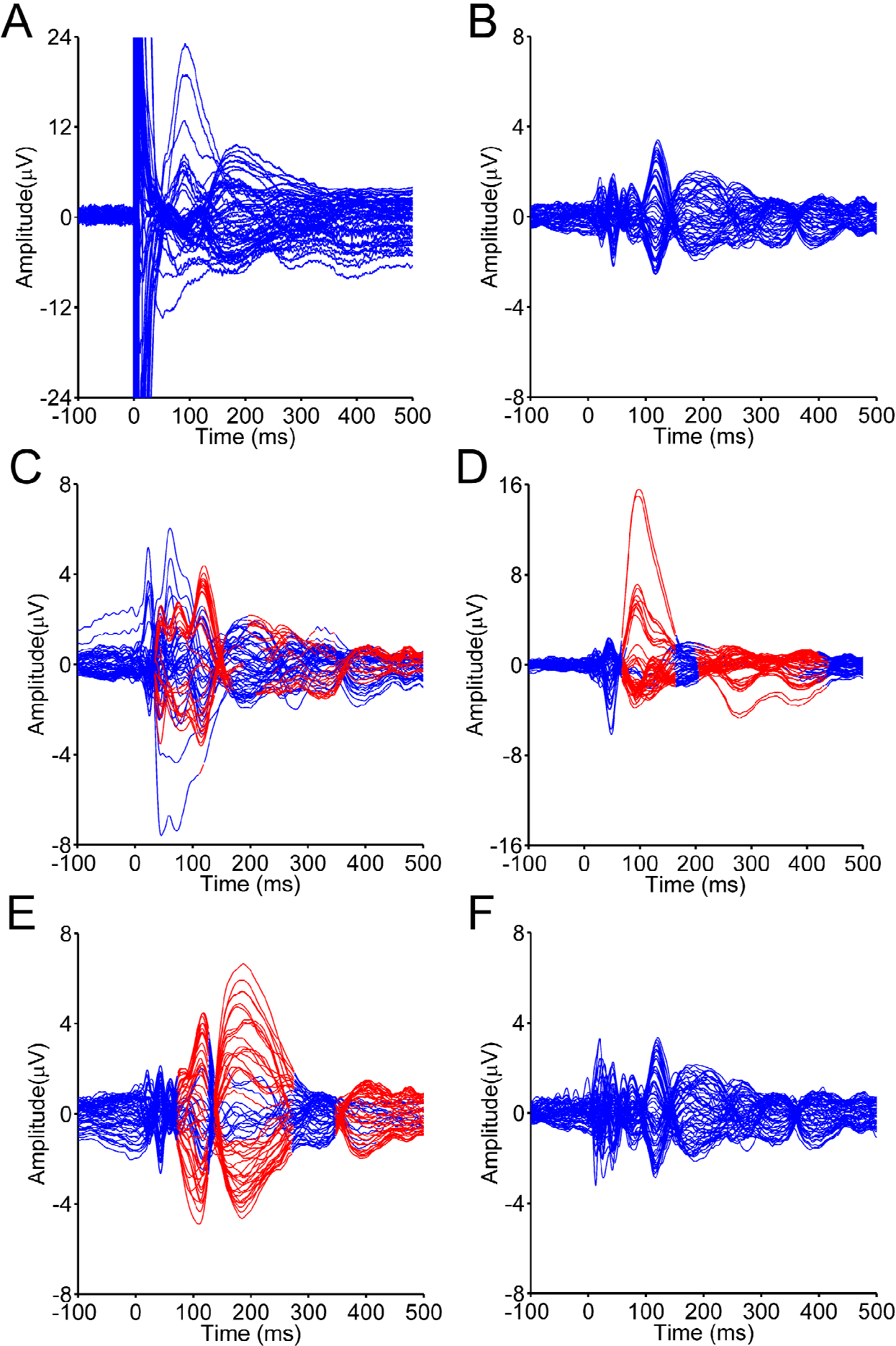


Figure 6: Butterfly plots demonstrating the effect of each artifact on spatiotemporal properties of the TMS-evoked potential (averaged across all participants). A) Raw, unprocessed signal prior to removal of any artifacts (re-referenced to average). B) Signal with all artifacts removed. Note the change in scale. C) Signal with slow decay artifacts present. D) Signal with blink artifacts present. Note the change in scale. E) Signal with auditory artifacts present. F) Signal with bad electrode artifacts present. Red lines in C-F indicate electrodes and time points significantly different to signal with all artifacts removed in B (cluster-based statistics, $p < 0.05$).

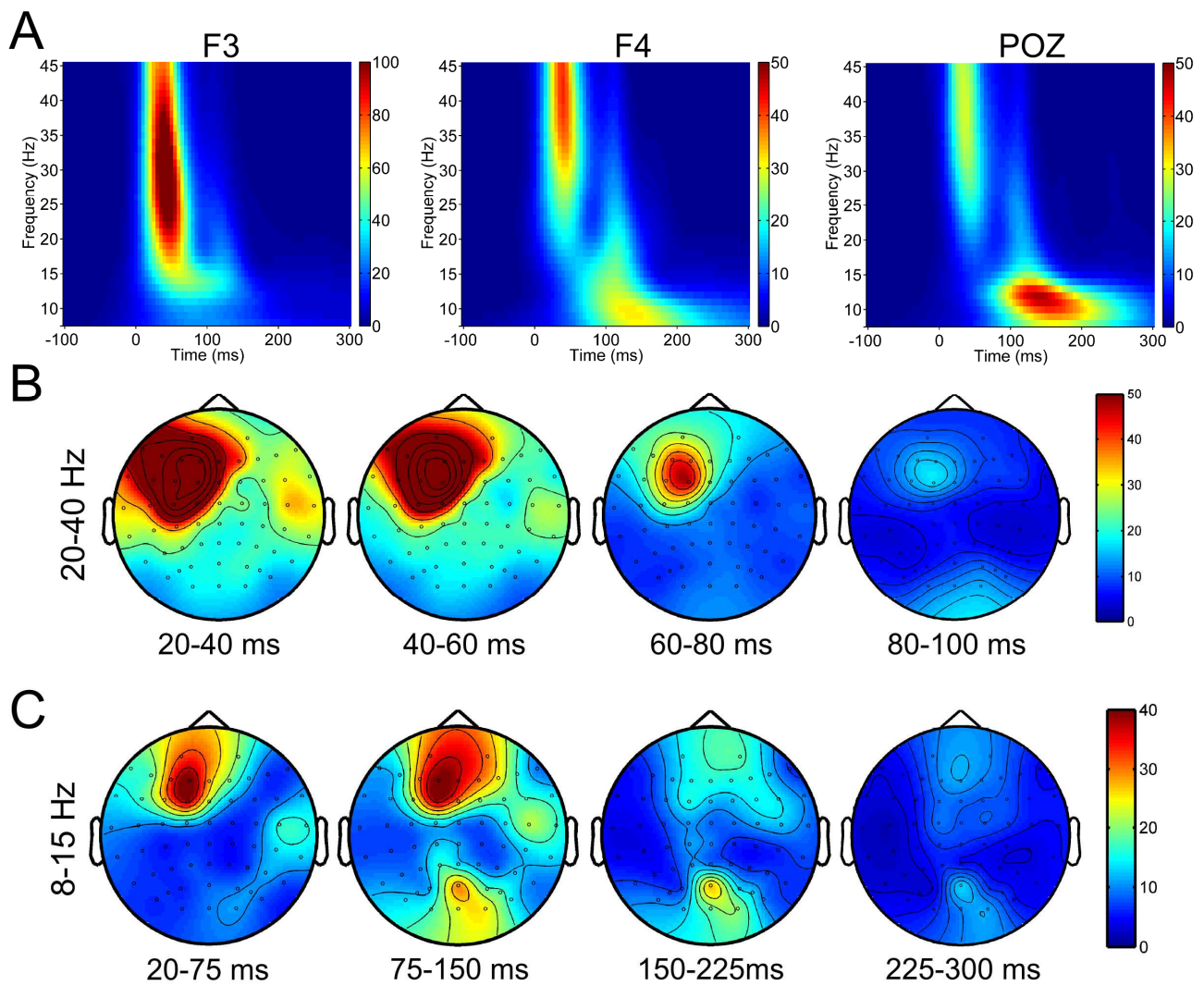


Figure 7: TMS-evoked oscillations following stimulation over left dorsolateral prefrontal cortex with artifacts removed (average across all participants). A) Time-frequency plots of TMS-evoked oscillations at F3, F4 and POZ electrodes. B) Spatiotemporal spread of 20-40Hz TMS-evoked oscillations over the first 100 ms. C) Spatiotemporal spread of 8-15 Hz TMS-evoked oscillations over the first 300 ms.

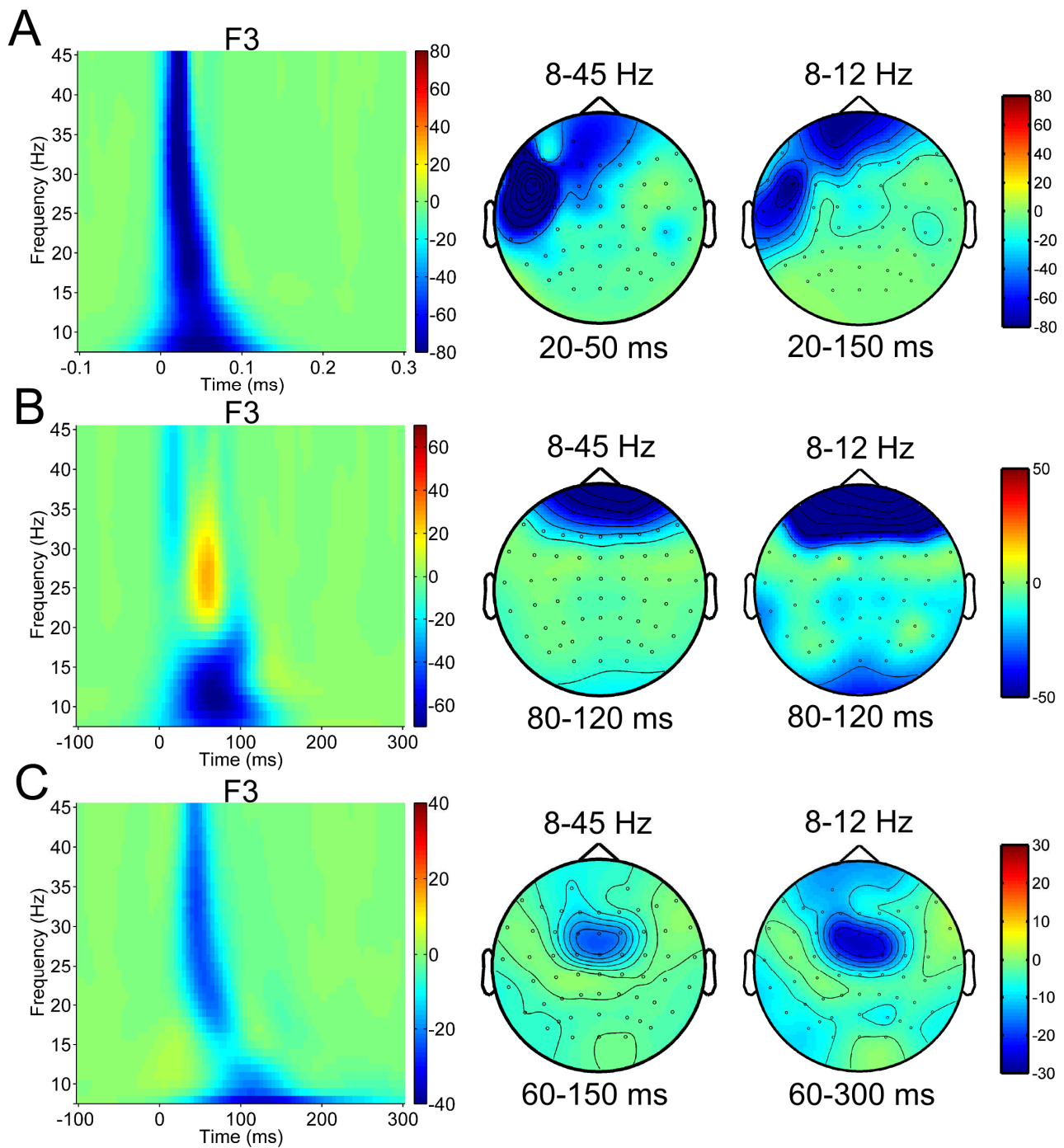


Figure 8: Time-frequency plots and topoplots demonstrating the effect of each artifact on TMS-evoked oscillations (averaged across all participants). Plots represent differences between conditions with and without artifacts removed. Blue = increase with artifact. A) Difference in TMS-evoked oscillations with slow decay artifacts present. B) Difference in TMS-evoked oscillations with blink artifacts present. C) Difference in TMS-evoked oscillations with auditory artifacts present.

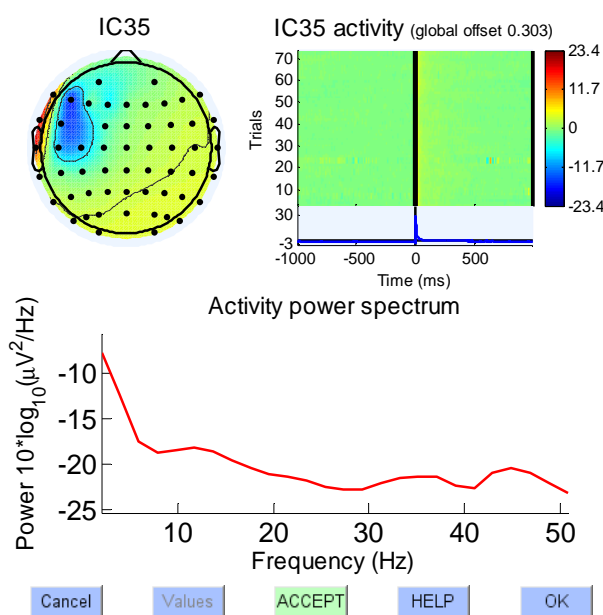
Supplementary material

In this document, we have provided descriptions and examples of independent components identified as artifacts from individual participants. These components have been grouped in to the sub-type categories described in the main text. Decisions on independent components were made taking in to account as much information as possible (i.e. topography, time course, spectral signature, consistency etc.). The examples were generated using the 'Reject data using ICA' option (Tools -> Reject data using ICA -> Reject components by map) in EEGLAB (Delorme and Makeig, 2004).

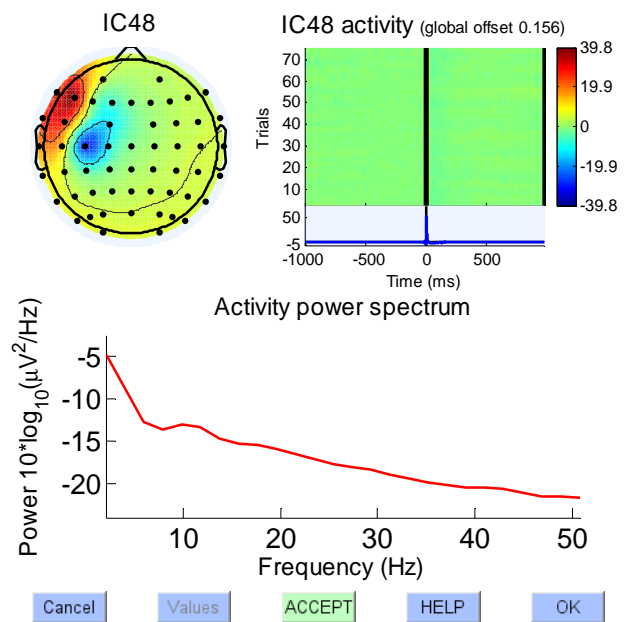
1. Fast decay artifacts

Fast decay artifacts were identified and removed following the first ICA run. This artifact subtype was characterised primarily by a large amplitude ($>10 \mu\text{V}$) signal occurring in the first 50 ms following TMS. The component was easy to identify as it was generally several orders larger than any other component. Due to the removal of the TMS pulse artifact and TMS-evoked muscle artifact prior to this ICA run, this artifact also presented with a sharp leading edge followed by an exponential decay. Polarity could be either positive or negative (examples 1.1-1.4).

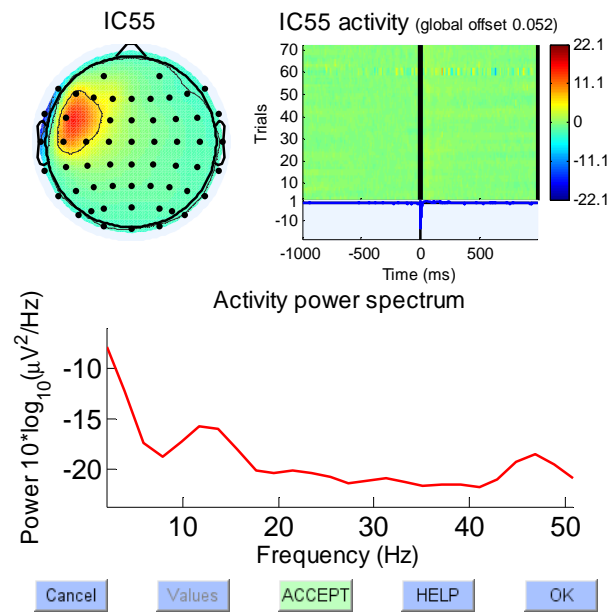
Example 1.1



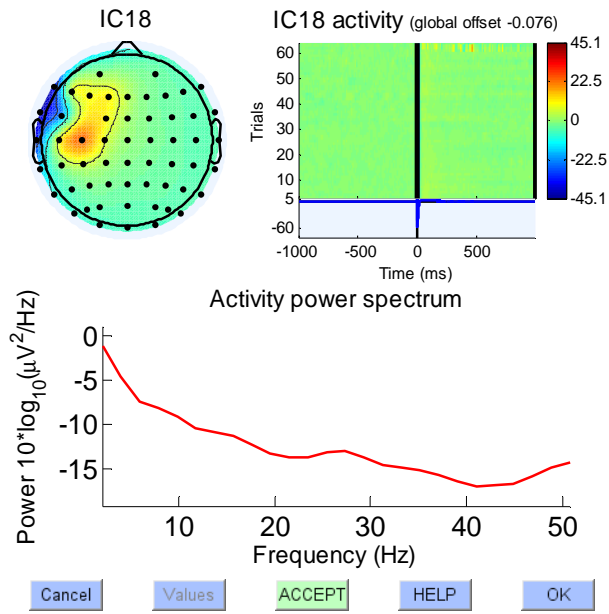
Example 1.2



Example 1.3



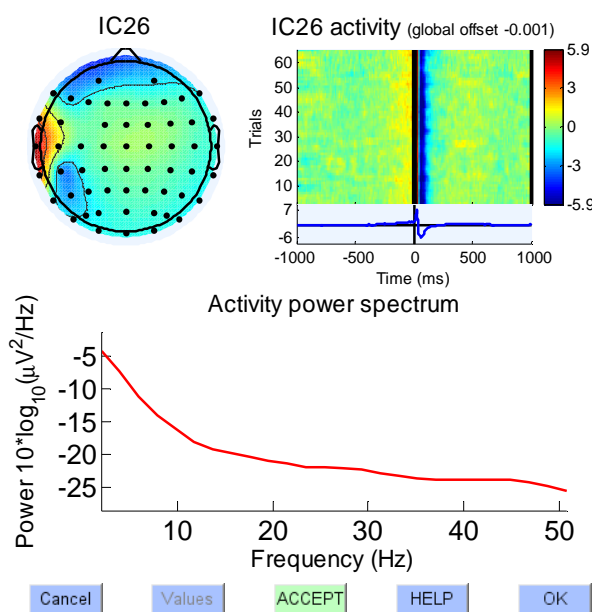
Example 1.4



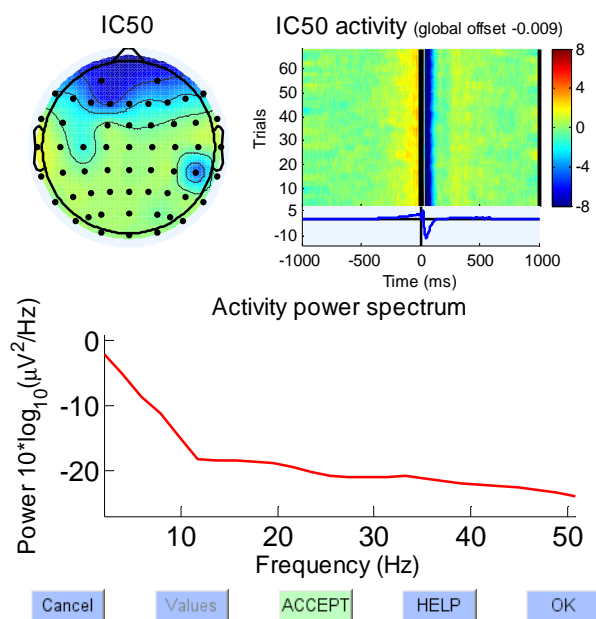
2. Slow decay artifacts

Slow decay artifacts were identified and removed following the second ICA run. This artifact subtype was characterised by a peak between 10-50 ms that was followed by an exponential decay. This artifact was often very consistent between trials. In participants with a large fast decay artifact, this slow decay artifact was often also large, especially compared with other components (examples 2.1-2.2), however smaller decay components were also present (example 2.3). In some participants, the slow decay artifact could separate in to multiple components. Examples 2.4-2.6 are from the same participant. Notice that the topography and shape of example 2.4 and 2.5 are almost identical, however example 2.5 has a later peak. Example 2.6 also has a similar topography to the earlier examples and the trial-by-trial activity (in the colour map) coincides with trials of smaller activity in example 2.5 suggesting these two components share the same source.

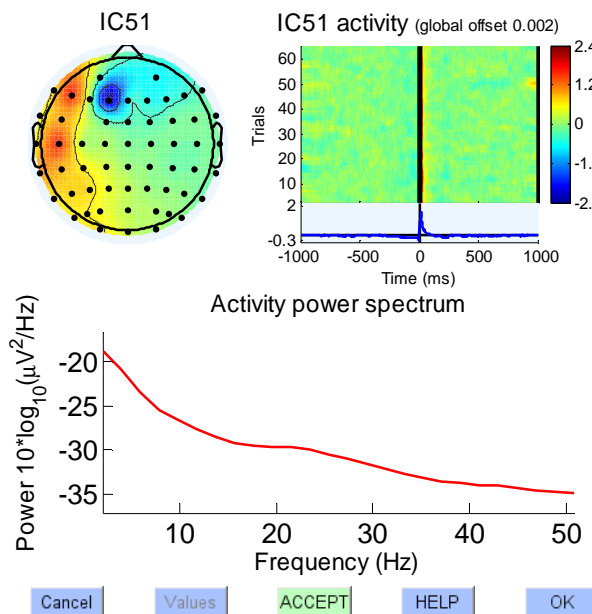
Example 2.1



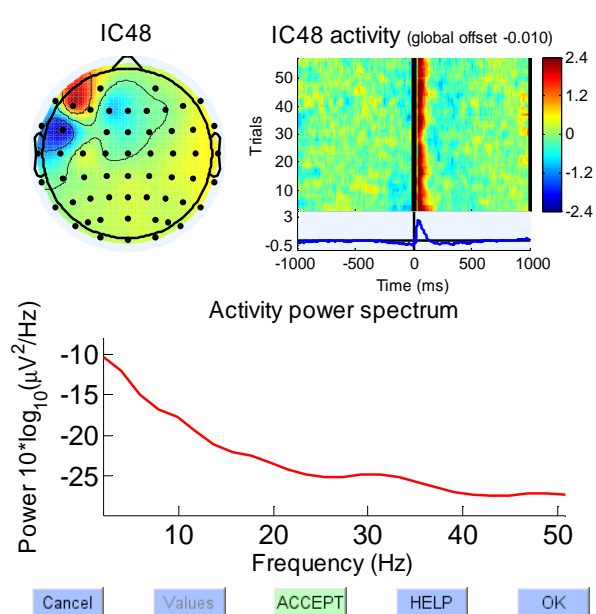
Example 2.2



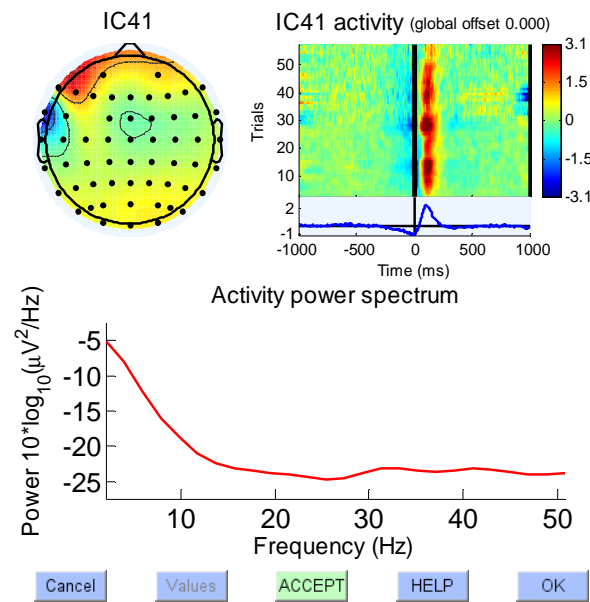
Example 2.3



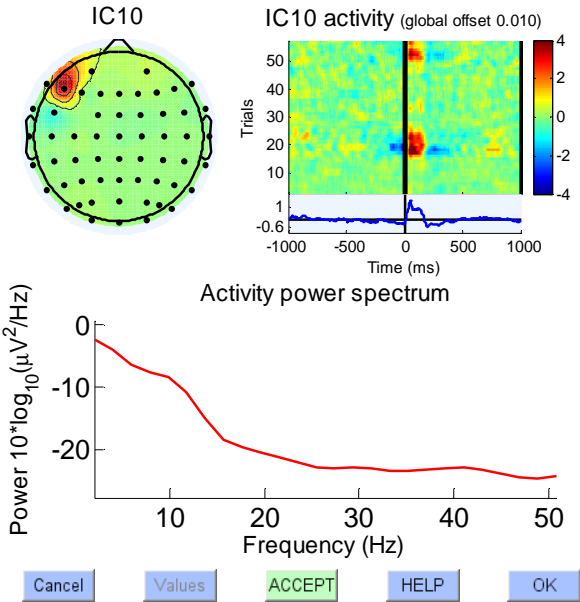
Example 2.4



Example 2.5



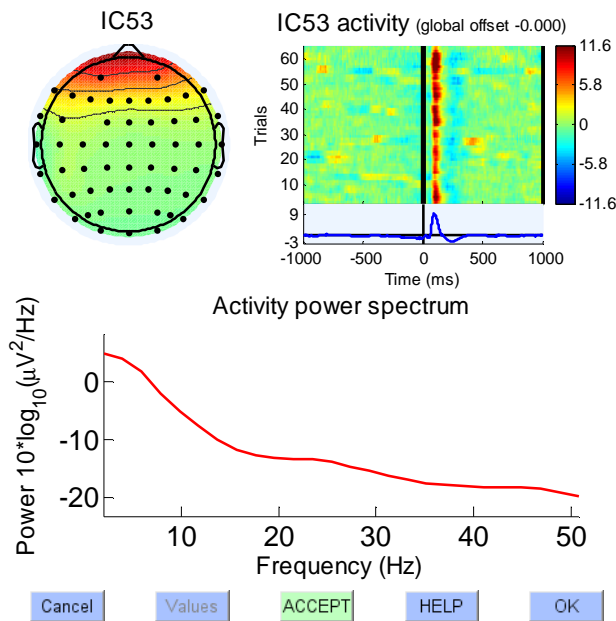
Example 2.6



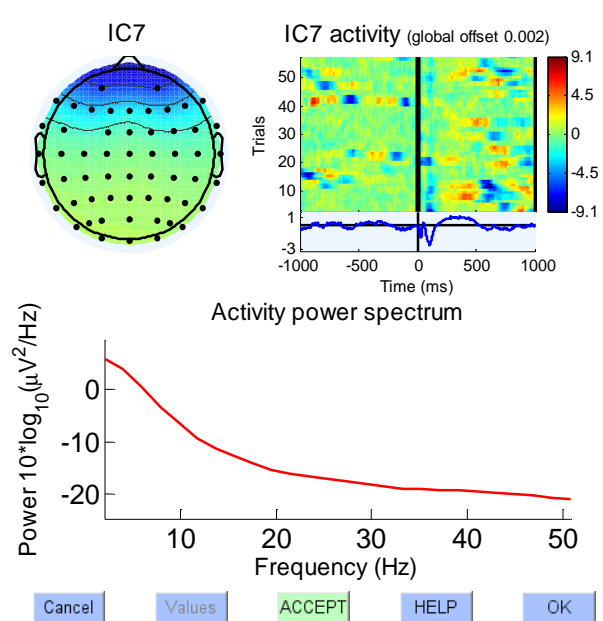
3. Blink artifacts

Blink artifacts were identified and removed following the second ICA run. This artifact subtype was characterised by activity concentrated over the frontal electrodes (AF3, AF4), which quickly decreased towards more posterior electrodes. Activity could be time-locked to the TMS pulse with peaks at approximately 90-100 ms (example 3.1), however spontaneous blinks occurring elsewhere in the trials were often also combined (example 3.2). In participants with particularly large blinks, this artifact could be separated in to two components made obvious by the identical topography (examples 3.3-3.4 from the same participant).

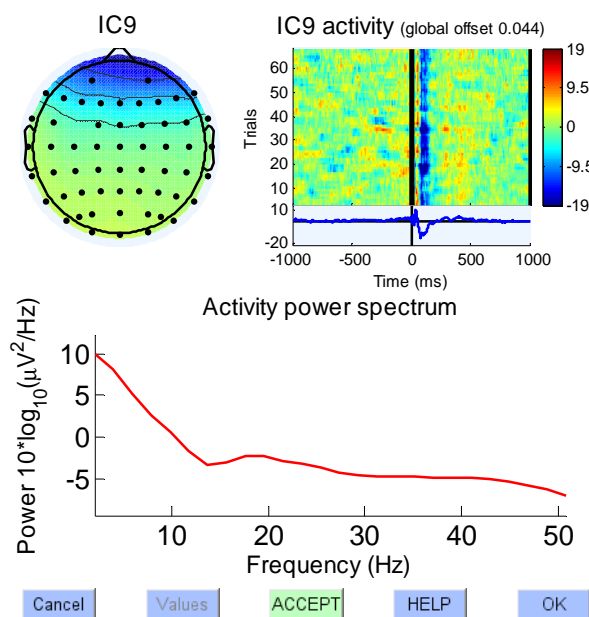
Example 3.1



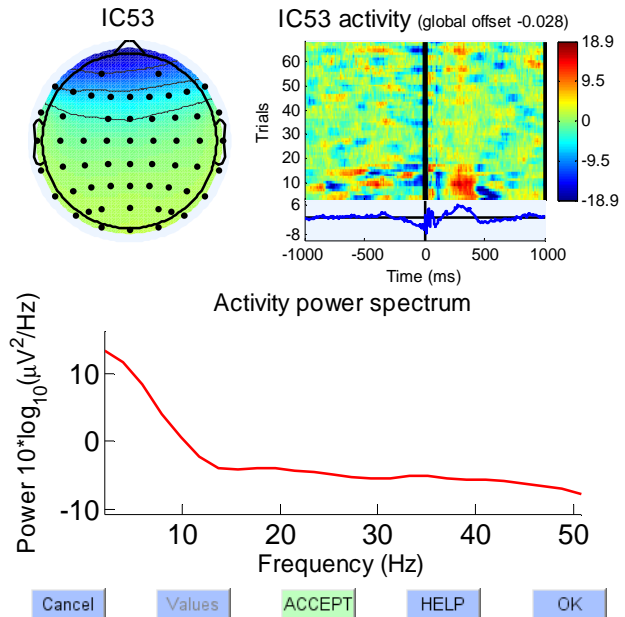
Example 3.2



Example 3.3



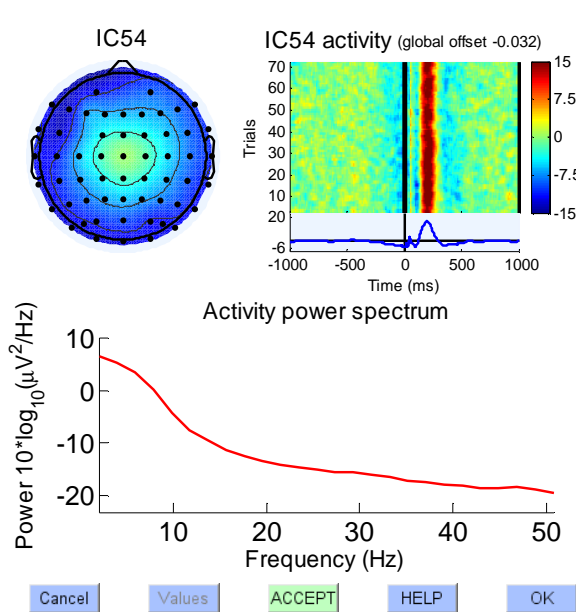
Example 3.4



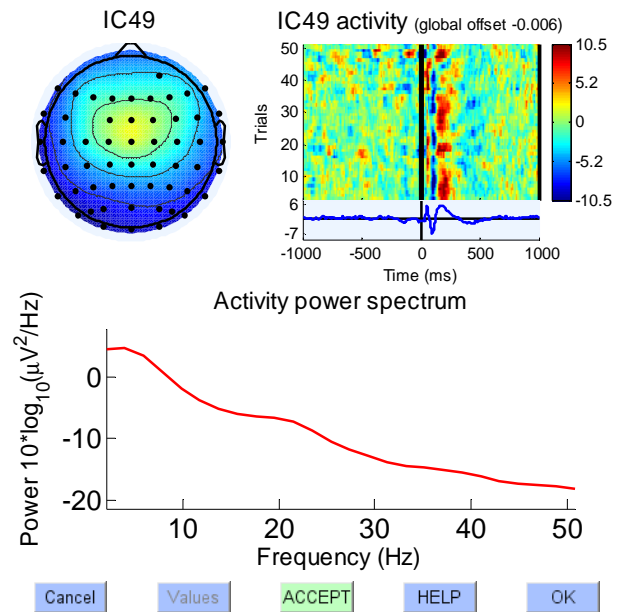
4. Auditory artifacts

Auditory artifacts was identified and removed following the second ICA run. This artifact sub-type was characterised by a topography centring over CZ to FZ and a time course with bipolar peaks at approximately 100-200 ms (examples 4.1-4.4). Note that the time course could vary by up to 50 ms in some participants. Also note that in some instances when the first and second peak were nearly identical in amplitude, the signal could cancel resulting in a difficult to distinguish topography (example 4.4; centre over CZ is present but faint, however the artifact can be identified by its time course).

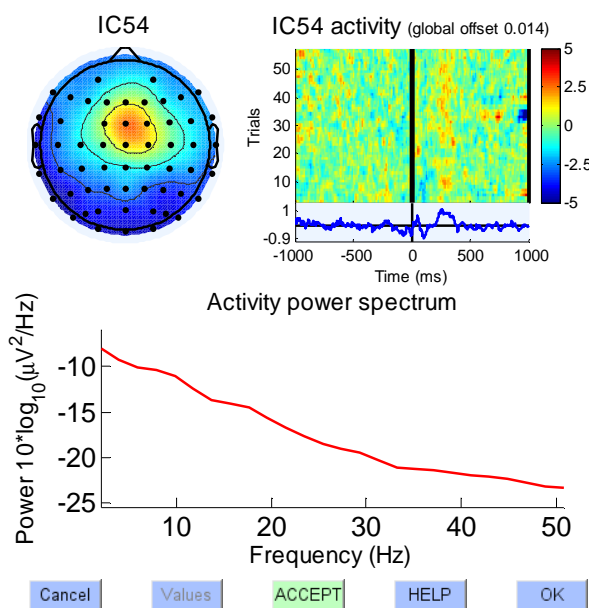
Example 4.1



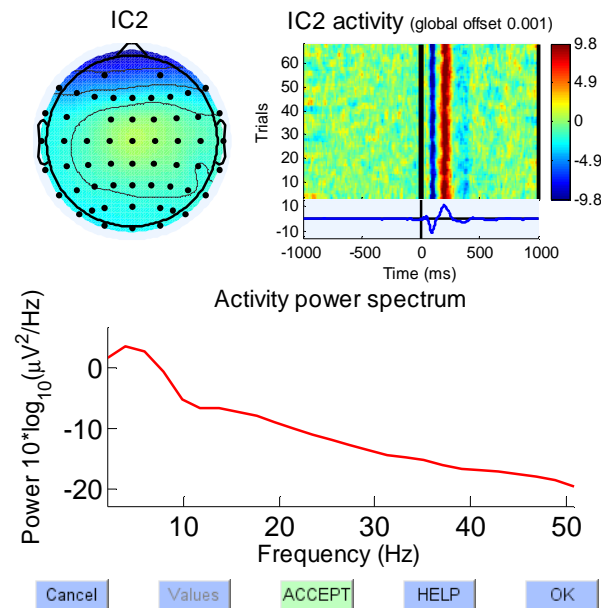
Example 4.2



Example 4.3



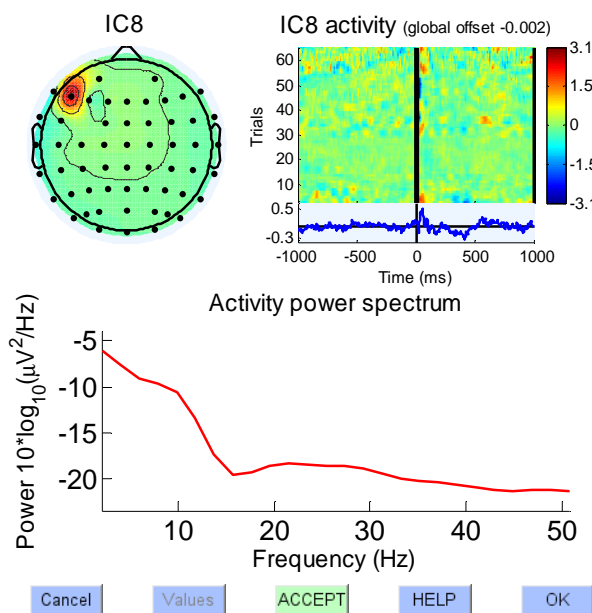
Example 4.4



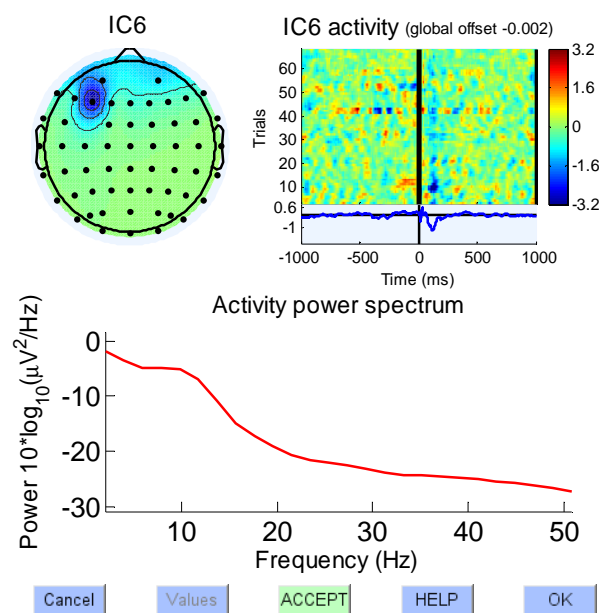
5. Bad electrodes

Bad electrode artifacts were identified and removed following the second ICA run. This sub-type captured several artifact categories. First, components with topographies centred on single electrodes or with bipolar topographies over neighbouring electrodes near the stimulation site (F3, F5, FC3, FC5) were identified (examples 5.1-5.4). These components resulted in unrealistic topographies (see figure 4, main text) and possibly resulted from coil-electrode contact. Second, components with a time course peaking during the interpolation period were identified (examples 5.5-5.6). These components represented artificially introduced signal and were therefore considered artifacts. Third, components consistent with persistent scalp muscle activity (i.e. positioned around lateral scalp positions, broad band frequency spectrums that either increased or remained stable above 10 Hz, no TMS time-locked activity etc.) were identified (examples 5.7-5.9). Finally, any other components with topographies centred on single electrodes and containing spurious activity were identified (example 5.10-5.12).

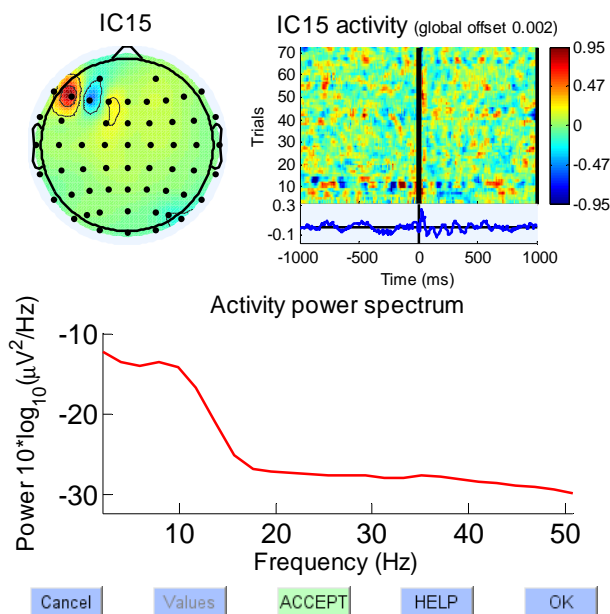
Example 5.1



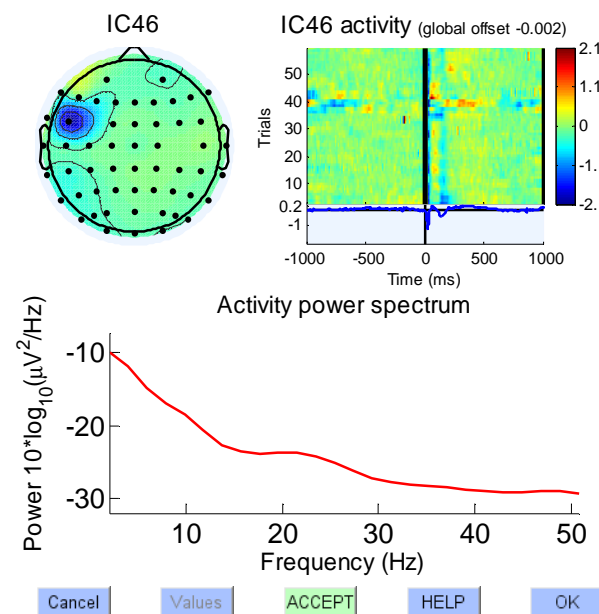
Example 5.2



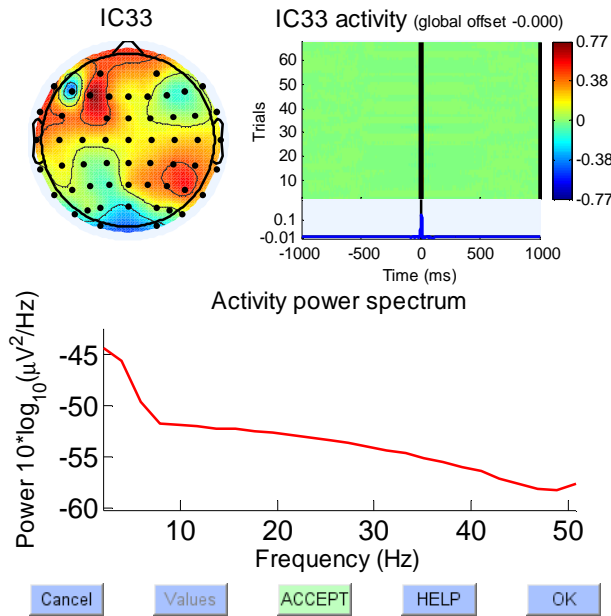
Example 5.3



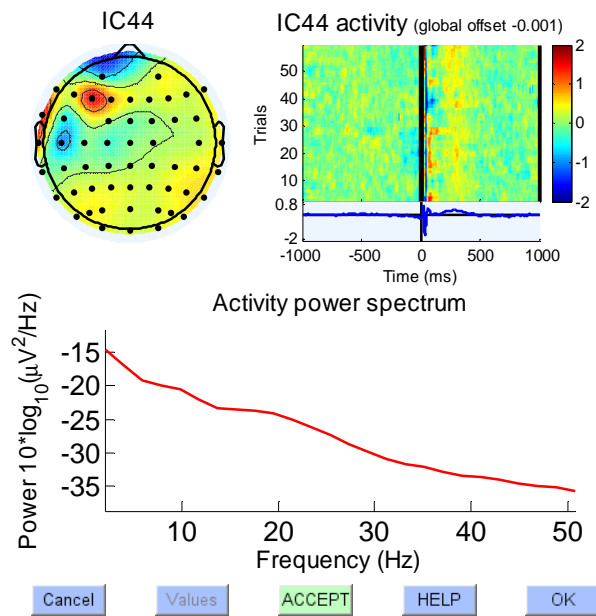
Example 5.4



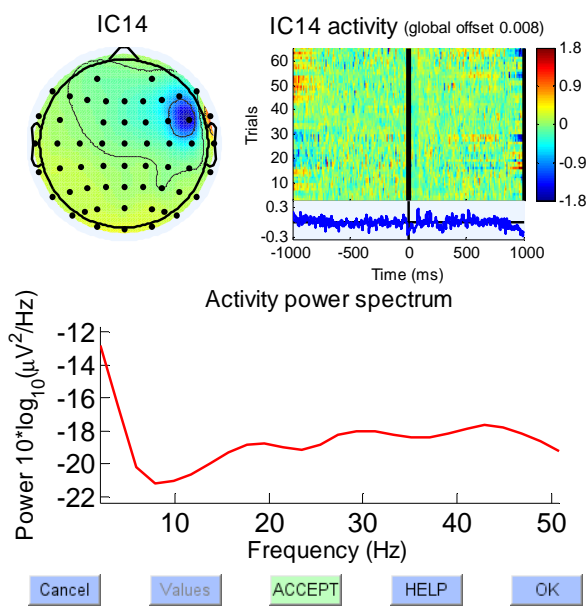
Example 5.5



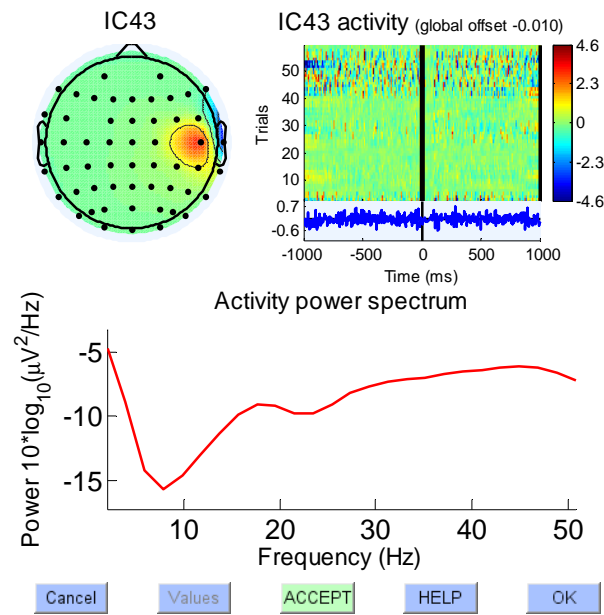
Example 5.6



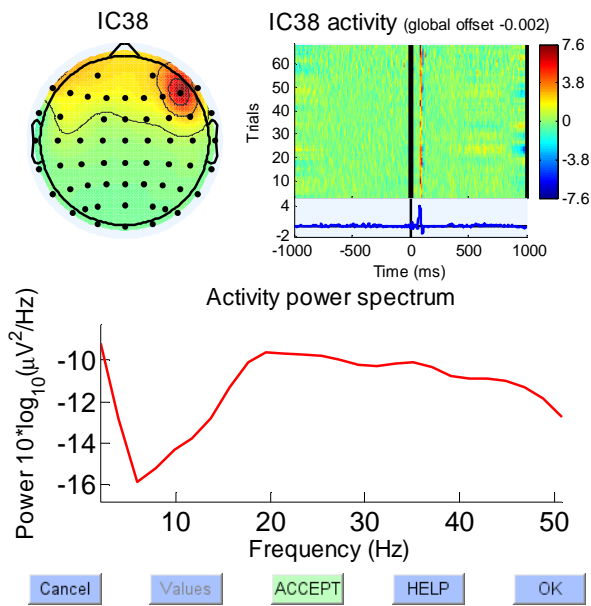
Example 5.7



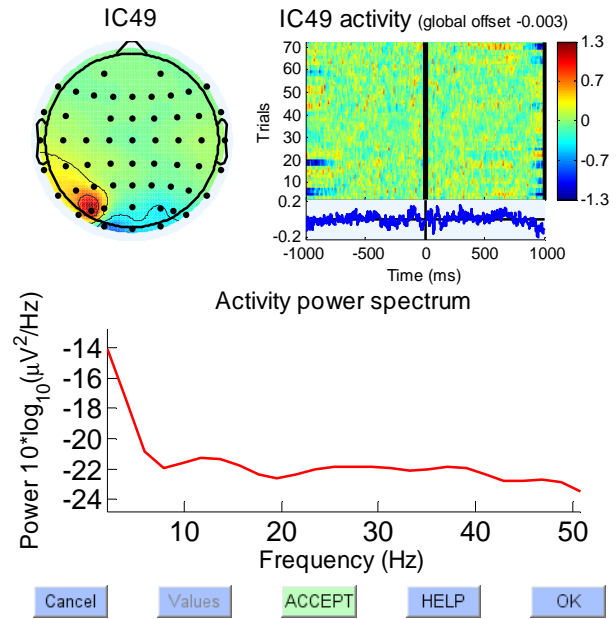
Example 5.8



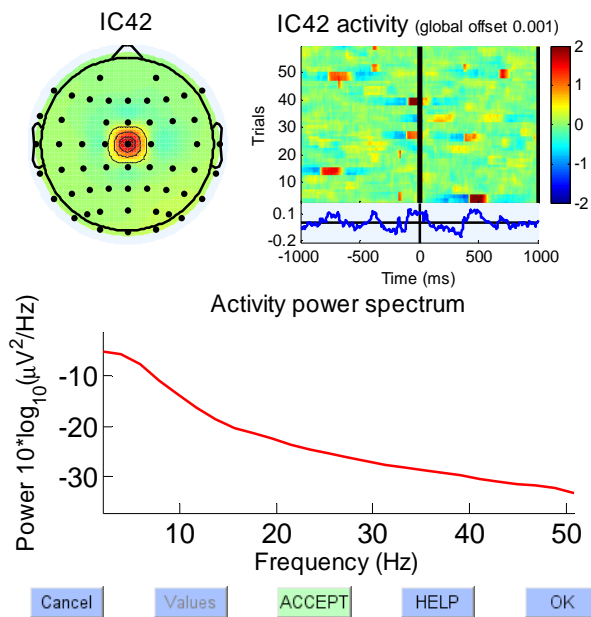
Example 5.9



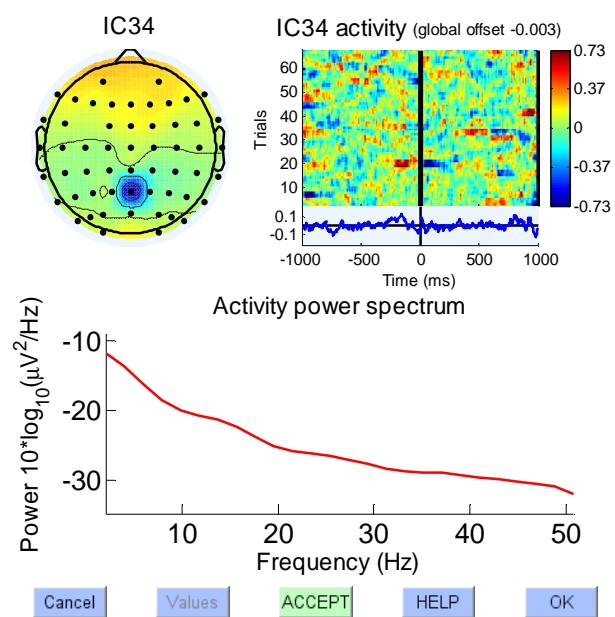
Example 5.10



Example 5.11



Example 5.12



REFERENCES

Delorme, A., Makeig, S., 2004. EEGLAB: an open source toolbox for analysis of single-trial EEG dynamics including independent component analysis. *Journal of neuroscience methods* 134, 9–21.

CHAPTER SIX

Mechanisms underlying TMS-evoked potentials in motor cortex

Rogasch NC, Daskalakis ZJ, Fitzgerald PB. (2013). Mechanisms underlying long-interval cortical inhibition in the human motor cortex: a TMS-EEG study. *Journal of Neurophysiology*. 109(1):89-99.

Preamble to empirical paper

Having established a method for removing artifacts in Chapter 5, we now focus on the information contained in TMS-evoked cortical potentials. Several studies over the motor cortex have provided evidence that early peaks of the TMS-evoked potential (i.e. N15, P30) share properties with excitatory neurotransmission (relationship with TMS intensity, coil angle, MEPs etc.; Bonato et al., 2006; Komssi et al., 2004; Mäki & Ilmoniemi, 2010), whereas later peaks (i.e. N100) share properties with inhibitory neurotransmission (modulation with tasks etc.; Bonnard, Spieser, Meziane, de Graaf, & Pailhous, 2009; Kicić, Lioumis, Ilmoniemi, & Nikulin, 2008; Nikulin et al., 2003). This pattern of activity following suprathreshold TMS is consistent with patterns observed using paired-pulse paradigms (i.e. facilitatory 25-45 ms, inhibitory 50-150 ms) recorded using MEPs and descending spinal volleys (Nakamura, Kitagawa, Kawaguchi, & Tsuji, 1997; Valls-Solé et al., 1992). In line with this research, our group has shown that TMS-evoked cortical activity recorded with EEG is also inhibited during long-interval cortical inhibition (LICI; paired-pulse with interstimulus interval of 100 ms; Daskalakis, Farzan, Barr, Maller, et al., 2008; Fitzgerald et al., 2008). However, the relationship between specific TEP peaks and LICI is unclear. We hypothesised that if early TEPs (P30) reflected excitatory neurotransmission, then altering LICI strength should result in a similar modulation of TEP size to that observed with MEPs (as MEP generation is dependent on pyramidal cell excitation). We also hypothesised that if later TEPs (N100) reflected inhibitory neurotransmission, then the slope of the signal immediately preceding the test pulse (i.e. the N100 evoked by the conditioning pulse) should predict LICI of MEPs and TEPs. In the following published paper, we applied single and paired pulse (LICI) TMS over motor cortex and measured MEPs and TEPs. We altered LICI strength by manipulating

the conditioning and test pulse intensity and observed the effect on the inhibition of MEPs and the peaks of several different TEPs.

Note that chronologically, the experiments presented in this chapter were performed before those reported in Chapter 5. Consequently ICA was not used to correct for artifacts. As this study was in the motor cortex, scalp muscle activation was considerably smaller than in the DLPFC and had recovered by 30 ms in all but one participant. In addition, blinks were considerably less prominent, however were corrected using a validated eye-correction algorithm (Croft & Barry, 2000). Finally, auditory components were minimised by auditory masking (white noise) during the experiment (Ter Braack, de Vos, & van Putten, 2013).

Due to copyright, readers are directed to the following reference:

Rogasch NC, Daskalakis ZJ, Fitzgerald PB. (2013). Mechanisms underlying long-interval cortical inhibition in the human motor cortex: a TMS-EEG study. *Journal of Neurophysiology*. 109(1):89-99. DOI: 10.1152/jn.00762.2012

CHAPTER SEVEN

Mechanisms underlying TMS-evoked potentials in DLPFC

Rogasch NC, Daskalakis ZJ, Fitzgerald PB. Mechanisms underlying markers of cortical inhibition in the dorsolateral prefrontal cortex: a TMS-EEG study. (Submitted).

Preamble to empirical paper

The results from Chapter 6 support evidence that the P30 over motor cortex reflects excitatory neurotransmission, whereas the N100 likely reflects inhibitory neurotransmission mediated by the GABA_B receptor. A peak similar to the N100 is also observed following stimulation of other cortical regions and has been reported from the DLPFC (Kähkönen et al., 2005; Lioumis, Kicić, Savolainen, Mäkelä, & Kähkönen, 2009). Although the DLPFC N100 has been attributed to inhibitory activity (Kähkönen et al., 2003), little to no empirical evidence exists supporting this assumption. In the following paper we adopted a similar paired pulse approach over the DLPFC and provide some of the first evidence that the N100 following DLPFC stimulation also reflects inhibitory neurotransmission. Additionally, we assessed inter-individual variation of the N100 slope and in LICI of different TEPs and TMS-evoked oscillations. We predicted that the N100 slope gradient would be related to LICI of an early peak (N40) and high-frequency TMS-evoked oscillations across individuals. We also predicted that LICI would not only suppress local activity, but would also reduce the TMS-evoked propagation of activity to distant cortical regions.

Mechanisms underlying markers of cortical inhibition in dorsolateral prefrontal cortex: a TMS-EEG study

Nigel C. Rogasch¹, Zafiris J. Daskalakis² and Paul B. Fitzgerald¹

1. Monash Alfred Psychiatry Research Centre, Central Clinical School, The Alfred and Monash University, Melbourne, Australia
2. Temerty Centre for Therapeutic Brain Intervention, Centre for Addiction and Mental Health, University of Toronto, Toronto, Canada

Running head: Cortical inhibition in prefrontal cortex.

Key words: Transcranial magnetic stimulation, electroencephalography, cortical inhibition, GABA_B receptor, dorsolateral prefrontal cortex.

Word count (abstract): 279

Word count (main text): 4,460

Figures: 6

Correspondence: Nigel C. Rogasch
Monash Alfred Psychiatry Research Centre
Level 4, 607 St. Kilda rd.
Melbourne,
Victoria, Australia, 3004

ABSTRACT

Background: Paired-pulse transcranial magnetic stimulation combined with electroencephalography (TMS-EEG) is a method for studying cortical inhibition from regions such as the dorsolateral prefrontal cortex (DLPFC). However, little is known about the mechanisms that underlie TMS-evoked potentials (TEPs) from the DLPFC, let alone inhibition of these components. Therefore, the aim of this study was to assess the mechanisms underlying cortical inhibition in the DLPFC measured using TMS-EEG.

Methods: 30 healthy volunteers received single and paired (interstimulus interval = 100 ms) TMS to the left DLPFC. Variations in long-interval cortical inhibition (LICI) of different TEP peaks (N40, P60, N100) and different TMS-evoked oscillations (alpha, lower beta, upper beta and gamma) over left DLPFC were compared between individuals. Variation in the slope of the N100 peak following single pulse TMS, another putative marker of inhibition, was also compared with LICI of each measure. Finally, the effect of LICI on TEP propagation and entrainment of TMS-evoked oscillations in distant cortical regions was assessed across the scalp.

Results: LICI resulted in significant suppression of all TEP peaks and TMS-evoked oscillations at the left DLPFC (all $p < 0.05$). Variation in LICI of P60 and N100 significantly correlated, however there was no relationship between these peaks and LICI of N40 or between LICI of any TMS-evoked oscillation frequency. Variation in N100 slope correlated with LICI of N40 and beta oscillations. In addition, propagation of TEPs and generation of TMS-evoked oscillations in distant cortical regions was also suppressed in the presence of LICI.

Conclusions: The LICI paradigm and N100 following single pulse TMS reflect complementary methods for assessing GABA_B-mediated cortical inhibition in the DLPFC. In addition to local TMS-evoked activity, LICI also suppresses TMS-evoked outputs from the DLPFC.

INTRODUCTION

Cortical inhibition refers to suppression of neuronal activity and is a fundamental mechanism for both the generation and control of coordinated cortical network activity [1]. In the mature cortex, cortical inhibition is largely governed by the neurotransmitter γ -amino butyric acid (GABA), which alters polarization of neuronal membranes via fast acting GABA_A receptors and slower acting GABA_B-receptors [2]. Many studies have focused on the role of GABA_A receptors in generating network activity such as gamma oscillations (30-80 Hz) [3–5], however the role of GABA_B-mediated inhibition is less understood. Recent work has suggested that GABA_B-mediated cortical inhibition plays an important role in modulating cortical network activity [6]. For instance, presynaptic GABA_B inhibition of inhibitory interneurons appears essential for modulating gamma activity [7], an oscillatory band which is implicated in a wide range of cognitive processes such as working memory and selective attention [8]. Importantly, dysfunction of GABA_B-mediated inhibition may play a crucial role in neurological and psychiatric conditions that are thought to result from impaired control of network activity, such as epilepsy [9] and schizophrenia [10,11].

In humans, GABA_B-mediated cortical inhibition can be assessed using transcranial magnetic stimulation (TMS). TMS utilizes electromagnetic induction to non-invasively depolarize excitatory and inhibitory cortical neurons across the scalp [12]. When a suprathreshold TMS pulse is preceded by a suprathreshold conditioning pulse at intervals of 50-200 ms (i.e. paired-pulse TMS), TMS-evoked neuronal activity is suppressed through a process known as long-interval cortical inhibition (LICI). This can be measured as either a decrease in motor cortical output via motor evoked potentials (MEPs) in peripheral muscles [13,14] or modulation of TMS-evoked cortical potentials (TEPs) assessed directly from the cortex using electroencephalography (EEG) [15,16]. LICI shares many similarities with GABA_B-mediated cortical inhibition measured in animal studies, such as time course [13,17], the intensity of stimulation required for activation [13,18–20], pre-and postsynaptic activity [21–24], reduction of descending volleys in the motor system [14,25] and enhancement with the GABA_B-agonist baclofen [26,27]. In addition to paired-pulse paradigms, a growing body of evidence suggests that GABA_B-mediated inhibition can also be measured following single pulses in TMS-EEG recordings [28,29]. The N100 peak is one of the most reproducible TEPs

following stimulation of the motor cortex [30] and has a similar time course to inhibitory postsynaptic potentials resulting from GABA_B receptor activation [31–33]. Accordingly, different motor tasks modulate N100 amplitude in a way consistent with cortical inhibition [34–38] and N100 amplitude correlates with the cortical silent period, another TMS-evoked motor measure of GABA_B-mediated inhibition [29].

Although useful for studying motor physiology, the real strength of combined TMS-EEG is the potential for studying inhibitory mechanisms outside of the motor cortex. Studying non-motor regions represents a vital step for understanding the functional role of GABA_B-mediated inhibition in tasks and illnesses which are associated with higher-order brain regions, such as the dorsolateral prefrontal cortex (DLPFC). LICI of both TMS-evoked activity [15,16] and TMS-evoked oscillations [39,40] has recently been demonstrated from the DLPFC using TMS-EEG. In addition, LICI strength from this region was found to correlate with performance on a working memory task [41,42], providing preliminary evidence for a role of GABA_B-mediated inhibition in cognition. However, very little is known about the mechanisms that underlie TEPs or TMS-evoked oscillations from the DLPFC, let alone inhibition of these measures. In addition, whether LICI suppresses TMS-evoked outputs to other cortical regions as well as local activity also remains unclear.

The aim of this study was to provide evidence for the mechanism underlying TMS-EEG measures of cortical inhibition in the DLPFC. We assessed natural variation in LICI strength across a population of healthy volunteers using paired-pulse TMS-EEG. First, we assessed whether variation in LICI of early and late TEPs from DLPFC were related or independent. Second, we evaluated whether the N100 slope following single pulse TMS was associated with LICI of TEPs and TMS-evoked oscillations. Finally, we assessed whether LICI suppressed TMS-evoked propagation from the DLPFC to wider cortical regions as well as local activity.

METHODS

30 volunteers participated in the current study (32.2 ± 11 years, 8 female). Volunteers had no history of neurological or psychiatric illnesses and provided informed written consent before commencement of the study. All experimental procedures were approved by the Monash University, Alfred Hospital and Centre for Addiction and Mental Health Human Research Ethics Committees in accordance with the declaration of Helsinki.

Procedures

Participants were seated comfortably with their hands resting in their laps. An EEG cap was fitted to their head and electrodes were placed over the right abductor pollicis brevis (APB) muscle for electromyographic (EMG) recordings. Resting motor threshold (RMT) and the TMS intensity required to evoke a motor evoked potential (MEP) of ~ 1 mV ($S1mV$) were then determined over the motor cortical region that produced the largest responses in APB. Following motor measures, the coil was positioned so the centre rested between the F3 and F5 electrode and the handle was rotated to a 45° angle relative to midline, producing a posterior-anterior current flow in the underlying cortex. This position provides the most accurate estimation of left DLPFC (border of BA9 and BA46) in the absence of neuronavigational equipment [43,44]. The coil border was marked using a felt tipped pen to allow repositioning. Participants then received 75 single and 75 paired (interstimulus interval = 100 ms) TMS pulses to the left DLPFC while they sat quietly and looked directly ahead with their eyes open. Single and paired pulses were randomly interleaved at a rate of 0.2 Hz (10 % jitter). Nine participants also received 50 single and 50 paired sham TMS pulses prior to real TMS.

Electromyography

EMG signal was recorded using bipolar Ag/AgCl electrodes positioned in a tendon-belly montage over APB. Signal was amplified (1000x) band-pass filtered (10-1000 Hz; PowerLab, ADInstruments, New Zealand) digitised (2000 Hz; Micro1401, Cambridge Electronic Design Ltd., UK), epoched around the TMS pulse (-200 to 500 ms) and displayed on a computer screen online.

Transcranial magnetic stimulation

Monophasic TMS pulses were delivered through a figure-of-eight coil (wingspan = 7 cm) connected to two Magstim 200 stimulators via a bistim module (Magstim Ltd., UK). RMT was determined as the stimulus intensity (% maximum stimulator output; MSO) required to evoke an MEP of amplitude $\pm 50 \mu\text{V}$ in at least 3 out of 6 consecutive trials [45]. S1mV was determined as the stimulus intensity (% MSO) required to evoke an MEP with average peak-to-peak amplitude between 0.7-1.3 mV over 5 trials (maximum stimulator output = $68.2 \pm 11 \%$; percentage of RMT = $120.3 \pm 6 \%$). For sham TMS, the coil was held over the same prefrontal position at 90° to the scalp with the wing resting on the head.

Electroencephalography

EEG was recorded using a cap with 57 electrodes (sintered Ag/AgCl) in standard 10-20 positions (Quickcap, Compumedics Ltd., Australia). To ensure cap position was as accurate as possible between participants, FPZ position was measured and marked on participant's heads and used to position the cap. EEG signal was amplified (1000x), filtered (DC-3500 Hz) and digitised (20 kHz; Synamps2, Compumedics Ltd.) and recorded on a computer for offline analysis. This arrangement along with the DC-coupling and large recording range of the amplifier captures the TMS artifact with minimal amplifier saturation and allows recording of neural signal within ~ 5 -10 ms following a pulse [46,47]. Electrode impedances were regularly checked and kept as low as possible throughout the experiment ($< 5 \text{ k}\Omega$).

Analysis

Analysis of EEG data were performed using EEGLAB [48], field trip [49] and custom scripts all on the MATLAB platform (R2013a, The Mathworks, USA). Single and paired pulse trials were analysed separately. EEG data were epoched around the TMS pulse (-1000 to 1000 ms), baseline corrected (-500 to -110 ms) and bad channels were removed. Data containing the TMS pulse artifact and peaks of any TMS-evoked muscle activity were truncated (-2 ms to $16.6 \pm 6 \text{ ms}$; cut-off altered on an individual basis) and the remaining data traces were concatenated together. Following truncation, data were downsampled to 1 kHz and trials

containing any large, paroxysmal artifacts were removed. Data were then passed through a first run of the fastICA algorithm [50] and components representing large decay components were removed. Data from the truncated window were then interpolated using a cubic function and all data were filtered using a butterworth, zero-phase band-pass filter (1-80 Hz). Epochs were then manually inspected and trials containing excessive muscle activity (i.e. from jaw clenching) or other uncharacterised activity were removed. The data was then passed through a second run of the fastICA algorithm and components representing slow decay artifacts, blink artifacts, auditory artifacts and bad electrode artifacts were removed. Following artifact removal, missing channels were replaced using spherical interpolation and data from each electrode were re-referenced to the average of all channels. Finally, butterfly plots were inspected for unusual activity (i.e. a single electrode with larger signal than all others). If unusual activity was detected, the artifact component identification and processing steps were repeated until this activity was removed. To ensure ICA was able to accurately decompose artifacts from paired pulse TMS in a similar fashion to single pulse TMS, trials containing voluntary blinks (collected at the beginning of the experiment; 40 blinks at approximately once per second) and trials containing paired sham TMS were concatenated to the paired pulse trials prior to ICA. Results from a representative individual are presented in figure 1. ICA consistently grouped fast decay, slow decay, blink and auditory artifacts into components following both pulses in the paired condition, indicating these artifacts could be reliably removed using this method.

-----Insert figure 1-----

TMS –evoked potentials

The effect of paired pulse TMS on TEPs was analysed in two ways; a region of interest analysis (ROI) to evaluate the local effects of paired pulse TMS and global scalp analysis to assess the effect of paired pulse TMS on outputs from the DLPFC across the cortex. For the ROI analysis, three peaks were analysed at the F3 electrode for both single and paired pulses; N40, P60 and N100. The N40 peak latency was calculated at the negative peak closest to 40 ms between 25-55 ms and the amplitude was calculated as the average signal between ± 5 ms of the peak latency. The P60 peak latency was calculated at the positive peak closest

to 60 ms between 45-75 ms and the amplitude was calculated as the average signal between ± 5 ms of the peak latency. The N100 peak latency was calculated at the negative peak closest to 100 ms between 85-145 ms and amplitude was calculated as the average signal between ± 10 ms of the peak latency. LICl of TEPs was quantified by normalising the difference between unconditioned (single test pulse) and conditioned (paired test pulse) TEPs to the overall size of the TEP (25-150 ms):

$$\text{Equation A: LICl}_{N40} = (N40_{\text{single}} - N40_{\text{paired}}) / (\text{Min}_{\text{single}} - \text{Max}_{\text{single}}) \times 100$$

$$\text{Equation B: LICl}_{P60} = (P60_{\text{single}} - P60_{\text{paired}}) / (\text{Max}_{\text{single}} - \text{Min}_{\text{single}}) \times 100$$

$$\text{Equation C: LICl}_{N100} = (N100_{\text{single}} - N100_{\text{paired}}) / (\text{Min}_{\text{single}} - \text{Max}_{\text{single}}) \times 100$$

Inspection of the trace following the test pulse (i.e. the period of interest to quantify LICl) revealed several peaks that were consistent with the latter peaks of the conditioning pulse (fig. 2). In order to account for this potential confound, the single-pulse trace was time-shifted 100 ms to match the conditioning pulse of the paired-pulse condition and was phase-subtracted from this trace (fig. 2C). Theoretically, this should leave only activity resulting from the test stimuli in the paired-pulse condition. LICl was then calculated again using the above formulas.

-----Insert figure 2-----

Slope analysis was used to compare the inhibitory measures of LICl and the N100 following single pulse TMS [31,51]. N100 slope was determined by calculating the mean first derivative between 90 and 98 ms following single pulse TMS, a period that corresponds to the inhibitory period of LICl. The effect of LICl on output from the DLPFC was assessed by comparing TEPs evoked by the unconditioned and conditioned TMS pulse over all electrodes between 25-300 ms.

TMS –evoked oscillations

The effect of paired pulse TMS on TMS-evoked oscillations was also assessed using an ROI analysis and a global scalp analysis. TMS-evoked oscillations were obtained using wavelet decomposition (3.5 oscillation cycles, steps of 1 Hz between 8-45 Hz) on averaged trials for each individual electrode. Oscillations were normalised by dividing the relative post TMS power by mean baseline power (-600 to -100) in each frequency bin. For ROI analysis at the F3 electrode, oscillations were averaged across frequency bands (alpha 8-12 Hz, lower beta 13-20 Hz, upper beta 21-30 Hz, gamma 31-45 Hz) and across time (25-200 ms for alpha and lower beta, 25-100 ms for upper beta and gamma). LICl of TMS-evoked oscillations was quantified by normalising the difference between unconditioned and conditioned oscillations in each frequency band to the mean power across all frequencies:

$$\text{Equation D: } \text{LICl}_{\text{freq}} = (\text{Single}_{\text{freq}} - \text{Paired}_{\text{freq}}) / \text{Single}_{\text{all}} \times 100$$

The effect of LICl on oscillations evoked in distant cortical regions was assessed by comparing the difference between unconditioned and conditioned TMS-evoked oscillations over time (25-250 ms), frequency (8-45 Hz) and space (all electrodes).

Statistics

Comparisons of single and paired pulses on ROI analyses (peak amplitudes, TMS-evoked frequency bands) were made between conditioned and unconditioned responses using paired t-tests. Correlations between LICl measures (different TEP peaks and different TMS-evoked oscillation frequencies) and between N100 slope and LICl measures were performed using Pearson's correlations (with and without outliers removed; outlier >3 × SD). Comparisons of single and paired pulses on global scalp TEPs (space and time) and global scalp TMS-evoked oscillations (space, time and frequency) were performed using non-parametric, cluster-based permutation statistics [52]. This approach controls for multiple-comparisons across any combination of space, time and frequency. Clusters were defined as two or more neighboring electrodes in which the t-statistic at a given time or frequency point exceeded a threshold of $p < 0.05$ (dependent t-test). Electrodes,

time points and/or frequency bins with above-threshold values were used for subsequent cluster-based permutation analysis. Monte Carlo p-values were calculated on 2000 random permutations and a value of $p < 0.05$ was used as the cluster-statistic significance threshold for all analyses.

RESULTS

TMS-evoked potentials

ROI analysis: Single-pulse TMS over DLPFC resulted in three consistent peaks measured at the F3 electrode (directly under the coil); a negative peak at 40.3 ± 7 ms (N40; distinguishable in 29 participants), a positive peak at 61.9 ± 11 ms (P60; distinguishable in 29 participants) and a second negative peak at 113.2 ± 14 ms (N100; distinguishable in 29 participants). Latter peaks at ~ 220 , 280 and 390 ms were also observed in most participants. Paired-pulse TMS resulted in TMS-evoked potentials after both the conditioning and test pulses (fig. 2). Inspection of the corrected paired-pulse trace revealed improved matching of shape between the single and paired test-pulses, suggesting the subtraction approach was successful (fig. 2D).

To quantify LICl, differences in N40, P60 and N100 amplitude following the test stimulus were compared between the single-pulse condition and both the uncorrected and corrected paired-pulse condition at the F3 electrode. N40 was significantly reduced following paired-pulse TMS in both conditions (uncorrected, $p=0.019$; corrected, $p=0.027$), P60 was significantly reduced in the corrected ($p=0.011$) and trended toward significance in the uncorrected condition ($p=0.098$) and N100 was significantly reduced in both conditions (uncorrected, $p<0.001$; corrected, $p=0.005$).

To assess whether LICl measured from different peaks reflected inhibition of related or independent mechanisms, correlation analyses were performed between normalised LICl scores from each peak. There was no significant relationship between LICl measured with N40 and P60 (uncorrected $p=0.32$, corrected $p=0.36$) or N40 and N100 (uncorrected $p=0.67$, corrected $p=0.37$), however LICl measured with P60 significantly correlated with N100 for the corrected condition ($r=-0.539$, $p=0.003$) and trended toward significance in the uncorrected condition ($p=0.096$).

To assess whether the N100 following single pulse TMS conveys similar inhibitory information to that as LICl measured with paired-pulses, the slope of the N100 (90-98 ms, analogous to the timing of LICl) from single pulse TMS was compared with normalised LICl measured from each peak. LICl from corrected N40

significantly correlated with N100 slope ($r=-0.47$, $p=0.010$) and trended towards significance with uncorrected N40 ($r=-0.35$, $p=0.063$), but did not correlate with any other peak (table 1). To assess whether the association with LICl measured from N40 was specific to the N100 slope, correlations between the preceding negative slope (60-70 ms) and positive slope (80-90 ms) were also assessed. There were no significant correlations between LICl of any peak and either slope (all $p>0.05$). Finally, the N100 slope was also significantly correlated with the N100 slope of the conditioning pulse (-10 to -2 ms, i.e. the slope immediately preceding the test pulse in the paired condition; $r=0.383$, $p=0.040$). Taken together, these findings suggest that the slope of the N100 represents a similar mechanism to LICl of N40 and supports LICl of N40, P60 and N100 reflecting inhibition of independent mechanisms. As correcting or not correcting the paired-pulse trace gave similar results and correcting resulted in a more plausible shape of the test TEP, the remaining analysis were completed on corrected paired-pulse traces.

-----Insert table 1-----

Global scalp analysis: To assess the spatiotemporal evolution of LICl, TMS-evoked potentials were compared between single and corrected paired conditions across space and time using cluster-based statistics. One significant negative cluster (109-283 ms, $p<0.001$; paired signal more negative than single) and one significant positive cluster (138-295 ms, $p<0.001$ paired signal more positive than single) was observed indicating reduced overall EEG signal following paired-pulse TMS compared with single-pulse TMS (fig. 4). Inspection of topographic plots revealed that inhibition began in a cluster of electrodes close to the site of stimulation and spread across the centre of the scalp to the contralateral frontal/temporal cortex. Over the next 30 ms, inhibition spread posteriorly and extended over bilateral parietal and occipital cortices while also developing over a fronto-central cluster. Inhibition of early latency TEPs did not survive correction for multiple comparisons at the global level.

-----Insert figure 4-----

TMS-evoked oscillations

ROI analysis: To quantify LICl of TMS-evoked oscillations, differences in TMS-evoked alpha, lower beta, upper beta and gamma oscillations were compared between single and corrected paired-pulse conditions at the F3 electrode. Evoked oscillations were significantly reduced in lower beta ($p=0.028$), upper beta ($p=0.005$) and gamma ($p=0.008$) frequency bands and trended toward significance in the alpha band ($p=0.067$) following paired-pulse TMS (fig. 5). To assess whether inhibition of different frequency bands represented similar or independent mechanisms, LICl was correlated between oscillatory bands. Data from one participant represented an extreme outlier and was excluded from all correlation analyses. LICl of alpha trended towards a significant correlation with LICl of gamma ($r=-0.361$, $p=0.054$), however there was no other significant correlation between LICl of any frequency band (all $p>0.15$).

To assess whether N100 following single pulse TMS was associated with inhibition of any particular frequency, N100 slope (90-98 ms) was correlated with LICl strength of each frequency band. N100 slope trended towards significant correlations with lower beta ($r=-0.264$, $p=0.17$) and upper beta inhibition ($r=-0.291$, $p=0.11$), but not alpha ($p=0.68$) or gamma inhibition ($p=0.94$). To further explore this relationship, LICl of individual frequencies in the beta band (13-30 Hz) were analysed. Significant correlations were found between N100 slope and LICl of oscillations from 16-23 Hz ($p<0.05$), suggesting individuals with steeper N100 slope gradients displayed increased LICl of mid-beta oscillations (fig. 5C). This relationship remained significant for oscillations between 17-22 Hz following removal of a second outlier ($p<0.05$). There were also no significant correlations between inhibition of any frequency band and slopes at either 60-70 ms or 80-90 ms (all $p>0.05$).

-----Insert figure 5-----

Global scalp analysis: To assess the spatiotemporal evolution of LICl in the frequency domain, TMS-evoked oscillations were compared between single and corrected paired conditions across space, time and

frequency using cluster-based statistics. One significant positive cluster ($p < 0.001$) was observed spanning all electrodes and multiple time points (25-185 ms; fig. 6). TMS-evoked alpha, lower beta, upper beta and gamma oscillations were inhibited over bilateral frontal electrodes up to 150 ms. Upper beta, gamma and particularly lower beta oscillations were also inhibited between 50-160 ms over right parieto-occipital electrodes. Inhibition was strongest at the site of stimulation and evolved over time to both frontal and parieto-occipital regions over the contralateral hemisphere.

-----Insert figure 6-----

DISCUSSION

There are three novel findings to the current study. First, LICl of early and late TEP peaks and LICl of different TMS-evoked oscillations varied independently, supporting independent underlying mechanisms of these measures. Second, the N100 slope following single pulse TMS correlated with LICl of N40 and mid-beta oscillations, suggesting that N100 over DLPFC also directly represents cortical inhibition. Finally, LICl suppressed propagation of the TEP and entrainment of TMS-evoked oscillations in distant cortical regions, suggesting TMS-evoked outputs from the DLPFC were also inhibited following paired-pulse TMS.

Mechanisms of TEPs over DLPFC

TEPs reflect the summation of a complex interplay between excitatory and inhibitory activity resulting from depolarisation of a heterogeneous neuronal population in the cortex following TMS [51]. However, characteristics of TEP peaks such as amplitude, latency and polarity appear to reflect properties of the dominant mechanism during a given period [28]. A growing body of evidence from the motor cortex suggests that earlier TEP peaks (10-50 ms) reflect excitatory neurotransmission, whereas later peaks (100-200 ms) reflect inhibitory neurotransmission, particularly at supathreshold intensities [33 for example]. In support, we recently demonstrated that LICl of early and late TEP peaks were independently modulated following systematic changes in conditioning and test intensity over motor cortex [31]. In the current study we have shown that LICl of early and late TEPs also vary independently across individuals in the DLPFC. In addition, we found that LICl of different TMS-evoked frequency bands also vary independently from each other. These findings support independent mechanisms generating different peaks and frequencies following TMS over DLPFC.

Despite the independence of TMS-evoked activity in the DLPFC, little is known about the underlying mechanisms of these peaks and frequencies. We found that the N100 slope was associated with LICl of the N40 and mid-beta oscillations over left DLPFC. Importantly, this relationship was not present for slopes from other peaks and also correlated with the N100 slope generated by the conditioning pulse. The link between N100 and LICl in DLPFC mirrors our recent finding of a similar relationship in the motor cortex

[31]. Although good evidence exists that the N100 generated by the motor cortex is related to cortical inhibition [29,33–38,53], this is the first empirical evidence we are aware of directly linking the DLPFC N100 with cortical inhibition. To confirm this relationship, pharmacological interventions using selective GABA_B-receptor agonists such as baclofen are required.

The relationship between N100 and LICl of N40 may also provide insight in to the underlying mechanism of early TEP peaks in DLPFC. In the motor cortex a range of evidence links early peaks with excitatory neurotransmission [33,54,55], including a relationship between LICl of P30, MEPs and the N100 slope [31]. We have replicated the relationship between LICl of N40 and N100 slope in the DLPFC, providing preliminary evidence that early peaks in this region may also reflect excitatory neurotransmission. Studies altering coil angle or pharmacological interventions targeting excitatory receptors will strengthen this evidence.

Suppression of DLPFC outputs by LICl

A single TMS pulse to the DLPFC not only activates local intracortical networks, but results in propagation of TEPs and entrainment of oscillations in (presumably) connected cortical regions. In the current study, we have demonstrated that this activation of wider cortical networks is reduced by LICl, suggesting output from the DLPFC is suppressed alongside local cortical activity by GABA_B-mediated inhibition. This finding agrees with studies in the motor cortex in which both the early and late phases of interhemispheric inhibition between motor cortices are reduced in the presence of LICl [56]. In the time domain, suppression was particularly evident from 100 ms onwards and evolved from the site of stimulation to contralateral and posterior regions. Suppression of earlier clusters (~40 and 60 ms) evident in the ROI analysis did not survive correction for multiple comparisons. This could reflect a known limitation of cluster based statistics in which large clusters, such as those between 100-300 ms, bias against smaller clusters [52]. Alternatively, inter-individual variation in latency of these early high frequency peaks could limit the sensitivity of this analysis in the time domain. In the frequency domain, inhibition of beta and gamma oscillations at the site of stimulation was evident within the first 100 ms. In addition, entrainment of later alpha (100-200) and

earlier gamma (25-50 ms) oscillations in contralateral and posterior sites were also suppressed. One proposed role of the DLPFC is selectively activating specific cortical networks required during a task [8,57,58]. GABA_B-dependent inhibition may sub-serve this role by mediating the output of the DLPFC during such events.

Limitations

There are several limitations to the current study. First, we did not use neuronavigation to target the DLPFC. However, we did use a site based on the 10/20 EEG system which provides the closest estimate to this region without using neuronavigation [43,44]. Second, stimulation parameters were based on the motor cortex, which does not necessarily translate to the DLPFC [59]. Currently, there is no consensus on a method for deciding TMS intensities outside of motor cortex. Motor cortex parameters were chosen as they produce consistent LICl in the DLPFC across sessions [40] and therefore are adequate for the purpose of this study. Finally, the TMS-evoked EEG signal was recovered from highly artifactual recordings using ICA. Although we have previously demonstrated that neural signal can be recovered with reasonable confidence using this method, complete certainty that TMS-evoked neural activity was not altered by removing these artifacts is not possible.

Conclusions

LICl over DLPFC suppresses both local TMS-evoked activity and TMS-evoked output to distant cortical regions. At the site of stimulation, different TEP peaks and different TMS-evoked oscillations reflect independent mechanisms. The N100 is consistent with the mechanism responsible for LICl, most likely GABA_B-mediated inhibition, whereas the N40 may reflect excitatory neurotransmission. The LICl paradigm and the N100 are different methods which provide complementary information on the generation and inhibitory role of GABA_B-mediated potentials. These methods will prove useful for investigating the role of GABA_B-mediated inhibition within the DLPFC in cognition and pathological conditions such as schizophrenia.

Acknowledgements: The authors wish to thank all volunteers for their participation. The following work will contribute to the doctoral thesis of NCR. NCR is supported by a postgraduate biomedical research scholarship (607223) from the National Health and Medical Research Council (NHMRC) of Australia. PBF is supported by a NHMRC Practitioner Fellowship.

Disclosures and conflict of interests: PBF has received equipment for research from MagVenture A/S, Medtronic Ltd and Brainsway Ltd and funding for research from Cervel Neurotech. ZJD received external funding through Neuronetics and Brainsway Inc, Aspect Medical and a travel allowance through Pfizer and Merck. ZJD has also received speaker funding through Sepracor Inc and served on the advisory board for Hoffmann-La Roche Limited. NCR reports no conflicts of interest.

REFERENCES

- [1] Isaacson JS, Scanziani M. How inhibition shapes cortical activity. *Neuron* 2011;72:231–43.
- [2] Krnjević K. Role of GABA in cerebral cortex. *Can J Physiol Pharmacol* 1997;75:439–51.
- [3] Whittington MA, Traub RD, Jefferys JG. Synchronized oscillations in interneuron networks driven by metabotropic glutamate receptor activation. *Nature* 1995;373:612–5.
- [4] Cardin J a, Carlén M, Meletis K, Knoblich U, Zhang F, Deisseroth K, et al. Driving fast-spiking cells induces gamma rhythm and controls sensory responses. *Nature* 2009;459:663–7.
- [5] Sohal VS, Zhang F, Yizhar O, Deisseroth K. Parvalbumin neurons and gamma rhythms enhance cortical circuit performance. *Nature* 2009;459:698–702.
- [6] Kohl MM, Paulsen O. The roles of GABAB receptors in cortical network activity. *Adv Pharmacol* 2010;58:205–29.
- [7] Brown JT, Davies CH, Randall AD. Synaptic activation of GABA(B) receptors regulates neuronal network activity and entrainment. *Eur J Neurosci* 2007;25:2982–90.
- [8] Benchenane K, Tiesinga PH, Battaglia FP. Oscillations in the prefrontal cortex: a gateway to memory and attention. *Curr Opin Neurobiol* 2011;21:475–85.
- [9] Schuler V, Lüscher C, Blanchet C, Klix N, Sansig G, Klebs K, et al. Epilepsy, hyperalgesia, impaired memory, and loss of pre- and postsynaptic GABA(B) responses in mice lacking GABA(B(1)). *Neuron* 2001;31:47–58.
- [10] Daskalakis ZJ, George TP. Clozapine, GABA(B), and the treatment of resistant schizophrenia. *Clin Pharmacol Ther* 2009;86:442–6.
- [11] Rogasch NC, Daskalakis ZJ, Fitzgerald PB. Cortical Inhibition, Excitation, and Connectivity in Schizophrenia: A Review of Insights From Transcranial Magnetic Stimulation. *Schizophr Bull* 2013;1–12.
- [12] Barker AT, Jalinous R, Freeston IL. Non-invasive magnetic stimulation of human motor cortex. *Lancet* 1985;1:1106–7.
- [13] Valls-Solé J, Pascual-Leone a, Wassermann EM, Hallett M. Human motor evoked responses to paired transcranial magnetic stimuli. *Electroencephalogr Clin Neurophysiol* 1992;85:355–64.
- [14] Nakamura H, Kitagawa H, Kawaguchi Y, Tsuji H. Intracortical facilitation and inhibition after transcranial magnetic stimulation in conscious humans. *J Physiol* 1997;498 (Pt 3:817–23.
- [15] Daskalakis ZJ, Farzan F, Barr MS, Maller JJ, Chen R, Fitzgerald PB. Long-interval cortical inhibition from the dorsolateral prefrontal cortex: a TMS-EEG study. *Neuropsychopharmacology* 2008;33:2860–9.
- [16] Fitzgerald PB, Daskalakis ZJ, Hoy K, Farzan F, Upton DJ, Cooper NR, et al. Cortical inhibition in motor and non-motor regions: a combined TMS-EEG study. *Clin EEG Neurosci* 2008;39:112–7.

- [17] McCormick DA. GABA as an inhibitory neurotransmitter in human cerebral cortex. *J Neurophysiol* 1989;62:1018–27.
- [18] Connors BW, Malenka RC, Silva LR. Two inhibitory postsynaptic potentials, and GABAA and GABAB receptor-mediated responses in neocortex of rat and cat. *J Physiol* 1988;406:443–68.
- [19] Tamás G, Lorincz A, Simon A, Szabadics J. Identified sources and targets of slow inhibition in the neocortex. *Science* 2003;299:1902–5.
- [20] Hammond GR, Garvey C-A. Asymmetries of long-latency intracortical inhibition in motor cortex and handedness. *Exp Brain Res* 2006;172:449–53.
- [21] Cash RFH, Ziemann U, Murray K, Thickbroom GW. Late cortical disinhibition in human motor cortex: a triple-pulse transcranial magnetic stimulation study. *J Neurophysiol* 2010;103:511–8.
- [22] Sanger TD, Garg RR, Chen R. Interactions between two different inhibitory systems in the human motor cortex. *J Physiol* 2001;530:307–17.
- [23] Davies CH, Davies SN, Collingridge GL. Paired-pulse depression of monosynaptic GABA-mediated inhibitory postsynaptic responses in rat hippocampus. *J Physiol* 1990;424:513–31.
- [24] Deisz R a. GABA(B) receptor-mediated effects in human and rat neocortical neurones in vitro. *Neuropharmacology* 1999;38:1755–66.
- [25] Di Lazzaro V, Oliviero a, Mazzone P, Pilato F, Saturno E, Insola a, et al. Direct demonstration of long latency cortico-cortical inhibition in normal subjects and in a patient with vascular parkinsonism. *Clin Neurophysiol* 2002;113:1673–9.
- [26] McDonnell MN, Orekhov Y, Ziemann U. The role of GABA(B) receptors in intracortical inhibition in the human motor cortex. *Exp Brain Res* 2006;173:86–93.
- [27] Florian J, Müller-Dahlhaus M, Liu Y, Ziemann U. Inhibitory circuits and the nature of their interactions in the human motor cortex a pharmacological TMS study. *J Physiol* 2008;586:495–514.
- [28] Rogasch NC, Fitzgerald PB. Assessing cortical network properties using TMS-EEG. *Hum Brain Mapp* 2013;34:1652–69.
- [29] Farzan F, Barr MS, Hoppenbrouwers SS, Fitzgerald PB, Chen R, Pascual-Leone A, et al. The EEG correlates of the TMS-induced EMG silent period in humans. *Neuroimage* 2013;83C:120–34.
- [30] Ilmoniemi RJ, Kicić D. Methodology for combined TMS and EEG. *Brain Topogr* 2010;22:233–48.
- [31] Rogasch NC, Daskalakis ZJ, Fitzgerald PB. Mechanisms underlying long-interval cortical inhibition in the human motor cortex: a TMS-EEG study. *J Neurophysiol* 2013;109:89–98.
- [32] Fitzgerald PB, Maller JJ, Hoy K, Farzan F, Daskalakis ZJ. GABA and cortical inhibition in motor and non-motor regions using combined TMS-EEG: a time analysis. *Clin Neurophysiol* 2009;120:1706–10.
- [33] Komssi S, Kähkönen S, Ilmoniemi RJ. The effect of stimulus intensity on brain responses evoked by transcranial magnetic stimulation. *Hum Brain Mapp* 2004;21:154–64.

- [34] Nikulin V V., Kicic D, Kahkonen S, Ilmoniemi RJ. Modulation of electroencephalographic responses to transcranial magnetic stimulation: evidence for changes in cortical excitability related to movement. *Eur J Neurosci* 2003;18:1206–12.
- [35] Bruckmann S, Hauk D, Roessner V, Resch F, Freitag CM, Kammer T, et al. Cortical inhibition in attention deficit hyperactivity disorder: new insights from the electroencephalographic response to transcranial magnetic stimulation. *Brain* 2012;135:2215–30.
- [36] Kicić D, Lioumis P, Ilmoniemi RJ, Nikulin V V. Bilateral changes in excitability of sensorimotor cortices during unilateral movement: combined electroencephalographic and transcranial magnetic stimulation study. *Neuroscience* 2008;152:1119–29.
- [37] Spieser L, Meziane HB, Bonnard M. Cortical mechanisms underlying stretch reflex adaptation to intention: a combined EEG-TMS study. *Neuroimage* 2010;52:316–25.
- [38] Bonnard M, Spieser L, Meziane HB, de Graaf JB, Pailhous J. Prior intention can locally tune inhibitory processes in the primary motor cortex: direct evidence from combined TMS-EEG. *Eur J Neurosci* 2009;30:913–23.
- [39] Farzan F, Barr MS, Wong W, Chen R, Fitzgerald PB, Daskalakis ZJ. Suppression of gamma-oscillations in the dorsolateral prefrontal cortex following long interval cortical inhibition: a TMS-EEG study. *Neuropsychopharmacology* 2009;34:1543–51.
- [40] Farzan F, Barr MS, Levinson a. J, Chen R, Wong W, Fitzgerald PB, et al. Reliability of Long-Interval Cortical Inhibition in Healthy Human Subjects: A TMS-EEG Study. *J Neurophysiol* 2010;104:1339–46.
- [41] Daskalakis ZJ, Farzan F, Barr MS, Rusjan PM, Favalli G, Levinson AJ, et al. Evaluating the relationship between long interval cortical inhibition, working memory and gamma band activity in the dorsolateral prefrontal cortex. *Clin EEG Neurosci* 2008;39:150–5.
- [42] Hoppenbrouwers SS, De Jesus DR, Stirpe T, Fitzgerald PB, Voineskos AN, Schutter DJLG, et al. Inhibitory deficits in the dorsolateral prefrontal cortex in psychopathic offenders. *Cortex* 2013;49:1377–85.
- [43] Rusjan PM, Barr MS, Farzan F, Arenovich T, Maller JJ, Fitzgerald PB, et al. Optimal transcranial magnetic stimulation coil placement for targeting the dorsolateral prefrontal cortex using novel magnetic resonance image-guided neuronavigation. *Hum Brain Mapp* 2010;31:1643–52.
- [44] Fitzgerald PB, Maller JJ, Hoy KE, Thomson R, Daskalakis ZJ. Exploring the optimal site for the localization of dorsolateral prefrontal cortex in brain stimulation experiments. *Brain Stimul* 2009;2:234–7.
- [45] Conforto AB, Z'Graggen WJ, Kohl AS, Rösler KM, Kaelin-Lang A. Impact of coil position and electrophysiological monitoring on determination of motor thresholds to transcranial magnetic stimulation. *Clin Neurophysiol* 2004;115:812–9.
- [46] Rogasch NC, Thomson RH, Daskalakis ZJ, Fitzgerald PB. Short-Latency Artifacts Associated with Concurrent TMS-EEG. *Brain Stimul* 2013:1–9.
- [47] Veniero D, Bortoletto M, Miniussi C. TMS-EEG co-registration: on TMS-induced artifact. *Clin Neurophysiol* 2009;120:1392–9.

- [48] Delorme A, Makeig S. EEGLAB: an open source toolbox for analysis of single-trial EEG dynamics including independent component analysis. *J Neurosci Methods* 2004;134:9–21.
- [49] Oostenveld R, Fries P, Maris E, Schoffelen J-M. FieldTrip: Open source software for advanced analysis of MEG, EEG, and invasive electrophysiological data. *Comput Intell Neurosci* 2011;2011:156869.
- [50] Hyvärinen a, Oja E. Independent component analysis: algorithms and applications. *Neural Netw* 2000;13:411–30.
- [51] Huber R, Mäki H, Rosanova M, Casarotto S, Canali P, Casali AG, et al. Human cortical excitability increases with time awake. *Cereb Cortex* 2013;23:332–8.
- [52] Maris E, Oostenveld R. Nonparametric statistical testing of EEG- and MEG-data. *J Neurosci Methods* 2007;164:177–90.
- [53] Bender S, Basseler K, Sebastian I, Resch F, Kammer T, Oelkers-Ax R, et al. Electroencephalographic response to transcranial magnetic stimulation in children: Evidence for giant inhibitory potentials. *Ann Neurol* 2005;58:58–67.
- [54] Bonato C, Miniussi C, Rossini PM. Transcranial magnetic stimulation and cortical evoked potentials: a TMS/EEG co-registration study. *Clin Neurophysiol* 2006;117:1699–707.
- [55] Mäki H, Ilmoniemi RJ. The relationship between peripheral and early cortical activation induced by transcranial magnetic stimulation. *Neurosci Lett* 2010;478:24–8.
- [56] Lee H, Gunraj C, Chen R. The effects of inhibitory and facilitatory intracortical circuits on interhemispheric inhibition in the human motor cortex. *J Physiol* 2007;580:1021–32.
- [57] Zanto TP, Rubens MT, Thangavel A, Gazzaley A. Causal role of the prefrontal cortex in top-down modulation of visual processing and working memory. *Nat Neurosci* 2011;14:656–61.
- [58] Fell J, Axmacher N. The role of phase synchronization in memory processes. *Nat Rev Neurosci* 2011;12:105–18.
- [59] Pell GS, Roth Y, Zangen A. Modulation of cortical excitability induced by repetitive transcranial magnetic stimulation: influence of timing and geometrical parameters and underlying mechanisms. *Prog Neurobiol* 2011;93:59–98.

Table 1: Correlations between LICl of TEP peaks and N100 slope gradient

	Correlation coefficient (r)	p-value
N40, uncorrected	-0.35	0.063
N40, corrected	-0.47	0.010*
P60, uncorrected	-0.08	0.685
P60, corrected	-0.15	0.426
N100, uncorrected	-0.07	0.712
N100 corrected	0.07	0.729

*p<0.05

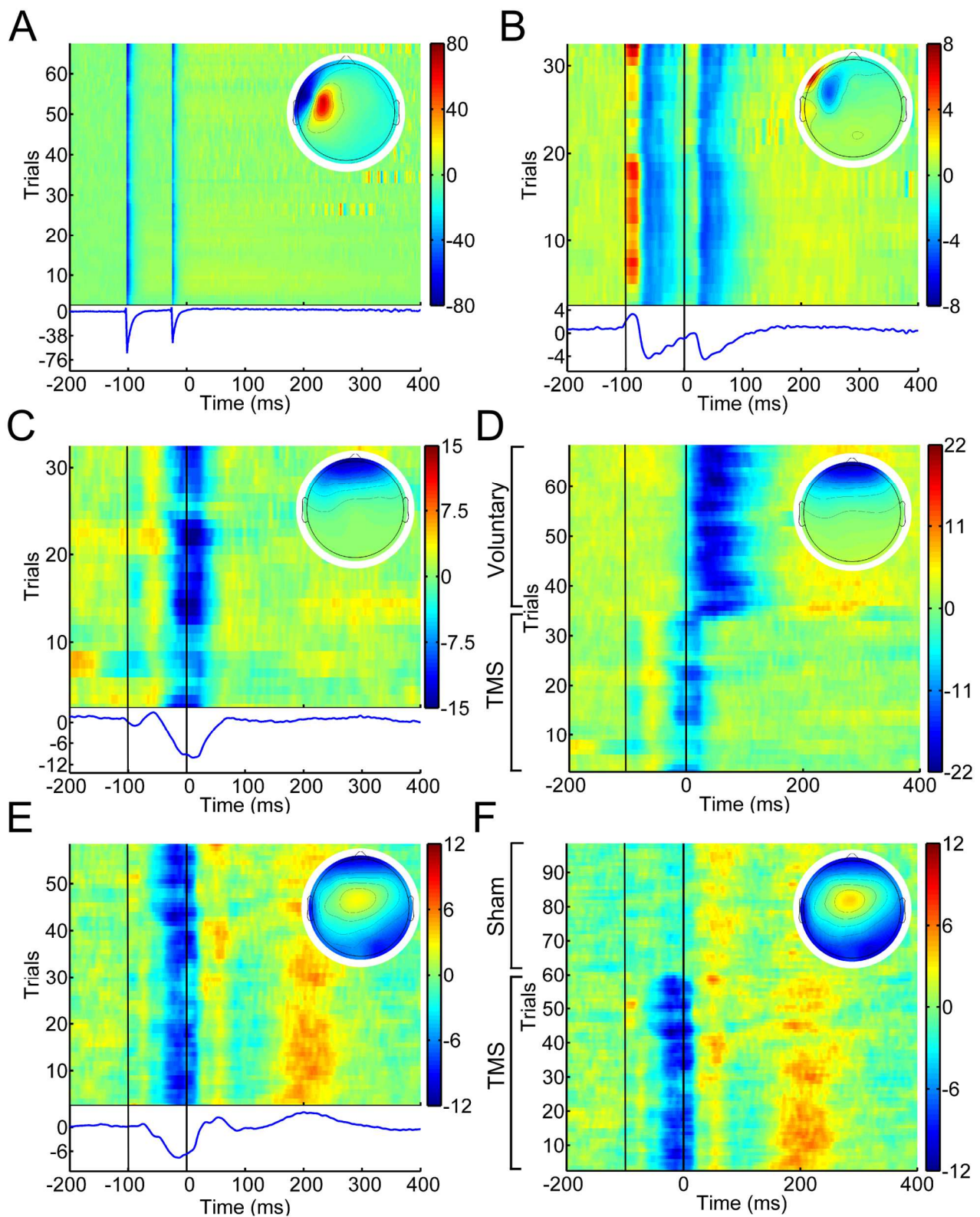


Figure 1. Independent components representing TMS-related EEG artifacts following paired pulse TMS (examples from representative individuals). A) Fast decay artifact. B) Slow decay artifact. C) TMS-evoked blink artifact. D) The TMS-evoked blink artifact combined with voluntary blinks confirming independent component analysis was capable of identifying this artifact following paired pulse TMS. E) TMS-evoked

auditory artifact. F) The auditory artifact following real TMS combined with auditory activity following sham TMS confirming independent component analysis was capable of identifying this artifact following paired pulse TMS.

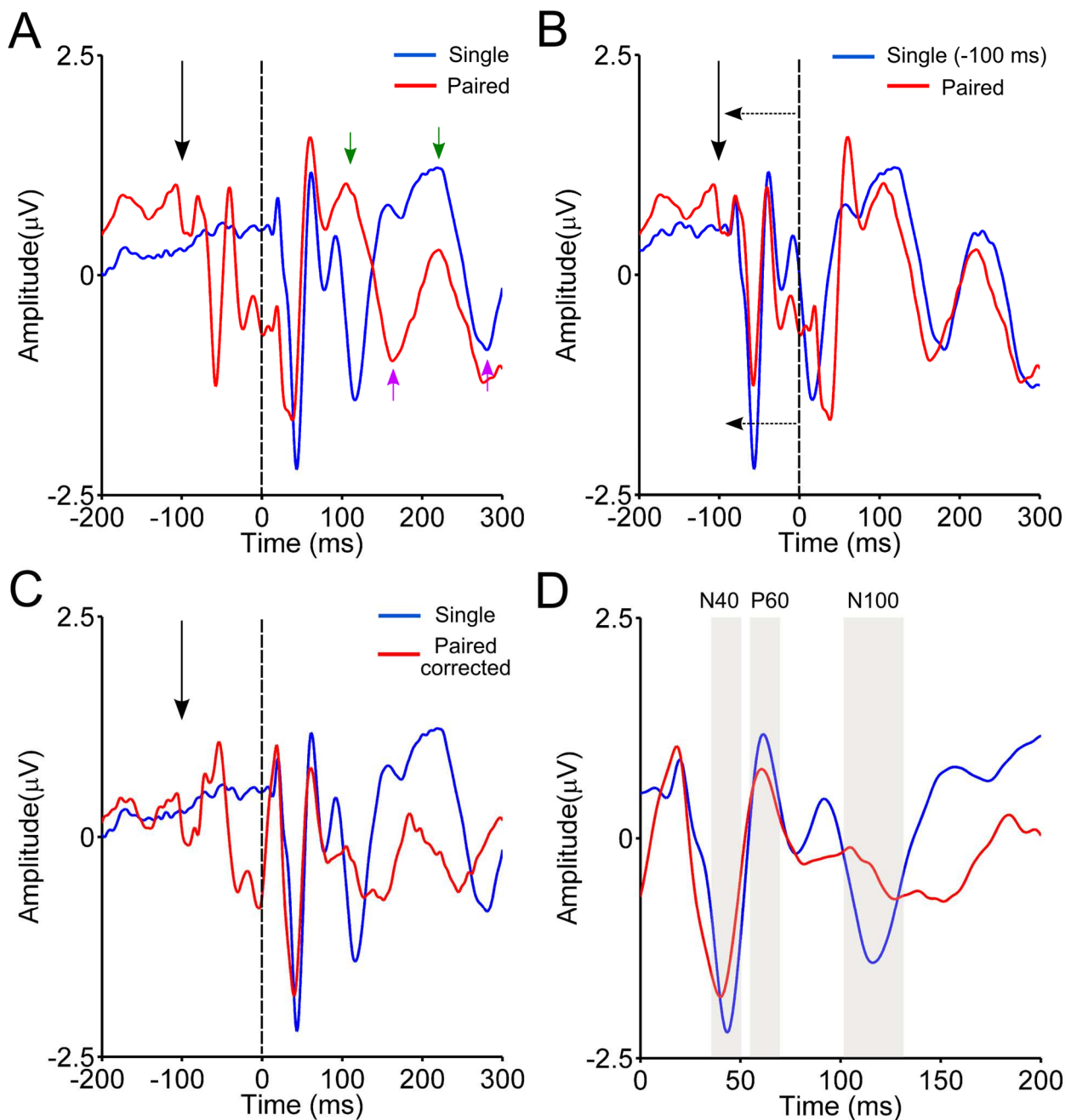


Figure 2. TMS-evoked potentials following single and paired TMS averaged across all participants at the F3 electrode. A) Dashed line represents timing of test pulse. Large arrow represents timing of the conditioning pulse (paired condition). Notice the similarity between peaks marked by green and purple arrows between conditions, suggesting continuation of the conditioning pulse into the single pulse analysis window. B) To demonstrate the coincidental peaks in A were likely residual activity from the conditioning pulse, the trace from the single pulse condition was shifted 100 ms to the left. Notice the alignment of peaks at 100, 180 and 220 ms. C) To account for this residual activity, the shifted single pulse trace was phase subtracted from the paired pulse trace (paired corrected). Notice the improvement in TEP shape following the test

pulse in the paired corrected condition. D) Enhanced view of C demonstrating the peaks used for long-interval cortical inhibition analysis.

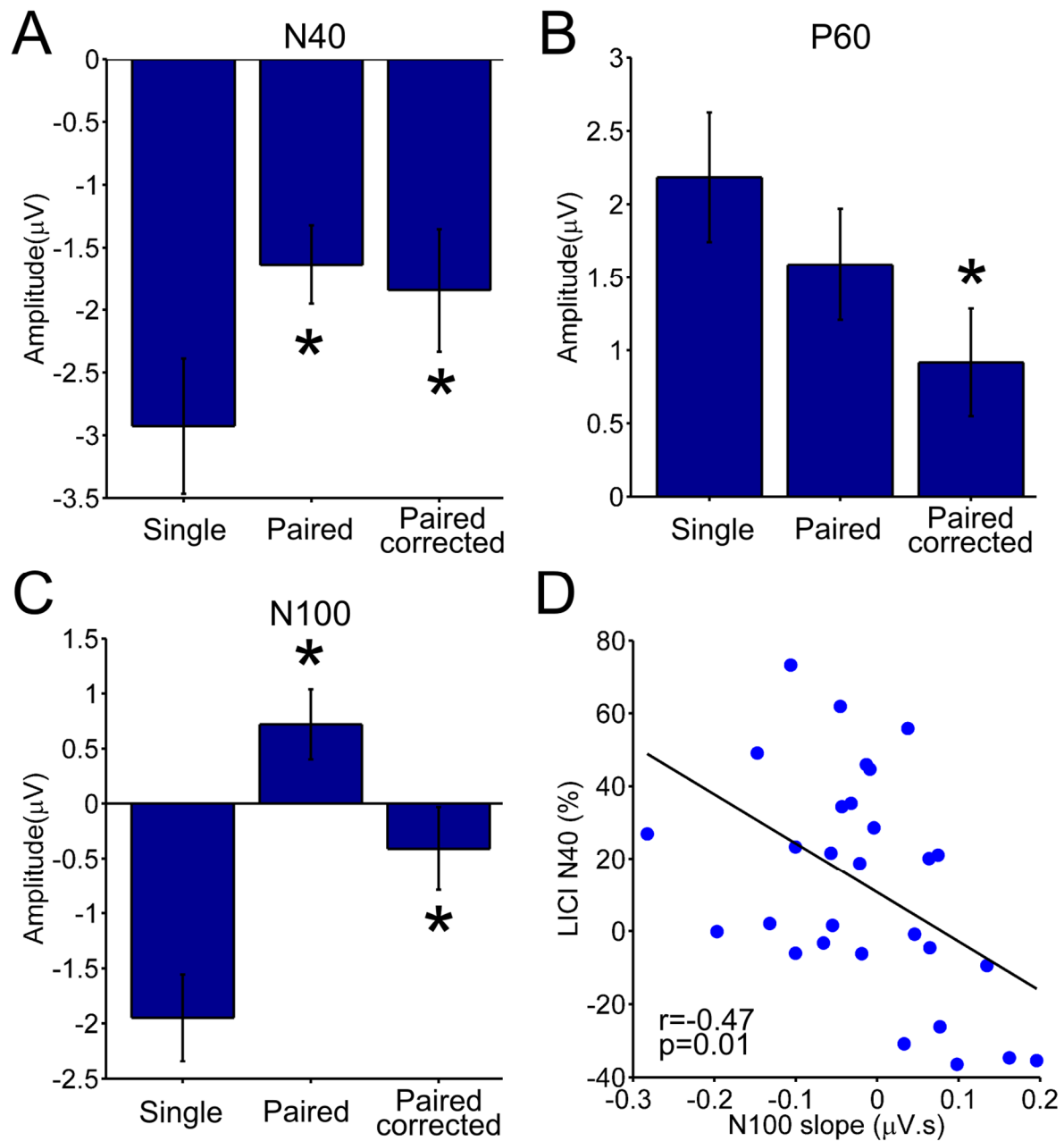


Figure 3: Long-interval cortical inhibition (LICI) of TMS-evoked potentials following paired-pulse TMS at the F3 electrode. A) N40 peak amplitude following single and paired TMS. B) P60 peak amplitude following single and paired TMS. C) N100 peak amplitude following single and paired TMS. D) Correlation between N100 slope and LICI of N40 peak. * indicates $p < 0.05$ compared with single pulse amplitude.

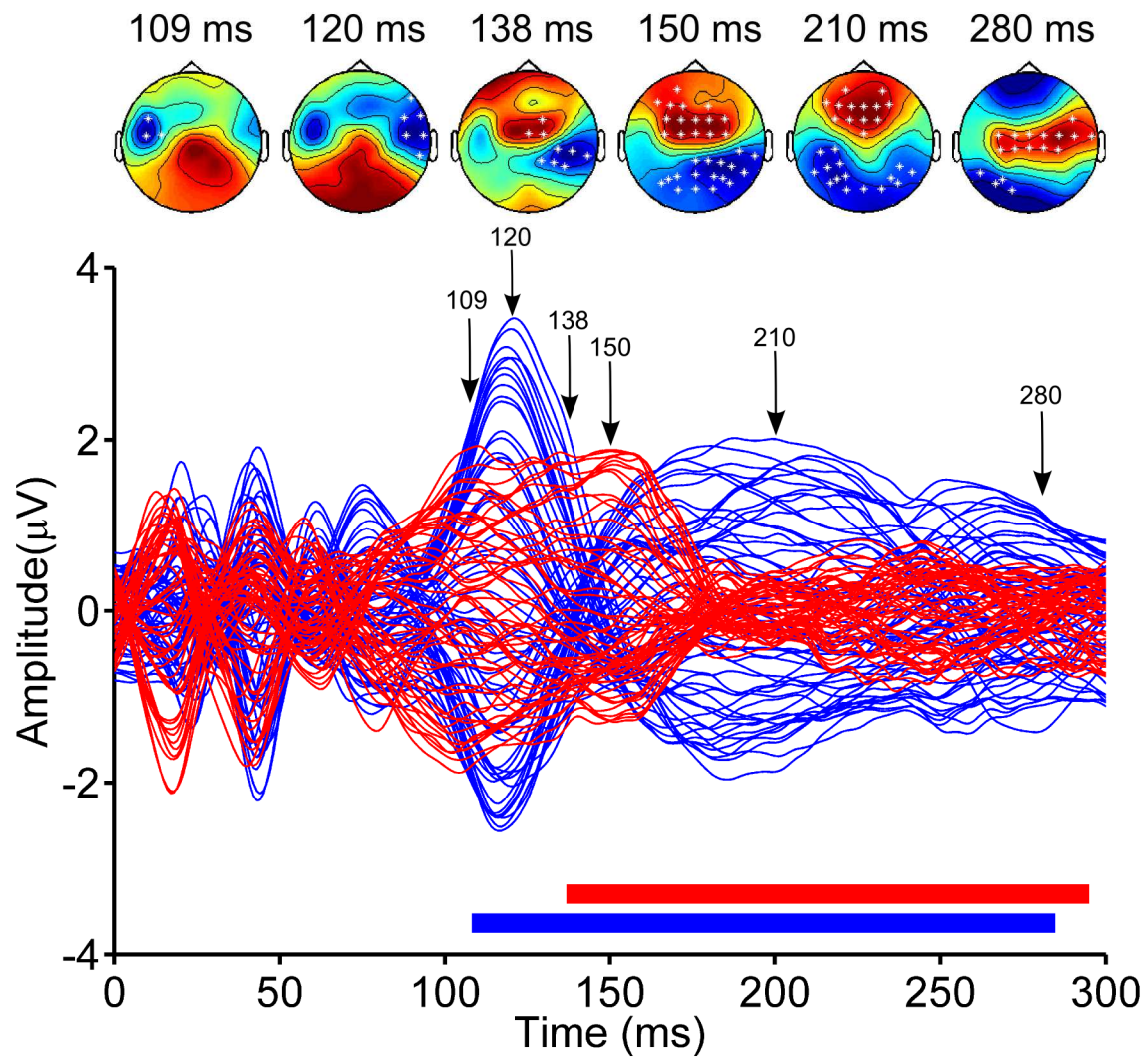


Figure 4: Butterfly plots averaged across all individuals demonstrating the difference in propagation of the TMS-evoked potential following single- (blue lines) and paired-pulse (red lines) TMS over DLPFC. Topoplots represent t-statistic values across the scalp at time points marked by arrows (blue = paired more negative than single, red=paired more positive than single). White crosses represents significantly different electrodes making up the cluster at these time points ($p < 0.05$, cluster based statistics). The blue bar represents timing of the significant negative cluster, the red bar represents timing of the significant positive cluster.

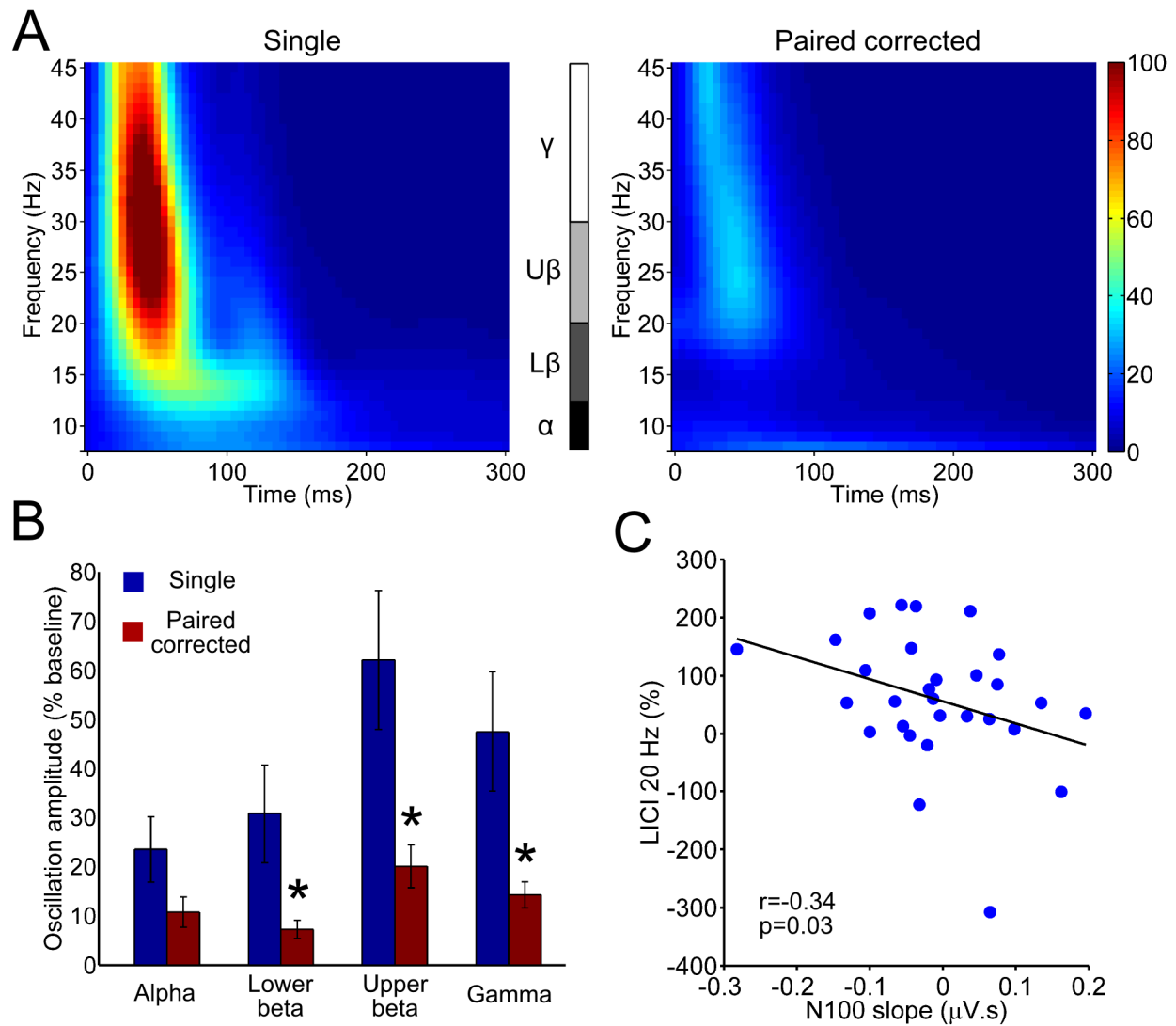


Figure 5: Long-interval cortical inhibition (LICI) of TMS-evoked potentials following paired-pulse TMS at the F3 electrode. A) Time-frequency plots from the averaged across all individuals following single and paired TMS (0 ms = timing of test pulse). B) TMS-evoked oscillations from different frequency bands following single and paired TMS (alpha and lower beta = 25-200 ms, upper beta and gamma = 25-100 ms). D) Correlation between N100 slope and LICI of TMS-evoked oscillations at 20 Hz. The correlation remained significant with removal of the outlier ($r = -0.328$, $p = 0.045$). * $p < 0.05$ compared with single.

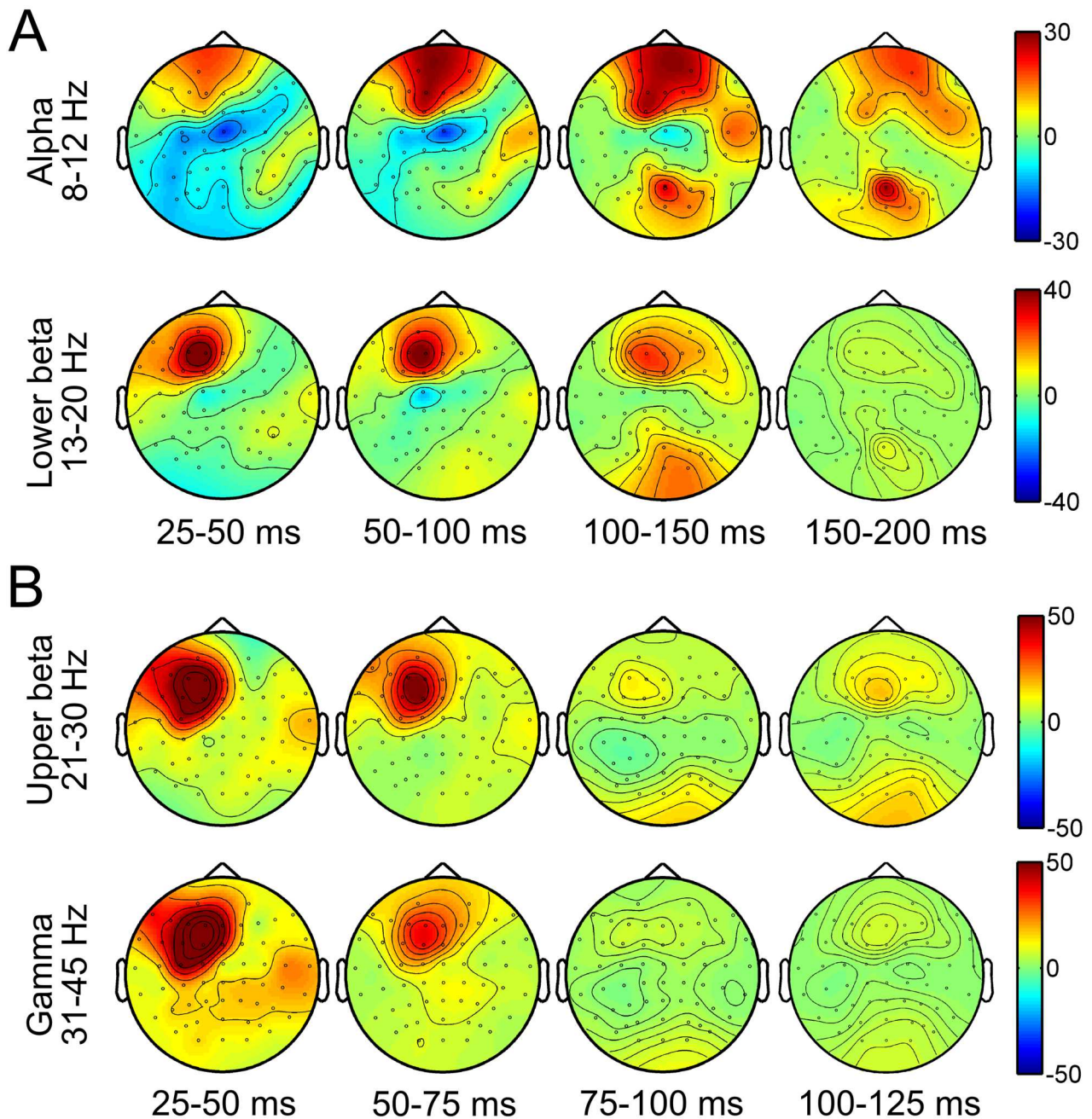


Figure 6: Topoplots averaged across all individual demonstrating the difference in TMS-evoked oscillations across the scalp following single and paired TMS. Red colours indicate a decrease in TMS-evoked oscillation frequency power (relative to baseline) following paired-pulse TMS. A) Inhibition of alpha and lower beta frequencies between 25-200 ms. B) Inhibition of upper beta and gamma oscillations between 25-125 ms.

CHAPTER EIGHT

DLPFC function in people with schizophrenia

Rogasch NC, Rajji TK, Tran LC, Bailey NW, Fitzgibbon BM, Daskalakis ZJ, Fitzgerald PB. Dorsolateral prefrontal cortex network properties are altered in schizophrenia: implications for working memory. (Submitted).

Preamble to empirical paper

In the previous chapters, we have established methods for recording TMS-evoked neural activity with minimal artifact from the DLPFC and have demonstrated that inhibitory neurotransmission is at least partially reflected by the DLPFC N100. Having developed these methods, TMS-EEG can now be used to address two important questions in the cortical inhibition/DLPFC/WM hypothesis of SCZ: 1) is DLPFC activation abnormal in SCZ independent of task activity and 2) is inhibitory neurotransmission deficient in the DLPFC of SCZ *in vivo*? In the final empirical paper of this thesis, we compared DLPFC network properties in people with and without SCZ using TMS-EEG and related this function to WM performance. We hypothesised that TMS-evoked gamma oscillations, a measure of DLPFC activation, would be impaired both locally and globally in SCZ. We also hypothesised that the DLPFC N100 would be reduced in SCZ, providing evidence for abnormal cortical inhibition. Finally, we predicted that these measures would relate to SCZ-related WM deficits.

Dorsolateral prefrontal cortex network properties are altered in schizophrenia: implications for working memory

Nigel C. Rogasch¹, Tarek K. Rajji², Lisa C. Tran², Neil W. Bailey¹, Bernadette M. Fitzgibbon¹, Zafiris J. Daskalakis² and Paul B. Fitzgerald¹

1. Monash Alfred Psychiatry Research Centre, Central Clinical School, The Alfred and Monash University, Melbourne, Australia
2. Temerty Centre for Therapeutic Brain Intervention, Centre for Addiction and Mental Health, University of Toronto, Toronto, Canada

Running head: TMS-EEG over prefrontal cortex in SCZ.

Key words: Transcranial magnetic stimulation, electroencephalography, cortical inhibition, GABA_B receptor, gamma oscillations, working memory.

Word count (abstract): 283

Word count (main text): 4,128

Tables: 1

Figures: 4

Correspondence: Nigel C. Rogasch
Monash Alfred Psychiatry Research Centre
Level 4, 607 St. Kilda rd.
Melbourne,
Victoria, Australia, 3004



ABSTRACT

Background: Dysfunctional dorsolateral prefrontal cortex (DLPFC) activation during working memory is a consistent finding in schizophrenia (SCZ). However, whether these deficits reflect aberrant DLPFC network properties or impaired sensory integration remains unclear. The aim of this study was to assess DLPFC function evoked by transcranial magnetic stimulation (TMS) and working memory performance in participants with and without SCZ.

Methods: 19 participants with SCZ (35.6 ± 9 years, 6 female) and 20 healthy participants (31.9 ± 10 , 5 females) received single TMS pulses to the left DLPFC while electroencephalography was recorded. Several indices of TMS-evoked cortical function were measured at the DLPFC and across the scalp including TMS-evoked cortical potentials such as the N100 and P180 (putative markers of cortical inhibition and excitation respectively) and TMS-evoked cortical oscillations were measured at the DLPFC and across the scalp. Working memory was assessed using the Sternberg letter recognition task with 5 and 7 letters.

Results: The N100 slope and amplitude were reduced over the DLPFC of participants with SCZ compared with healthy participants, whereas the P180 was increased. TMS-evoked oscillations (13-45 Hz) at the DLPFC were also reduced, as was propagation of gamma (31-45 Hz) oscillations to the left parietal cortex and upper beta (21-30 Hz) oscillations to contralateral DLPFC. Participants with SCZ who had low working memory capacity displayed reduced TMS-evoked gamma oscillations over the DLPFC compared with participants with SCZ who did not demonstrate working memory impairments and healthy participants.

Discussion: Intrinsic DLPFC network properties such as cortical inhibition and the ability to entrain high frequency oscillations in local and distant cortical regions are altered in SCZ. A reduced capability of the DLPFC to generate gamma oscillations may contribute to SCZ-related working memory deficits.

INTRODUCTION

Schizophrenia (SCZ) is a debilitating mental illness that affects between 0.5-1% of the world's population (1). Although SCZ is characterised by positive (e.g. psychosis, thought disorder) and negative (e.g. amotivation, flat affect) symptoms, cognitive symptoms such as impaired memory, attention and executive function are also core features of the illness (2). Understanding the pathophysiology of cognitive symptoms in SCZ is of paramount importance as these symptoms are minimally affected by current pharmacological treatments (3) and severity of cognitive impairment strongly predicts functional outcomes of the illness such as vocational and social function (4).

Deficits in working memory, the ability to retain and manipulate information over brief periods (5), are particularly prevalent in SCZ (6). Typically, these impairments in working memory are accompanied by abnormal hemodynamic activation of the dorsolateral prefrontal cortex (DLPFC) (7; 8); however, the physiological mechanisms underlying these changes remain unclear. Post mortem studies have revealed abnormalities in specific inhibitory interneuron sub-types in the DLPFC of people with SCZ (9), suggesting that impaired cortical inhibition as an underlying mechanism for working memory deficits. Cortical inhibition is a fundamental mechanism for the generation and control of high frequency cortical oscillations (25-100 Hz) (10; 11). Oscillations reflect synchronous firing of neuronal ensembles (12) and high frequency oscillations are thought to represent a key mechanism for the encoding and maintenance of information within cortical networks (13). Numerous studies have reported abnormal high frequency oscillations in the DLPFC of patients with SCZ during working memory (14–17) and over various stages of the illness such as in recent onset (18). These findings persist in both unmedicated (19) and medicated patients (20–23) indicating that abnormal oscillations are not a result of treatment or illness chronicity. However, whether DLPFC oscillation abnormalities during working memory reflect aberrant DLPFC circuitry or instead reflect a secondary or compensatory response to up-stream impairments in sensory integration and encoding, i.e. from the visual system (22; 24), remains unclear.

An alternative method for assessing cortical function is transcranial magnetic stimulation (TMS). TMS utilises electromagnetic induction to non-invasively stimulate cortical neurons through the scalp (25). The combination of TMS with electroencephalography (EEG) has enabled the assessment of oscillatory activity in local stimulated networks (26; 27) and the entrainment of oscillations in wider cortical networks in which the stimulated region plays a causal role (28–30). In addition, characteristics of certain time-locked TMS-evoked cortical potentials (TEPs) such as slope and amplitude appear to directly reflect excitatory and inhibitory neurotransmission (31). For instance, the N100 has been linked with cortical inhibition in the motor cortex (32–36) and may reflect TMS-evoked generation of inhibitory potentials mediated by postsynaptic GABA_B-receptors. Therefore, TMS-EEG can be used to assess various functional cortical network properties relevant to SCZ, such as oscillatory activity and cortical inhibition.

The aim of this study was to assess DLPFC network properties using TMS-EEG and working memory performance in participants with and without SCZ. We hypothesised that those with SCZ would demonstrate impaired markers of TMS-evoked cortical inhibitory function (i.e. N100 slope, high frequency oscillations) over the DLPFC and in wider networks activated by the DLPFC and that deficits in these network properties would relate to impaired working memory performance.

METHODS AND MATERIALS

Participants

Twenty volunteers with SCZ (n=12) or schizoaffective disorder (n=8) and 20 aged matched healthy comparisons participants (controls) were recruited (table 1). One participant with SCZ had difficulties staying awake during the session and data from this participant was discarded (n=19). Each participant provided written informed consent prior to participation and all experimental procedures were approved by the Alfred Hospital, Monash University and the Centre for Addiction and Mental Health Human Research Ethics Committees. For participants with SCZ, diagnosis was confirmed by DSM-IV-TR structured interviews. Symptom severity was assessed using the Positive And Negative Syndrome Scale (PANSS) (37). Healthy controls were screened for psychopathology using the Personality Assessment Screener (an abbreviated version of the Personality Assessment Inventory; Psychological Assessment Resources Inc.). 17 of the participants with SCZ were receiving either one or two second generation antipsychotics, 10 were receiving additional antidepressants or mood stabilisers and 1 was unmedicated. For analysis, dosages were converted to chlorpromazine (CPZ) equivalents (38). No healthy controls were receiving medication.

-----Insert table 1-----

Procedures

Participants were seated comfortably with their hands resting in their laps. The experiment contained two sessions. In session 1 participants performed the Sternberg letter recognition task (39). In session 2 participants received 75 single TMS pulses to the DLPFC while EEG was recorded. To avoid order effects, the order in which the sessions were administered was counterbalanced across participants.

Sternberg task

For the Sternberg task, participants were asked to remember a set of presented letters over a brief period and then indicate whether a single probe letter was present or not present in the memory set using a button press. The memory set was presented with either five (low load) or seven (high load) simultaneous letters (3017ms, all consonants), followed by a blank screen (3017ms). The probe letter was then presented (2017ms) and followed by a brief visual mask (133ms). Responses were required within this window to be deemed correct. The probe letter was present in the memory set in 50% of trials, the order of which was pseudorandomised across trials. Participants completed six blocks of twenty trials per block (total = 120) and both accuracy (% correct) and reaction time to correct responses were calculated as measures of performance.

EEG

EEG was recorded using a cap with 57 electrodes (sintered Ag/AgCl) in standard 10-20 positions (Quickcap, Compumedics Ltd., Australia). EEG signal was amplified (1000x), filtered (DC-3500 Hz), digitised (20 kHz; Synamps2, Compumedics Ltd.) and recorded on a computer for offline analysis. This arrangement, along with the DC-coupling and large recording range of the amplifier, captures the TMS artifact with minimal amplifier saturation and allows for recording of neural signals within ~5-10 ms following a pulse (40; 41). Electrode impedances were checked regularly and kept as low as possible throughout the experiment (<5 k Ω).

TMS

Monophasic TMS pulses were delivered through a figure of eight coil connected to a Magstim 200 stimulator. In all conditions, the coil was held with the handle angled 45° to the midline pointing backwards, resulting in a posterior to anterior current flow in the underlying cortex. Motor evoked potentials (MEPs) were recorded from Ag/AgCl electrodes attached in a belly-tendon montage over the

right abductor pollicis brevis (APB) muscle. Electromyographic signal was amplified (1000x) band-pass filtered (10-1000 Hz; PowerLab, ADInstruments, New Zealand) digitised (2000 Hz; Micro1401, Cambridge Electronic Design Ltd., UK), epoched around the TMS pulse (-200 to 500 ms) and displayed on a computer screen online. Resting motor threshold (RMT) was determined as the minimum stimulus intensity required to evoke at least 3 of 6 MEPs $>50 \mu\text{V}$ in amplitude from the motor cortical region that produced the largest responses in the APB. Next, the stimulus intensity required to evoke an MEP with average peak-to-peak amplitude between 0.7-1.3 mV over 5 trials (S1mV) was determined. This intensity was used for stimulation of the DLPFC. For DLPFC stimulation, the coil was positioned with its centre resting between the F3 and F5 electrodes. This position provides the most accurate estimation of the left DLPFC (border of BA9 and BA46) in the absence of neuronavigational equipment (42; 43). The coil border was marked using a felt tipped pen to allow for repositioning. TMS was delivered at a rate of 0.2 Hz (10 % jitter) throughout the experiment and participants were asked to stare directly ahead with their eyes open during stimulation.

EEG Analysis

Analysis of EEG data was performed using EEGLAB (44), field trip (45) and custom scripts all on the MATLAB platform (R2013a, The Mathworks, USA). EEG data were epoched around the TMS pulse (-1000 to 1000 ms), baseline corrected (-500 to -110 ms) and bad channels were removed. Data containing the TMS pulse artifact and peaks of any TMS-evoked muscle activity were truncated (-2 ms to 16.6 ± 6 ms; cut-off altered on an individual basis) and the remaining data traces were concatenated together. Following truncation, data were downsampled to 1 kHz and trials containing any large, paroxysmal artifacts were removed. Data were then passed through the fastICA algorithm (46) and components representing large decay components were removed. Data from the truncated window were then interpolated using a cubic function and all data were filtered using a butterworth, zero-phase band-pass filter (1-80 Hz). Epochs were then manually inspected and trials containing excessive muscle activity (i.e. from jaw clenching) or other uncharacterised activity were removed. The data was then passed through the fastICA algorithm a second time and components representing slow decay artifacts, blink artifacts, auditory artifacts and bad electrode

artifacts were removed. Eye movement and auditory artifacts have a large effect on TEPs and on TMS-evoked oscillations between 70-200 ms. There was no significant difference in the number of independent components identified as eye (control= 1.1 ± 0.5 , SCZ= 1.3 ± 0.9 ; $p=0.14$) or auditory (control= 1.2 ± 0.4 , SCZ= 1.3 ± 0.5 ; $p=0.11$) artifacts between groups. Following artifact removal, missing channels were replaced using spherical interpolation and data from each electrode were re-referenced to the average of all channels. Finally, butterfly plots were inspected for unusual activity (i.e. a single electrode with larger signal than all others). If unusual activity was detected, the above steps were repeated until this activity was removed.

TMS –evoked potentials

TEPs were analysed in two ways; a region of interest analysis (ROI) to evaluate the local effects of TMS and global scalp analysis to assess connectivity of the DLPFC with other regions. For the ROI analysis, four peaks (N40, P60, N100, P180) were analysed at the F3 electrode. The N40 peak amplitude and latency were calculated at the peak closest to 40 ms (± 15 ms), the P60 at the peak closest to 60 ms (± 15 ms), the N100 at the peak closest to 120 ms (± 25 ms) and the P180 at the peak closest to 180 ms (± 25 ms). N100 slope, a putative marker of GABA_B-mediated cortical inhibition (47), was determined by calculating the mean first derivative between 90-100 ms and 100-110 ms following TMS. DLPFC connectivity was assessed by comparing TEPs over all electrodes in four blocks based around peaks in the butterfly plot: 35-55 ms, 65-85 ms, 90-130 ms and 180-220 ms.

TMS –evoked oscillations

TMS-evoked oscillations were also assessed using an ROI analysis and global scalp analysis. TMS-evoked oscillations were obtained using wavelet decomposition (3.5 oscillation cycles, steps of 1 Hz between 8-45 Hz) on averaged trials for each individual electrode. Oscillations were normalised by subtracting the mean baseline power (-600 to -100) in each frequency bin. For ROI analysis at the F3 electrode, oscillations were averaged across discrete frequency bands (alpha 8-12 Hz, lower beta 13-20 Hz, upper beta 21-30 Hz, gamma 31-45 Hz) and across time. As lower and higher frequencies occur across different time periods,

alpha and lower beta oscillations were analysed between 25-200 ms and upper beta and gamma between 25-100 ms. DLPFC connectivity was assessed by comparing TMS-evoked oscillations in each frequency band over all electrodes in three time periods: early (25-40 ms), mid (40-75 ms) and late (75-150 ms).

Statistics

Outliers ($> 3 \times \text{SD}$ from the mean) were identified and z-score corrected to within 3.29 standard deviations from the mean calculated without outliers. Comparisons between groups on local DLPFC properties (N100 slope, peak amplitudes, peak latencies, TMS-evoked frequency bands) and working memory performance (accuracy, reaction time) were made using two-tailed independent sample t-tests. Within group comparisons between working memory load were made using two-tailed dependent sample t-tests and Bonferroni corrections for multiple comparisons were applied. Correlations between local DLPFC properties and low load working memory performance were made using Pearson's correlations (with outliers removed). Comparisons of global scalp TEPs (space and time) and global scalp TMS-evoked oscillations (space, time and frequency) were performed using non-parametric, cluster-based permutation statistics (48). This approach controls for multiple-comparisons across any combination of space, time and frequency. Clusters were defined as two or more neighbouring electrodes in which the t-statistic at a given time or frequency point exceeded a threshold of $p < 0.05$ (independent t-test). Electrodes, time points and/or frequency bins with above-threshold values were used for subsequent cluster-based permutation analysis. Monte Carlo p-values were calculated on 2000 random permutations and a value of $p < 0.05$ was used as the cluster-statistic significance threshold for all analyses.

RESULTS

Local DLPFC properties

The gradient of the N100 slope between 100-110 ms was significantly reduced in participants with SCZ when compared with healthy controls ($p=0.03$; fig. 1A-B). This reduction was accompanied by significantly reduced N100 amplitudes ($p=0.04$; fig. 1C) and longer N100 latencies ($p=0.03$; fig. 1D). We did not detect significant differences in N100 slope between 90-100 ms ($p=0.43$), other peak amplitudes (P60, $p=0.31$; P180, $p=0.17$) or peak latency (N40, $p=0.45$; P60, $p=0.14$; P180, $p=0.39$). However, overall peak-to-peak amplitude of the TEP ($p=0.08$) and N40 ($p=0.07$) tended to be smaller in participants with SCZ. To control for differences in overall TEP amplitude, we normalised N100 slope and each peak amplitude to the overall peak-to-peak amplitude for each individual. N100 slope ($p=0.05$) and amplitude ($p=0.03$) remained significantly smaller in participants with SCZ following normalisation. We did not detect any differences in normalised N40 ($p=0.26$) or P60 ($p=0.49$) amplitude between groups. Normalised P180 amplitude was larger in participants with SCZ compared with controls ($p=0.02$). As the N100 slope is a putative marker of cortical inhibition (47), we compared participants taking GABAergic medications to SCZ participants taking non-GABAergic medications. There was no significant difference in N100 slope between SCZ participants treated with lorazepam ($n=4$, $p=0.16$) or clozapine ($n=5$, $p=0.24$) compared to those taking other antipsychotic medications.

-----Insert figure 1-----

In the frequency domain, TMS-evoked oscillations in the DLPFC (8-45 Hz) were significantly reduced in participants with SCZ compared with controls ($p=0.03$; fig. 2A-B). When separated into discrete frequency bands, TMS-evoked oscillations in SCZ were significantly reduced in the lower beta ($p=0.04$), upper beta ($p=0.02$) and gamma ($p=0.02$) bands and trended towards significance in the alpha band ($p=0.06$; fig. 2C). In order to determine whether differences represented alterations specific to these frequencies rather than simply reduced response to TMS in SCZ, we normalised each frequency band to the overall peak-to-peak TEP amplitude for each individual. Upper-beta frequencies remained significantly reduced following

normalisation ($p=0.01$); however, we did not detect any significant differences in normalised alpha ($p=0.29$), lower beta ($p=0.08$) or gamma ($p=0.29$) oscillations between groups.

-----Insert figure 2-----

DLPFC connectivity

For TEP analysis, a significant positive cluster between 106-128 ms ($p=0.04$) revealed a positive TEP over parieto/occipital electrodes that was reduced in amplitude in people with SCZ (fig. 3A). We did not detect any other clusters which survived correction for multiple comparisons during other time periods between groups (all $p>0.05$).

For TMS-evoked oscillation analysis, TMS-evoked gamma oscillations were significantly reduced under left frontal and left parietal electrodes between 25-40 ms in SCZ compared with controls (fig. 3B). TMS-evoked upper beta oscillations under bilateral frontal electrodes between 40-75 ms were also reduced in SCZ (fig. 3C). We did not detect significant differences for any other frequency bands or time period between groups (all $p>0.05$).

-----Insert figure 3-----

Working memory

One participant with SCZ performed below 60% accuracy in both the low and high load working memory task conditions. As this score approached chance in both loads and could reflect a lack of effort, this data was removed from analysis. For both SCZ and controls, accuracy was significantly lower (HC and SCZ, $p<0.001$) and reaction time was significantly slower (HC and SCZ, $p<0.001$) in the high load compared to the low load (fig. 4A-B). Compared with controls, participants with SCZ performed with less accuracy (low load, $p=0.04$; high load, $p=0.012$) and slower reaction times (low load, $p=0.004$; high load, $p=0.004$) over both loads. Of the remaining 18 participants with SCZ, 5 scored below 60% in the high, but not low load task, suggesting they had exceeded their working memory capacity. Removing these participants from the

analysis improved accuracy so the SCZ group did not significantly differ from controls (low, $p=0.31$; high, $p=0.44$); however, high load reaction times remained slower in SCZ (low load, $p=0.08$; high load, $p=0.04$).

To assess the relationship between DLPFC function and working memory performance, we correlated low load accuracy and reaction times with measures of DLPFC function that significantly differed between groups separately for controls and SCZ. TMS-evoked oscillations from one participant with SCZ were outliers for all frequencies and were removed from analysis. In both participants with SCZ and controls, we found a significant negative correlation between TMS-evoked lower beta frequencies and task accuracy (HC, $p<0.001$; SCZ, $p=0.009$; fig. 4C) and a positive correlation between lower beta frequencies and reaction time in controls only ($p=0.03$). We did not detect any significant relationship between working memory and any other measure of DLPFC function (N100 slope, N100 amplitude, P180 amplitude, upper beta oscillations, gamma oscillations, TEP connectivity or oscillatory connectivity; all $p>0.05$).

To assess whether differences in working memory capacity were accompanied by any specific changes in DLPFC function in SCZ, the SCZ group was stratified into two groups: low performers who exceeded their working memory capacity in the high load task (accuracy $<60\%$ in high load task, $n=5$) and high performers who did not ($>60\%$ high load task, $n=13$). Measures of DLPFC function were compared between these two groups. TMS-evoked gamma oscillations were significantly reduced in low compared to high SCZ performers ($p=0.047$) and gamma oscillations were significantly reduced in both sub-groups compared to controls (low, $p=0.001$; high, $p=0.024$; fig. 4D). We did not detect any significant differences between SCZ subgroups and other measures of DLPFC function (N100 slope, overall TEP amplitude, N100 amplitude, P180 amplitude, lower beta oscillations, upper beta oscillations, TEP connectivity or oscillatory connectivity; all $p>0.05$) or demographic measures (age, RMT, S1mV, CPZ equivalent dosage, PANSS total; all $p>0.05$).

-----Insert figure 4-----

Symptoms and medication

We did not detect any significant relationships between positive symptoms, negative symptoms or CPZ equivalent antipsychotic dosages and any measure of DLPFC function in SCZ (N100 slope, N100 amplitude, P180 amplitude, lower beta oscillations, upper beta oscillations, gamma oscillations, TEP connectivity or oscillatory connectivity; all $p > 0.05$).

DISCUSSION

There were three novel findings from the current study. First, participants with SCZ displayed reduced N100 slope, amplitude and increased latency and increased P180 amplitude at the DLPFC compared with controls, suggesting altered inhibition and excitation in the cortex. Second, high frequency TMS-evoked oscillations in fronto-parietal and frontal interhemispheric networks were reduced in SCZ compared with controls, suggesting the ability of the DLPFC to entrain oscillations in distant cortical regions is impaired in SCZ. Third, TMS-evoked gamma band oscillations were reduced in participants with SCZ who had low working memory capacity compared with other participants, suggesting the ability of the DLPFC to generate high frequency oscillations may be important for working memory performance.

Reduced DLPFC Inhibition in SCZ

Evidence from several fields suggests that cortical inhibition is impaired in SCZ. Post mortem studies have found reduced glutamic acid decarboxylase (GAD67; an enzyme responsible for GABA synthesis) mRNA levels across various cortical regions in SCZ (49; 50), participants with SCZ show impaired P50 suppression (an EEG correlate of sensorimotor gating) (51) and several TMS measures of motor cortical inhibition are impaired in people with SCZ (52–54). In addition, a recent paired-pulse TMS-EEG study revealed impaired long-interval cortical inhibition (LICI) of TMS-evoked DLPFC gamma oscillations which was specific to SCZ diagnosis (55). The N100 slope following single pulse TMS also cortical inhibition (32), most likely a postsynaptic inhibitory potential mediated by GABA_B receptors. In the current study, we found that N100 slope, amplitude and latency were all altered in the DLPFC of participants with SCZ, providing further evidence for prefrontal GABA_B-mediated inhibitory deficits in SCZ. The relevance of this deficit to SCZ symptomatology remains unclear, as we could not find any relationships with reduced N100 slope and working memory deficits, positive symptoms or negative symptoms. A more comprehensive battery assessing a wider variety of cognitive symptoms is required to fully characterise any possible relationships.

The balance between inhibition and excitation in the cortex is vital for neuronal dynamics and information processing (56) and an imbalance between these mechanisms may represent the pathophysiological

mechanism important for SCZ symptoms (57). A recent TMS-EEG study in the motor cortex found increased TMS-evoked activity at 200 ms and at 400-700 ms in people with SCZ (58), which was interpreted as possible evidence for excessive excitation resulting from reduced inhibitory tone. In the current study, we also found increased amplitude of the P180 relative to overall TEP size in the DLPFC of participants with SCZ. Intriguingly, TMS studies in the motor cortex have revealed a period of increased cortical excitation following TMS that results from presynaptic inhibition of inhibitory interneurons between 190-210 ms (59; 60). Although speculative, the P180 may reflect a similar mechanism, providing a direct measure of excessive excitation in SCZ resulting from disinhibition. Further work comparing TMS-EEG and TMS motor measures at these later intervals is required to better understand these mechanisms in both healthy individuals and people with SCZ.

Reduced oscillations in SCZ

Another important role of cortical inhibition is the generation and modulation of cortical oscillations, particularly in higher frequency bands (10; 11). Two recent TMS-EEG studies have shown reduced upper beta/gamma TMS-evoked oscillations in the premotor (27) and superior frontal gyrus (26) of people with SCZ, the latter also demonstrating a relationship between peak oscillation frequencies and working memory performance. We have replicated and extended these findings, demonstrating that the ability of the DLPFC to entrain upper beta/gamma oscillations in distant cortical regions such as the parietal and contralateral DLPFC is also impaired in SCZ. Importantly, we have also shown TMS-evoked gamma oscillations are particularly diminished in participants with SCZ who have low working memory capacity. This finding suggests that TMS-evoked oscillations may, at least in part, represent activation of neural networks that are important for working memory capacity. In turn, these findings provide independent confirmation that the neural circuits responsible for gamma oscillations are impaired in SCZ, as predicted by post mortem anatomical studies (61).

In addition to gamma oscillations, we also observed that controls and SCZ participants with higher working memory performance showed reduced TMS-evoked lower beta oscillations. Lower beta oscillations

decrease over frontal regions with increasing working memory load (16; 62), suggesting that reductions in lower beta oscillations may be advantageous for working memory performance. Despite overall lower working memory performance, participants with SCZ demonstrated reduced lower beta TMS-evoked oscillations compared with controls. This reduction may therefore reflect a compensatory mechanism following the failure of other mechanisms, such as those responsible for higher frequency oscillations.

Limitations

Several limitations to the current study should be considered. First, all but one of the participants with SCZ were medicated, potentially confounding our between group comparisons of DLPFC function. However, we could not detect any relationships between CPZ equivalent antipsychotic dosage and any measure of TMS-evoked DLPFC function. Moreover, N100 measures were similar in those participants on medications with high affinity for GABA receptors to other SCZ participants, suggesting that medication was not mediating this effect. Second, we used measures from the motor cortex to set stimulation intensities for the DLPFC. SCZ is associated with reduced cortical thickness in the prefrontal cortex (63), which could increase the scalp-to-cortex distance and result in less effective neuronal activation by TMS. To account for this potential difference, we normalised measures of DLPFC function to the overall TEP amplitude in each individual. With this normalisation, participants with SCZ still displayed N100 and upper beta deficits compared with controls, suggesting that these deficits were independent of evoked activity size. Third, we did not use neuronavigation to localise the DLPFC. Instead, we used anatomical landmarks based on the 10-20 system which provide the most accurate estimation of DLPFC location in the absence of neuronavigation (42; 43). Fourth, we did not compare measures of TMS response in other brain regions to the DLPFC. Therefore, it is unclear whether these alterations are specific to the DLPFC, or whether they reflect more global changes in cortical function. Finally, it will be important to replicate this current study using a larger sample, particularly when stratifying the SCZ group based on working memory performance, as was done here.

Conclusions

DLPFC network properties assessed with TMS-EEG are altered in people with SCZ. In particular, people with SCZ displayed reduced markers of TMS-evoked inhibitory neurotransmission, as well as impaired generation of TMS-evoked high frequency oscillations in fronto-parietal and contralateral DLPFC networks. A reduced ability of the DLPFC to generate gamma oscillations may contribute to impaired working memory capacity in people with SCZ. The mechanisms underlying high frequency oscillations, such as cortical inhibition, are prime candidates for developing novel treatments targeting cognitive symptoms in SCZ.

Acknowledgements: The authors wish to thank all volunteers for their participation. The following work will contribute to the doctoral thesis of NCR. NCR is supported by a postgraduate biomedical research scholarship (607223) from the National Health and Medical Research Council (NHMRC) of Australia. PBF is supported by a NHMRC Practitioner Fellowship.

Disclosures and conflict of interests: PBF has received equipment for research from MagVenture A/S, Medtronic Ltd and Brainsway Ltd and funding for research from Cervel Neurotech. ZJD received external funding through Neuronetics and Brainsway Inc, Aspect Medical and a travel allowance through Pfizer and Merck. ZJD has also received speaker funding through Sepracor Inc and served on the advisory board for Hoffmann-La Roche Limited. NCR, TKR, LCT, NWB and BMF report no conflicts of interest.

REFERENCES

1. MacDonald AW, Schulz SC (2009): What we know: findings that every theory of schizophrenia should explain. *Schizophr Bull* 35: 493–508.
2. Insel TR (2010): Rethinking schizophrenia. *Nature* 468: 187–93.
3. Goldberg TE, Goldman RS, Burdick KE, Malhotra AK, Lencz T, Patel RC, *et al.* (2007): Cognitive improvement after treatment with second-generation antipsychotic medications in first-episode schizophrenia: is it a practice effect? *Arch Gen Psychiatry* 64: 1115–22.
4. Green MF (1996): What are the functional consequences of neurocognitive deficits in schizophrenia? *Am J Psychiatry* 153: 321–30.
5. Baddeley A (1992): Working memory. *Science* 255: 556–9.
6. Forbes NF, Carrick L a, McIntosh a M, Lawrie SM (2009): Working memory in schizophrenia: a meta-analysis. *Psychol Med* 39: 889–905.
7. Barch DM, Ceaser A (2012): Cognition in schizophrenia: core psychological and neural mechanisms. *Trends Cogn Sci* 16: 27–34.
8. Minzenberg MJ, Laird AR, Thelen S, Carter CS, Glahn DC (2009): Meta-analysis of 41 functional neuroimaging studies of executive function in schizophrenia. *Arch Gen Psychiatry* 66: 811–22.
9. Lewis D a, Hashimoto T, Volk DW (2005): Cortical inhibitory neurons and schizophrenia. *Nat Rev Neurosci* 6: 312–24.
10. Sohal VS, Zhang F, Yizhar O, Deisseroth K (2009): Parvalbumin neurons and gamma rhythms enhance cortical circuit performance. *Nature* 459: 698–702.
11. Cardin J a, Carlén M, Meletis K, Knoblich U, Zhang F, Deisseroth K, *et al.* (2009): Driving fast-spiking cells induces gamma rhythm and controls sensory responses *Nature*. 459: 663–7.
12. Buzsáki G, Draguhn A (2004): Neuronal oscillations in cortical networks. *Science* 304: 1926–9.
13. Lisman J, Buzsáki G (2008): A neural coding scheme formed by the combined function of gamma and theta oscillations. *Schizophr Bull* 34: 974–80.
14. Barr MS, Farzan F, Tran LC, Chen R, Fitzgerald PB, Daskalakis ZJ (2010): Evidence for excessive frontal evoked gamma oscillatory activity in schizophrenia during working memory. *Schizophr Res* 121: 146–52.
15. Basar-Eroglu C, Brand A, Hildebrandt H, Karolina Kedzior K, Mathes B, Schmiedt C (2007): Working memory related gamma oscillations in schizophrenia patients. *Int J Psychophysiol* 64: 39–45.
16. Haenschel C, Bittner R a, Waltz J, Haertling F, Wibral M, Singer W, *et al.* (2009): Cortical oscillatory activity is critical for working memory as revealed by deficits in early-onset schizophrenia. *J Neurosci* 29: 9481–9.
17. Cho RY, Konecky RO, Carter CS (2006): Impairments in frontal cortical gamma synchrony and cognitive control in schizophrenia. *Proc Natl Acad Sci U S A* 103: 19878–83.

18. Minzenberg MJ, Firl AJ, Yoon JH, Gomes GC, Reinking C, Carter CS (2010): Gamma oscillatory power is impaired during cognitive control independent of medication status in first-episode schizophrenia. *Neuropsychopharmacology* 35: 2590–9.
19. Gallinat J, Winterer G, Herrmann CS, Senkowski D (2004): Reduced oscillatory gamma-band responses in unmedicated schizophrenic patients indicate impaired frontal network processing. *Clin Neurophysiol* 115: 1863–74.
20. Kwon JS, O'Donnell BF, Wallenstein G V, Greene RW, Hirayasu Y, Nestor PG, *et al.* (1999): Gamma frequency-range abnormalities to auditory stimulation in schizophrenia. *Arch Gen Psychiatry* 56: 1001–5.
21. Spencer KM, Nestor PG, Niznikiewicz M a, Salisbury DF, Shenton ME, McCarley RW (2003): Abnormal neural synchrony in schizophrenia. *J Neurosci* 23: 7407–11.
22. Spencer KM, Niznikiewicz M a, Shenton ME, McCarley RW (2008): Sensory-evoked gamma oscillations in chronic schizophrenia. *Biol Psychiatry* 63: 744–7.
23. Spencer KM, Nestor PG, Perlmuter R, Niznikiewicz M a, Klump MC, Frumin M, *et al.* (2004): Neural synchrony indexes disordered perception and cognition in schizophrenia. *Proc Natl Acad Sci U S A* 101: 17288–93.
24. Dias EC, Butler PD, Hoptman MJ, Javitt DC (2011): Early sensory contributions to contextual encoding deficits in schizophrenia. *Arch Gen Psychiatry* 68: 654–64.
25. Hallett M (2007): Transcranial magnetic stimulation: a primer. *Neuron* 55: 187–99.
26. Ferrarelli F, Sarasso S, Guller Y, Riedner B a, Peterson MJ, Bellesi M, *et al.* (2012): Reduced natural oscillatory frequency of frontal thalamocortical circuits in schizophrenia. *Arch Gen Psychiatry* 69: 766–74.
27. Ferrarelli F, Massimini M, Peterson MJ, Riedner B a, Lazar M, Murphy MJ, *et al.* (2008): Reduced evoked gamma oscillations in the frontal cortex in schizophrenia patients: a TMS/EEG study. *Am J Psychiatry* 165: 996–1005.
28. Massimini M, Ferrarelli F, Huber R, Esser SK, Singh H, Tononi G (2005): Breakdown of cortical effective connectivity during sleep. *Science* 309: 2228–32.
29. Cona F, Zavaglia M, Massimini M, Rosanova M, Ursino M (2011): A neural mass model of interconnected regions simulates rhythm propagation observed via TMS-EEG. *Neuroimage* 57: 1045–58.
30. Garcia JO, Grossman ED, Srinivasan R (2011): Evoked potentials in large-scale cortical networks elicited by TMS of the visual cortex. *J Neurophysiol* 106: 1734–46.
31. Rogasch NC, Fitzgerald PB (2013): Assessing cortical network properties using TMS-EEG. *Hum Brain Mapp* 34: 1652–69.
32. Rogasch NC, Daskalakis ZJ, Fitzgerald PB (2013): Mechanisms underlying long-interval cortical inhibition in the human motor cortex: a TMS-EEG study. *J Neurophysiol* 109: 89–98.
33. Farzan F, Barr MS, Hoppenbrouwers SS, Fitzgerald PB, Chen R, Pascual-Leone A, Daskalakis ZJ (2013): The EEG correlates of the TMS-induced EMG silent period in humans. *Neuroimage* 83: 120–134.

34. Bonnard M, Spieser L, Meziane HB, de Graaf JB, Pailhous J (2009): Prior intention can locally tune inhibitory processes in the primary motor cortex: direct evidence from combined TMS-EEG. *Eur J Neurosci* 30: 913–23.
35. Spieser L, Meziane HB, Bonnard M (2010): Cortical mechanisms underlying stretch reflex adaptation to intention: a combined EEG-TMS study. *Neuroimage* 52: 316–25.
36. Komssi S, Kähkönen S, Ilmoniemi RJ (2004): The effect of stimulus intensity on brain responses evoked by transcranial magnetic stimulation. *Hum Brain Mapp* 21: 154–64.
37. Kay SR, Qpjer LA (1982): The Positive and Negative Syndrome Scale (PANSS) for Schizophrenia. *Schizophr Bull* 13: 261-76 .
38. Woods SW (2003): Chlorpromazine equivalent doses for the newer atypical antipsychotics. *J Clin Psychiatry* 64: 663–7.
39. Sternberg S (1966): High-speed scanning in human memory. *Science* 153: 652–4.
40. Rogasch NC, Thomson RH, Daskalakis ZJ, Fitzgerald PB (2013): Short-Latency Artifacts Associated with Concurrent TMS-EEG. *Brain Stimul* 1–9.
41. Veniero D, Bortoletto M, Miniussi C (2009): TMS-EEG co-registration: on TMS-induced artifact. *Clin Neurophysiol* 120: 1392–9.
42. Rusjan PM, Barr MS, Farzan F, Arenovich T, Maller JJ, Fitzgerald PB, Daskalakis ZJ (2010): Optimal transcranial magnetic stimulation coil placement for targeting the dorsolateral prefrontal cortex using novel magnetic resonance image-guided neuronavigation. *Hum Brain Mapp* 31: 1643–52.
43. Fitzgerald PB, Maller JJ, Hoy KE, Thomson R, Daskalakis ZJ (2009): Exploring the optimal site for the localization of dorsolateral prefrontal cortex in brain stimulation experiments. *Brain Stimul* 2: 234–7.
44. Delorme A, Makeig S (2004): EEGLAB: an open source toolbox for analysis of single-trial EEG dynamics including independent component analysis. *J Neurosci Methods* 134: 9–21.
45. Oostenveld R, Fries P, Maris E, Schoffelen J-M (2011): FieldTrip: Open source software for advanced analysis of MEG, EEG, and invasive electrophysiological data. *Comput Intell Neurosci* 2011: 1568-69.
46. Hyvärinen a, Oja E (2000): Independent component analysis: algorithms and applications. *Neural Netw* 13: 411–30.
47. Rogasch NC, Daskalakis ZJ, Fitzgerald PB (2013): Mechanisms underlying long-interval cortical inhibition in the human motor cortex: a TMS-EEG study. *J Neurophysiol* 109: 89–98.
48. Maris E, Oostenveld R (2007): Nonparametric statistical testing of EEG- and MEG-data. *J Neurosci Methods* 164: 177–90.
49. Akbarian S, Kim JJ, Potkin SG, Hagman JO, Tafazzoli A, Bunney WE, Jones EG (1995): Gene expression for glutamic acid decarboxylase is reduced without loss of neurons in prefrontal cortex of schizophrenics. *Arch Gen Psychiatry* 52: 258–66.
50. Volk DW, Austin MC, Pierri JN, Sampson AR, Lewis DA (2000): Decreased glutamic acid decarboxylase67 messenger RNA expression in a subset of prefrontal cortical gamma-aminobutyric acid neurons in subjects with schizophrenia. *Arch Gen Psychiatry* 57: 237–45.

51. Freedman R, Adler LE, Myles-Worsley M, Nagamoto HT, Miller C, Kisley M, *et al.* (1996): Inhibitory gating of an evoked response to repeated auditory stimuli in schizophrenic and normal subjects. Human recordings, computer simulation, and an animal model. *Arch Gen Psychiatry* 53: 1114–21.
52. Daskalakis ZJ, Christensen BK, Chen R, Fitzgerald PB, Zipursky RB, Kapur S (2002): Evidence for impaired cortical inhibition in schizophrenia using transcranial magnetic stimulation. *Arch Gen Psychiatry* 59: 347–54.
53. Fitzgerald PB, Brown TL, Daskalakis ZJ, Kulkarni J (2002): A transcranial magnetic stimulation study of inhibitory deficits in the motor cortex in patients with schizophrenia. *Psychiatry Res* 114: 11–22.
54. Rogasch NC, Daskalakis ZJ, Fitzgerald PB (2013): Cortical Inhibition, Excitation, and Connectivity in Schizophrenia: A Review of Insights From Transcranial Magnetic Stimulation. *Schizophr Bull* 1–12.
55. Farzan F, Barr MS, Levinson AJ, Chen R, Wong W, Fitzgerald PB, Daskalakis ZJ (2010): Evidence for gamma inhibition deficits in the dorsolateral prefrontal cortex of patients with schizophrenia. *Brain* 133: 1505–14.
56. Yizhar O, Fenno LE, Prigge M, Schneider F, Davidson TJ, O’Shea DJ, *et al.* (2011): Neocortical excitation/inhibition balance in information processing and social dysfunction. *Nature* 477: 171–8.
57. Lisman J (2012): Excitation, inhibition, local oscillations, or large-scale loops: what causes the symptoms of schizophrenia? *Curr Opin Neurobiol* 22: 537–44.
58. Frantseva M, Cui J, Farzan F, Chinta L V, Perez Velazquez JL, Daskalakis ZJ (2012): Disrupted Cortical Conductivity in Schizophrenia: TMS-EEG Study. *Cereb Cortex* 1–11.
59. Cash RFH, Ziemann U, Murray K, Thickbroom GW (2010): Late cortical disinhibition in human motor cortex: a triple-pulse transcranial magnetic stimulation study. *J Neurophysiol* 103: 511–8.
60. Chu J, Gunraj C, Chen R (2008): Possible differences between the time courses of presynaptic and postsynaptic GABAB mediated inhibition in the human motor cortex. *Exp Brain Res* 184: 571–7.
61. Gonzalez-Burgos G, Lewis D a (2008): GABA neurons and the mechanisms of network oscillations: implications for understanding cortical dysfunction in schizophrenia. *Schizophr Bull* 34: 944–61.
62. Michels L, Bucher K, Lüscher R, Klaver P, Martin E, Jeanmonod D, Brandeis D (2010): Simultaneous EEG-fMRI during a working memory task: modulations in low and high frequency bands. *PLoS One* 5: e10298.
63. Honea R, Crow TJ, Passingham D, Mackay CE (2005): Regional deficits in brain volume in schizophrenia: a meta-analysis of voxel-based morphometry studies. *Am J Psychiatry* 162: 2233–45.

Table 1: Description of participants

	Healthy control participants (n=20)	Participants with schizophrenia (n=19)	p-value
Age, years	31.9 ± 10	35.6 ± 9	0.12
Male/female, no.	15/5	13/6	0.65
RMT, % MSO	56.6 ± 11	57.4 ± 8	0.40
S1mV, %MSO	68.5 ± 13	70.0 ± 9	0.34
PANSS positive	-	12.5 ± 6	-
PANSS negative	-	11.3 ± 4	-
PANSS general	-	25.1 ± 8	-

RMT, resting motor threshold; MSO, maximum stimulator output; S1mV, stimulus intensity for 1 mV; PANSS, positive and negative syndrome scale.

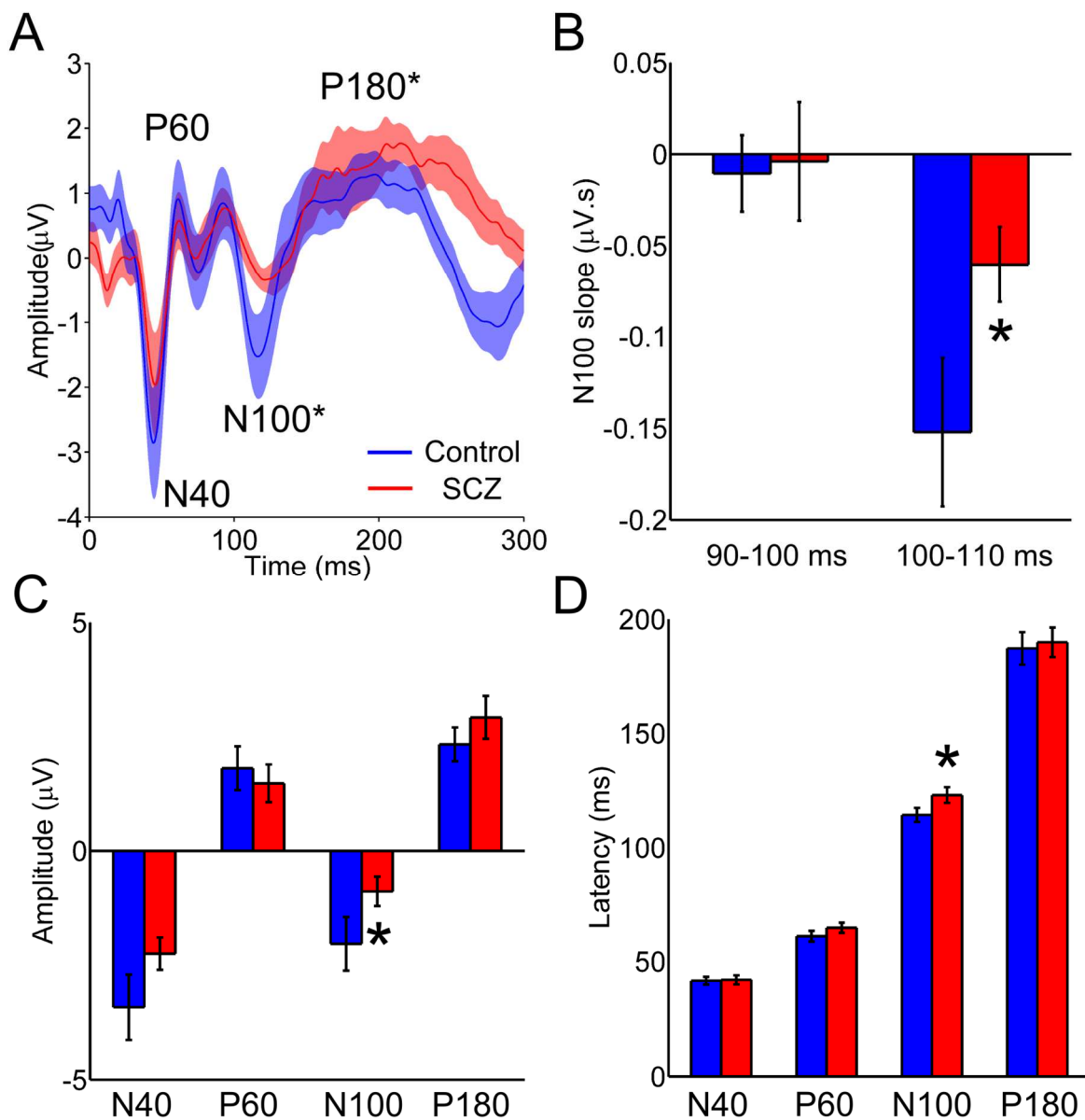


Figure 1: Transcranial magnetic stimulation (TMS)-evoked potentials (TEPs) in the dorsolateral prefrontal cortex of people with and without schizophrenia (SCZ). A) Averaged TEP traces from the F3 electrode across all participants demonstrating analysed peaks. TMS was given at 0 ms. Shaded area represents standard error. B) N100 slope measured across two time points. C) Amplitude of TEP peaks. D) Latency of TEP peaks.

* $p < 0.05$ compared with controls.

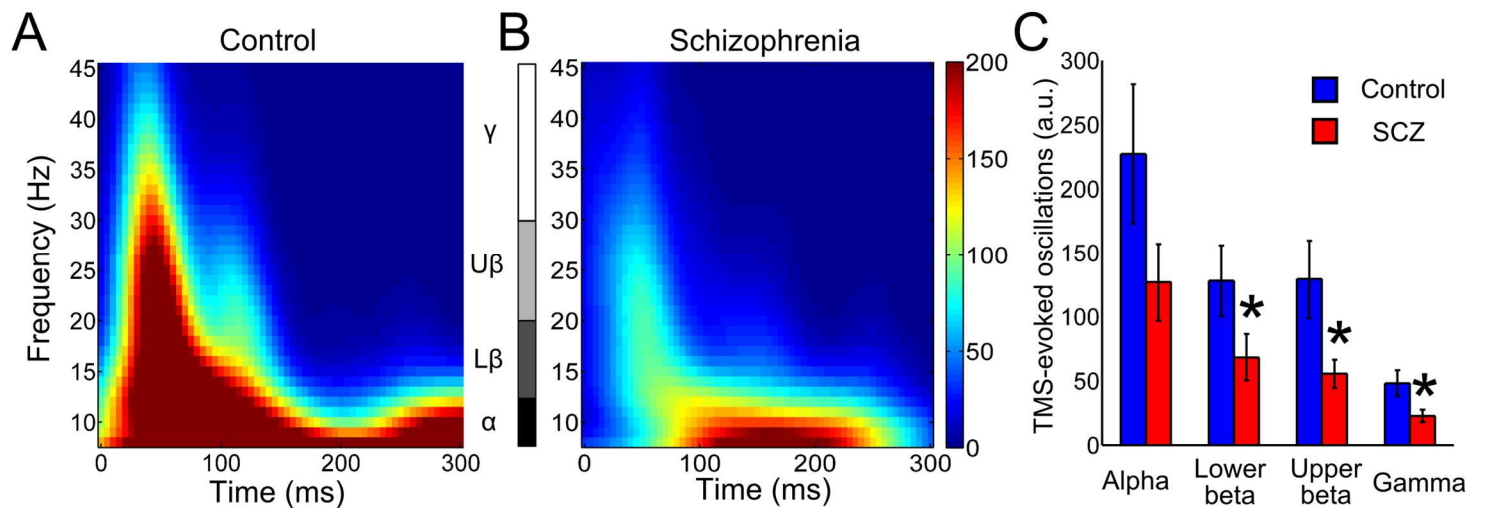


Figure 2: Transcranial magnetic stimulation (TMS)-evoked oscillations in the dorsolateral prefrontal cortex of people with and without schizophrenia (SCZ). Averaged time-frequency plots following TMS (time = 0 ms) in controls (A) and participants with SCZ (B) at the F3 electrode. Breakdown of analysis into discrete frequency bands is shown by the central bar. C) TMS-evoked oscillations amplitude measured in discrete frequency bands over time (alpha, lower beta = 25-200 ms; upper beta, gamma = 25-100 ms). Alpha, 8-12 Hz; Lower beta, 13-20 Hz; Upper beta, 21-30 Hz; Gamma, 31-45 Hz. * $p < 0.05$ compared with controls.

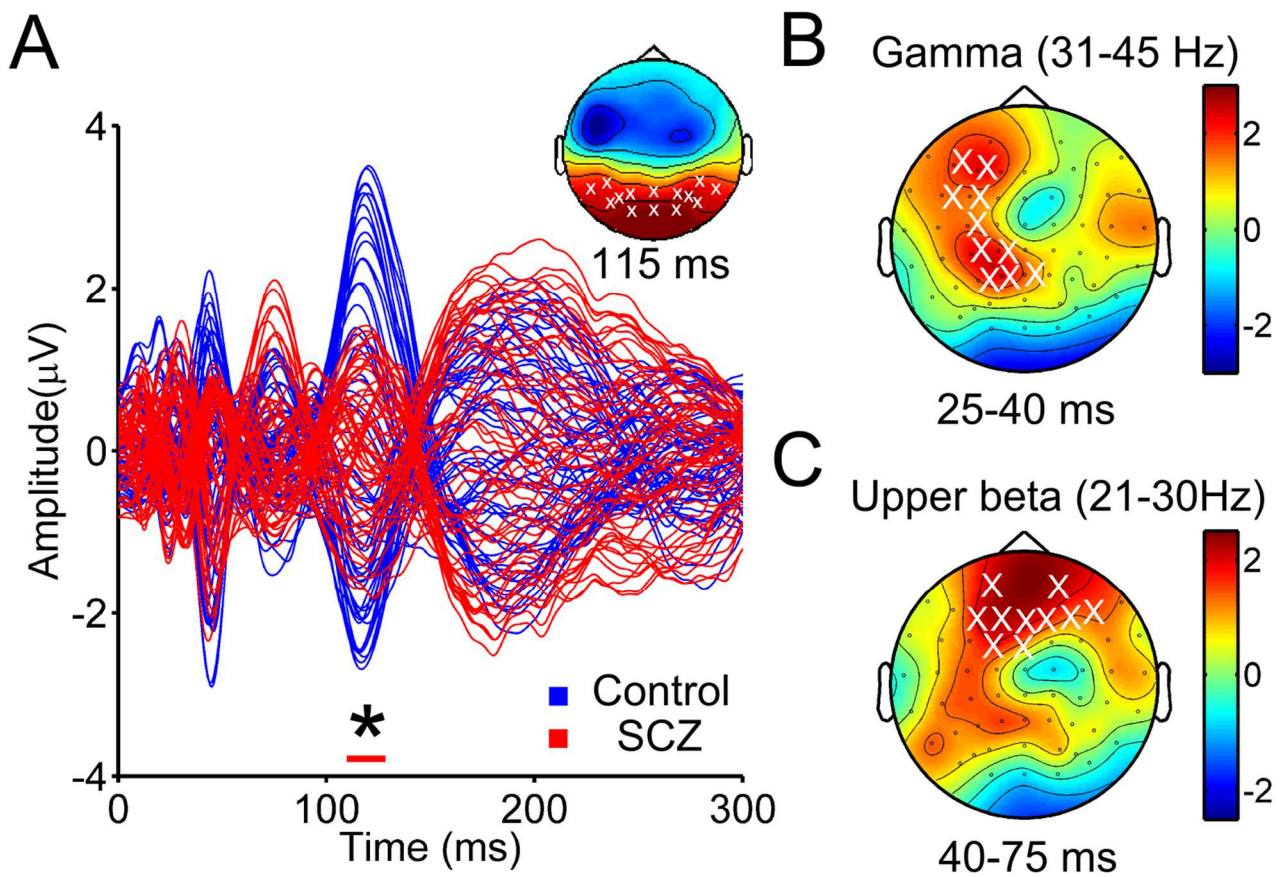


Figure 3: Differences in transcranial magnetic stimulation (TMS)-evoked activity across the scalp between participants with and without schizophrenia (SCZ). A) Butterfly plot of all electrodes averaged across all participants. The red bar indicates timing of a significant positive cluster (EEG signal more positive for controls than SCZ, $p < 0.05$, cluster statistics). White crosses on imbedded topoplot demonstrate the electrodes which were significantly different between controls and SCZ at the 115 ms time point. B) Topoplot with t-statistics comparing TMS-evoked gamma oscillation between controls and SCZ across the scalp over 25-40 ms. White crosses demonstrate electrodes forming a significant positive cluster (TMS-evoked oscillations higher in controls than SCZ, $p < 0.05$, cluster statistics). C) Topoplot with t-statistics comparing TMS-evoked upper beta oscillations between controls and SCZ across the scalp over 40-75 ms. White crosses demonstrate electrodes forming a significant positive cluster (TMS-evoked oscillations higher in controls than SCZ, $p < 0.05$, cluster statistics).

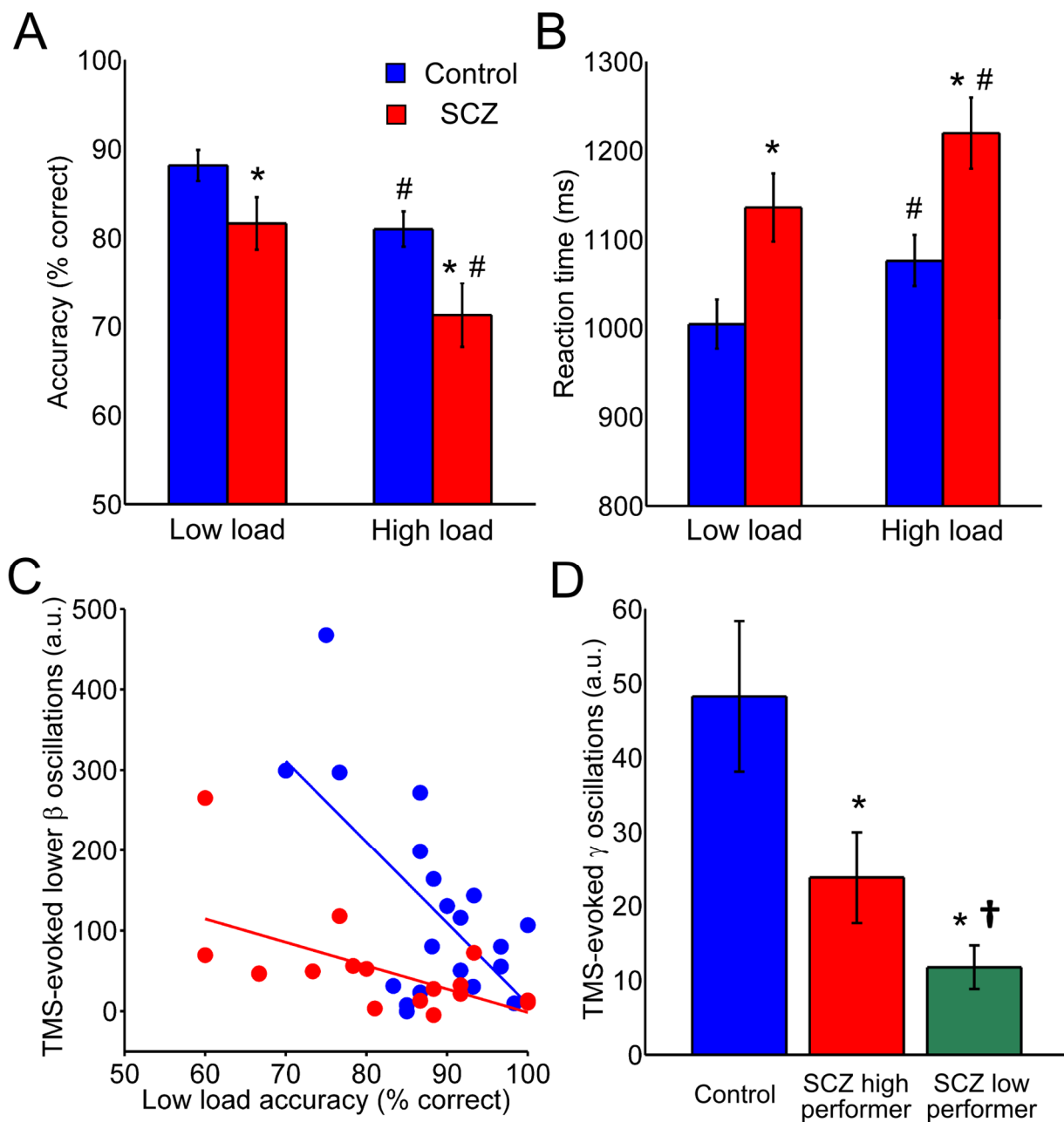


Figure 4: Working memory performance in the Sternberg task following low (five letters) and high (seven letters) loads in people with and without schizophrenia (SCZ). A) Working memory accuracy. B) Reaction time to correct responses. C) The relationship between transcranial magnetic stimulation (TMS)-evoked lower beta (13-20 Hz) oscillations and low load accuracy (controls, $p < 0.001$, $r = -0.63$; SCZ, $p = 0.009$, $r = -0.69$). D) TMS-evoked gamma (31-45 Hz) oscillations in controls, high SCZ performers (>60% accuracy in high load) and low SCZ performers (<60% accuracy in high load).

CHAPTER NINE

Discussion and conclusions

In this thesis, combined TMS-EEG was developed to allow recording of neurophysiological mechanisms from the DLFPC of people with and without SCZ. The following discussion provides an overview of the main findings from each empirical investigation. The implications of these findings are then discussed, followed by the limitations of the research and suggestions for future research.

Summary of main findings

Study one (chapter four): Short-Latency Artifacts Associated with Concurrent TMS-EEG.

In the study described in Chapter 4, we measured TMS-evoked EEG artifacts in phantoms (melons) and human participants across a range of conditions and equipment and using non-specialised EEG amplifiers. There were three main findings. First, different TMS machines resulted in different EEG artifact profiles. Whereas artifacts recovered relatively quickly (<3 ms) following stimulation with magstim machines as previously reported, magventure machines resulted in several additional high amplitude artifacts which prevented return of the signal to a useable recording range for several 100 ms. Second, when these additional artifacts were accounted for by preventing coil/electrode contact, EEG signal returned to a reasonable recording range within 10 ms for all arrangements. Third, additional physiological artifacts were present in human recordings. In particular, a large bipolar potential immediately following the TMS pulse was observed that took over 50 ms to recover. This large artifact was present with both stimulators, increased over lateral scalp positions, increased with increasing TMS intensity and was not inhibited by the LICl paradigm whereas the later signal was. This data combined with the topography of the artifact led us to conclude that this potential most likely resulted from TMS-evoked scalp muscle activation as opposed to large TMS-evoked cortical potentials as posited by others.

The significance of this study lies in its practical application; the results suggest that non-specialised EEG arrangements can be used to successfully record TMS-evoked neural activity. However, caution is required as both recording and physiological artifacts can be altered by different experimental arrangements. The methods of this paper will hopefully provide a guideline for other laboratories wishing to assess artifacts in their systems before beginning TMS-EEG research.

Study two (Chapter 5): Removing artifacts from TMS-EEG recordings using independent component analysis: importance for assessing prefrontal cortex network properties.

In Chapter 5, we assessed the utility of using ICA to separate TMS-evoked neural activity from TMS-evoked artifacts following stimulation over the DLPFC. There were three main findings to this study. First, we provided evidence that ICA could be used to identify several different kinds of TMS-evoked artifact following DLPFC stimulation: a fast and slow decay artifact, a blink artifact, an auditory artifact and artifacts most likely resulting from coil/electrode contact. Second, we provided evidence that these artifacts could be removed using ICA while minimally affecting the underlying TMS-evoked neural activity. Third, we demonstrated that if not removed, each artifact distorted TEPs and TMS-evoked oscillations both at the site of stimulation and across the scalp. Although it is not possible to conclusively demonstrate that the TMS-evoked neural signal was completely conserved following removal of artifacts with ICA, our data suggest that removing these artifacts is more beneficial than not removing them for evaluating DLPFC activity.

These findings extend previous work assessing the use of ICA to remove TMS-evoked muscle artifacts and provide one of the first attempts to validate the use of ICA for removing TMS-related blink and auditory artifacts. Our results indicate the extent to which artifacts can distort TMS-evoked neural activity and suggest that ICA can be used to recover TMS-evoked neural activity from the DLPFC.

Study three (Chapter 6): Mechanisms underlying long-interval cortical inhibition in the human motor cortex: a TMS-EEG study.

In Chapter 6, we investigated the origin of different TEP components. We varied conditioning and test intensities of the LICI paired pulse paradigm over motor cortex and measured changes in LICI strength of MEPs and different TEP peaks. There were two main findings. First, LICI of different TEP peaks were modulated independently of each other. LICI of the P30 peak increased with increasing conditioning intensity and decreased with increasing test intensity, correlating with LICI of MEPs. LICI of the P60 peak was also modulated in a similar fashion and correlated with P30 LICI, but not MEP LICI. In contrast, LICI of the N100 was not modulated by either condition. Second, the slope gradient of the EEG signal preceding the test pulse in the paired condition (i.e. the N100 evoked by the conditioning pulse) correlated with both LICI of P30 and with LICI of MEPs, suggesting this slope represented the mechanism responsible for LICI - most likely a GABA_B-mediated inhibitory potential.

These findings provide greater insight into the cortical mechanism underlying both MEP and TEP inhibition using the LICI paradigm. In addition, these results add to the growing body of evidence suggesting that early TEP components reflect excitatory neurotransmission, whereas later components reflect cortical inhibition.

Study four (Chapter 7): Mechanisms underlying markers of cortical inhibition in the dorsolateral prefrontal cortex: a TMS-EEG study.

In Chapter 7, we translated the findings of Chapter 6 in to the DLPFC. A group of healthy participants received single and paired pulse (LICI) TMS to the DLPFC and inter-individual variation in N100 slope gradient and LICI strength of different TEPs and TMS-evoked oscillations was observed. There were two main findings. First, variations in N100 slope gradient correlated with variations in LICI of early (N40) but not later (P60 or N100) TEP peaks, mirroring our findings from the motor cortex. N100 slope gradient also

correlated with LICl of TMS-evoked oscillations in the beta band (16-23 Hz). Second, we demonstrated that LICl not only suppressed local TMS-evoked activity (i.e. under the coil), but also inhibited the spread of TEPs and the entrainment of cortical oscillations in connected cortical regions. This finding suggests that both local and output networks are inhibited by the LICl paradigm.

The significance of this study is the demonstration that the N100 following TMS over the DLPFC is related to cortical inhibitory activity of both TEPs and oscillations. Although several studies have suggested a link between the DLPFC N100 and inhibition, this is the first empirical evidence, of which we are aware, to demonstrate this link. The finding that both local and global activity is suppressed by LICl also offers an interesting insight in to the role of GABA_B-mediated cortical inhibition in controlling network activity. This finding highlights the information that can be gained by using TMS-EEG to study cortical neurophysiology.

Study five (Chapter 8): Dorsolateral prefrontal cortex network properties are altered in schizophrenia: implications for working memory.

In Chapter 8, we applied the knowledge gained in Chapters 4-7 to study DLPFC network properties in people with and without SCZ using TMS-EEG. Participants received single pulse TMS over the DLPFC while EEG was recorded. Participants also completed a WM task. There were three main findings to this study. First, participants with SCZ displayed a smaller N100 and larger P180 following TMS compared with controls, suggesting impaired generation of inhibitory potentials and possibly excessive excitability in SCZ. Second, TMS-evoked upper beta and gamma oscillations were reduced in SCZ both at the site of stimulation and in fronto-parietal and interhemispheric networks, suggesting the ability to entrain oscillations in local and distant regions is impaired in SCZ. Finally, SCZ participants with lower WM capacity displayed reduced TMS-evoked gamma oscillations compared with other SCZ participants and controls, suggesting the ability to generate high frequency oscillations may be important for WM performance.

The findings from this study are significant as they directly address two outstanding questions in a prominent hypothesis on WM pathophysiology in SCZ. First, TMS-evoked activation of the DLPFC (i.e. upper beta and gamma oscillations) is reduced in SCZ independent of task activation and sensory input. Second, a marker of inhibitory neurotransmission is reduced in the DLPFC of people with SCZ *in vivo*. Thus, the findings of this study support dysfunctional DLPFC inhibitory networks in people with SCZ, which may underlie WM impairments.

Implications

The results from this series of studies have significant implications for the way in which we study cortical function, from the development of TMS-EEG as a robust neurophysiological technique to our causal understanding of cortical mechanisms such as inhibition, excitation, connectivity and intrinsic network dynamics. In addition, these findings also significantly inform our understanding of DLPFC network properties in SCZ and their potential involvement in WM impairments.

TMS-EEG methods

Since the first successful combination of TMS and EEG using a sample-and-hold circuit published in 1997 (Ilmoniemi et al., 1997) and the release of commercial Nexstim system, the use of TMS-EEG to study cortical networks has steadily grown. This growth has been aided by overall improvements in EEG amplifier quality, with many brands of non-specialised EEG amplifier now capable of capturing the main TMS artifact without saturation. As specialised TMS-EEG systems are expensive and not available in all parts of the world (for example Australia), the desire to combine existing TMS and EEG hardware is high (Fitzgerald, 2010). Perhaps the largest prohibitive factor for the wide spread use of TMS-EEG has been the difficulty in identifying and minimising the numerous artifacts associated with the technique, particularly in non-specialised systems which have not had the benefit of dedicated engineering. Chapters 4 and 5 directly

address this growing need, providing a detailed description of artifact in non-specialised TMS-EEG systems and methods for preventing and removing such artifacts.

From a practical perspective, the finding in Chapter 4 that different TMS machines can result in differing artifact profiles is important for the field. This finding highlights the importance of thoroughly testing the combination of existing hardware to ensure idiosyncratic recording artifacts are properly accounted for. Two separate artifacts were introduced by magventure stimulators. One resulted from recharge of the capacitors and could be removed by delaying the recharge until after the window of interest for TEPs. The origin of the second artifact was less clear and seemed to reflect activity from the machine that was propagated down the coil. Although the artifacts introduced by magventure stimulators could be ameliorated by preventing coil/electrode contact, this introduced its own practical difficulties. Higher stimulation intensities were required for equivalent cortical activation and the use of foam padding etc. was awkward and made coil repositioning difficult. The decay artifact introduced by the magventure stimulators seemed relatively stable and correction methods such as ICA (see Chapter 5) or fitting and subtracting exponential curves may prove useful in removing these artifacts offline. When these additional artifacts were accounted for, the DC-coupling and large operating range of the Synamps² amplifiers (Compumedics Ltd.) allowed recovery from the TMS artifact within 3-10 ms, which is comparable to that of the specialised Nexstim system (Virtanen et al., 1999) and BrainAmp amplifiers (Veniero et al., 2009). In line with previous research (Veniero et al., 2009), different pulse shapes had minimal effect on recovery times following the TMS artifact between magstim (mono) and magventure (bi), although monophasic pulses from the magventure stimulators did perform slightly worst. In addition, increasing stimulator intensity, changing scalp position and 10 Hz stimulation (i.e. LICI paired pulse) all had little effect on recovery time from the TMS pulse artifact, suggesting this type of artifact was reasonably stable.

In addition to the main TMS artifact, in Chapters 4 and 5 we have also described a large bipolar waveform which peaked within the first 10 ms following TMS, recovered after ~50 ms and has also been described

using Nexstim (Korhonen et al., 2011; Mutanen et al., 2012) and BrainAmp systems (Veniero, Maioli, & Miniussi, 2010). The origin of this waveform remains controversial, with muscle activity (Ilmoniemi & Kicić, 2010; Korhonen et al., 2011; Mäki & Ilmoniemi, 2011; Mutanen et al., 2012; Siebner et al., 2009), stored electrical charges at the skin/electrode interface (Julkunen et al., 2008), residual induced artifacts (Litvak et al., 2007), electromotive forces (Sekiguchi et al., 2011) and even large cortical-evoked potentials (Veniero, Bortoletto, & Miniussi, 2012; Veniero et al., 2010) all offered as explanations. We found that this waveform was not related to blinks, was not inhibited by LICI, had topography consistent with scalp muscle activity and increased in amplitude with more lateral scalp stimulation. Considering as well the size of the waveform ($>5000 \mu\text{V}$ in some cases), we conclude that this response is consistent with TMS-evoked scalp muscle activity and is extremely unlikely to solely represent TMS-evoked cortical activity. This interpretation is in line with another recent study, which also found an increase in amplitude of this early potential over lateral scalp positions using a different system (Mutanen et al., 2012). This is not to say that cortical activity is not represented in this early signal along with artifact. As recently demonstrated by Hernandez-Pavon et al. (2012), early TEP components can be recovered despite this large artifact using ICA along with various suppression techniques. A mixing of artifact and TEP might also reconcile the findings that this early response is modulated following repetitive TMS (Veniero et al., 2012, 2010). Further work is required to fully characterise the contribution of muscle and cortical activity to this early response.

Of note, the presence of the larger early artifact occurred at different lateral scalp positions between individuals, with approximately 40% of people displaying this artifact over the motor cortex, a finding also consistent with other research (Mutanen et al., 2012). In contrast, nearly all participants displayed this artifact over the DLPFC (between F3 and F5) and over more lateral central regions (between C3 and C5; Chapters 4 and 5). In fact, the DLPFC was particularly problematic for other physiological artifacts also, as TMS-evoked blinks proved common from this region. These artifacts were non-trivial and severely distorted measures of TMS-evoked neural activity in the time and frequency domain (Chapter 5). One easy approach to deal with these artifacts is to only stimulate close to the midline, where both blink and muscle artifacts

are minimised (Massimini et al., 2005). However, this approach is not an option for the DLPFC (Korhonen et al., 2011). Therefore, both Chapters 4 and 5 demonstrate the difficulty in using TMS-EEG to target regions such as the DLPFC due to physiological artifacts, noting this as a clear limitation of the technique.

In Chapter 5, we also investigated the use of ICA to separate TMS-evoked neural activity from TMS-evoked artifacts. This approach is well validated for removing blink (Plöchl, Ossandón, & König, 2012) and muscle activity (McMenamin et al., 2010) from regular EEG recordings and has also been applied to TMS-EEG data (Hamidi et al., 2010; Iwahashi, Arimatsu, Ueno, & Iramina, 2008; Korhonen et al., 2011; Rajji et al., 2013; Verhagen, Dijkerman, Medendorp, & Toni, 2013; Vernet et al., 2013). One challenge of ICA is that it is blind technique; the signal is separated into different components and then left to the experimenter to decide what to keep and what to discard (Onton et al., 2006). The significance of Chapter 5 is twofold. Firstly, we sought to provide evidence that the components we identified as artifacts were actually artifacts. This serves as an important validation for the use of ICA in TMS-EEG as certain artifacts such as the large muscle response and other related decay artifacts are specific to TMS-EEG research. Secondly, we attempted to quantify the success of the ICA algorithm in separating neural and artifact data. This is important as several properties of TMS-EEG artifacts such as the size of the muscle response (Hernandez-Pavon et al., 2012) and time locking of the blink response (Li & Principe, 2006) weaken certain assumptions of ICA. This can result in unsuccessful separation of neural signal and, therefore, invalidated data. Although complete certainty that the neural signal underlying TMS is unaffected by removing ICA components is not possible, the evidence we present in Chapter 5 suggests that removing artifacts with ICA provides a more accurate representation of the neural response following TMS over the DLPFC than the uncorrected signal. The evidence from Chapter 5 can be viewed as a foundation for developing more robust protocols that will allow consistency in data cleaning across the field.

Although we focused on the DLPFC, this research has implications for TMS-EEG over other regions also. For instance, auditory artifacts will result from any TMS experiment regardless of stimulation site if auditory masking is not employed (Massimini et al., 2005; Nikouline et al., 1999; Ter Braack et al., 2013; Tiitinen et al., 1999). In addition, blink artifacts can prove more common in certain groups of participants such as children even from stimulation of the motor cortex (Bruckmann et al., 2012). Therefore, a method for removing these artifacts is required when avoidance is not possible. The aim of this work was not to provide a comprehensive list of all artifacts resulting from TMS. For instance, we did not address somatosensory artifacts resulting from scalp muscle movement of direct stimulation of the trigeminal nerve (Ilmoniemi & Kicić, 2010), which are likely to be more common over certain regions. Instead, it is hoped that Chapter 5 will serve as a reference point for other researchers within the field and will improve consistency in accurately reporting artifacts removed from individual datasets using ICA. This will hopefully improve the comparability of data between studies and between research groups, further strengthening the use of TMS-EEG as a validated neurophysiological technique.

Evaluating cortical mechanisms with TMS

Having identified artifacts and established a method for artifact correction, Chapters 6 and 7 were dedicated to improving our understanding of the mechanisms responsible for TMS-evoked cortical potentials. Paired-pulse paradigms in the motor cortex have established that a complex interplay between excitatory and inhibitory neurotransmission follows stimulation of cortical neurons with TMS (Kujirai et al., 1993; Valls-Solé et al., 1992), which is likely to be reflected in EEG (Ferreri et al., 2011; Komssi et al., 2004). TMS causes a synchronous firing of excitatory and inhibitory neurons, which results in both glutamatergic and GABAergic neurotransmission (Paulus et al., 2008). These neurotransmitter bind to their respective pre- and post-synaptic receptors leading to excitatory and inhibitory currents which result in either hyper – or de-polarisation of the postsynaptic (and presynaptic) neurons (Esser, Hill, & Tononi, 2005). The predominance of excitation or inhibition in turn affects the net excitability of the stimulated region for several 100 ms following stimulation (Reis et al., 2008). The resultant fluctuations in net excitability

following TMS are thought to reflect the dominant activity of certain interneuron sub-types and the dynamics of postsynaptic receptors. Traditionally, net excitability has been gauged by testing the ability to generate subsequent output in corticospinal pyramidal neurons across time (i.e. a paired-pulse paradigms), which is quantified by measuring MEP size relative to a single suprathreshold TMS pulse. For instance, a subthreshold (i.e. below the threshold to evoke an MEP) TMS pulse is immediately followed by a period of reduced net excitability (2-6 ms; Kujirai et al., 1993) which is dependent on the GABA_A receptor (Ziemann, Lönnecker, et al., 1996) and is likely to reflect activity of inhibitory interneurons (Di Lazzaro et al., 1998a). This is followed by a period of increased net excitability likely dependent on glutamatergic neurotransmission of excitatory neurons (Kujirai et al., 1993; Ziemann, Rothwell, & Ridding, 1996) and possibly mediated by the NMDA receptor (Ziemann, Chen, Cohen, & Hallett, 1998). Following suprathreshold TMS, the early period of net inhibition is interleaved by periods of net excitation at intervals of approximately 1.5 ms (Ziemann, Tergau, Wassermann, et al., 1998). This excitation is strong enough to depolarise pyramidal neurons and results in several descending volleys which can be measured either with EMG and paired pulse paradigms (Ziemann, Tergau, Wassermann, et al., 1998) or using epidural electrodes at the spinal cord (Di Lazzaro et al., 1998b). The timing of these peaks could reflect arrival of excitatory input from other stimulated neurons several synapses away (Di Lazzaro, Ziemann, & Lemon, 2008) or possibly reflect the intrinsic firing properties of stimulated neurons (Esser et al., 2005). At longer intervals (25-45 ms) another period of net excitation is observed (Nakamura et al., 1997; Valls-Solé et al., 1992) which is not strong enough depolarise pyramidal cells and is followed by a long (50-180 ms) period of reduced net excitation dependent on the GABA_B receptor (Florian, Müller-Dahlhaus, Liu, & Ziemann, 2008; Fuhr et al., 1991; McDonnell et al., 2006; Valls-Solé et al., 1992). Following this period, another period of increased excitation, possibly reflecting disinhibition as a result of elongated presynaptic inhibition of inhibitory interneurons, has also been reported (Cash, Ziemann, Murray, & Thickbroom, 2010; Cash, Ziemann, & Thickbroom, 2011). The fluctuation in excitability following TMS shares many similarities with excitatory and inhibitory postsynaptic potentials observed in animal studies following electrical stimulation of the cortical surface (Connors, Malenka, & Silva, 1988; Moliadze, Zhao, Eysel, & Funke, 2003; Rosenthal, Waller, & Amassian, 1967; Stern, Edwards, & Sakmann, 1992; Sutor & Hablitz, 1989a, 1989b).

EEG signal reflects the difference between two points (i.e. recording electrodes) in the sum of extracellular voltage potentials resulting from synchronous activity of large population of cortical pyramidal neurons (Buzsáki et al., 2012). This signal is considerably smoothed and attenuated due to the distance and surfaces (hard and soft tissues) between the current source and scalp. Despite the warping of signal, we have argued in Chapter 3 that the fluctuations in net excitability evident with paired-pulse TMS should be at least partly reflected in the fluctuations of the TMS-evoked potential recorded with EEG. In accordance, the shape of the TEP following single-pulse stimulation of the motor cortex bares remarkable similarities with the pattern of net excitability described by paired-pulse studies. For instance, the P30 coincides with an early period of excitation, the N100 with a late period of inhibition and the P180 with a late period of excitation (Komssi et al., 2004). In Chapter 6, we directly assessed this hypothesis using the LICI paired pulse paradigm and demonstrated that the slope of the N100 was related to the inhibitory mechanism responsible for suppression of both MEP and early TEP size. Although circumstantial, we also observed a positive relationship between LICI of the MEP and P30, suggesting the two may also reflect similar excitatory mechanisms most likely mediated by glutamatergic neurotransmission. Both lines of evidence add to a steadily growing literature supporting independent mechanisms underlying different TEP peaks (Bonato et al., 2006; Bonnard et al., 2009; Ferreri et al., 2011; Komssi et al., 2004).

LICI of TEPs over motor cortex appears robust and has been replicated numerous times by our group (Daskalakis, Farzan, Barr, Maller, et al., 2008; Daskalakis, Farzan, Barr, Rusjan, et al., 2008; Farzan et al., 2010; Fitzgerald et al., 2008; Fitzgerald, Maller, Hoy, Farzan, & Daskalakis, 2009). However, modulation of TEPs by other paired pulse paradigms such as short-interval intracortical inhibition (SICI) and intracortical facilitation (ICF) have produced mixed results (Ferreri et al., 2011; Paus et al., 2001). The reasons for the discrepancies between findings within these studies remain unclear. It is possible that the activity evoked by the conditioning pulse needs to be removed from the test pulse in order to more accurately describe the modulatory effects of these paradigms as we have shown in Chapter 7. Alternatively, it may be that these

paradigms mainly alter early components, which are more difficult to measure. Regardless, the finding of Ferreri et al. (2011) demonstrating differential modulation of TEP peaks by these paradigms agrees with our LICl finding from the motor cortex.

Perhaps the most exciting implication of the findings from Chapter 6, from a neurophysiological perspective at least, is the potential to directly investigate excitatory and inhibitory mechanisms in regions outside of the motor cortex using TMS-EEG. However, TMS results in TEPs of slightly different morphologies from different regions (Kähkönen, Wilenius, Komssi, & Ilmoniemi, 2004; Massimini et al., 2007), possibly reflecting different intrinsic properties of either the neurons or their organisation across the cortex. It was therefore unclear whether the findings from the motor cortex would translate in to other cortical regions. To address this issue, we applied the LICl paradigm to the DLPFC and observed a similar relationship between the N100 following single pulse TMS and the suppression of an early TEP (N40) and TMS-evoked oscillations (16-23 Hz) with LICl. This evidence from Chapter 7 is the first we are aware of demonstrating that the N100 over the DLPFC also represents inhibitory neurotransmission. The results from Chapter 7 serve as a proof-of-principle that TMS-EEG can be used to study markers of cortical inhibition in non-motor regions.

One of the real advantages of TMS-EEG is the holistic view it provides on the effect of TMS on wider cortical networks. Twin coil TMS studies in the motor cortex have demonstrated that TMS not only activates local cortical circuits, but also stimulates cortico-cortical output neurons which result in activation of connected cortical regions (Daskalakis, Christensen, Fitzgerald, Roshan, & Chen, 2002; Ferbert et al., 1992). Using TMS-EEG, one can observe the propagation of current density to distant cortical regions (Ilmoniemi et al., 1997; Komssi et al., 2002; Massimini et al., 2005) and observe the effect of stimulating one region on entraining oscillations in other regions (Garcia, Grossman, & Srinivasan, 2011; Rosanova et al., 2009). For instance, in Chapters 5 and 8 we demonstrated that stimulation of the DLPFC resulted in alpha and gamma activity in

contralateral and posterior cortical regions. This measure of effective connectivity and network dynamics could prove useful in studying the functional role of certain brain regions within wider cortical networks. For instance, this technique could be used to map the functional anatomy of different brain regions (Garcia et al., 2011), such as sub-regions of the DLPFC. This finding also has important implications for cognitive research. Often, TMS is applied over a given region during a task in a 'virtual lesion' model, and resultant alterations in task performance are taken as causal evidence for a role of that region in the task (Pascual-Leone et al., 2000). However, as TMS not only activates the stimulated region, these changes in behaviour or task performance could reflect indirect stimulation of other cortical region, more relevant to actual task performance. Finally, we exploited this measure of TMS-evoked propagation to investigate the effect of LICI on DLPFC output to distant cortical regions. We demonstrated that LICI not only inhibits local circuits, but also suppresses the spread of TEPs and the entrainment of cortical oscillations across the cortex. This finding has implications for understanding the role of cortical inhibition in mediating top-down influences of the DLPFC on other cortical regions. Further research investigating the state-dependent alterations between inhibition and connectivity will provide greater insight in to this possibility (Bergmann et al., 2012; Johnson, Kundu, Casali, & Postle, 2012).

Understanding SCZ pathophysiology

The motivation for Chapters 4-7 was to develop a method for studying DLPFC neurophysiology in people with SCZ. In Chapter 8, we demonstrated the applicability of our methods to address two outstanding questions in the prominent hypothesis of WM impairment in SCZ. The first question relates to abnormal activation of the DLPFC in SCZ. One of the most replicated findings in SCZ is abnormal activity of the DLPFC during WM task performance, a finding evident across several neuroimaging modalities (Minzenberg et al., 2009). However, it remains unclear if this abnormal DLPFC activation is a causal factor related to the illness, or instead represents a secondary or compensatory activation resulting from deficits in sensory integration and encoding (Dias et al., 2011). We posited that TMS-EEG was ideally suited to test whether DLPFC activation was abnormal in SCZ, as TMS directly stimulates cortical networks and therefore by-passes the

need for sensory input or task performance. We demonstrated that participants with SCZ showed less TMS-evoked activity in the beta and gamma bands compared with controls. Importantly, the deficits in upper beta oscillations remained when overall TMS response size was taken in to account, confirming this alteration was not simply reflective of insufficient cortical stimulation due to cortical thinning in SCZ. In addition, we also demonstrated reduced upper beta and gamma band activity in the contralateral DLPFC and ipsilateral parietal cortex respectively, suggesting that the ability of the DLPFC to entrain oscillations in distant cortical regions was also reduced in SCZ. This finding directly supports abnormal DLPFC activation in people with SCZ.

The finding from the study described in Chapter 8 of reduced oscillatory activation in the DLPFC of people with SCZ compliments two other recent TMS-EEG studies, which also reported reduced beta/gamma oscillations in the premotor and superior frontal gyrus of participants with SCZ (Ferrarelli et al., 2008, 2012). Participants also demonstrated reduced propagation of TMS-evoked activity compared with controls (Ferrarelli et al., 2008). In both of these studies, participants with SCZ demonstrated reduced peak oscillation frequency following frontal TMS. TMS-evoked oscillatory deficit increased in a posterior to anterior direction along the cortex, with no deficits observed in the parietal, mild deficits in the motor and strong deficits in the prefrontal cortex. In addition, reduced peak frequency correlated with WM deficits in the frontal cortex (Ferrarelli et al., 2012). The relationship between TMS-evoked activity and task-evoked activity is somewhat unclear. TMS results in a non-selective, synchronous firing of neurons underneath the coil, which is likely very different from the activation of specific neural circuits which underlie tasks such as WM. Although we did not find a linear relationship between TMS-evoked gamma and WM, we did find that SCZ participants with low WM capacity displayed lower TMS-evoked gamma oscillations compared with other SCZ participants and with controls. This finding suggests that TMS-evoked oscillations may at least in part represent activation of neural networks that are important for WM performance. In turn, these findings provide independent confirmation that the neural circuits responsible for gamma oscillations are deficient in SCZ, as predicted by post mortem anatomical studies (Gonzalez-Burgos & Lewis, 2008). This

finding represents an important step in determining the link between abnormal DLPFC activation and WM impairments in SCZ. However, as we didn't test other cortical sites, it remains unclear whether TMS-evoked gamma deficits specific to the DLPFC are important for WM performance in SCZ, or whether global deficits may also contribute.

The second question relates to findings from post mortem studies, which have reported deficits in mRNA and protein related to GABA synthesis and release across the cortex in SCZ (Lewis, Curley, Glausier, & Volk, 2012). Despite sensorimotor gating evidence in the auditory cortex (Freedman et al., 1996) and TMS evidence from the motor cortex (Daskalakis et al., 2002; Fitzgerald et al., 2002; discussed in chapter 2), little to no direct evidence exists for cortical inhibitory deficits in the DLPFC. In fact, magnetic resonance spectroscopy of GABA concentrations in the frontal cortex of SCZ has produced largely mixed results with both decreases (Goto, Yoshimura, Moriya, et al., 2009) and increases (Kegeles et al., 2012) reported relative to controls. Using the measures validated in Chapters 6 and 7, we demonstrated that TMS-evoked N100 slope and amplitude was reduced in the DLPFC of SCZ compared with controls. This finding provides some of the first direct evidence that inhibitory neurotransmission is deficient in the DLPFC of people with SCZ. These results compliment another TMS-EEG which recently found reduced LICl of gamma oscillations in the DLPFC of people with SCZ, but not with bipolar disorder (Farzan et al., 2010). Reduced N100 may indeed reflect the mechanism responsible for reduced LICl of oscillations in SCZ (see Chapter 7). The specificity of LICl deficits to SCZ as opposed to other psychotic illnesses (i.e. bipolar disorder) suggest this measure may serve as a potential endophenotype for the illness (Farzan et al., 2010). Whether N100 deficits are also specific to SCZ and are present through different stages of the illness requires further investigation.

The relevance of reduced N100 to WM performance and impaired gamma oscillation generation in SCZ is unclear. We could not find any relationship between N100 and WM deficits in SCZ, however, we only tested one WM task which may not have been sensitive enough to detect a relationship. WM tasks involving

manipulation as well as maintenance, such as the n-back task, result in larger DLPFC activation and might be more suitable for detecting any potential relationships (Rottschy et al., 2012). In addition, we have suggested that the N100 most likely reflects inhibitory potentials generated by postsynaptic GABA_B receptors. GABA_B receptors are mainly located extra-synaptically on postsynaptic neurons and are activated by excessive GABA that spills from the synaptic cleft (Chalifoux & Carter, 2011; Kohl & Paulsen, 2010). Some evidence also exists that neurogliaform cells, a sub-type of inhibitory interneuron, can specifically activate post-synaptic GABA_B-receptors (Tamás, Lorincz, Simon, & Szabadics, 2003). Alternatively, gamma oscillations are dependent on fast spiking, PV-positive inhibitory interneurons which mediate their inhibitory effect primarily through the GABA_A receptor (Cardin et al., 2009; Sohal et al., 2009). It is therefore unclear whether deficits in the N100 reflect abnormal GABA neurotransmission from inhibitory interneurons, which could affect both GABA_A and GABA_B-mediated cortical inhibition, or whether this deficit reflects impaired GABA_B receptor or neurogliaform cell function in SCZ. Measuring specific GABA_A-mediated inhibitory potentials is required to address this problem. At present, this is not possible or controversial using TMS-EEG over DLPFC. Measuring this activity in a way similar to the N100 requires accurate TEP recordings within 5-6 ms following the TMS pulse, which is not possible using our experiment arrangement (see Chapter 4). In addition, paired-pulse paradigms that assess GABA_A-mediated inhibition over motor cortex such as SICI have produced mixed results with TMS-EEG and appear unreliable (Ferreri et al., 2011; Paus et al., 2001). Regardless, we have demonstrated that participants with SCZ display deficient inhibitory neurotransmission in the DLPFC. These findings suggest that new treatments targeting cortical inhibitory circuits may prove useful in improving DLPFC function in SCZ.

In addition to inhibitory deficits, we also reported increased P180 relative to other peaks in SCZ. This finding supports an emerging trend in the response of participants with SCZ to TMS. Whereas early activity within the first 150 ms following TMS appears reduced in SCZ (Ferrarelli et al., 2008, 2012; Levitt-Binnun et al., 2010), this study is the second to report an increase in later (150 ms onwards) TMS-evoked activity (Frantseva et al., 2012), and the first to report this in the DLPFC. Frantseva and colleagues interpreted

increased TMS-evoked activity as a potential indication of excessive signal propagation resulting from disinhibition in SCZ. Intriguingly, the P180 coincides with a period of disinhibition observed in the motor cortex (Cash et al., 2010, 2011), most likely resulting from presynaptic autoinhibition of inhibitory interneurons. The P180 may directly reflect a similar mechanism, therefore indicating a functional consequence of reduced inhibitory tone in SCZ. Further research using both TMS-EMG and TMS-EEG is required to investigate this possibility. Taken together, these findings of impaired activation and abnormal inhibition/excitation in the DLPFC of SCZ highlight the utility of TMS-EEG to investigate cortical function in health and disease.

Limitations

Limitations specific to each study are discussed in detail in the relevant chapters. To prevent repetition, we will only cover the main limitations that apply to all or most studies. First, in order to measure activity from the DLPFC we needed to remove a large amount of non-TMS related data, which obscures the TMS-evoked response, using ICA. This process resulted in a considerable change to the data (see Chapter 5). It is impossible to be completely certain that by doing this we have not altered TMS-evoked neural activity in some way. It is also impossible to be completely certain that artifacts are removed in a uniform way between individuals. In addition, as the decision of which artifacts to remove involves a subjective decision by the experimenter, it is therefore difficult to remain certain that each data set is treated in the exact same way. This point is particularly important when comparing TEPs between groups such as in Chapter 8. We took several steps to minimise these limitation as much as possible. 1) We compared ICA removal using different methods such as compression to improve confidence that we were not over correcting the data. 2) We provided evidence of the origin of each artifact we removed and used this information to create some general guidelines for identifying artifacts (supplementary material, Chapter 5). 3) ICA removal was repeated by a second experimenter to assess the reproducibility of the resultant TEPs. To further strengthen this work, comparison with suppression techniques that prevent distortion of neural components in the presence of high amplitude artifacts is required (Hernandez-Pavon et al., 2012). It is

worth noting that the recovered DLPFC TEP following ICA correction was remarkably similar to that reported elsewhere using a different system, with a similar number of peaks at comparable latencies and with comparable scalp distributions (S Kähkönen et al., 2005; Lioumis et al., 2009). Although it is not possible to completely address this limitation, the evidence we have provided in Chapter 5 improves confidence that the recovered signal largely reflects TMS-evoked neural activity.

Second, in all DLPFC experiments, we used measures from the motor cortex to set stimulation intensities. This approach is flawed in logic as there is no correlation between the scalp-to-cortex distance of the motor cortex and the DLPFC (Stokes et al., 2005). Therefore, using motor measures to set intensities for the DLPFC could result in over or under stimulating this region (Pell, Roth, & Zangen, 2011). However, there is currently no consensus within the brain stimulation community on how to adequately address this issue. Some neuronavigational systems come with software that estimates the electric field induced by the TMS pulse in the underlying cortex (Massimini et al., 2005). This approach is prohibitive to most groups, as it requires expensive hardware. Several laboratories are developing sophisticated finite element models of TMS-evoked electric field (Opitz et al., 2013; Opitz, Windhoff, Heidemann, Turner, & Thielscher, 2011) that might become available to the wider brain stimulation community. In addition, a basic ratio has also been calculated for estimating intensities for other regions based on the resting motor threshold (Stokes et al., 2005, 2007). However both of these approaches still require an MRI scan for all individuals, which is not always practical for financial and logistical reasons. One interesting idea is to use TMS-EEG to determine thresholds from non-motor regions (Komssi, Savolainen, Heiskala, & Kähkönen, 2007). Although appealing in theory, the poor signal-to-noise ratio of EEG recordings would potentially require a large number of stimuli that may not be practical. Therefore, we used either resting motor threshold or the intensity required to evoke a 1 mV response over motor cortex to set DLPFC stimulation parameters, fully acknowledging the potential limitation of this technique. To account for potential group differences resulting from this measure in chapter 8, we normalised our measure to overall TMS-evoked response size. This approach might prove useful for others studies faced with similar limitations.

Finally, we did not use neuronavigation to target the DLPFC. Activation of the cortex by TMS is dependent on the position of the induced electrical current relative to the peak of the gyri, with optimal stimulation achieved when the coil is perpendicular to gyral direction (Kammer, Beck, Thielscher, Laubis-Herrmann, & Topka, 2001). This is easy to determine over motor cortex as the optimal site can be determined by measuring MEP amplitude online. This is obviously not an option for regions such as the DLPFC, hence the need for neuronavigation. To account for this, we based our DLPFC positioning on 10-20 electrode positions (between F3 and F5). This position has been shown to provide the most accurate estimation of the DLPFC position in the absence of neuronavigation (Fitzgerald, Maller, Hoy, Thomson, & Daskalakis, 2009; Rusjan et al., 2010). We reasoned that, over enough participants, small differences in position of the coil relative to prefrontal gyri would be averaged out. However, we acknowledge that ideally neuronavigation should be used and could reduce variability between individuals.

Future directions

As with limitations, suggestions for future directions for each study are discussed in the relevant chapters. To avoid repetition, we will not repeat them all here, however we will highlight the most important. First, we have demonstrated in Chapter 5 that ICA has the potential to recover TMS-evoked neural activity from regions such as the DLPFC. However, the use of ICA to remove artifacts requires further validation.

Introducing known signals into data is one approach that is particularly useful for evaluating the efficacy of ICA in accurately decomposing EEG signal (Hernandez-Pavon et al., 2012). This method may help to confirm that muscle, blink and auditory artifacts can be removed without affecting time-locked neural activity. In addition, improved methods and pipelines are required to streamline analysis. The method used in Chapter 5 was extremely time consuming. Using suppression methods to limit the number of independent components could make this decision making process easier and faster (Hernandez-Pavon et al., 2012; Korhonen et al., 2011). Ideally, some kind of consensus on methods for cleaning TMS-EEG data should be

reached within the brain stimulation community. To facilitate this, comparisons of different methods such as PCA (Litvak et al., 2007; Mäki & Ilmoniemi, 2011; ter Braack, de Jonge, & van Putten, 2013) and curve fitting (Verhagen et al., 2013) are required to determine the best technique for recovering neural data. It may be that a combination of techniques is required to adequately remove different artifacts. Having a standardised method will improve comparability of results across the field.

Second, the use of TMS-EEG to study cortical mechanisms such as excitation and inhibition in motor and non-motor areas is extremely promising. In Chapters 6 and 7 we have provided some of the first evidence that the N100 represents inhibitory activity in different cortical regions. However, significantly more research is required to better understand the origin of different TEP peaks. Paired-pulse approaches such as the one we have employed could be used to target specific TEP. Facilitation or inhibition of subsequent TEPs would provide evidence of excitatory or inhibitory activity. Alternatively, detailed inhibition/excitation curves tested across a large number of inter-stimulus intervals acquired from MEP data could be mapped on to TEPs to identify periods of particular interest. Importantly, volume conduction also needs to be taken in to account to determine which peaks represents excitation/inhibition of local circuits and which represent excitation/inhibition of the spread of TMS-evoked activity. Pharmacological approaches are an ideal way of determining the relationship between different peaks and excitatory and inhibitory mechanisms. Such approaches have been used extensively in the TMS-EMG literature, particularly for paired-pulse studies (Paulus et al., 2008) and would greatly benefit knowledge of TEP mechanisms. Once these methods are better established, TMS-EEG will allow comparisons of excitability/inhibition between different brain regions, during different states such as functional tasks and in different pathological conditions.

Thirdly, a more detailed account of TMS-evoked cortical activation is required in SCZ. We have shown in Chapter 8 that DLPFC activation is reduced in SCZ, particularly in people with low WM capacity. In addition,

we also demonstrated that a marker of cortical inhibition was reduced in the DLPFC of people with SCZ. However, it remains unclear whether other cortical regions are also impaired. A more comprehensive evaluation of TMS-evoked cortical activity from other cortical regions will assist in clarifying this point. It is also unclear how impaired TMS-evoked activity relates to impaired task-evoked activity in the DLPFC. A comparison of DLPFC activity assessed during a task is required to compare with TMS-evoked activity. Finally, assessing the TMS-evoked response during a WM task might provide further insight in to the role of GABA_B-mediated inhibition in cognitive control and provide context for dysfunctional inhibition in SCZ-related WM impairment.

Conclusions

The findings presented in this thesis contribute to the development of combined TMS-EEG as a technique for studying cortical network properties in conscious humans. In addition, we have demonstrated the application of TMS-EEG for studying DLPFC neurophysiology in healthy people and in people with SCZ. It is hoped this research will broaden the use of TMS-EEG as neurophysiological method and play a role in identifying novel biological targets to develop effective treatments for cognitive impairment in SCZ.

REFERENCES

- Akbarian, S., Kim, J. J., Potkin, S. G., Hagman, J. O., Tafazzoli, A., Bunney, W. E., & Jones, E. G. (1995). Gene expression for glutamic acid decarboxylase is reduced without loss of neurons in prefrontal cortex of schizophrenics. *Archives of general psychiatry*, 52(4), 258–66.
- Amassian, V. E., Cracco, R. Q., & Maccabee, P. J. (1989). Focal stimulation of human cerebral cortex with the magnetic coil: a comparison with electrical stimulation. *Electroencephalography and clinical neurophysiology*, 74(6), 401–16.
- Amassian, V. E., Eberle, L., Maccabee, P. J., & Cracco, R. Q. (1992). Modelling magnetic coil excitation of human cerebral cortex with a peripheral nerve immersed in a brain-shaped volume conductor: the significance of fiber bending in excitation. *Electroencephalography and clinical neurophysiology*, 85(5), 291–301.
- American Psychiatric Association. (2000). *Diagnostic and Statistical Manual of Mental Disorders, Fourth Edition, Text Revision (DSM-IV-TR)*. Text (Vol. 1, p. 943). Arlington, VA: American Psychiatric Association.
- Baddeley, A. (1992). Working memory. *Science*, 255(5044), 556–9.
- Barch, D. M., & Ceaser, A. (2012). Cognition in schizophrenia: core psychological and neural mechanisms. *Trends in cognitive sciences*, 16(1), 27–34.
- Barker, A. T., Jalinous, R., & Freeston, I. L. (1985). Non-invasive magnetic stimulation of human motor cortex. *Lancet*, 1(8437), 1106–7.
- Baron, M., Gruen, R., Asnis, L., & Kane, J. (1983). Familial relatedness of schizophrenia and schizotypal states. *The American journal of psychiatry*, 140(11), 1437–42.
- Barr, M. S., Farzan, F., Tran, L. C., Chen, R., Fitzgerald, P. B., & Daskalakis, Z. J. (2010). Evidence for excessive frontal evoked gamma oscillatory activity in schizophrenia during working memory. *Schizophrenia research*, 121(1-3), 146–52.
- Basar-Eroglu, C., Brand, A., Hildebrandt, H., Karolina Kedzior, K., Mathes, B., & Schmiedt, C. (2007). Working memory related gamma oscillations in schizophrenia patients. *International journal of psychophysiology*, 64(1), 39–45.
- Benes, F. M., Vincent, S. L., Marie, A., & Khan, Y. (1996). Up-regulation of GABAA receptor binding on neurons of the prefrontal cortex in schizophrenic subjects. *Neuroscience*, 75(4), 1021–31.
- Bergmann, T. O., Mölle, M., Schmidt, M. a, Lindner, C., Marshall, L., Born, J., & Siebner, H. R. (2012). EEG-guided transcranial magnetic stimulation reveals rapid shifts in motor cortical excitability during the human sleep slow oscillation. *The Journal of neuroscience*, 32(1), 243–53.
- Bitanirwe, B. K. Y., Lim, M. P., Kelley, J. F., Kaneko, T., & Woo, T. U. W. (2009). Glutamatergic deficits and parvalbumin-containing inhibitory neurons in the prefrontal cortex in schizophrenia. *BMC psychiatry*, 9, 71.

- Bonato, C., Miniussi, C., & Rossini, P. M. (2006). Transcranial magnetic stimulation and cortical evoked potentials: a TMS/EEG co-registration study. *Clinical neurophysiology*, 117(8), 1699–707.
- Bonnard, M., Spieser, L., Meziane, H. B., de Graaf, J. B., & Pailhous, J. (2009). Prior intention can locally tune inhibitory processes in the primary motor cortex: direct evidence from combined TMS-EEG. *The European journal of neuroscience*, 30(5), 913–23.
- Bowie, C. R., Reichenberg, A., Patterson, T. L., Heaton, R. K., & Harvey, P. D. (2006). Determinants of real-world functional performance in schizophrenia subjects: correlations with cognition, functional capacity, and symptoms. *The American journal of psychiatry*, 163(3), 418–25.
- Braver, T. S., Cohen, J. D., Nystrom, L. E., Jonides, J., Smith, E. E., & Noll, D. C. (1997). A parametric study of prefrontal cortex involvement in human working memory. *NeuroImage*, 5(1), 49–62.
- Bray, N. J., Leweke, F. M., Kapur, S., & Meyer-Lindenberg, A. (2010). The neurobiology of schizophrenia: new leads and avenues for treatment. *Current opinion in neurobiology*, 20(6), 810–5.
- Brignani, D., Manganotti, P., Rossini, P. M., & Miniussi, C. (2008). Modulation of cortical oscillatory activity during transcranial magnetic stimulation. *Human brain mapping*, 29(5), 603–12.
- Brown, J. T., Davies, C. H., & Randall, A. D. (2007). Synaptic activation of GABA(B) receptors regulates neuronal network activity and entrainment. *The European journal of neuroscience*, 25(10), 2982–90.
- Bruckmann, S., Hauk, D., Roessner, V., Resch, F., Freitag, C. M., Kammer, T., ... Bender, S. (2012). Cortical inhibition in attention deficit hyperactivity disorder: new insights from the electroencephalographic response to transcranial magnetic stimulation. *Brain*, 135(Pt 7), 2215–30.
- Buchanan, R. W., Keefe, R. S. E., Lieberman, J. A., Barch, D. M., Csernansky, J. G., Goff, D. C., ... Marder, S. R. (2011). A randomized clinical trial of MK-0777 for the treatment of cognitive impairments in people with schizophrenia. *Biological psychiatry*, 69(5), 442–9.
- Buzsáki, G., Anastassiou, C. a, & Koch, C. (2012). The origin of extracellular fields and currents--EEG, ECoG, LFP and spikes. *Nature reviews. Neuroscience*, 13(6), 407–20.
- Buzsáki, G., & Draguhn, A. (2004). Neuronal oscillations in cortical networks. *Science*, 304(5679), 1926–9.
- Buzsáki, G., & Wang, X.-J. (2012). Mechanisms of gamma oscillations. *Annual review of neuroscience*, 35, 203–25.
- Callicott, J H, Mattay, V. S., Bertolino, a, Finn, K., Coppola, R., Frank, J. a, ... Weinberger, D. R. (1999). Physiological characteristics of capacity constraints in working memory as revealed by functional MRI. *Cerebral cortex*, 9(1), 20–6.
- Callicott, Joseph H, Mattay, V. S., Verchinski, B. a, Marenco, S., Egan, M. F., & Weinberger, D. R. (2003). Complexity of prefrontal cortical dysfunction in schizophrenia: more than up or down. *The American journal of psychiatry*, 160(12), 2209–15.
- Cannon, T. D., Kaprio, J., Lönnqvist, J., Huttunen, M., & Koskenvuo, M. (1998). The genetic epidemiology of schizophrenia in a Finnish twin cohort. A population-based modeling study. *Archives of general psychiatry*, 55(1), 67–74.

- Cardin, J. a, Carlén, M., Meletis, K., Knoblich, U., Zhang, F., Deisseroth, K., ... Moore, C. I. (2009). Driving fast-spiking cells induces gamma rhythm and controls sensory responses. *Nature*, 459(7247), 663–7.
- Cash, R. F. H., Ziemann, U., Murray, K., & Thickbroom, G. W. (2010). Late cortical disinhibition in human motor cortex: a triple-pulse transcranial magnetic stimulation study. *Journal of neurophysiology*, 103(1), 511–8.
- Cash, R. F. H., Ziemann, U., & Thickbroom, G. W. (2011). Inhibitory and disinhibitory effects on I-wave facilitation in motor cortex. *Journal of neurophysiology*, 105(1), 100–6.
- Chalifoux, J. R., & Carter, A. G. (2011). GABAB receptor modulation of synaptic function. *Current opinion in neurobiology*, 21(2), 339–44.
- Cho, R. Y., Konecky, R. O., & Carter, C. S. (2006). Impairments in frontal cortical gamma synchrony and cognitive control in schizophrenia. *Proceedings of the National Academy of Sciences of the United States of America*, 103(52), 19878–83.
- Colton, C. W., & Manderscheid, R. W. (2006). Congruencies in increased mortality rates, years of potential life lost, and causes of death among public mental health clients in eight states. *Preventing chronic disease*, 3(2), A42.
- Cona, F., Zavaglia, M., Massimini, M., Rosanova, M., & Ursino, M. (2011). A neural mass model of interconnected regions simulates rhythm propagation observed via TMS-EEG. *NeuroImage*, 57(3), 1045–58.
- Connors, B. W., Malenka, R. C., & Silva, L. R. (1988). Two inhibitory postsynaptic potentials, and GABAA and GABAB receptor-mediated responses in neocortex of rat and cat. *The Journal of physiology*, 406, 443–68.
- Cracco, R. Q., Amassian, V. E., Maccabee, P. J., & Cracco, J. B. (1989). Comparison of human transcallosal responses evoked by magnetic coil and electrical stimulation. *Electroencephalography and clinical neurophysiology*, 74(6), 417–24.
- Croft, R. J., & Barry, R. J. (2000). EOG correction of blinks with saccade coefficients: a test and revision of the aligned-artefact average solution. *Clinical neurophysiology*, 111(3), 444–51.
- Curtis, C. E., & D’Esposito, M. (2003). Persistent activity in the prefrontal cortex during working memory. *Trends in Cognitive Sciences*, 7(9), 415–423.
- Curtis, V. a, Bullmore, E. T., Brammer, M. J., Wright, I. C., Williams, S. C., Morris, R. G., ... McGuire, P. K. (1998). Attenuated frontal activation during a verbal fluency task in patients with schizophrenia. *The American journal of psychiatry*, 155(8), 1056–63.
- Daskalakis, Z. J, Christensen, B. K., Fitzgerald, P. B., Roshan, L., & Chen, R. (2002). The mechanisms of interhemispheric inhibition in the human motor cortex. *The Journal of Physiology*, 543(1), 317–326.
- Daskalakis, Zafiris J, Christensen, B. K., Chen, R., Fitzgerald, P. B., Zipursky, R. B., & Kapur, S. (2002). Evidence for impaired cortical inhibition in schizophrenia using transcranial magnetic stimulation. *Archives of general psychiatry*, 59(4), 347–54.

- Daskalakis, Zafiris J, Farzan, F., Barr, M. S., Maller, J. J., Chen, R., & Fitzgerald, P. B. (2008). Long-interval cortical inhibition from the dorsolateral prefrontal cortex: a TMS-EEG study. *Neuropsychopharmacology*, 33(12), 2860–9.
- Daskalakis, Zafiris J, Farzan, F., Barr, M. S., Rusjan, P. M., Favalli, G., Levinson, A. J., & Fitzgerald, P. B. (2008). Evaluating the relationship between long interval cortical inhibition, working memory and gamma band activity in the dorsolateral prefrontal cortex. *Clinical EEG and neuroscience*, 39(3), 150–5.
- Di Lazzaro, V, Restuccia, D., Oliviero, a, Profice, P., Ferrara, L., Insola, a, ... Rothwell, J. C. (1998a). Magnetic transcranial stimulation at intensities below active motor threshold activates intracortical inhibitory circuits. *Experimental brain research*, 119(2), 265–8.
- Di Lazzaro, V, Restuccia, D., Oliviero, a, Profice, P., Ferrara, L., Insola, a, ... Rothwell, J. C. (1998b). Effects of voluntary contraction on descending volleys evoked by transcranial stimulation in conscious humans. *The Journal of physiology*, 508, 625–33.
- Di Lazzaro, Vincenzo, Ziemann, U., & Lemon, R. N. (2008). State of the art: Physiology of transcranial motor cortex stimulation. *Brain stimulation*, 1(4), 345–62.
- Dias, E. C., Butler, P. D., Hoptman, M. J., & Javitt, D. C. (2011). Early sensory contributions to contextual encoding deficits in schizophrenia. *Archives of general psychiatry*, 68(7), 654–64.
- Doherty, J. L., O'Donovan, M. C., & Owen, M. J. (2012). Recent genomic advances in schizophrenia. *Clinical genetics*, 81(2), 103–9.
- Edin, F., Klingberg, T., Johansson, P., McNab, F., Tegnér, J., & Compte, A. (2009). Mechanism for top-down control of working memory capacity. *Proceedings of the National Academy of Sciences of the United States of America*, 106(16), 6802–7.
- Ellison-Wright, I., & Bullmore, E. (2010). Anatomy of bipolar disorder and schizophrenia: a meta-analysis. *Schizophrenia research*, 117(1), 1–12.
- Esser, S. K., Hill, S. L., & Tononi, G. (2005). Modeling the effects of transcranial magnetic stimulation on cortical circuits. *Journal of neurophysiology*, 94(1), 622–39.
- Farzan, F., Barr, M. S., Levinson, a. J., Chen, R., Wong, W., Fitzgerald, P. B., & Daskalakis, Z. J. (2010). Reliability of Long-Interval Cortical Inhibition in Healthy Human Subjects: A TMS-EEG Study. *Journal of Neurophysiology*, 104(3), 1339–1346.
- Farzan, Faranak, Barr, M. S., Levinson, A. J., Chen, R., Wong, W., Fitzgerald, P. B., & Daskalakis, Z. J. (2010). Evidence for gamma inhibition deficits in the dorsolateral prefrontal cortex of patients with schizophrenia. *Brain*, 133(Pt 5), 1505–14.
- Ferbert, A., Priori, A., Rothwell, J. C., Day, B. L., Colebatch, J. G., & Marsden, C. D. (1992). Interhemispheric inhibition of the human motor cortex. *The Journal of physiology*, 453, 525–46.
- Ferrarelli, F., Massimini, M., Peterson, M. J., Riedner, B. a, Lazar, M., Murphy, M. J., ... Tononi, G. (2008). Reduced evoked gamma oscillations in the frontal cortex in schizophrenia patients: a TMS/EEG study. *The American journal of psychiatry*, 165(8), 996–1005.

- Ferrarelli, F., Sarasso, S., Guller, Y., Riedner, B. a, Peterson, M. J., Bellesi, M., ... Tononi, G. (2012). Reduced natural oscillatory frequency of frontal thalamocortical circuits in schizophrenia. *Archives of general psychiatry*, 69(8), 766–74.
- Ferreri, F., Pasqualetti, P., Määttä, S., Ponzo, D., Ferrarelli, F., Tononi, G., ... Rossini, P. M. (2011). Human brain connectivity during single and paired pulse transcranial magnetic stimulation. *NeuroImage*, 54(1), 90–102.
- Fitzgerald, P B, Brown, T. L., Daskalakis, Z. J., DeCastella, A., & Kulkarni, J. (2002). A study of transcallosal inhibition in schizophrenia using transcranial magnetic stimulation. *Schizophrenia research*, 56(3), 199–209.
- Fitzgerald, P., de Castella, A., Arya, D., Simons, W. R., Eggleston, A., Meere, S., & Kulkarni, J. (2009). The cost of relapse in schizophrenia and schizoaffective disorder. *Australasian psychiatry : bulletin of Royal Australian and New Zealand College of Psychiatrists*, 17(4), 265–72.
- Fitzgerald, Paul B. (2010). TMS-EEG: a technique that has come of age? *Clinical neurophysiology*, 121(3), 265–7.
- Fitzgerald, Paul B, Brown, T. L., Daskalakis, Z. J., & Kulkarni, J. (2002). A transcranial magnetic stimulation study of inhibitory deficits in the motor cortex in patients with schizophrenia. *Psychiatry research*, 114(1), 11–22.
- Fitzgerald, Paul B, Brown, T. L., Marston, N. A. U., Oxley, T. J., de Castella, A., Daskalakis, Z. J., & Kulkarni, J. (2003). A transcranial magnetic stimulation study of abnormal cortical inhibition in schizophrenia. *Psychiatry research*, 118(3), 197–207.
- Fitzgerald, Paul B, Daskalakis, Z. J., Hoy, K., Farzan, F., Upton, D. J., Cooper, N. R., & Maller, J. J. (2008). Cortical inhibition in motor and non-motor regions: a combined TMS-EEG study. *Clinical EEG and neuroscience*, 39(3), 112–7.
- Fitzgerald, Paul B, Maller, J. J., Hoy, K. E., Thomson, R., & Daskalakis, Z. J. (2009). Exploring the optimal site for the localization of dorsolateral prefrontal cortex in brain stimulation experiments. *Brain stimulation*, 2(4), 234–7.
- Fitzgerald, Paul B, Maller, J. J., Hoy, K., Farzan, F., & Daskalakis, Z. J. (2009). GABA and cortical inhibition in motor and non-motor regions using combined TMS-EEG: a time analysis. *Clinical neurophysiology*, 120(9), 1706–10.
- Florian, J., Müller-Dahlhaus, M., Liu, Y., & Ziemann, U. (2008). Inhibitory circuits and the nature of their interactions in the human motor cortex a pharmacological TMS study. *The Journal of physiology*, 586(2), 495–514.
- Forbes, N. F., Carrick, L. a, McIntosh, a M., & Lawrie, S. M. (2009). Working memory in schizophrenia: a meta-analysis. *Psychological medicine*, 39(6), 889–905.
- Foster, A., Gable, J., & Buckley, J. (2012). Homelessness in schizophrenia. *The Psychiatric clinics of North America*, 35(3), 717–34.
- Frantseva, M., Cui, J., Farzan, F., Chinta, L. V, Perez Velazquez, J. L., & Daskalakis, Z. J. (2012). Disrupted Cortical Conductivity in Schizophrenia: TMS-EEG Study. *Cerebral cortex*, 1–11.

- Freedman, R., Adams, C. E., Adler, L. E., Bickford, P. C., Gault, J., Harris, J. G., ... Leonard, S. (2000). Inhibitory neurophysiological deficit as a phenotype for genetic investigation of schizophrenia. *American journal of medical genetics*, 97(1), 58–64.
- Freedman, R., Adler, L. E., Myles-Worsley, M., Nagamoto, H. T., Miller, C., Kisley, M., ... Waldo, M. (1996). Inhibitory gating of an evoked response to repeated auditory stimuli in schizophrenic and normal subjects. Human recordings, computer simulation, and an animal model. *Archives of general psychiatry*, 53(12), 1114–21.
- Fuggetta, G., Fiaschi, A., & Manganotti, P. (2005). Modulation of cortical oscillatory activities induced by varying single-pulse transcranial magnetic stimulation intensity over the left primary motor area: a combined EEG and TMS study. *NeuroImage*, 27(4), 896–908.
- Fuhr, P., Agostino, R., & Hallett, M. (1991). Spinal motor neuron excitability during the silent period after cortical stimulation. *Electroencephalography and clinical neurophysiology*, 81(4), 257–62.
- Funahashi, S. (2006). Prefrontal cortex and working memory processes. *Neuroscience*, 139(1), 251–61.
- Garcia, J. O., Grossman, E. D., & Srinivasan, R. (2011). Evoked potentials in large-scale cortical networks elicited by TMS of the visual cortex. *Journal of neurophysiology*, 106(4), 1734–46.
- Glantz, L. a, & Lewis, D. a. (2000). Decreased dendritic spine density on prefrontal cortical pyramidal neurons in schizophrenia. *Archives of general psychiatry*, 57(1), 65–73.
- Gold, J. M. (2004). Cognitive deficits as treatment targets in schizophrenia. *Schizophrenia research*, 72(1), 21–8.
- Goldberg, T. E., Goldman, R. S., Burdick, K. E., Malhotra, A. K., Lencz, T., Patel, R. C., ... Robinson, D. G. (2007). Cognitive improvement after treatment with second-generation antipsychotic medications in first-episode schizophrenia: is it a practice effect? *Archives of general psychiatry*, 64(10), 1115–22.
- Goldman-Rakic, P. S. (1995). Cellular basis of working memory. *Neuron*, 14(3), 477–85.
- Gonzalez-Burgos, G., & Lewis, D. a. (2008). GABA neurons and the mechanisms of network oscillations: implications for understanding cortical dysfunction in schizophrenia. *Schizophrenia bulletin*, 34(5), 944–61.
- Gonzalez-Burgos, G., & Lewis, D. a. (2012). NMDA receptor hypofunction, parvalbumin-positive neurons, and cortical gamma oscillations in schizophrenia. *Schizophrenia bulletin*, 38(5), 950–7.
- Goto, N., Yoshimura, R., Kakeda, S., Moriya, J., Hayashi, K., Ikenouchi-Sugita, A., ... Nakamura, J. (2009). Associations between plasma levels of 3-methoxy-4-hydroxyphenylglycol (MHPG) and negative symptoms or cognitive impairments in early-stage schizophrenia. *Human psychopharmacology*, 24(8), 639–45.
- Goto, N., Yoshimura, R., Moriya, J., Kakeda, S., Ueda, N., Ikenouchi-Sugita, A., ... Nakamura, J. (2009). Reduction of brain gamma-aminobutyric acid (GABA) concentrations in early-stage schizophrenia patients: 3T Proton MRS study. *Schizophrenia research*, 112(1-3), 192–3.
- Green, M. F. (1996). What are the functional consequences of neurocognitive deficits in schizophrenia? *The American journal of psychiatry*, 153(3), 321–30.

- Haenschel, C., Bittner, R. a, Waltz, J., Haertling, F., Wibrall, M., Singer, W., ... Rodriguez, E. (2009). Cortical oscillatory activity is critical for working memory as revealed by deficits in early-onset schizophrenia. *The Journal of neuroscience*, 29(30), 9481–9.
- Hallett, M. (2007). Transcranial magnetic stimulation: a primer. *Neuron*, 55(2), 187–99.
- Hamidi, M., Slagter, H. a, Tononi, G., & Postle, B. R. (2010). Brain responses evoked by high-frequency repetitive transcranial magnetic stimulation: an event-related potential study. *Brain stimulation*, 3(1), 2–14.
- Harrison, G. (2001). Recovery from psychotic illness: a 15- and 25-year international follow-up study. *The British Journal of Psychiatry*, 178(6), 506–517.
- Hashimoto, T., Bazmi, H. H., Mirnics, K., Wu, Q., Sampson, A. R., & Lewis, D. a. (2008). Conserved regional patterns of GABA-related transcript expression in the neocortex of subjects with schizophrenia. *The American journal of psychiatry*, 165(4), 479–89.
- Hashimoto, T., Volk, D. W., Eggan, S. M., Mirnics, K., Pierri, J. N., Sun, Z., ... Lewis, D. a. (2003). Gene expression deficits in a subclass of GABA neurons in the prefrontal cortex of subjects with schizophrenia. *The Journal of neuroscienc*, 23(15), 6315–26.
- Heinrichs, R. W., & Zakzanis, K. K. (1998). Neurocognitive deficit in schizophrenia: a quantitative review of the evidence. *Neuropsychology*, 12(3), 426–45.
- Hernandez-Pavon, J. C., Metsomaa, J., Mutanen, T., Stenroos, M., Mäki, H., Ilmoniemi, R. J., & Sarvas, J. (2012). Uncovering neural independent components from highly artifactual TMS-evoked EEG data. *Journal of neuroscience methods*, 209(1), 144–57.
- Hershman, K. M., Freedman, R., & Bickford, P. C. (1995). GABAB antagonists diminish the inhibitory gating of auditory response in the rat hippocampus. *Neuroscience letters*, 190(2), 133–6.
- Hoff, a L., Sakuma, M., Wieneke, M., Horon, R., Kushner, M., & DeLisi, L. E. (1999). Longitudinal neuropsychological follow-up study of patients with first-episode schizophrenia. *The American journal of psychiatry*, 156(9), 1336–41.
- Howard, M. W. (2003). Gamma Oscillations Correlate with Working Memory Load in Humans. *Cerebral Cortex*, 13(12), 1369–1374.
- Ilmoniemi, R J, Virtanen, J., Ruohonen, J., Karhu, J., Aronen, H. J., Näätänen, R., & Katila, T. (1997). Neuronal responses to magnetic stimulation reveal cortical reactivity and connectivity. *Neuroreport*, 8(16), 3537–40.
- Ilmoniemi, Risto J, & Kicić, D. (2010). Methodology for combined TMS and EEG. *Brain topography*, 22(4), 233–48.
- Impagnatiello, F., Guidotti, A. R., Pesold, C., Dwivedi, Y., Caruncho, H., Pisu, M. G., ... Costa, E. (1998). A decrease of reelin expression as a putative vulnerability factor in schizophrenia. *Proceedings of the National Academy of Sciences of the United States of America*, 95(26), 15718–23.
- Insel, T. R. (2010). Rethinking schizophrenia. *Nature*, 468(7321), 187–93.

- Iwahashi, M., Arimatsu, T., Ueno, S., & Iramina, K. (2008). Differences in evoked EEG by transcranial magnetic stimulation at various stimulus points on the head. *Conference proceedings : ... Annual International Conference of the IEEE Engineering in Medicine and Biology Society. IEEE Engineering in Medicine and Biology Society. Conference, 2008*, 2570–3.
- Izumi, S., Takase, M., Arita, M., Masakado, Y., Kimura, a, & Chino, N. (1997). Transcranial magnetic stimulation-induced changes in EEG and responses recorded from the scalp of healthy humans. *Electroencephalography and clinical neurophysiology*, 103(2), 319–22.
- Johnson, J. S., Kundu, B., Casali, A. G., & Postle, B. R. (2012). Task-dependent changes in cortical excitability and effective connectivity: a combined TMS-EEG study. *Journal of neurophysiology*, 107(9), 2383–92.
- Jonides, J., Smith, E. E., Koeppe, R. A., Awh, E., Minoshima, S., & Mintun, M. A. (1993). Spatial working memory in humans as revealed by PET. *Nature*, 363(6430), 623–5.
- Julkunen, P., Pääkkönen, a, Hukkanen, T., Könönen, M., Tiihonen, P., Vanhatalo, S., & Karhu, J. (2008). Efficient reduction of stimulus artefact in TMS-EEG by epithelial short-circuiting by mini-punctures. *Clinical neurophysiology*, 119(2), 475–81.
- Kähkönen, S., Komssi, S., Wilenius, J., & Ilmoniemi, R. J. (2005). Prefrontal transcranial magnetic stimulation produces intensity-dependent EEG responses in humans. *NeuroImage*, 24(4), 955–60.
- Kähkönen, Seppo, Wilenius, J., Komssi, S., & Ilmoniemi, R. J. (2004). Distinct differences in cortical reactivity of motor and prefrontal cortices to magnetic stimulation. *Clinical neurophysiology*, 115(3), 583–8.
- Kähkönen, Seppo, Wilenius, J., Nikulin, V. V., Ollikainen, M., & Ilmoniemi, R. J. (2003). Alcohol reduces prefrontal cortical excitability in humans: a combined TMS and EEG study. *Neuropsychopharmacology*, 28(4), 747–54.
- Kammer, T., Beck, S., Thielscher, a, Laubis-Herrmann, U., & Topka, H. (2001). Motor thresholds in humans: a transcranial magnetic stimulation study comparing different pulse waveforms, current directions and stimulator types. *Clinical neurophysiology*, 112(2), 250–8.
- Kegeles, L. S., Mao, X., Stanford, A. D., Girgis, R., Ojeil, N., Xu, X., ... Shungu, D. C. (2012). Elevated prefrontal cortex γ -aminobutyric acid and glutamate-glutamine levels in schizophrenia measured in vivo with proton magnetic resonance spectroscopy. *Archives of general psychiatry*, 69(5), 449–59.
- Kicić, D., Lioumis, P., Ilmoniemi, R. J., & Nikulin, V. V. (2008). Bilateral changes in excitability of sensorimotor cortices during unilateral movement: combined electroencephalographic and transcranial magnetic stimulation study. *Neuroscience*, 152(4), 1119–29.
- Kohl, M. M., & Paulsen, O. (2010). The roles of GABAB receptors in cortical network activity. *Advances in pharmacology*, 58(10), 205–29.
- Komssi, S., Aronen, H. J., Huttunen, J., Kesäniemi, M., Soinne, L., Nikouline, V. V., ... Ilmoniemi, R. J. (2002). Ipsi- and contralateral EEG reactions to transcranial magnetic stimulation. *Clinical neurophysiology*, 113(2), 175–84.
- Komssi, S., Kähkönen, S., & Ilmoniemi, R. J. (2004). The effect of stimulus intensity on brain responses evoked by transcranial magnetic stimulation. *Human brain mapping*, 21(3), 154–64.

- Komssi, S., Savolainen, P., Heiskala, J., & Kähkönen, S. (2007). Excitation threshold of the motor cortex estimated with transcranial magnetic stimulation electroencephalography. *Neuroreport*, 18(1), 13–6.
- Korhonen, R. J., Hernandez-Pavon, J. C., Metsomaa, J., Mäki, H., Ilmoniemi, R. J., & Sarvas, J. (2011). Removal of large muscle artifacts from transcranial magnetic stimulation-evoked EEG by independent component analysis. *Medical & biological engineering & computing*, 49(4), 397–407.
- Kujirai, T., Caramia, M. D., Rothwell, J. C., Day, B. L., Thompson, P. D., Ferbert, A., ... Marsden, C. D. (1993). Corticocortical inhibition in human motor cortex. *The Journal of physiology*, 471, 501–19.
- Levit-Binnun, N., Litvak, V., Pratt, H., Moses, E., Zaroor, M., & Peled, A. (2010). Differences in TMS-evoked responses between schizophrenia patients and healthy controls can be observed without a dedicated EEG system. *Clinical neurophysiology*, 121(3), 332–9.
- Lewis, D. a, Cho, R. Y., Carter, C. S., Eklund, K., Forster, S., Kelly, M. A., & Montrose, D. (2008). Subunit-selective modulation of GABA type A receptor neurotransmission and cognition in schizophrenia. *The American journal of psychiatry*, 165(12), 1585–93.
- Lewis, D. a, Curley, A. a, Glausier, J. R., & Volk, D. W. (2012). Cortical parvalbumin interneurons and cognitive dysfunction in schizophrenia. *Trends in neurosciences*, 35(1), 57–67.
- Lewis, D. a, Hashimoto, T., & Volk, D. W. (2005). Cortical inhibitory neurons and schizophrenia. *Nature reviews. Neuroscience*, 6(4), 312–24.
- Li, R., & Principe, J. C. (2006). Blinking artifact removal in cognitive EEG data using ICA. *Conference proceedings : ... Annual International Conference of the IEEE Engineering in Medicine and Biology Society. IEEE Engineering in Medicine and Biology Society. Conference*, 1(3), 5273–6.
- Lioumis, P., Kicić, D., Savolainen, P., Mäkelä, J. P., & Kähkönen, S. (2009). Reproducibility of TMS-Evoked EEG responses. *Human brain mapping*, 30(4), 1387–96.
- Lisman, J., & Buzsáki, G. (2008). A neural coding scheme formed by the combined function of gamma and theta oscillations. *Schizophrenia bulletin*, 34(5), 974–80.
- Lisman, J. E., & Idiart, M. A. (1995). Storage of 7 +/- 2 short-term memories in oscillatory subcycles. *Science*, 267(5203), 1512–5.
- Litvak, V., Komssi, S., Scherg, M., Hoechstetter, K., Classen, J., Zaaroor, M., ... Kahkonen, S. (2007). Artifact correction and source analysis of early electroencephalographic responses evoked by transcranial magnetic stimulation over primary motor cortex. *NeuroImage*, 37(1), 56–70.
- MacDonald, A. W., & Schulz, S. C. (2009). What we know: findings that every theory of schizophrenia should explain. *Schizophrenia bulletin*, 35(3), 493–508.
- Mäki, H., & Ilmoniemi, R. J. (2010). The relationship between peripheral and early cortical activation induced by transcranial magnetic stimulation. *Neuroscience letters*, 478(1), 24–8.
- Mäki, H., & Ilmoniemi, R. J. (2011). Projecting out muscle artifacts from TMS-evoked EEG. *NeuroImage*, 54(4), 2706–10.
- Malhotra, D., & Sebat, J. (2012). CNVs: harbingers of a rare variant revolution in psychiatric genetics. *Cell*, 148(6), 1223–41.

- Manoach, D. S., Gollub, R. L., Benson, E. S., Searl, M. M., Goff, D. C., Halpern, E., ... Rauch, S. L. (2000). Schizophrenic subjects show aberrant fMRI activation of dorsolateral prefrontal cortex and basal ganglia during working memory performance. *Biological psychiatry*, 48(2), 99–109.
- Marwaha, S., & Johnson, S. (2004). Schizophrenia and employment - a review. *Social psychiatry and psychiatric epidemiology*, 39(5), 337–49.
- Massimini, M., Ferrarelli, F., Esser, S. K., Riedner, B. a, Huber, R., Murphy, M., ... Tononi, G. (2007). Triggering sleep slow waves by transcranial magnetic stimulation. *Proceedings of the National Academy of Sciences of the United States of America*, 104(20), 8496–501.
- Massimini, M., Ferrarelli, F., Huber, R., Esser, S. K., Singh, H., & Tononi, G. (2005). Breakdown of cortical effective connectivity during sleep. *Science (New York, N.Y.)*, 309(5744), 2228–32.
- McCarthy, G., Blamire, a M., Puce, a, Nobre, a C., Bloch, G., Hyder, F., ... Shulman, R. G. (1994). Functional magnetic resonance imaging of human prefrontal cortex activation during a spatial working memory task. *Proceedings of the National Academy of Sciences of the United States of America*, 91(18), 8690–4.
- McDonnell, M. N., Orekhov, Y., & Ziemann, U. (2006). The role of GABA(B) receptors in intracortical inhibition in the human motor cortex. *Experimental brain research*, 173(1), 86–93.
- McEvoy, J. P., Meyer, J. M., Goff, D. C., Nasrallah, H. a, Davis, S. M., Sullivan, L., ... Lieberman, J. a. (2005). Prevalence of the metabolic syndrome in patients with schizophrenia: baseline results from the Clinical Antipsychotic Trials of Intervention Effectiveness (CATIE) schizophrenia trial and comparison with national estimates from NHANES III. *Schizophrenia research*, 80(1), 19–32.
- McMenamin, B. W., Shackman, A. J., Maxwell, J. S., Bachhuber, D. R. W., Koppenhaver, A. M., Greischar, L. L., & Davidson, R. J. (2010). Validation of ICA-based myogenic artifact correction for scalp and source-localized EEG. *NeuroImage*, 49(3), 2416–32.
- Meda, S. A., Bhattarai, M., Morris, N. A., Astur, R. S., Calhoun, V. D., Mathalon, D. H., ... Pearlson, G. D. (2008). An fMRI study of working memory in first-degree unaffected relatives of schizophrenia patients. *Schizophrenia research*, 104(1-3), 85–95.
- Merabet, L. B., Theoret, H., & Pascual-Leone, A. (2003). Transcranial magnetic stimulation as an investigative tool in the study of visual function. *Optometry and vision science : official publication of the American Academy of Optometry*, 80(5), 356–68.
- Michels, L., Bucher, K., Lüchinger, R., Klaver, P., Martin, E., Jeanmonod, D., & Brandeis, D. (2010). Simultaneous EEG-fMRI during a working memory task: modulations in low and high frequency bands. *PloS one*, 5(4), e10298.
- Miller, E. K., & Cohen, J. D. (2001). An integrative theory of prefrontal cortex function. *Annual review of neuroscience*, 24, 167–202.
- Minzenberg, M. J., Firl, A. J., Yoon, J. H., Gomes, G. C., Reinking, C., & Carter, C. S. (2010). Gamma oscillatory power is impaired during cognitive control independent of medication status in first-episode schizophrenia. *Neuropsychopharmacology : official publication of the American College of Neuropsychopharmacology*, 35(13), 2590–9.

- Minzenberg, M. J., Laird, A. R., Thelen, S., Carter, C. S., & Glahn, D. C. (2009). Meta-analysis of 41 functional neuroimaging studies of executive function in schizophrenia. *Archives of general psychiatry*, 66(8), 811–22.
- Moliadze, V., Zhao, Y., Eysel, U., & Funke, K. (2003). Effect of transcranial magnetic stimulation on single-unit activity in the cat primary visual cortex. *The Journal of physiology*, 553(Pt 2), 665–79.
- Morbidi, F., Garulli, A., Prattichizzo, D., Rizzo, C., Manganotti, P., & Rossi, S. (2007). Off-line removal of TMS-induced artifacts on human electroencephalography by Kalman filter. *Journal of neuroscience methods*, 162(1-2), 293–302.
- Morey, R. a, Inan, S., Mitchell, T. V, Perkins, D. O., Lieberman, J. a, & Belger, A. (2005). Imaging frontostriatal function in ultra-high-risk, early, and chronic schizophrenia during executive processing. *Archives of general psychiatry*, 62(3), 254–62.
- Murray, C. J. L., Richards, M. a, Newton, J. N., Fenton, K. a, Anderson, H. R., Atkinson, C., ... Davis, A. (2013). UK health performance: findings of the Global Burden of Disease Study 2010. *Lancet*, 381(9871), 997–
- Mutanen, T., Mäki, H., & Ilmoniemi, R. J. (2012). The effect of stimulus parameters on TMS-EEG muscle artifacts. *Brain stimulation*, 1–6.
- Nakamura, H., Kitagawa, H., Kawaguchi, Y., & Tsuji, H. (1997). Intracortical facilitation and inhibition after transcranial magnetic stimulation in conscious humans. *The Journal of physiology*, 498, 817–23.
- Nikouline, V., Ruohonen, J., & Ilmoniemi, R. J. (1999). The role of the coil click in TMS assessed with simultaneous EEG. *Clinical neurophysiology*, 110(8), 1325–8.
- Nikulin, V. V., Kicic, D., Kahkonen, S., & Ilmoniemi, R. J. (2003). Modulation of electroencephalographic responses to transcranial magnetic stimulation: evidence for changes in cortical excitability related to movement. *European Journal of Neuroscience*, 18(5), 1206–1212.
- Onton, J., Westerfield, M., Townsend, J., & Makeig, S. (2006). Imaging human EEG dynamics using independent component analysis. *Neuroscience and biobehavioral reviews*, 30(6), 808–22.
- Opitz, A., Legon, W., Rowlands, A., Bickel, W. K., Paulus, W., & Tyler, W. J. (2013). Physiological observations validate finite element models for estimating subject-specific electric field distributions induced by transcranial magnetic stimulation of the human motor cortex. *NeuroImage*, 81, 253–64.
- Opitz, A., Windhoff, M., Heidemann, R. M., Turner, R., & Thielscher, A. (2011). How the brain tissue shapes the electric field induced by transcranial magnetic stimulation. *NeuroImage*, 58(3), 849–59.
- Pascual-Leone, a, Walsh, V., & Rothwell, J. (2000). Transcranial magnetic stimulation in cognitive neuroscience--virtual lesion, chronometry, and functional connectivity. *Current opinion in neurobiology*, 10(2), 232–7.
- Paulus, W., Classen, J., Cohen, L. G., Large, C. H., Di Lazzaro, V., Nitsche, M., ... Ziemann, U. (2008). State of the art: Pharmacologic effects on cortical excitability measures tested by transcranial magnetic stimulation. *Brain stimulation*, 1(3), 151–63.

- Paus, T., Sipila, P. K., & Strafella, P. (2001). Synchronization of neuronal activity in the human primary motor cortex by transcranial magnetic stimulation: an EEG study. *Journal of neurophysiology*, 86(4), 1983–90.
- Pell, G. S., Roth, Y., & Zangen, A. (2011). Modulation of cortical excitability induced by repetitive transcranial magnetic stimulation: influence of timing and geometrical parameters and underlying mechanisms. *Progress in neurobiology*, 93(1), 59–98.
- Pesaran, B., Pezaris, J. S., Sahani, M., Mitra, P. P., & Andersen, R. a. (2002). Temporal structure in neuronal activity during working memory in macaque parietal cortex. *Nature neuroscience*, 5(8), 805–11.
- Petrides, M., Alivisatos, B., Meyer, E., & Evans, C. (1993). Functional activation of the human frontal cortex during the performance of verbal working memory tasks. *Proceedings of the National Academy of Sciences of the United States of America*, 90(3), 878–82.
- Plöchl, M., Ossandón, J. P., & König, P. (2012). Combining EEG and eye tracking: identification, characterization, and correction of eye movement artifacts in electroencephalographic data. *Frontiers in human neuroscience*, 6, 278.
- Rajji, T. K., Sun, Y., Zomorodi-Moghaddam, R., Farzan, F., Blumberger, D. M., Mulsant, B. H., ... Daskalakis, Z. J. (2013). PAS-Induced Potentiation of Cortical-Evoked Activity in the Dorsolateral Prefrontal Cortex. *Neuropsychopharmacology*, 1–8.
- Reichenberg, A., Caspi, A., Harrington, H., Houts, R., Keefe, R. S. E., Murray, R. M., ... Moffitt, T. E. (2010). Static and dynamic cognitive deficits in childhood preceding adult schizophrenia: a 30-year study. *The American journal of psychiatry*, 167(2), 160–9.
- Reis, J., Swayne, O. B., Vandermeeren, Y., Camus, M., Dimyan, M. a, Harris-Love, M., ... Cohen, L. G. (2008). Contribution of transcranial magnetic stimulation to the understanding of cortical mechanisms involved in motor control. *The Journal of physiology*, 586(2), 325–51.
- Rosanova, M., Casali, A., Bellina, V., Resta, F., Mariotti, M., & Massimini, M. (2009). Natural frequencies of human corticothalamic circuits. *The Journal of neuroscience*, 29(24), 7679–85.
- Rosenthal, J., Waller, H. J., & Amassian, V. E. (1967). An analysis of the activation of motor cortical neurons by surface stimulation. *Journal of neurophysiology*, 30(4), 844–58.
- Rothwell, J. C. (1997). Techniques and mechanisms of action of transcranial stimulation of the human motor cortex. *Journal of neuroscience methods*, 74(2), 113–22.
- Rothwell, J. C., Thompson, P. D., Day, B. L., Boyd, S., & Marsden, C. D. (1991). Stimulation of the human motor cortex through the scalp. *Experimental physiology*, 76(2), 159–200.
- Rotzschy, C., Langner, R., Dogan, I., Reetz, K., Laird, R., Schulz, J. B., ... Eickhoff, S. B. (2012). Modelling neural correlates of working memory: a coordinate-based meta-analysis. *NeuroImage*, 60(1), 830–46.
- Rusjan, P. M., Barr, M. S., Farzan, F., Arenovich, T., Maller, J. J., Fitzgerald, P. B., & Daskalakis, Z. J. (2010). Optimal transcranial magnetic stimulation coil placement for targeting the dorsolateral prefrontal cortex using novel magnetic resonance image-guided neuronavigation. *Human brain mapping*, 31(11), 1643–52.

- Saha, S., Chant, D., & McGrath, J. (2007). A systematic review of mortality in schizophrenia: is the differential mortality gap worsening over time? *Archives of general psychiatry*, 64(10), 1123–31.
- Saha, S., Chant, D., Welham, J., & McGrath, J. (2005). A systematic review of the prevalence of schizophrenia. *PLoS medicine*, 2(5), e141.
- Sekiguchi, H., Takeuchi, S., Kadota, H., Kohno, Y., & Nakajima, Y. (2011). TMS-induced artifacts on EEG can be reduced by rearrangement of the electrode's lead wire before recording. *Clinical neurophysiology*, 122(5), 984–90.
- Selemon, L. D., Rajkowska, G., & Goldman-Rakic, P. S. (1995). Abnormally high neuronal density in the schizophrenic cortex. A morphometric analysis of prefrontal area 9 and occipital area 17. *Archives of general psychiatry*, 52(10), 805–18;
- Siebnner, H. R., Bergmann, T. O., Bestmann, S., Massimini, M., Johansen-Berg, H., Mochizuki, H., ... Rossini, P. M. (2009). Consensus paper: combining transcranial stimulation with neuroimaging. *Brain stimulation*, 2(2), 58–80.
- Siegel, M., Warden, M. R., & Miller, E. K. (2009). Phase-dependent neuronal coding of objects in short-term memory. *Proceedings of the National Academy of Sciences of the United States of America*, 106(50), 21341–6.
- Silver, H., Feldman, P., Bilker, W., & Gur, R. C. (2003). Working memory deficit as a core neuropsychological dysfunction in schizophrenia. *The American journal of psychiatry*, 160(10), 1809–16.
- Singer, W., & Gray, C. M. (1995). Visual feature integration and the temporal correlation hypothesis. *Annual review of neuroscience*, 18, 555–86.
- Smith, E. E., Jonides, J., & Koeppe, R. A. (1996). Dissociating verbal and spatial working memory using PET. *Cerebral cortex (New York, N.Y. : 1991)*, 6(1), 11–20.
- Snitz, B. E., Macdonald, A. W., & Carter, C. S. (2006). Cognitive deficits in unaffected first-degree relatives of schizophrenia patients: a meta-analytic review of putative endophenotypes. *Schizophrenia bulletin*, 32(1), 179–94.
- Sohal, V. S., Zhang, F., Yizhar, O., & Deisseroth, K. (2009). Parvalbumin neurons and gamma rhythms enhance cortical circuit performance. *Nature*, 459(7247), 698–702.
- Sørensen, H. J., Mortensen, E. L., Schiffman, J., Reinisch, J. M., Maeda, J., & Mednick, S. A. (2010). Early developmental milestones and risk of schizophrenia: a 45-year follow-up of the Copenhagen Perinatal Cohort. *Schizophrenia research*, 118(1-3), 41–7.
- Spencer, K. M., Nestor, P. G., Niznikiewicz, M. a, Salisbury, D. F., Shenton, M. E., & McCarley, R. W. (2003). Abnormal neural synchrony in schizophrenia. *The Journal of neuroscience : the official journal of the Society for Neuroscience*, 23(19), 7407–11.
- Spencer, K. M., Nestor, P. G., Perlmuter, R., Niznikiewicz, M. a, Klump, M. C., Frumin, M., ... McCarley, R. W. (2004). Neural synchrony indexes disordered perception and cognition in schizophrenia. *Proceedings of the National Academy of Sciences of the United States of America*, 101(49), 17288–93.

- Spencer, K. M., Niznikiewicz, M. a, Shenton, M. E., & McCarley, R. W. (2008). Sensory-evoked gamma oscillations in chronic schizophrenia. *Biological psychiatry*, 63(8), 744–7.
- Stern, P., Edwards, F. A., & Sakmann, B. (1992). Fast and slow components of unitary EPSCs on stellate cells elicited by focal stimulation in slices of rat visual cortex. *The Journal of physiology*, 449, 247–78.
- Stokes, M. G., Chambers, C. D., Gould, I. C., English, T., McNaught, E., McDonald, O., & Mattingley, J. B. (2007). Distance-adjusted motor threshold for transcranial magnetic stimulation. *Clinical neurophysiology*, 118(7), 1617–25.
- Stokes, M. G., Chambers, C. D., Gould, I. C., Henderson, T. R., Janko, N. E., Allen, N. B., & Mattingley, J. B. (2005). Simple metric for scaling motor threshold based on scalp-cortex distance: application to studies using transcranial magnetic stimulation. *Journal of neurophysiology*, 94(6), 4520–7.
- Sun, Y., Farzan, F., Barr, M. S., Kirihaara, K., Fitzgerald, P. B., Light, G. a, & Daskalakis, Z. J. (2011). Γ Oscillations in Schizophrenia: Mechanisms and Clinical Significance. *Brain research*, 1413, 98–114.
- Sutor, B., & Hablitz, J. J. (1989a). EPSPs in rat neocortical neurons in vitro. I. Electrophysiological evidence for two distinct EPSPs. *Journal of neurophysiology*, 61(3), 607–20.
- Sutor, B., & Hablitz, J. J. (1989b). EPSPs in rat neocortical neurons in vitro. II. Involvement of N-methyl-D-aspartate receptors in the generation of EPSPs. *Journal of neurophysiology*, 61(3), 621–34.
- Swartz, B. E., Halgren, E., Fuster, J. M., Simpkins, E., Gee, M., & Mandelkern, M. (1995). Cortical metabolic activation in humans during a visual memory task. *Cerebral cortex*, 5(3), 205–14.
- Tallon-Baudry, C., Bertrand, O., Peronnet, F., & Pernier, J. (1998). Induced gamma-band activity during the delay of a visual short-term memory task in humans. *The Journal of neuroscience*, 18(11), 4244–54.
- Tamás, G., Lorincz, A., Simon, A., & Szabadics, J. (2003). Identified sources and targets of slow inhibition in the neocortex. *Science*, 299(5614), 1902–5.
- Ter Braack, E. M., de Jonge, B., & van Putten, M. J. a M. (2013). Reduction of TMS induced artifacts in EEG using principal component analysis. *IEEE transactions on neural systems and rehabilitation engineering : a publication of the IEEE Engineering in Medicine and Biology Society*, 21(3), 376–82.
- Ter Braack, E. M., de Vos, C. C., & van Putten, M. J. a M. (2013). Masking the Auditory Evoked Potential in TMS-EEG: A Comparison of Various Methods. *Brain topography*. doi:10.1007/s10548-013-0312-z
- Thompson, M., Weickert, C. S., Wyatt, E., & Webster, M. J. (2009). Decreased glutamic acid decarboxylase(67) mRNA expression in multiple brain areas of patients with schizophrenia and mood disorders. *Journal of psychiatric research*, 43(11), 970–7.
- Tiitinen, H., Virtanen, J., Ilmoniemi, R. J., Kamppuri, J., Ollikainen, M., Ruohonen, J., & Näätänen, R. (1999). Separation of contamination caused by coil clicks from responses elicited by transcranial magnetic stimulation. *Clinical neurophysiology*, 110(5), 982–5.
- Tsujimoto, S., & Sawaguchi, T. (2004). Properties of delay-period neuronal activity in the primate prefrontal cortex during memory- and sensory-guided saccade tasks. *The European journal of neuroscience*, 19(2), 447–57.

- Uhlhaas, P. J., & Singer, W. (2010). Abnormal neural oscillations and synchrony in schizophrenia. *Nature reviews. Neuroscience*, 11(2), 100–13.
- Valls-Solé, J., Pascual-Leone, a, Wassermann, E. M., & Hallett, M. (1992). Human motor evoked responses to paired transcranial magnetic stimuli. *Electroencephalography and clinical neurophysiology*, 85(6), 355–64.
- Van Der Werf, Y. D., & Paus, T. (2006). The neural response to transcranial magnetic stimulation of the human motor cortex. I. Intracortical and cortico-cortical contributions. *Experimental brain research*, 175(2), 231–45. doi:10.1007/s00221-006-0551-2
- Van Os, J., & Kapur, S. (2009). Schizophrenia. *Lancet*, 374(9690), 635–45.
- Veniero, D., Bortoletto, M., & Miniussi, C. (2009). TMS-EEG co-registration: on TMS-induced artifact. *Clinical neurophysiology*, 120(7), 1392–9.
- Veniero, D., Bortoletto, M., & Miniussi, C. (2012). Cortical modulation of short-latency TMS-evoked potentials. *Frontiers in human neuroscience*, 6(January), 352.
- Veniero, D., Maioli, C., & Miniussi, C. (2010). Potentiation of short-latency cortical responses by high-frequency repetitive transcranial magnetic stimulation. *Journal of neurophysiology*, 104(3), 1578–88.
- Verhagen, L., Dijkerman, H. C., Medendorp, W. P., & Toni, I. (2013). Hierarchical organization of parietofrontal circuits during goal-directed action. *The Journal of neuroscience*, 33(15), 6492–503.
- Vernet, M., Bashir, S., Yoo, W.-K., Perez, J. M., Najib, U., & Pascual-Leone, A. (2013). Insights on the neural basis of motor plasticity induced by theta burst stimulation from TMS-EEG. *The European journal of neuroscience*, 37(4), 598–606.
- Virtanen, J., Ruohonen, J., Näätänen, R., & Ilmoniemi, R. J. (1999). Instrumentation for the measurement of electric brain responses to transcranial magnetic stimulation. *Medical & biological engineering & computing*, 37(3), 322–6.
- Voineskos, A. N., Farzan, F., Barr, M. S., Lobaugh, N. J., Mulsant, B. H., Chen, R., ... Daskalakis, Z. J. (2010). The role of the corpus callosum in transcranial magnetic stimulation induced interhemispheric signal propagation. *Biological psychiatry*, 68(9), 825–31.
- Volk, D., Austin, M., Pierri, J., Sampson, a, & Lewis, D. (2001). GABA transporter-1 mRNA in the prefrontal cortex in schizophrenia: decreased expression in a subset of neurons. *The American journal of psychiatry*, 158(2), 256–65.
- Volk, D. W., Austin, M. C., Pierri, J. N., Sampson, A. R., & Lewis, D. A. (2000). Decreased glutamic acid decarboxylase67 messenger RNA expression in a subset of prefrontal cortical gamma-aminobutyric acid neurons in subjects with schizophrenia. *Archives of general psychiatry*, 57(3), 237–45.
- Volz, H., Gaser, C., Häger, F., Rzanny, R., Pönisch, J., Mentzel, H., ... Sauer, H. (1999). Decreased frontal activation in schizophrenics during stimulation with the continuous performance test--a functional magnetic resonance imaging study. *European psychiatry*, 14(1), 17–24.

- Werhahn, K. J., Kunesch, E., Noachtar, S., Benecke, R., & Classen, J. (1999). Differential effects on motorcortical inhibition induced by blockade of GABA uptake in humans. *The Journal of physiology*, 517, 591–7.
- Whittington, M. A., Traub, R. D., & Jefferys, J. G. (1995). Synchronized oscillations in interneuron networks driven by metabotropic glutamate receptor activation. *Nature*, 373(6515), 612–5.
- Whittington, M. A., Traub, R. D., Kopell, N., Ermentrout, B., & Buhl, E. H. (2000). Inhibition-based rhythms: experimental and mathematical observations on network dynamics. *International journal of psychophysiology*, 38(3), 315–36.
- Wiersma, D., Wanderling, J., Dragomirecka, E., Ganev, K., Harrison, G., An Der Heiden, W., ... Walsh, D. (2000). Social disability in schizophrenia: its development and prediction over 15 years in incidence cohorts in six European centres. *Psychological medicine*, 30(5), 1155–67.
- Woodberry, K. A., Giuliano, A. J., & Seidman, L. J. (2008). Premorbid IQ in schizophrenia: a meta-analytic review. *The American journal of psychiatry*, 165(5), 579–87.
- Ziemann, U., Chen, R., Cohen, L. G., & Hallett, M. (1998). Dextromethorphan decreases the excitability of the human motor cortex. *Neurology*, 51(5), 1320–4.
- Ziemann, U., Lönnecker, S., Steinhoff, B. J., & Paulus, W. (1996). The effect of lorazepam on the motor cortical excitability in man. *Experimental brain research*, 109(1), 127–35.
- Ziemann, U., Rothwell, J. C., & Ridding, M. C. (1996). Interaction between intracortical inhibition and facilitation in human motor cortex. *The Journal of physiology*, 496, 873–81.
- Ziemann, U., Tergau, F., Wassermann, E. M., Wischer, S., Hildebrandt, J., & Paulus, W. (1998). Demonstration of facilitatory I wave interaction in the human motor cortex by paired transcranial magnetic stimulation. *The Journal of physiology*, 511, 181–90.
- Ziemann, U., Tergau, F., Wischer, S., Hildebrandt, J., & Paulus, W. (1998). Pharmacological control of facilitatory I-wave interaction in the human motor cortex. A paired transcranial magnetic stimulation study. *Electroencephalography and clinical neurophysiology*, 109(4), 321–30.

APPENDICES

Appendix A

Abstract: Australian Cognitive Neurosciences Conference. Melbourne, Australia. 2010.

Long interval cortical inhibition measured in humans using concurrent TMS-EEG.

Rogasch NC, Fitzgerald PB.

Transcranial magnetic stimulation (TMS) can be used to estimate cortical inhibition in conscious humans using paired-pulse paradigms. For instance, a suprathreshold conditioning TMS pulse inhibits the response to TMS at interstimulus intervals between 50 – 250 ms. Such inhibition is termed long-interval cortical inhibition (LICI) and is thought to reflect GABA_B- mediated cortical inhibition. Recently TMS has been combined with electroencephalography (EEG) to directly measure LICI from the cortex instead of inferring inhibition via motor-evoked responses in muscles. By using TMS-EEG, LICI can be measured from any cortical area such as motor, prefrontal and parietal cortices. However, little is known about how TMS-EEG measured LICI is affected by altered stimulation parameters. Therefore, the aim of this study was to evaluate the effect of altering conditioning and test intensities on LICI measured with TMS-EEG. Cortically-evoked potentials (CEPs) were measured from the scalp using EEG and motor-evoked potentials (MEPs) were measured from a target muscle using electromyography in healthy volunteers while single and paired-pulse TMS was given over motor or prefrontal cortex. In block 1, conditioning intensities were altered (100%, 120%, 140% of resting motor threshold; RMT) while test intensities remained constant and in block 2, conditioning intensities remained constant while test intensities were altered (110%, 125%, 140% RMT). LICI measured from CEPs over motor cortex were compared between different conditioning and test intensities and between LICI measured from MEPs in the target muscle and LICI measured from CEPs in the prefrontal cortex. Experimental results and interpretations are to be discussed.

Appendix B

Abstract: Society for Neuroscience, Washington DC, USA. 2011

Optimal parameters for measuring long-interval cortical inhibition using TMS-EEG.

Rogasch NC, Fitzgerald PB.

Introduction: The recent development of concurrent transcranial magnetic stimulation-electroencephalography (TMS-EEG) has allowed cortical inhibition to be measured directly from motor and non-motor regions in conscious humans. Using paired-pulse TMS-EEG, a GABA_B-mediated form of inhibition termed long-interval cortical inhibition (LICI) has been linked with working memory function and the pathophysiology of schizophrenia. However, the optimal parameters for measuring LICI directly from the cortex using TMS-EEG remain unclear.

Aim: To investigate the optimal stimulation parameters for measuring LICI with TMS-EEG.

Methods: Single (test) and paired (conditioning and test; interstimulus interval = 100 ms) TMS was given over the left motor cortex of 6 healthy volunteers. Cortically-evoked potentials (CEPs) resulting from TMS were measured from the left hemisphere using EEG and motor-evoked potentials (MEPs) were recorded from right first dorsal interosseus muscle using electromyography (EMG). Two blocks of stimulation were given which have previously been shown to modulate LICI strength using MEPs. In block 1, conditioning TMS intensities were altered (100%, 120%, 140% resting motor threshold; RMT) while test TMS intensities remained constant. In block 2, conditioning TMS intensities remained constant while test TMS intensities were altered (110%, 125%, 140% RMT).

Results: LICI strength measured with MEPs in block 1 increased with increasing conditioning intensities resulting in significant inhibition at 120% and 140% RMT ($p < 0.02$). In contrast, LICI strength measured with CEPs displayed an inverted-U shape being strongest at 120% RMT. In block 2, increasing test TMS intensity increased single pulse MEP and CEP size ($p < 0.01$). MEPs were significantly inhibited at each test intensity

($p < 0.001$) and LICI strength tended to decrease as test intensities increased. However, CEP inhibition was only significant at test intensities of 125% RMT ($p = 0.02$).

Conclusions: Altering conditioning and test intensities resulted in differential patterns of LICI modulation between TMS-EMG and TMS-EEG. For TMS-EEG, LICI is strongest with conditioning intensities at approximately 120% RMT and test intensities at approximately 125% RMT. These results provide a guide for future research utilising TMS-EEG to measure LICI.

Appendix C

Abstract: Biological Psychiatry Australia. Melbourne, Australia. 2012

*This poster won best student poster award, clinical research.

Plasticity in the prefrontal cortex: relationship with working memory and schizophrenia.

Rogasch NC, Rajji TK, Tran LC, Fitzgerald PB, Daskalakis ZJ.

Plasticity refers to reorganisation of neural structure and is fundamental for brain function. Short-term plasticity is important in working memory (WM), the ability to retain and manipulate information for a brief period, and dysfunctional plasticity may underlie WM impairment in schizophrenia (SCZ). In humans, plasticity can be measured as changes in cortical excitability using combined electroencephalography and transcranial magnetic stimulation (TMS-EEG), a non-invasive form of brain stimulation. The aim of this study was to assess plasticity in dorsolateral prefrontal cortex (DLPFC), a region involved in WM, of people with and without SCZ. Study 1 assessed the temporal relationship between WM and plasticity in healthy participants. Study 2 assessed DLPFC plasticity in participants with SCZ. DLPFC plasticity was induced in participants using paired associative stimulation (PAS). PAS involved pairing peripheral nerve stimulation with TMS over DLPFC (interstimulus interval (ISI) = 25 ms) every 10 s for 30 mins. TMS-evoked potentials (TEPs) following single- and paired-pulse (ISI = 100 ms) TMS were used to assess DLPFC excitability and inhibition at baseline and 5 mins following PAS. In study 1, seven healthy participants (29.3 ± 10 years, 1 F) performed a WM task (Sternberg letter recognition) 30 mins before PAS (group 1) and seven healthy participants (34.0 ± 13 years, 3 F) performed WM immediately before PAS (group 2). In study 2, seven people with SCZ (medicated, 37.0 ± 9 years, 2 F) performed a WM 30 mins before PAS and results were compared with healthy participants (group 1). *Study 1:* Single-pulse TEP facilitation following PAS was significantly larger in group 1 (WM 30 mins before PAS) compared with group 2 (WM immediately before PAS; $p=0.03$). Baseline cortical inhibition tended to be reduced following WM in group 1 ($p=0.2$) and less cortical inhibition correlated with greater plasticity induction between groups ($r=-0.6$, $p=0.02$). *Study 2:* TEP facilitation was significantly reduced in SCZ compared with controls ($p=0.04$) when both groups performed

WM 30 mins before PAS. There was no significant difference in baseline cortical inhibition between groups ($p=0.6$), however cortical inhibition strength still correlated with plasticity induction ($r=-0.6$, $p=0.03$). There is a temporal relationship between WM and PAS-induced plasticity in DLPFC of healthy participants. Reduced cortical inhibition following WM performance may explain facilitated DLPFC plasticity. Despite optimal conditions, DLPFC plasticity was impaired in SCZ. These preliminary findings suggest meta-plasticity in DLPFC following WM and support dysfunctional plasticity in SCZ.

Appendix D

Abstract: Australian Neuroscience Society Annual Meeting, Melbourne, Australia. 2013.

Plasticity induced in the prefrontal cortex is impaired in people with schizophrenia.

Rogasch NC, Rajji TK, Tran LC, Fitzgerald PB, Daskalakis ZJ.

Purpose: Recent studies have attributed cognitive impairments in schizophrenia (SCZ) to deficits in neural plasticity. However, assessments of neural plasticity in brain regions relevant to cognition, such as the prefrontal cortex (PFC), are lacking in humans. The aim of this study was to compare plasticity in the PFC and working memory (WM) function in individuals with and without SCZ. **Methods:** Paired associative stimulation (PAS) was used to induce PFC plasticity in seven healthy participants (29.3 ± 10 years, 1 F) and seven people with SCZ (medicated, 37.0 ± 9 years, 2 F). PAS involved pairing peripheral nerve stimulation with transcranial magnetic stimulation (TMS, a non-invasive method of brain stimulation) over PFC (interstimulus interval (ISI)=25 ms) every 10 s for 30 mins. TMS-evoked potentials (TEPs) following single- and paired-pulse (ISI=100 ms) TMS were measured using electroencephalography (EEG) to assess PFC excitability and inhibition at baseline and 5 mins following PAS. Participants performed a WM task 30 mins before PAS to assess WM function. **Results:** SCZ showed slower performance during the WM task compared to controls ($p=0.03$). Facilitation of PFC excitability following PAS (i.e. plasticity) was also significantly reduced in SCZ compared with controls ($p=0.04$). There was no significant difference in baseline cortical inhibition between groups ($p=0.6$), however lower cortical inhibition correlated with greater plasticity induction ($r=-0.6$, $p=0.03$). **Conclusions:** These preliminary findings suggest that people with SCZ have impaired plasticity in the PFC. The impact of this impairment on WM function requires further investigation.

Appendix E

Abstract: Australasian Schizophrenia Conference. Melbourne, Australia. 2013.

Brain stimulation-induced associative plasticity is reduced in the prefrontal cortex of people with schizophrenia.

Rogasch NC, Rajji TK, Tran LC, Fitzgerald PB, Daskalakis ZJ.

Objective: Associative plasticity refers to timing-dependent alterations in synaptic efficacy which underlie learning and memory. Memory deficits are a core feature of schizophrenia (SCZ) and abnormal plasticity may contribute to memory dysfunction. The aim of this pilot study was to assess associative plasticity in the prefrontal cortex (PFC; a region involved in short-term memory) in people with and without SCZ. We hypothesised that people with SCZ would demonstrate impaired plasticity compared with healthy controls.

Methods: Seven healthy participants (29.3 ± 10 years, 1 F) and seven people with SCZ (medicated, 37.0 ± 9 years, 2 F) participated in this study. Baseline PFC excitability and inhibition was assessed using combined transcranial magnetic stimulation (TMS, a non-invasive form of brain stimulation) and electroencephalography. 75 single (excitability) and 75 paired (inhibition) TMS pulses were given over PFC and the amplitude of TMS-evoked cortical potentials were measured. To induce associative plasticity in the PFC, we adapted a TMS paradigm developed in the motor system called paired associative stimulation (PAS). PAS involved pairing single pulse TMS over PFC with somatosensory-evoked potentials resulting from peripheral nerve stimulation. Stimuli were delivered at an interstimulus interval of 25 ms every 10 s for 30 mins. To quantify PAS-induced plastic change, PFC excitability and inhibition was assessed again following PAS and compared with baseline measures.

Results: In controls, PFC excitability increased following PAS (i.e. plasticity). However, facilitation of PFC excitability following PAS was significantly reduced in SCZ compared with controls ($p=0.04$). There was no significant difference in baseline cortical inhibition between groups ($p=0.6$), however lower inhibition correlated with greater plasticity induction ($r=-0.6$, $p=0.03$) across all participants.

Conclusions: This preliminary data suggest that associative plasticity is reduced in the PFC of people with SCZ, however age-related plasticity decline may also factor. The contribution of plasticity impairment to memory dysfunction in SCZ warrants further investigation.

Appendix F

Abstract: World Congress of Biological Psychiatry. Kyoto, Japan. 2013.

Brain stimulation-induced associative plasticity is reduced in the prefrontal cortex of people with schizophrenia.

Rogasch NC, Rajji TK, Tran LC, Fitzgerald PB, Daskalakis ZJ.

Objective: Associative plasticity refers to timing-dependent alterations in synaptic efficacy which underlie learning and memory. Memory deficits are a core feature of schizophrenia (SCZ) and abnormal plasticity may contribute to memory dysfunction. The aim of this pilot study was to assess associative plasticity in the prefrontal cortex (PFC; a region involved in short-term memory) in people with and without SCZ. We hypothesised that people with SCZ would demonstrate impaired plasticity compared with healthy controls.

Methods: Seven healthy participants (29.3 ± 10 years, 1 F) and seven people with SCZ (medicated, 37.0 ± 9 years, 2 F) participated in this study. Baseline PFC excitability and inhibition was assessed using combined transcranial magnetic stimulation (TMS, a non-invasive form of brain stimulation) and electroencephalography. 75 single (excitability) and 75 paired (inhibition) TMS pulses were given over PFC and the amplitude of TMS-evoked cortical potentials were measured. To induce associative plasticity in the PFC, we adapted a TMS paradigm developed in the motor system called paired associative stimulation (PAS). PAS involved pairing single pulse TMS over PFC with somatosensory-evoked potentials resulting from peripheral nerve stimulation. Stimuli were delivered at an interstimulus interval of 25 ms every 10 s for 30 mins. To quantify PAS-induced plastic change, PFC excitability and inhibition was assessed again following PAS and compared with baseline measures.

Results: In controls, PFC excitability increased following PAS (i.e. plasticity). However, facilitation of PFC excitability following PAS was significantly reduced in SCZ compared with controls ($p=0.04$). There was no significant difference in baseline cortical inhibition between groups ($p=0.6$), however lower inhibition correlated with greater plasticity induction ($r=-0.6$, $p=0.03$) across all participants.

Conclusions: This preliminary data suggest that associative plasticity is reduced in the PFC of people with SCZ, however age-related plasticity decline may also factor. The contribution of plasticity impairment to memory dysfunction in SCZ warrants further investigation.

Appendix G

Abstract: Australasian Brain Stimulation Meeting. Melbourne, Australia. 2013.

Artifacts associated with combined TMS-EEG.

Rogasch NC, Thomson RH, Bailey NW, Daskalakis ZJ, Fitzgerald PB.

Background: Combined transcranial magnetic stimulation and electroencephalography (TMS-EEG) is an emerging technique for assessing cortical network properties in both health and disease. However, various recording and physiological artifacts can obscure TMS-evoked cortical potentials (TEPs). The aim of these experiments was to identify artifacts in TMS-EEG recordings made using non-specialised TMS- EEG equipment.

Methods: Recovery time from TMS-related artifacts were measured on a phantom head (melon; *Cucumis Melo*) and compared between different TMS stimulators (Magstim, Magventure). Findings were then confirmed in healthy humans (n=32) and additional physiological artifacts were identified. The origin of these artifacts was determined using independent component analysis (ICA) and the effect of different stimulus intensities, different scalp positions and paired-pulse TMS on artifact amplitude was assessed. Finally, the use of ICA for artifact correction was trialled.

Results: Phantom head experiments revealed differing TMS artifact profiles between different stimulators. These differences could be accounted for by preventing coil and electrode contact in both phantom and human heads, resulting in recovery within 5-10 ms. In humans, a large artifact, presumably resulting from stimulation of scalp muscles, obscured TEPs up to 25-40 ms following TMS over lateral scalp positions, but not following TMS closer to the mid-line. Eye-blink artifacts time-locked to the TMS pulse obscured TEPs in

frontal channels between 60-120 ms. EEG signal resulting from eye-blinks could be removed using ICA without removing TMS-evoked neural activity.

Conclusion: TEPs occurring within 5-10 ms of TMS can be measured using EEG, however care must be taken to either avoid or remove recording and physiological artifacts.